Valorization of Kraft lignin via alkaline and acid-mediated aerobic oxidation processes

Submitted by

Shrikanta Sutradhar

A dissertation submitted to the department of Chemistry and Materials Science in conformity with the requirements of the degree of Doctor of Philosophy.

Lakehead University

I dedicate this thesis to my parents,

Haradhan Sutradhar

&

Mina Rani Sutradhar

ABSTRACT

Lignin is a complex heterogeneous aromatic compound derived from renewable plant biomass. Due to its aromatic backbone, it has grown interested in producing biochemicals and other polymeric applications. Depending on the sources and isolation methods, lignin has a wide range of functional groups, such as aliphatic/aromatic hydroxyl, carboxylic, sulphonic, and methoxyl groups, which make lignin chemically reactive for modification towards versatile applications. The main goals of this dissertation are categorized into two main sections. Firstly, KOH mediated aerobic oxidation of kraft lignin (KL) was performed to produce water-soluble KL that was applied as green fertilizer on maize seedlings and a mid-range cement plasticizer. Secondly, oxalic acid mediated oxidation of KL was conducted to produce aromatic biochemicals such as vanillin and vanillic acid.

In this dissertation, the KL was aerobically oxidized in KOH solution to produce water-soluble anionic lignin. The oxidation reaction was optimized to achieve the maximum carboxylic acid groups and charge density. The XPS, ^{1}H-NMR, and ^{31}P-NMR confirmed the introduction of the carboxylic acid groups, while the FTIR, and HSQC-NMR confirmed the structural alterations in the oxidized lignin. The extensive degradations of the aromatic moieties (G-units) of lignin confirmed its ring openings during the alkaline oxidation. The fertilizing effects of the modified lignin were investigated on *Zea mays* seedlings. Compared with commercial humic acid, the results showed excellent physiological effects, such as improved plant growth, chlorophyll content in leaves and organic content. On the other note, cement paste flowability, adsorption on cement particles, compressive strength of the hardened cement, and water reducibility were tested to investigate the performance of the oxidized lignin as a green cement plasticizer. The

results confirmed that the KOH-mediated oxidized lignin has great potential to be used as a plasticizer.

The OA-mediated aerobic oxidation of KL was studied to produce aromatic compounds, such as vanillin and vanillic acid. The effects of reaction parameters on the yields of phenolic compounds were thoroughly studied. The study aimed to investigate the catalytic activity of niobium pentoxide in combination with OA. The product mixtures were identified and quantified by HPLC analysis. ^{13}C NMR and HSQC NMR confirmed the abundance of the phenolic moieties in the ethyl acetate soluble fractions, while ^{1}H and HSQC-NMR confirmed the structural changes of KL during the oxidation reaction. Interestingly, the absence of the β-O-4 linkages in unmodified lignin confirmed the selective degradation of lignin. The recyclability of the recovered oxalic acid showed no significant reduction in vanillin and vanillic acid yield. Finally, the current study showed a high yield of phenolic compounds with greater selectivity toward vanillin production.

Based on the results obtained in this thesis, it is apparent that the modification of KL via KOH-catalyzed oxidation to water-soluble lignin and OA-mediated oxidation to produce vanillin and vanillic acid can be technically feasible for generating value-added lignin-based products.

ACKNOWLEDGEMENTS

First, I would like to offer my heartfelt gratitude and respect to my honorable supervisor, Dr. Pedram Fatehi, for allowing me to work under his supervision. I thank him for his scholarly guidance, research insight, expert suggestions and finally for his active engagement and tireless efforts throughout the period of my research work.

Next, I would like to express my heartfelt gratitude to Dr. Nur Alam for giving me the Ph.D. opportunity, his encouragement, and constructive suggestions during the research.

I would also like to thank my Ph.D. committee members, Dr. Ebrahim Rezaei and Dr. Kang Kang for their constructing suggestions and encouragements.

I would like to thank and show my gratitude to Dr. Gousheng Wu, Mr. Michael Sorokopud, and Mr. Greg Krepka, LUIL department, Lakehead University for helping me with the analytical instruments.

Also, I would like to thank the faculty and the Department of Chemistry staff for their assistance, especially Dr. Christine Gottardo and Dr. Robert Mawhinney for their guidelines in my chemistry challenges and Dr. Brenda Magajna for her technical support.

I would like to express my special thanks to Dr. Abu Hena Md Billah, Mr. Morgan Ellis and Corry Hubbard from Civil engineering department of Lakehead University for their technical support and help.

I would also like to thank all previous and current lab members for encouraging me with and providing me an ideal workplace environment. I especially thank Dr. Weijue Gao, Dr. Mohan Konduri, Yichen Liao, Farzad Gholami, Jonathan A. Diaz Baca and Ameena Bacchus for their continued assistance and guidelines in the lab.

I am grateful to all my friends Md Shariful Islam, Adarsh Chowdhury, Rakibul Hasan Dhrubo, Niravkumar Kosamia, Md Hafizur Rahman, my roommates and all of those who have directly or indirectly helped me during the period of my Ph.D. study.

I must mention my respect and heartfelt gratitude towards my family members, Haradhan Sutradhar (father), Mina Rani Sutradhar (Mother), Ajit Sutradhar (brother) and Sheuli Sutradhar (sister) for their all-time love, blessings and sacrifice, inspiration, and mental support. Finally, I cannot express my heartfelt feelings to my beloved wife and forever life partner, Neela Sutradhar, for her patient and mental support throughout my Ph.D. study.

The financial assistant from NSERC, Canada is also much appreciated.

List of Abbreviations

AAO	Alkaline aerobic oxidation
ACD	Acid-catalyzed depolymerization
ALH	Artificial lignohumate
AOD	Alkaline oxidative digestion
ASAM	Alkaline Sulfite Anthraquinone and Methanol
BCD	Base-catalyzed depolymerization
FA	Fulvic acid
FTIR	Fourier transform infrared spectroscopy
GA	Gibberellin
HA	Humic acid
HMW	High molecular weight
HPLC	High performance Liquid Chromatography
HS	Humic Substances
IAA	Auxin
KL	Kraft lignin
LS	Lignosulphonates
LMW	Low molecular weight
N-ALH	Nitrogen enriched ALH
OA	Oxidative Ammonolysis
OL	Organosolv lignin
OxA	Oxalic acid
ROS	Reactive oxygen species
SL	Soda lignin
XPS	X-ray photoelectron spectroscopy

Table of Contents

List of Tables

List of Figures

Chapter 1

2.1. Introduction

2.1.1. Overview

Lignin is one of the most complex biopolymers on the earth, having heterogeneous aromatic structures [1]. Softwoods, hardwoods, and non-woods contain 25-35%, 18-28% and 9-20% of lignin respectively [2, 3]. Structurally, lignin is composed of three phenylpropane precursors, such as sinapyl alcohol, coniferyl alcohol and *p*-coumaryl alcohol, where the aromatic ring of these alcohols is called syringyl (S), guaiacyl (G) and p-hydroxyphenyl (H) units, respectively [2, 3]. Softwood lignin mostly contains G with a small portion of H-types, hardwood lignin contains a different proportion of G and S, whereas the non-wood plants mostly contain H with a small portion of G and S types of lignin. The major inter-unit linkages in lignin are ether linkages (α-O-4 and β-O-4) and carbon-carbon linkages (β-β, β-5, 5–5, β-1) [4-6]. Depending on the plant sources, β-O-4 linkages share around 50-60%, while the other linkages, such as 5–5 (18–25%), β-5 (9–12%), β-1 (7–10%), α-O-4, (6–8%) and β-β (0–3%) share the rest parts [2, 6, 7] .

In order to increase lignin reactivity and homogenization, scientists depolymerize lignin into oligomers and monomers and introduce several reactive sites [8]. Various thermochemical processes, such as oxidation, pyrolysis, gasification, hydrolysis, and hydrogenation, have been extensively studied over the years [12]. Generally, the depolymerization of lignin by the oxidation process is conducted to produce various biochemicals, such as aromatic aldehydes (vanillin, syringaldehyde, guaicol, phenol), phenolic acids and aliphatic acids in alkaline or acidic media [3, 9-11]. The commonly used oxidizing agents for lignin oxidation are air/molecular oxygen, hydrogen peroxide and some transitional metal oxides/salts [12]. Lignin

oxidation can be broadly classified as base-catalyzed depolymerization (BCD) and acid-catalyzed depolymerization (ACD). Depending on the end products, BCD can be sub-categorized into two pathways: 1) alkaline oxidation for fine biochemicals and 2) alkaline oxidation towards water-soluble anionic lignin. Regardless of the end products, oxidation by BCD is carried out in the aqueous solution of NaOH, KOH, Na_2CO_3, NH_4OH, $Ca(OH)_2$, LiOH, etc, at a temperature range of 100-300 °C with or without catalysts in the presence of oxidizing agents (air, oxygen or hydrogen peroxide [5, 10, 13-18]. However, ACD is carried out for fine chemicals in the presence of different inorganic (HCl, H_2SO_4, H_3PO_4) [19] or organic acids (formic acid, peracetic acid etc)[20, 21] at a temperature range of 60-300 °C. Based on our literature search, no study reported direct KOH catalysed (BCD) aerobic oxidation of KL to produce water-soluble lignin as plant growth stimulator (humic acid like substances) and green cement plasticizer.

According to the Food and Agricultural organization (FAO), the world population will increase to 34% and at the same time, the food demand will increase to 70% by 2050 [22]. For these over-growing food demands, inorganic chemical-based fertilizers are widely used to increase crop productivity. However, the excessive usages of these chemical fertilizers have severe environmental effects including soil compaction, deficiency of organic matters in soil and surface water contaminations [23]. Moreover, chemical fertilizers may cause serious health hazards to human body due to heavy metal contaminations in the grains and vegetables [24-26]. Therefore, producing renewable and environmentally friendly green fertilizers is essential for sustainable agricultural development. In this regard, lignin-based fertilizers could open windows of opportunities in the agricultural sector.

Commercial plasticizers are produced from petroleum-based chemicals, which are neither environmentally friendly nor sustainable. Lignosulfonates have been used as a bio-based green cement plasticizer for decades due to their excellent anionic hydrophilic nature [27-29]. However, the global production of lignosulfonates is in decline significantly. Alternatively, KL is hydrophobic, the widely available lignin (90% of produced lignin globally), considered underutilized by-products of the pulping industries, and mostly burnt as low-grade fuel on-site for steam generation[30, 31].

In addition, the ACD of lignin is carried out in harsh reaction conditions (including strong acidic media and operating conditions). However, recent studies investigated the oxidative depolymerization of lignin and lignin model compounds by peracetic acid (PAA) and oxalic acid (OxA) respectively in milder reaction conditions and produced monomeric phenolic compounds [21, 32]. Although PAA is a strong oxidizing reagent, it has carcinogenic effects and is a potential fire hazard [33]. Alternatively, oxalic acid is a strong reducing agent, safe, renewable, and can be recovered for recycling [32].

2.1.3. Research gaps

1. No other studies exploited the aerobic oxidation of KL in the presence of KOH to produce green fertilizers and investigated the physiological responses on *Zea mays* seedlings.
2. No studies were found regarding the aerobic oxidation of softwood KL in alkaline media (KOH) to produce a water-soluble anionic green cement plasticizer and optimized the reaction parameters.
3. No other studies reported oxalic acid-mediated direct oxidative depolymerization of commercial softwood KL towards vanillin and vanillic acid production. Moreover, no

other studies were found reporting the catalytic activity of niobium pentoxide with oxalic acid for KL depolymerization.

In chapter one, a brief overview of lignin, the recent research gaps, the objectives of this dissertation, and a summary of the next chapters are discussed.

2.1.2. Objectives of the dissertation

The objectives of this thesis were to:

1. Conduct KOH-catalyzed aerobic oxidation of KL to produce water-soluble lignin and optimize the reaction parameters to achieve oxidized lignin having the maximum carboxylic acid groups;
2. Investigate the use of soluble lignin as a lignin-derived humic substances for plant growth;
3. Investigate the use of water-soluble oxidized lignin as a green cement plasticizer; and
4. Conduct OA-mediated oxidation of KL to produce vanillin and vanillic acid.

The following chapters in this dissertation describe the proposed objectives.

Chapter two provides a comprehensive literature review on natural humic substances and artificial humic substances. The historical origin of HS, including the past theories, definitions, and components, are discussed with references. A brief definition of lignin and its structural connections to natural HS are also discussed. Recent studies and advances on the transformations of the technical lignin to HS and potential applications of lignin-derived artificial HS are

thoroughly reviewed. The challenges and future direction toward possible solutions are discussed.

Chapter three presents the KOH-catalyzed aerobic KL oxidation to produce lignin based fertilizer. This chapter describes the different oxidation approaches and the structural changes of the modified lignin analyzed by advanced analytical methods, such as FTIR, ^{1}H-NMR, ^{31}P-NMR, HSQC-NMR and XPS. The fertilizing effects of the modified water-soluble lignin was investigated on maize seedlings. The physiological effects, such as plant growth, dry weights of plants, chlorophyll content on leaves and the mineral contents in plant biomass, were extensively studied on a laboratory scale.

Chapter four describes the KOH- mediated oxidation of KL to achieve a cement plasticizer. The reaction parameters were thoroughly investigated. The chemical characterizations, such as carboxylic acid groups, charge density, and molecular weights, provided detailed relationships of the reaction parameters. The structural changes were also examined by FTIR, HSQC-NMR and XPS. The samples with highest carboxylic acid group and charge density was tested as a cement plasticizer and its performance was compared with that of LS and a commercial plasticizer. The flowability, adsorption, zeta potential, compressive strength, and water reducibility analyzes were conducted for understanding the behavior of oxidized KL, LS, and commercial plasticizers.

Chapter five presents OA-mediated oxidative depolymerization of KL to produce aromatic biochemicals, such as vanillin and vanillic acid. This chapter describes the effects of reaction parameters, such as reagents, temperatures, time and oxalic acid concentration, on the lignin depolymerizations towards the product yields. The oxidative depolymerized products are identified and quantified by HPLC analysis. In this study, the recyclability of the recovered OA was studied for industrial viability. A primary mass balance analysis was also studied and

presented. A reaction scheme was proposed and described in the chapter. Finally, product yields from previously studied literatures and from the current study were compared.

Chapter six provides conclusions and suggestions for future research.

References

[1] C. Crestini, M. Crucianelli, M. Orlandi, R. Saladino, Oxidative strategies in lignin chemistry: A new environmental friendly approach for the functionalisation of lignin and lignocellulosic fibers, 156(1-2) (2010) 8-22.

[2] A. Lourenço, H. Pereira, Compositional variability of lignin in biomass, Lignin-trends and applications (2018) 65-98.

[3] S. Laurichesse, L. Avérous, Chemical modification of lignins: Towards biobased polymers, J Progress in Polymer Science 39(7) (2014) 1266-1290.

[4] J. Ralph, K. Lundquist, G. Brunow, F. Lu, H. Kim, P.F. Schatz, J.M. Marita, R.D. Hatfield, S.A. Ralph, J.H. Christensen, Lignins: natural polymers from oxidative coupling of 4-hydroxyphenyl-propanoids, Phytochemistry reviews 3(1) (2004) 29-60.

[5] W. Schutyser, J.S. Kruger, A.M. Robinson, R. Katahira, D.G. Brandner, N.S. Cleveland, A. Mittal, D.J. Peterson, R. Meilan, Y. Román-Leshkov, Revisiting alkaline aerobic lignin oxidation, Green chemistry 20(16) (2018) 3828-3844.

[6] F. Wang, D. Ouyang, Z. Zhou, S.J. Page, D. Liu, X. Zhao, Lignocellulosic biomass as sustainable feedstock and materials for power generation and energy storage, Journal of Energy Chemistry 57 (2021) 247-280. https://doi.org/https://doi.org/10.1016/j.jechem.2020.08.060.

[7] C. Li, X. Zhao, A. Wang, G.W. Huber, T. Zhang, Catalytic transformation of lignin for the production of chemicals and fuels, Chemical Reviews 115(21) (2015) 11559-11624.

[8] A.G. Vishtal, A. Kraslawski, Challenges in industrial applications of technical lignins, BioResources 6(3) (2011) 3547-3568.

[9] J.D. Araújo, C.A. Grande, A.E. Rodrigues, Design, Vanillin production from lignin oxidation in a batch reactor, J Chemical Engineering Research 88(8) (2010) 1024-1032.

[10] A.G. Demesa, A. Laari, I. Turunen, M. Sillanpää, Alkaline partial wet oxidation of lignin for the production of carboxylic acids, Chemical Engineering &Technology 38(12) (2015) 2270-2278.

[11] J. Villar, A. Caperos, F. García-Ochoa, Oxidation of hardwood kraft-lignin to phenolic derivatives with oxygen as oxidant, Wood Science &Technology 35(3) (2001) 245-255.

[12] M.P. Pandey, C.S. Kim, Lignin depolymerization and conversion: a review of thermochemical methods, Chemical Engineering and Technology 34(1) (2011) 29-41.

[13] S. Sutradhar, N. Alam, L.P. Christopher, P. Fatehi, KOH catalyzed oxidation of kraft lignin to produce green fertilizer, Catalysis Today 404 (2022) 49-62.

[14] A. Toledano, L. Serrano, J. Labidi, Organosolv lignin depolymerization with different base catalysts, Journal of chemical technology & biotechnology 87(11) (2012) 1593-1599.

[15] C. Chio, M. Sain, W. Qin, Lignin utilization: A review of lignin depolymerization from various aspects, Renewable and Sustainable Energy Reviews 107 (2019) 232-249. https://doi.org/https://doi.org/10.1016/j.rser.2019.03.008.

[16] H. Paananen, E. Eronen, M. Mäkinen, J. Jänis, M. Suvanto, T.T. Pakkanen, Base-catalyzed oxidative depolymerization of softwood kraft lignin, Industrial Crops and Products 152 (2020) 112473. https://doi.org/https://doi.org/10.1016/j.indcrop.2020.112473.

[17] U. Junghans, J.J. Bernhardt, R. Wollnik, D. Triebert, G. Unkelbach, D. Pufky-Heinrich, Valorization of Lignin via Oxidative Depolymerization with Hydrogen Peroxide: Towards Carboxyl-Rich Oligomeric Lignin Fragments, Molecules 25(11) (2020) 2717.

[18] A. Kalliola, T. Vehmas, T. Liitiä, T. Tamminen, Alkali-O2 oxidized lignin–A bio-based concrete plasticizer, Industrial Crops and Products 74 (2015) 150-157.

[19] P. Asawaworarit, P. Daorattanachai, W. Laosiripojana, C. Sakdaronnarong, A. Shotipruk, N. Laosiripojana, Catalytic depolymerization of organosolv lignin from bagasse by carbonaceous solid acids derived from hydrothermal of lignocellulosic compounds, Chemical Engineering Journal 356 (2019) 461-471.

[20] A. Rahimi, A. Ulbrich, J.J. Coon, S.S. Stahl, Formic-acid-induced depolymerization of oxidized lignin to aromatics, Nature 515(7526) (2014) 249-252.

[21] R. Ma, U. Sanyal, M.V. Olarte, H.M. Job, M.S. Swita, S.B. Jones, P.A. Meyer, S.D. Burton, J.R. Cort, M.E. Bowden, Role of peracetic acid on the disruption of lignin packing structure and its consequence on lignin depolymerisation, Green Chemistry 23(21) (2021) 8468-8479.

[22] T.A. Wise, Can we feed the world in 2050, A scoping paper to assess the evidence. Global Development and Environment Institute Working Paper (13-04) (2013).

[23] M.T. Bashir, S. Ali, M. Ghauri, A. Adris, R. Harun, Impact of excessive nitrogen fertilizers on the environment and associated mitigation strategies, Asian Journal of Microbiology, Biotechnology and Environmental Sciences 15(2) (2013) 213-221.

[24] X.-X. Chen, Y.-M. Liu, Q.-Y. Zhao, W.-Q. Cao, X.-P. Chen, C.-Q. Zou, Health risk assessment associated with heavy metal accumulation in wheat after long-term phosphorus fertilizer application, Environmental Pollution 262 (2020) 114348.

[25] R. Kumar, R. Kumar, O. Prakash, Chapter-5 the Impact of Chemical Fertilizers on Our Environment and Ecosystem, Chief Ed 35 (2019) 69.

[26] N. Sharma, R. Singhvi, Effects of chemical fertilizers and pesticides on human health and environment: a review, International Journal of Agriculture, Environment and Biotechnology 10(6) (2017) 675-680.

[27] S. Hanehara, K. Yamada, Interaction between cement and chemical admixture from the point of cement hydration, absorption behaviour of admixture, and paste rheology, Cement and Concrete Research 29(8) (1999) 1159-1165.

[28] İ.B. Topçu, Ö. Ateşin, Effect of high dosage lignosulphonate and naphthalene sulphonate based plasticizer usage on micro concrete properties, Construction and Building Materials 120 (2016) 189-197.

[29] G. Telysheva, T. Dizhbite, E. Paegle, A. Shapatin, I. Demidov, Surface- active properties of hydrophobized derivatives of lignosulfonates: effect of structure of organosilicon modifier, Journal of Applied Polymer Science 82(4) (2001) 1013-1020.

[30] D. Bajwa, G. Pourhashem, A.H. Ullah, S. Bajwa, A concise review of current lignin production, applications, products and their environmental impact, Industrial Crops and Products 139 (2019) 111526.

[31] L. Dessbesell, M. Paleologou, M. Leitch, R. Pulkki, C.C. Xu, Global lignin supply overview and kraft lignin potential as an alternative for petroleum-based polymers, Renewable and Sustainable Energy Reviews 123 (2020) 109768.

[32] A.C. Lindsay, S. Kudo, J. Sperry, Cleavage of lignin model compounds and lignin ox using aqueous oxalic acid, Organic & Biomolecular Chemistry 17(31) (2019) 7408-7415.

[33] S.C. Gad, Peracetic Acid, in: P. Wexler (Ed.), Encyclopedia of Toxicology (Third Edition), Academic Press, Oxford, 2014, pp. 788-790. https://doi.org/https://doi.org/10.1016/B978-0-12-386454-3.01197-0.

Chapter 2

Latest Development in the Fabrication and Use of Lignin-derived Humic Acid

Abstract

Humic substances (HS) are originated from naturally decaying biomass. The main products of HS are humic acids, fulvic acids, and humins. HS are extracted from different natural origins (e.g., coals, lignite, forest, and river sediments). However, the production of HS from these resources is not environmentally friendly, potentially impacting ecological systems. Earlier theories claimed that the HS might be transformed from lignin by enzymatic or aerobic oxidation. On the other hand, lignin is a by-product of pulp and paper production processes and is available commercially. However, it is still under-utilized. To address the challenges of producing environmentally friendly HS and accommodating lignin in valorized processes, the

production of lignin-derived HS has attracted attention. Currently, several chemical modification pathways can be followed to convert lignin into HS-like materials, such as alkaline aerobic oxidation, alkaline oxidative digestion, and oxidative ammonolysis of lignin. This review paper discusses the fundamental aspects of lignin transformation to HS comprehensively. The applications of natural HS and lignin-derived HS in various fields, such as soil enrichment, fertilizers, wastewater treatment, water decontamination, and medicines, were comprehensively discussed. Furthermore, the current challenges associated with the production and use of HS from lignin were described.

*Chapter 2 is accepted for publication as a review paper in the BMC Biotechnology for Biofuels and Bioproducts.

2.1. Introduction

Although the global population has been increasing at an alarming rate, agricultural land has not expanded significantly [1, 2]. In this circumstance, improving the human ability to grow grains in a limited space, e.g., in small fields, is critical. Farmers depend on inorganic chemical fertilizers to keep the soil fertile for cultivation. However, the overused lands become unfertile and saline with a different pH in the long run. Soil salinity is characterized by high amounts of Na^{+}, Mg^{+2}, Ca^{+2}, Cl^{-}, HCO_3^{-}, and SO_4^{-2}, affecting plant growth [3]. Moreover, the total carbon content in the soil decreases daily. The organic matter of soil contains the residues of plants and animals and other organic compounds that form during the biomass decomposition processes in the soil. In this case, about 60% of the organic matter of soil are humic substances (HS) [4-7], which play a vital role in the health of soil for cultivation.

HS are mainly composed of humic acids (HA), fulvic acids (FA), and humins [8]. Structurally, although HA and FA share similar functional groups, FA have a lower molecular weight than

HA do. As HS are the oxidized products of degraded biomass (e.g., lignin), they contain many oxygen-containing functional groups, such as aliphatic/phenolic hydroxyl groups, carboxylic acid groups and quinones [9, 10]. These materials can probably be fabricated from other materials.

HS can play a vital role in managing the essential organic content of soil. However, their complicated chemical structures are not easily degraded by the soil's microorganisms. Moreover, their close interaction with soil minerals helps them remain intact for a long period. Organic fertilizers, such as composts and cattle manures, are primarily used to balance the humus and mineral content and act as natural pesticides [11]. Like organic fertilizers, humic substances (HS) are used in a few countries to improve soil quality [3]. It is well documented that the HS plays a vital role in atmospheric nitrogen management by increasing the soil's exchangeable NH_4^+ and available NO_3^-, thus preventing nitrogen leaching and stimulating nitrifying bacteria [12-14]. Moreover, HS hinders the precipitation of soil minerals, such as iron and aluminum, by complexation reactions [15-18]. Previous studies also claimed that HS could form complexes with soil minerals (including toxic metals), hydroxides, and organic compounds[19-22] . However, the sources of natural HS are limited. Thus, the incentives for generating HS artificially from natural biopolymers, such as lignin, are high.

Lignin is the most abundant aromatic biopolymer on earth, containing many active functional groups, e.g., aliphatic and phenolic moieties. Lignin is a three-dimensional, highly cross-linked macromolecule composed of three substituted phenols of coniferyl, sinapyl and p-coumaryl alcohols generated by enzymatic polymerization, yielding a vast number of functional groups and linkages [23, 24]. The primary source of lignin is plant biomass [24-27], mainly produced as the byproduct of the pulping processes of wood and other plant resources. The chemical

characteristics of lignin differ depending on the pulping processes and the origin of the lignin resources. Although unmodified lignin has a limited application today, many applications have been proposed for chemically modified lignin derivatives, such as fine chemicals, emulsifiers, flocculants, synthetic floorings, sequestering, binders, thermosets, paints, adhesives, and fuels [28-34]. There are various ways to modify lignin for valorization, such as pyrolysis [35-37], hydrolysis [38, 39], hydrogenolysis [40-42], gasification [43, 44], hydrothermal conversion [45] and oxidation [46-48]. Oxidation is the most popular route for lignin modification and depolymerization for vanillin and organic acid production [49, 50]. Oxidation can be conducted using different oxidizing agents or various catalysts and enzymes [47-49, 51-53]. Alkaline aerobic oxidation could be an efficient chemical process to convert lignin and lignocellulosic biomass into HS.

Earlier studies reported a direct connection between natural humification and lignin due to aromatic structures and other common functional groups found in HS and lignin [54, 55]. It was also illustrated that artificial humification by alkaline oxidation or oxidative ammonolysis/ammoxidation of technical lignin would be possible [56-61]. This review article describes the complete historical origin of HS and the similarities between HS and lignin comprehensively. Also, the natural humification process and recent approaches to transforming lignin into HS-like materials are extensively discussed. Furthermore, this review article extends the discussion on the application of lignin-derived HS.

2.2. Origin of humic substances: Historical review

Humic substances were first defined in 1761 by Wallerius as decomposed organic matter [62]. In 1786, Achard extracted a brown substance from soil and peat using KOH solution and named it

humic acid [63, 64]. Humus, a Latin word suggesting a soil-like substance, was first introduced by de Saussure in 1804, referring to dark soil organic matter [62]. In 1837, Sprengel developed several methods for preparing humic acid by pretreating soil with dilute mineral acids before alkaline extraction [62]. Sven Oden (1919) postulated that HS is the light to dark brown substances of unknown materials, which are formed in nature by the decomposition of organic matter through the actions of microorganisms or in a laboratory by oxidizing chemical reagents. Alternatively, it was suggested that humus is the product of the condensation reaction between carbohydrates and amino acids in a microorganism-free environment [65]. It was also stated that the oxidation of phenol, quinone, and hydroquinone in an alkaline solution yields compounds similar to humic acids [66].

In 1936, Waksman proposed the "Lignin-protein theory" and stated that HS could be generated from the microbial attack of lignin [67]. According to this theory, the incomplete microbial attack of lignin molecules fragments lignin into smaller units and residues, which become part of the soil humus. In the degradation process, the methoxyl groups of lignin decompose into o-hydroxy phenols, and the oxidation of the aliphatic side chain converts into carboxylic acid groups. Moreover, Waksman reported that the presence of nitrogen compounds in the HS might result from the condensation of lignin with the microbial protein and other nitrogenous compounds. However, the final transformation of modified lignin residues to humic acids followed by fulvic acids was unclear in theory. Although the concept of Waksman's theory is controversial to many researchers, scientists agree with the theory that HS originates from plant residues and lignin-based materials. In 1982, Stevenson proposed the polyphenol theory of HS generation, as presented in Figure 2.1. According to this theory, lignocellulosic biomass decomposes into lignin, cellulose, and other non-lignin compounds (tannins, flavonoids,

carotenoids, etc.). The lignin is fragmented into phenolic aldehydes and acids by the action of soil microorganisms. Some parts of these phenolic compounds (mainly phenolic acids) may oxidize to carbon dioxide by different enzymes. Later, these phenolic and non-lignin compounds are attacked by soil microorganisms and transformed into polyphenols. By enzymatic oxidation, the polyphenols convert to quinones. Finally, condensation occurs between animal protein amino compounds/acids in soil and the quinones to transform into the natural HS in soil[55] .

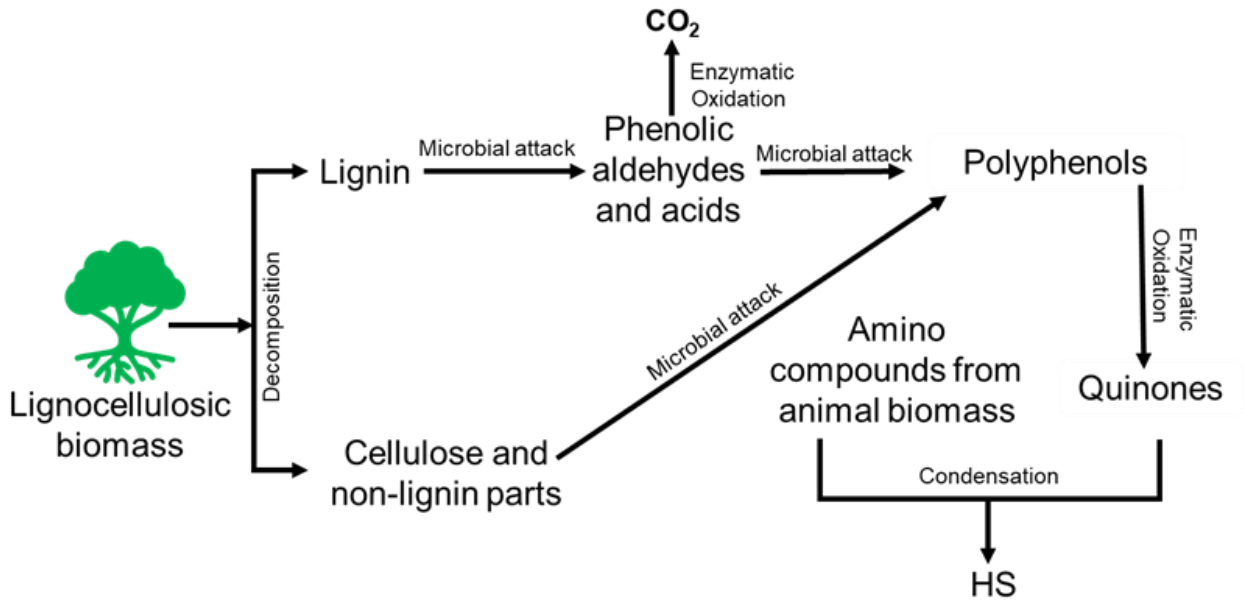

Figure 2.1: Polyphenol theory of HS formation from biomass proposed by Stevenson (1982); adapted and redrawn from [68]

In 1988, Flaig proposed a model reaction scheme for a natural humification process (Figure 2.2). According to the model, the lignin macromolecule would fragment into precursors (1). Through microbial action and demethylation, the lignin units and other phenolic compounds from non-lignin parts (2, 3) would convert to catechols (4, 5). Further aerobic or enzymatic oxidation of

those compounds would lead to quinone formation. Following condensation reactions, the amino acids from proteins and ammonia (degraded from protein by anaerobic digestion) would react with the quinones to transform into dark-brown HS polymers containing nitrogen [69]. It is also postulated that lignin's carbon and methoxyl contents would degrade, and other functional groups, such as hydroxyl, carbonyl, and a carboxylic acid, would increase due to oxidation reactions. It was reported that when oxidized under pressure, lignin is converted to humic acid-like compounds and finally to aromatic compounds containing acid groups [50, 59].

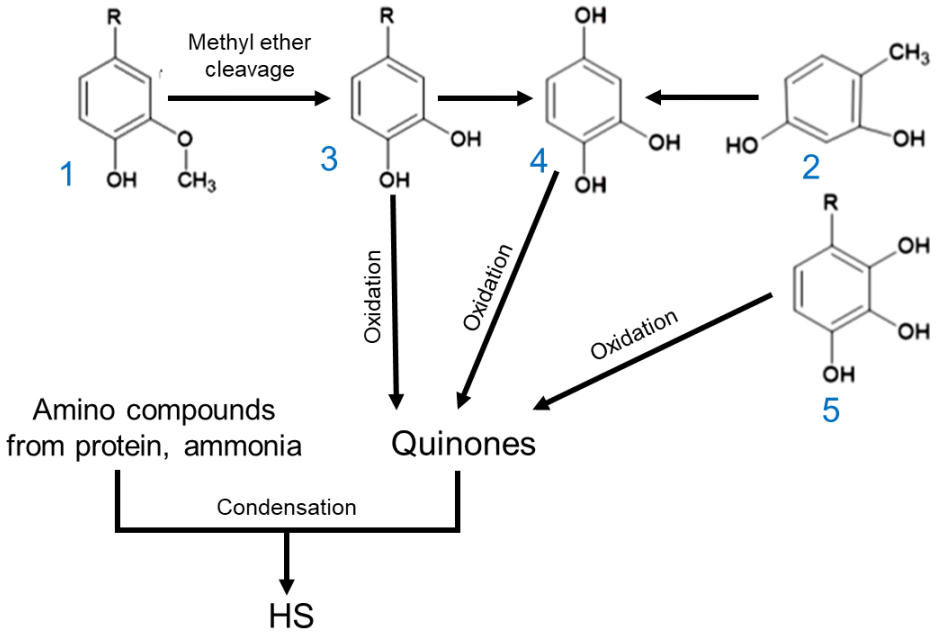

Figure 2.2: Reaction scheme for natural humification discovered by Flaig (1988); adapted and redrawn from[69] .

2.3. Properties of HS

The origin, location, and extraction methods are the main factors that are responsible for the different chemical properties of HS [70]. The main constituents of HS are humin, HA, and FA.

Figure 2.3 represents the tentative structures of HA and FA, while Table 2.1 describes the physicochemical properties of these compounds.

Humins are the insoluble fractions of HS, whereas HA and FA are the soluble fractions. The solubility of HA is pH-dependent (Table 2.1). When the HA are dispersed in alkaline solutions, deprotonation happens, and the anionic hydrophilic groups, such as carboxylate and phenolates dissociate in the solutions. On the other hand, in acidic media, due to protonation, HA precipitate [70, 71]. The FA have a smaller degree of polymerization, less organic carbon, more oxygen contents, and high acidity; consequently, their solubility is higher than HA [72].

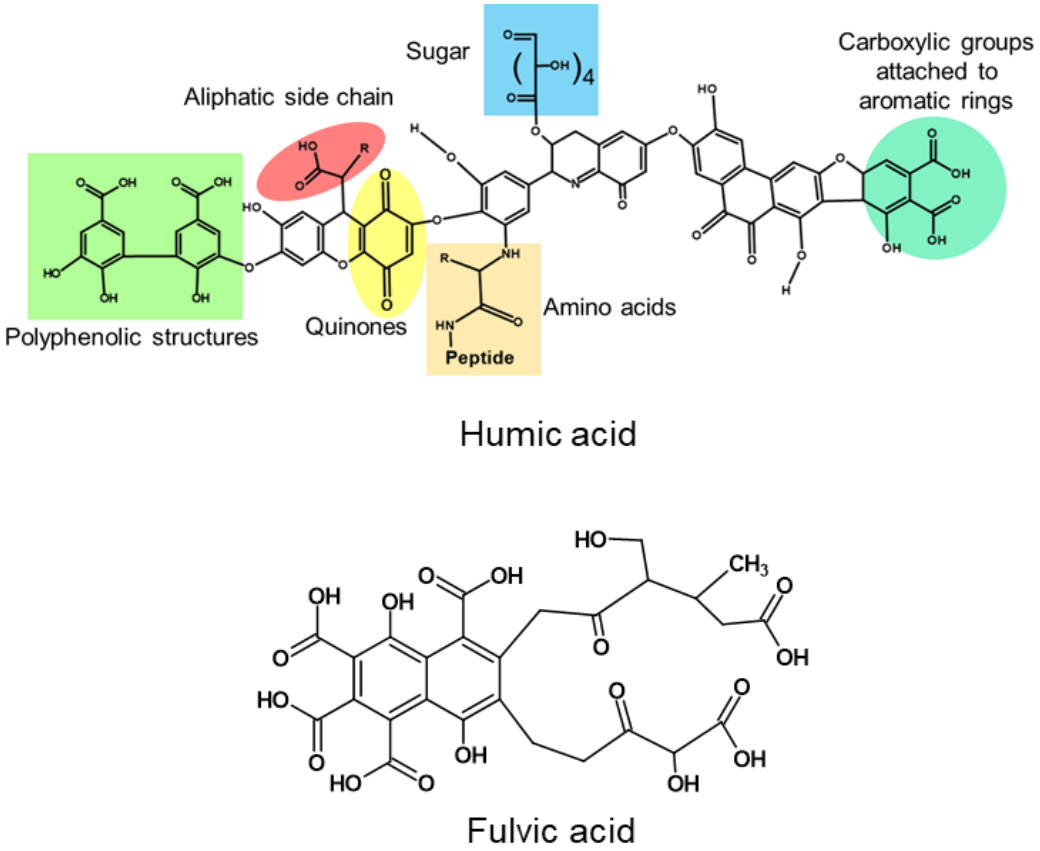

Figure 2.3: Chemical structures of Humic acid (HA) and fulvic acid (FA); adapted and redrawn from[68]

Depending on the source, HA have a wide range of functional groups, such as carboxylic, hydroxylic (both aliphatic and aromatic), quinones, amino acid groups, and carbohydrates [73]. Due to the significant amounts of carboxylic and phenolic OH, HA and FA show acidic behavior (Table 2.1). HA have comparatively higher molecular weights than FA (Table 2.1).

The carbon to nitrogen ratio (C/N) is one of the essential properties of HS. Due to microbial action, degradation, and condensation with the amino compounds in the soil, natural HS are enriched with nitrogen. Therefore, the nitrogen content is higher in HA and FA than in lignin (Table 2.1). Also, a smaller C/N is better for plant habitat applications, including agricultural land.

Table 2.1: Chemical properties of humin, HA, FA, and different types of lignin

Type of lignin	**Solubility**	**Carboxylic acid group, mmol/g**	**Phenolic OH, mmol/g**	**Aliphatic-OH, mmol/g**	**Molecular weight (Mw, g/mol)**	**C/N**	**Ref.**
Humin	Not soluble	3-4	2	NA	> 300000	NA	[70, 74-76]
HA	pH>2	2-5	2-6	1-4	2000-1000000	8-61	[70, 74-77]
FA	soluble	8-9	3-6	3-5	600-900	6.7-9.2	[70, 74-76]
Kraft lignin (KL)	pH>7	0.3	2.6	2.45	1000-15000	135	[51, 78, 79]
Lignosulphonate (LS)	soluble	0.1-0.53	1.5-2	1.9-4	1000-50000	240	[51, 79-81]
Organosolv lignin	pH>7	0.05-0.25	2.6-5.1	1.3	500-5000	203	[53, 79, 80, 82]
Soda lignin	pH>7	0.9-1	2.5-3.7	2.4	800-3000	68	[53, 79, 80, 83]

2.4. Humification of waste-biomass and non-lignin biomass materials

Table 2.2 describes recent developments on transformation of waste-biomass and non-lignin biomass materials into HS by hydrothermal (HT) and alkali pre-treatment [84-91]. A two-stage HT process (200 ºC) was developed and successfully generated 28.74 wt.% of HA from corn

stalks [84]. The study reported that transforming biomass to HA by HT depends on the pH of the solution. In the first stage of acidic-HT, the corn stalks generated precursors, such as carbohydrates, furans, phenols and different organic acids. Later, the alkaline-HT process converted those precursors into artificial HA. An earlier study also reported that under acidic conditions (pH 1 to 5), the carbohydrates (i.e., glucose or saccharides) convert to 5-hydroxymethyl-furfural-1-aldehyde (HMF) through dehydration[85]. A condensation reaction combines organic acids with the HMF to generate branched HS-like products (HA and FA) [85]. The pH effects on HT processes suggested that under acidic conditions insoluble HS (humins) formations are dominant while in alkaline-HT, soluble-HA forms and collected through acidification[91]. The yields of HS (HA or FA) in HT processes also depend on the reaction temperature. Earlier study reported that increasing temperature increased the HS formation. In this context, the HT treatment of broccoli stem conducted by Sui and the co-workers found that increasing temperature from 184 ºC to 220 ºC, increased the HA yield from 30.9 to 50.7 g/kg respectively[90]. Moreover, alkaline-HT processes towards the formation of HA depend on the strength of the alkali. The effects of different alkali such as, KOH and NH_4OH, were studied to observe the HA formation from cabbage leaves and reported that strong alkali increase HA yield due to higher delignification rate[88]. The main drawback of direct alkali-HT process (Table 2.4) is the lower yield (1.8-2.3 %) which might hinder the formation of HMF in high alkaline environment. Few studies reported neutral-HT treatment (water) of waste biomass (i.e., wheat straw, sugarcane exocarp and food wastes) and reported significant yield of HA (15-44 %)[87, 89, 92]. Due to the self-ionization at a high temperature, water can generate H^+ ions that hydrolyzes the macromolecules (i.e., cellulose, hemicellulose, lignin and protein) of biomass to their monomers (i.e., glucose, xylose, HMF, phenolic monomers, formic acid, lactic acids, amino

acids etc.) [87, 92]. Furthermore, under the acidic environment (generated organic acids) amino acids, phenolic compounds and the HMF derivatives may polymerize to form HS[92]. The HT process is carried at high operating temperature (Table 2.4) to generate the HMF which is considered one of the important precursors for the HS formation. In addition to those acidic and alkaline-HT, carbohydrates monomers (i.e., glucose, fructose) can be converted to HS through HMF formation in the presence of different ionic liquids such as 1-butyl-3-methylimidazolium chloride ([BMIM]Cl) with transitional metal salts as catalysts (i.e., $CrCl_3$)[93] at comparatively lower temperature. Xu et al reported the production of water-soluble humins (HA) can be achieved up to 56.6 % at 110 ºC [93]. Alkali treatment (8% KOH solution) of pre-fermented furfural (FR) residue can also be utilized for artificial humification followed by acidification to achieve a material with 49% HA[86]. However, the formation of humins from carbohydrates are considered undesirable by-products that reduce the yield of HMF[93]. In addition to the HT process of the waste-biomass, direct alkaline oxidation process could be an alternative way of transforming lignin materials into HS.

Table 2.2: Humification of biomass and non-lignin materials by alternative methods

Raw material	Chemical Processes	Conditions	Yield	Ref.
Corn stalk (0.5g)	Two-stage Hydrothermal	180 ºC, 4h, pH 1 180 ºC, 4h, pH 13	HA- 28.7%	[84]
Wheat straw	Hydrothermal	220 ºC, 4h	HA-30.2%	[89]
Broccoli stem (250 g)	Hydrothermal	204-220 ºC, 10min	HS-198 g/kg HA-50.7 g/kg FA-28 g/kg	[90]
Sugarcane exocarp	Hydrothermal	200 ºC, 1 h	HA-14.85%	[87]

Cabbage leaf	Alkali- Hydrothermal	KOH (25%), NH4OH (20%), 195 ºC, 4h	Not available	[88]
Glucose, saw dust, tulip tree leaves	Alkali-Hydrothermal	KOH	HA-1.8 %	[85]
Food wastes (rice, meat, cabbage, potatoes)	Hydrothermal	215 ºC, 1h	HA-43.5	[92]
Fermented Furfural	Alkali dissolution and acidification	KOH (8%) 70 ºC, 2.5 h	HA-49 %	[86]
Carbohydrates monomer (5g)	Hydrothermal	([BMIM]Cl (10g) $CrCl_3$ (0.74g) 110 ºC, 4h	HA-56.6 %	[93]

2.5. Lignin: types, properties, and applications

The plant biomass contains cellulose, hemicellulose, lignin, and a small number of extractives. Lignin is the most abundant natural aromatic compound. The functional groups of lignin include methoxyl, carbonyl, carboxyl, and hydroxy, linking to aromatic or aliphatic moieties in various amounts and proportions, which make lignin with different chemical structures [94, 95]. Up to 30% of the organic carbon on earth is sourced from lignin [96]. The typical lignin content of softwoods is 24–33%, hardwoods is 19–28%, and grasses is 15–25% [53, 97]. Various linkages in lignin molecules are shown in Figure 2.4. The three-dimensional heterogenous lignin structure is formed in plants by the radical polymerization of three aromatic precursors, such as p-coumaryl, coniferyl, and sinapyl alcohols [98]. During the biosynthesis of lignin in plants, these monolignols are radically coupled with each other to form different interunit linkages, such as β-O-4 (45–50%), 5–5 (18–25%), β-5 (9–12%), β-1 (7–10%), α-O-4, (6–8%) and β-β (0–3%) [99,

100]. Due to its high content of phenolic precursors, lignin could potentially be a renewable source for aromatic chemical production [101, 102].

The most widely produced technical lignins are kraft, lignosulphonates, soda, and organosolv lignin. Some chemical properties of different lignins are presented in Table 2.1. Kraft lignin (KL) is produced by the sulfate pulping process, which accounts for nearly 85-90% of the world's total lignin production and mostly, burnt on-site for steam generation [103, 104]. In this process, the wood biomass is delignified by an aqueous solution of sodium hydroxide and sodium sulfide at 140-170 ºC [51]. The recovered KL is not water-soluble but highly soluble in an alkaline solution (Table 1). Moreover, KL has the highest number of phenolic hydroxyl groups due to the extensive cleavage of β-aryl bonds. In addition, it has a significant amount of quinone, catechol, and carboxylic groups due to the delignification in the oxidative conditions [105]. The sulfite pulping process produces Lignosulphonates (LS), and the delignification is carried out at 120-180 ºC in the presence of alkali metal sulfites and sulfur dioxide [106]. LS contains many anionic functional groups (Table 2.1), such as carboxylic, sulphonate, and phenolic hydroxylic groups [107-109]. The unique functional and structural properties of lignosulphonates make them excellent raw materials as dispersants [110], binders [111], and adhesives [112], artificial HS [59], and cement additives [113, 114]. Due to a lack of economic viability, only 2% of lignin are utilized as a value-added product, such as vanillin. In contrast, the remainder is burned as a low-grade source of energy [115, 116]. Soda lignin (SL) is a by-product of pulping of mainly annual plants, like flax, straws, bagasse, etc. [117-119]. In this process, biomass is delignified by 13-16 wt.% of NaOH solution at 140-170 ºC [51]. Soda lignin is highly pure due to its production in a sulfur-free pulping process. The applications of the soda lignins are suggested in phenolic resins, animal nutrition, and dispersants in polymer synthesis [103,

120-122]. Organosolv lignin (OL) is isolated from the black liquor of organosolv pulping, where biomass is digested at temperature ranges of 100 and 190 °C with organic solvents, such as acetic acid, formic acid ethanol, etc. [51, 123]. This lignin contains minimal sulfur content rendering it chemically pure [124, 125]. The potential applications of OL were suggested in ink formulations, varnishes, and paints [108] due to their lower molecular weight (Table 2.1). Also, OL gained attraction towards the preparation of wood adhesives and fillers [126].

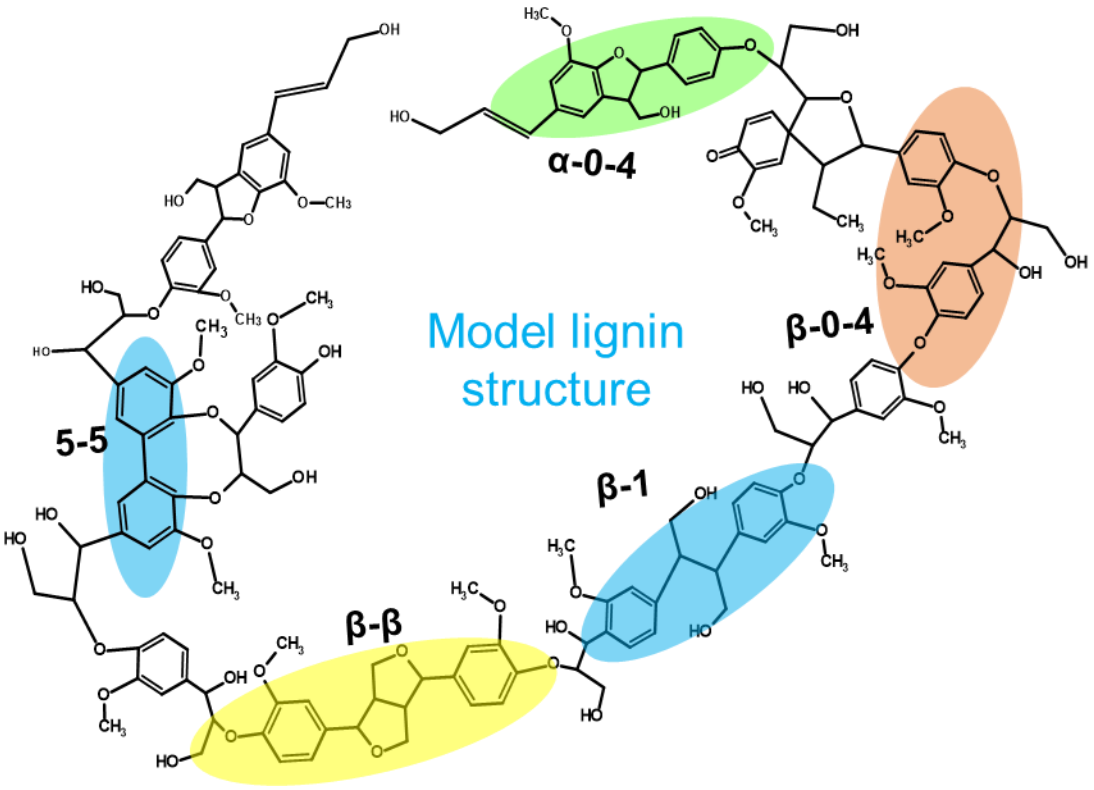

Figure 2.4: A model structure of lignin and common lignin linkages; Adapted and modified from [127]

2.6. Structural similarities between lignin and HS

Recent studies support the similarities between lignin and HS. Chemically, both lignin and humic acid have similar functional groups, such as carboxyl, phenolic/aliphatic hydroxyl, and methoxyl, and most importantly, the aromatic moieties [55, 128, 129]. In soil's organic matter, polyphenols and aromatic carboxylic acids are believed to be formed from lignin degradation and several microbial syntheses [130]. Oxidized lignin-derived phenyl propane has also been confirmed to be present in coal-based HS [131-133], suggesting that similar functional groups are shared between HS and lignins. Also, small aromatics identified by the pyrolysis of HS belong to lignin moieties [128, 134].

The oxidation (using CuO, $KMnO_4$, and H_2O_2 in an alkaline environment) products of humic and fulvic acids are similar to lignin aromatic moieties [135-137]. Yan et al. reported that 2-3 mmol/g of phenolic-OH groups are found in different sources of HAs [137]. It was also suggested that the degradation products of HS are similar to lignin-based phenolic compounds [54, 138]. Other studies showed that structural units and some typical inter-unit linkages were preserved during the transformation of lignin into HS [139, 140]. A recent study on composted grass lignin and humic acids showed that both materials have a similar range of phenolic-OH contents (1.2-1.5 mmol/g) [141]. This study reported different carboxylic acid groups of ~0.8 and 2.3-2.7 mmol/g in lignin and HAs, respectively. Also, the methoxy groups of lignin were found almost 5 times as much as that of HA. These results support the earlier theories regarding higher carboxylic acid groups and demethylation in HS than in lignin. Interestingly, the alkaline nitrobenzene oxidation of the grass lignin and HA provided similar phenolic compounds, such as vanillin, vanillic acid, syringyl and guaiacyl units etc., at varied amounts [141].

2.7. Natural sources, drawbacks of collecting HS and alternative solutions

Humification is a complex biochemical process. It was observed that the polyphenol structures of the HS originate from the plant's lignin [142], and the sources of some nitrogenous bonds may be due to the protein degradation of the microorganisms and the biomass from other dead animals. The characteristics of HS differ depending on the source and their extraction methods [131, 143]. Currently, the primary sources of HS are peat, leonardite, lignite, and river sediments, which are non-renewable sources [144]. Moreover, the excessive extraction of HS from natural sources may cause severe health hazards and ecological disturbance, including global warming, climate change, and land erosion in the long run, similar to coal mining [145]. It was reported that coal or lignite mining might release harmful organic substances that mix with surface water, and drinking those water may cause severe kidney failure [145]. In addition, collecting HS from the river sediments would remove the under-water microorganisms, which can directly hinder the aquatic ecosystem. The helpful microorganisms facilitate the decomposition of dead biomass to adjust the ecological balance. Considering the drawbacks of natural HS resources, it is necessary to consider alternative ways for preparing HS from renewable sources, like lignin. As discussed, a considerable number of HS are directly linked to biomass conversion (mostly lignins), and the artificial humification process can open windows of opportunities for utilizing lignin. However, the humification of technical lignins is yet to commercialize because of the complexity of the lignin structure. There are two major methods for converting technical lignins to HS: direct oxidation [58, 59] and oxidative ammonolysis (OA) [60, 142].

2.8. Humification of technical lignin by direct oxidation

Due to active hydroxyl groups, lignin acts as an excellent raw material for oxidative cracking and the production of various aromatic fine chemicals, including organic acids, aldehydes, and hydrophilic anionic lignin [37, 146-148]. The oxidation of lignin involves the depolymerization and fragmentation of the aryl ether bonds and other linkages [146]. Alkaline wet oxidation of lignin requires a high temperature (125-320 °C) and pressure (up to 2 MPa) in the presence of air or molecular oxygen [149]. Moreover, the post-treatment to separate the chemicals from the mixture is not economically feasible. According to the recent approaches, the direct oxidation of technical lignin towards transformation into HS-like materials can be categorized mainly in three ways, such as alkaline aerobic oxidation (AAO) of technical lignin, alkaline oxidative digestion (AOD) of lignocellulosic biomass by hydrogen peroxide, and Fenton reagent-based oxidation of lignin by hydrogen peroxide. Table 2.3 summarizes the different approaches of lignin and biomass oxidation toward artificial humification.

2.8.1. Alkaline aerobic oxidation (AAO) of lignin

Figure 2.5 demonstrates the schematic flow diagram for producing artificial lignohumate (ALH) from technical lignin by AAO [59, 147]. In this process, lignin is dissolved in alkaline solutions, such as KOH or NaOH (as a catalyst), to activate the phenolic-OH groups of lignin and later is oxidized by air/oxygen or hydrogen peroxide. After the reaction, the product can be used directly, either in liquid or solid form. However, the AAO generated by NaOH treatment may need to be purified by dialysis as Na^+ may increase salinity and inhibit plant growth when applied as a fertilizer [147].

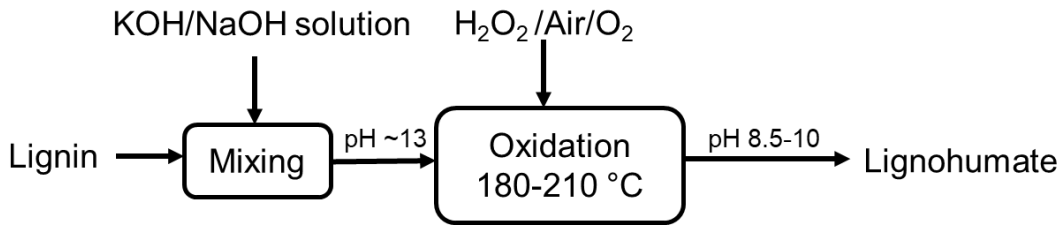

Figure 2.5: A schematic flow diagram of alkaline aerobic oxidation for lignohumate production from lignin

Figure 6 represents the simplified mechanism of AAO of lignin towards forming HA-like materials. Initially, lignin's free phenolic hydroxyl groups are ionized to produce phenolates in an alkaline environment. Then, O^{2-} reacts with phenolate and forms phenoxyl radicals, i.e., the first oxidation product. The superoxide radical anion (O^{2}•-) attacks in the meta position and breaks the methoxy groups of lignin to convert into quinones [147, 150]. Further oxidation leads to aromatic ring cleavage and the formation of dicarboxylic acid (or any orthoquinone compounds) [150, 151]. Route B in Figure 2.6 represents the undesirable coupling of phenolate ions to form biphenyl compounds, which leads to the repolymerization of lignin.

Naturally, the HS are enriched with organic acid groups. Therefore, the fundamental target of alkaline aerobic oxidation is to convert the phenolic and aliphatic hydroxyl groups of lignin into carboxylic groups [50]. Significant structural changes are observed during this oxidation, such as decreasing methoxyl, aliphatic, and phenolic hydroxyl groups while increasing aliphatic and aromatic acid groups [147]. These anionic groups increase the hydrophilicity of the oxidized lignin materials and play a significant role in mineral transportation toward the roots [147]. In one study, lignosulphonate was oxidized with hydrogen peroxide in an aerobic system, which increased the mass shares of HA up to 77% [59]. It was reported that similar to naturally

occurring HS, the oxidized KL and LS showed positive physiological effects on plant growth, such as increased length, dry weights, carbohydrate/sugar synthesis in the plants, and chlorophyll contents on the leaves [147, 152]. However, the AAO of lignin generates a wide range of phenolic monomers and derivatives, which not only improve the aforementioned physiological effects but also stimulate hormonal activities, such as auxin (IAA) and Gibberellin (GA) [152-155]. However, depending on the structural conformation and concentrations, some phenolic acids may show inhibitory effects on plant growth and other bioactivities [156-158].

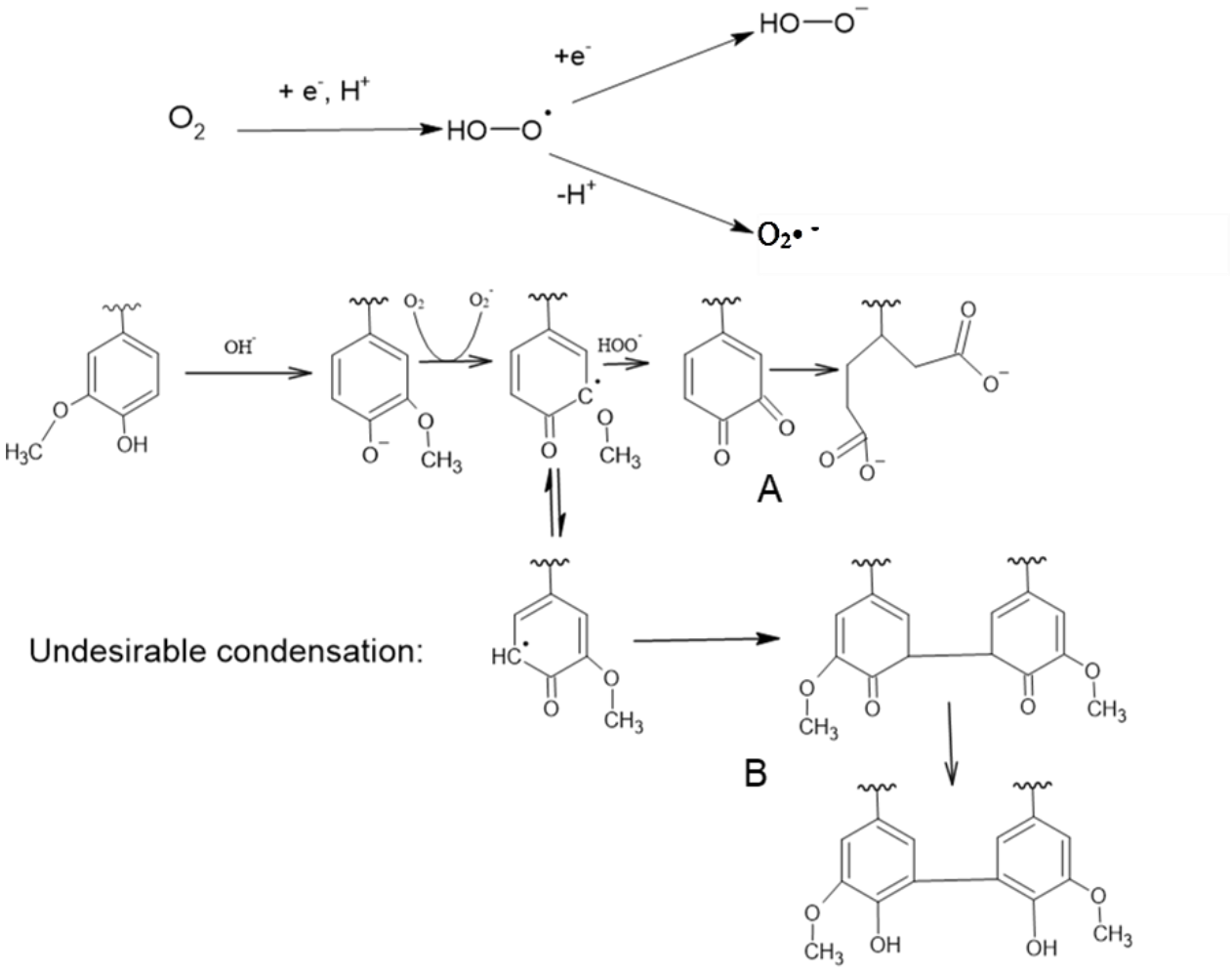

Figure 2.6: Reaction pathways for the alkaline aerobic oxidation of lignin adapted from [147, 151, 159, 160]. Route A: degradation (simplification). Route B: Undesired coupling)

Table 2.3: Different oxidation approaches for lignin and biomass conversion for HS-like lignin material productions.

Raw materials	**Chemical/reagents used**	**Temperature (°C), time (min)**	**Carboxylic groups, mmol/g**	**Mw, g/mol**	**Application Remarks**	**Ref.**
LS	NaOH, H_2O_2 /air	170-190, 180	NA	NA	Transformed LS to HA (77 wt.% yield)	[59]
LS	KOH, air/O_2	NA	NA	NA	Increased corn root dry weight and chlorophyll by 18% and 45%, respectively at 1 mgC/L dose	[58]
KL	KOH, O_2	195, 30	2.6	3500-4000	Increased fresh corn plant length, dry weight, and chlorophyll content by 27, 92 and 32 %, respectively at 10 mgC/L dose	[147]
KL	$FeSO_4$, H_2O_2	RT, 120	NA	NA	Increased seeds germinations and two folds of chlorophyll contents in leaves at 860 ppm dose	[133]
Giant reed	KOH/H_20_2	50, ON	NA	NA	Enhanced tomato seed germination and early hypocotyl growth by 10% at 10 ppm	[161]
Giant reed and Macanthus	KOH, H_20_2	50, ON	1.02		Enhanced germination of maize seeds and root elongation increased by 50% at 10 ppm dose	[158]

Cardoon, Eucalyptus, and black poplar woods	NaOH, H_20_2	50, ON	0.4-1.4	NA	Increased maize seedling growth by 72% at 10 ppm dose	[162]

*NA=Not Available; RT=Room Temperature; ON= Overnight.

2.8.2. Alkaline oxidative digestion (AOD) of biomass

In another pathway, lignocellulosic biomass was modified to water-soluble lignin via an alkaline oxidation digestion procedure for producing HS-like materials [161-163]. A schematic flow diagram of this process is presented in Figure 2.7. In this system, biomass is allowed to digest in an alkaline (KOH/NaOH) oxidative environment in the presence of an oxidant, e.g., hydrogen peroxide. After the digestion, the insoluble cellulosic fibers are removed by filtration, and the filtrate is acidified to separate hemicelluloses/sugars from lignin. After that, the separated lignin is suspended in water and neutralized to get water-soluble fractions, which are considered lignohumate. The oxidative reaction mechanism on lignin should follow a similar path as alkaline aerobic oxidation.

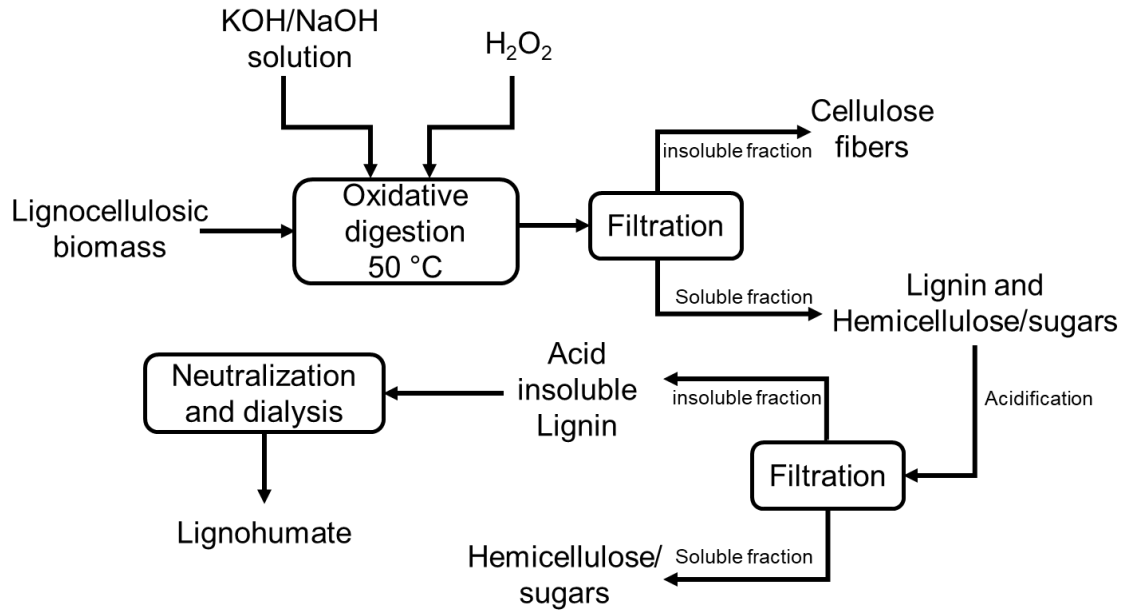

Figure 2.7: A schematic flow diagram of alkaline oxidative digestion for lignohumate production from lignin

Transforming biomass through the AOD process has a few advantages, such as direct use of biomass for conversion, low operating temperature (50 ºC, overnight), and obtaining cellulose fibers as by-products. Moreover, monomeric toxic phenolic compounds (also known as phytotoxic chemicals) free HS can be achieved due to the acidification step (Figure 2.7). The carboxylic acid groups can be achieved up to 1.4 mmol/g [158, 161, 162]. The bioactivity of the extracted lignin towards any plant depends on the hydrophilicity of lignin samples. Several studies on the oxidative digestion of biomass showed that non-wood water-soluble lignin (i.e., isolated from giant reed, miscanthus, cardoon, etc.) had higher hydrophilicity and bio-stimulating performance on plant growth [158, 161, 162]. On the other hand, oxidized eucalyptus lignin was

the least effective for plant stimulations following this oxidation method, which may be attributed to their poor hydrophilicity due to less hydroxylated long aliphatic chain, which inhibited the release of bioactive molecules to the aqueous environment [162].

2.8.3. Fenton reagent-based oxidation of lignin

A new method was developed for the oxidation of lignin, e.g., kraft lignin, by hydrogen peroxide in the presence of a Fenton reagent catalyst at room temperature [133]. Figure 2.8 represents the schematic flow diagram of this method. In this process, lignin is mixed with a hydrogen peroxide solution. After the mixing, the solution is oxidized at room temperature in the presence of iron (ii) sulfate heptahydrate. After the oxidation reaction, the solution is centrifuged and washed several times with deionized water to remove any unreacted chemicals and some toxic phenolic compounds. The solid residue (oxidized lignin) is lyophilized for further application as lignohumate.

The Fenton reagent-based lignin depolymerization is considered a nonspecific oxidation process. The Fenton reactions would allow lignin particles to mimic commercial HA because of the presence of the oxidized iron-based inorganics deposited on the lignin-based products. The primary goal of this oxidation is to increase the O/C ratio, which would indicate the formation of oxygenated functional groups, such as quinones, carbonyl, and carboxylic acid groups in the oxidized lignin. The outcomes of this process mainly depend on the organic structures of lignin and the ratio of hydrogen peroxide and iron (ii) sulfate [133, 164]. However, the Fenton-induced oxidation may generate some phytotoxic phenolic compounds [165]. Therefore, a post-separation of the soluble fractions (containing phenolics) is recommended to obtain a purified product.

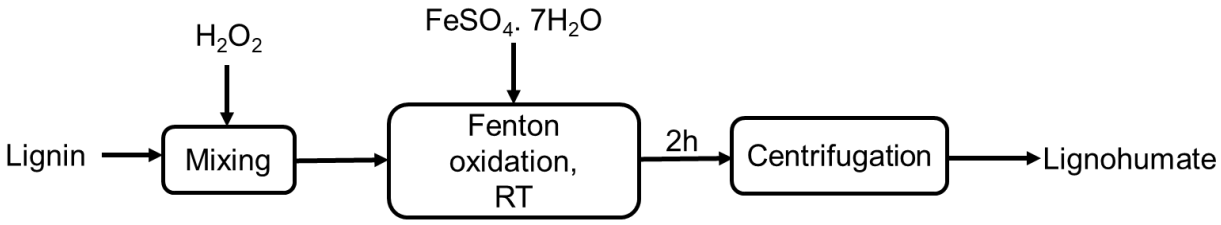

Figure 2.8: A schematic flow diagram of Fenton reagent-based oxidation for lignohumate production form lignin; RT- Room temperature.

2.8.4. Humification of lignin by oxidative ammonolysis (OA)

The artificial humification can be carried out by the OA process of lignin, which can incorporate a considerable amount of nitrogen in the humified lignin in different forms. Generally, soil's organic matter, such as HS, must have nitrogen for efficient biodegradation affinity. Research showed that a C/N ratio under 20 facilitates biological degradation [60], whereas a higher value than 25 can hinder the degradation process. Natural humification could be conducted artificially by reacting technical lignin with ammonium hydroxide/ammonia solution, increasing the C/N ratio and crop productivity [142].

Figure 2.9 demonstrates the preparation of nitrogen-enriched lignohumates (N-ALH) following the oxidative ammonolysis (OA) process [56, 57, 166]. In this method, lignin is suspended in different concentrations of NH_4OH solution. The reaction is carried out in the temperature ranges of 130-150 ºC and treated with or without any oxidants (air/oxygen). The water-soluble and insoluble parts are separated after the reaction and can be utilized as different grades of fertilizers [167]. The reaction mechanism of the OA system is shown in Figure 2.10. It is seen that lignin

fragmentation occurs at the aliphatic side chain during the OA process resulting in the cleavage of β-O-4 linkages [142]. The aromatic part of the lignin provides substituted acid derivatives, such as amide and nitrile compounds. Due to the oxidizing environment, some aromatic rings of lignin are degraded to convert into aliphatic dicarboxylic acids through quinone formations. Later, these aliphatic acids may react with available ammonium ions to form their salts. In addition, as the OA is carried out at a fairly high temperature and pressure, the produced CO_2 can react with the unreacted ammonia gas to produce urea as the final product [142].

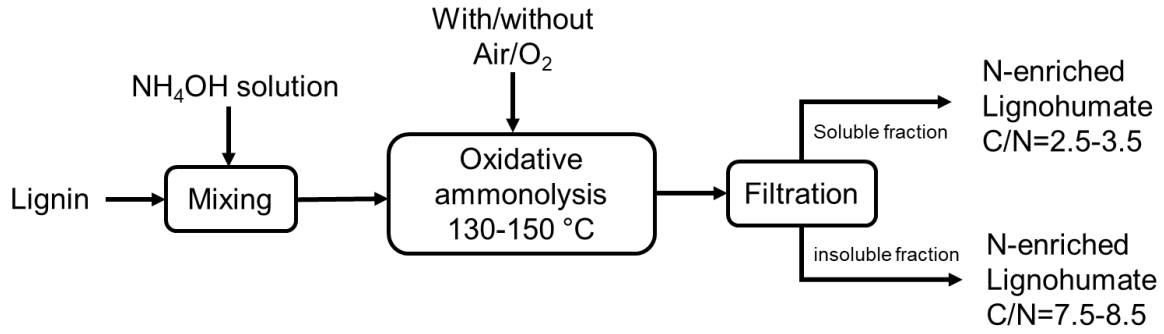

Figure 2.9: A schematic flow diagram of oxidative ammonolysis for N-enriched lignohumate production from lignin.

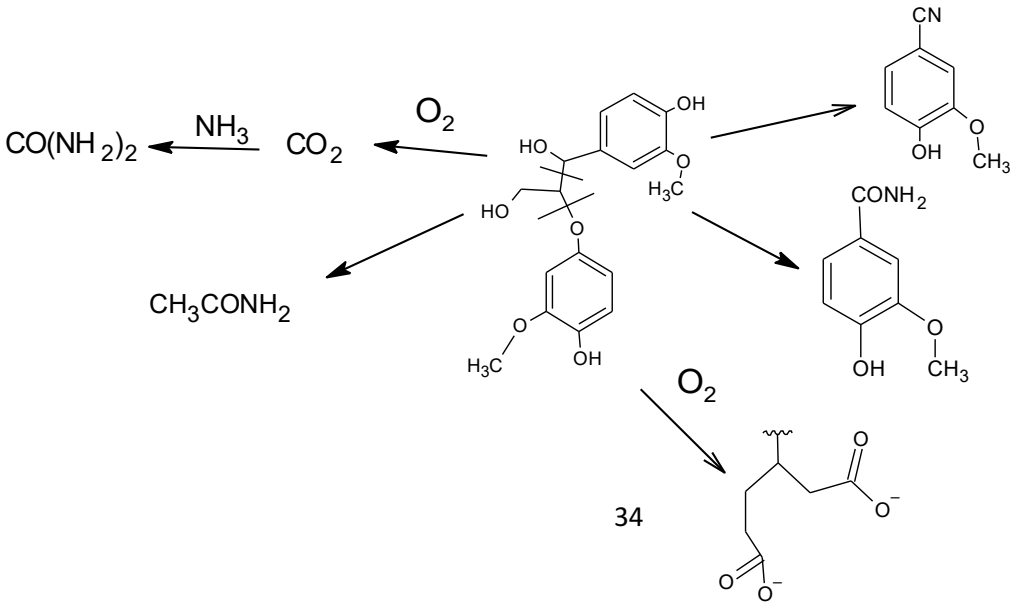

Figure 2.10: Model reaction scheme for the oxidative ammonolysis of lignin; adapted and redrawn from [142]

Different approaches to lignin modification by OA are listed in Table 2.4. The primary target of the OA process is to incorporate nitrogen into lignin molecules in the form of ammonium salts, amides, and urea-type structures, but not amines or heterocyclic [56, 168]. The transformation of KL, LS and OL into N-enriched fertilizers via the OA was exploited in the past [56, 57, 167, 169]. KL showed a higher reactivity towards OA among all lignin due to abundant phenolic hydroxyl groups [167]. Some studies investigated the effect of the reaction parameters on nitrogen incorporation in lignin [56, 57, 169]. It was observed that lignin's methoxyl and carbon content would decrease with nitrogen incorporation during the OA reaction [57, 167]. Interestingly, an increase in the reaction solution's pH increased the lignin oxidation rate and consequently increased its nitrogen incorporation [169]. It was stated that when increasing the concentration of ammonium hydroxide from 0.4 to 1.6 M, the lignin solubility in the reaction mixture increased to almost 75% thus enhancing the reactivity towards OA and increasing the nitrogen incorporation [56, 169]. Also, the rate-determining step of the OA reaction is the oxidative cleavage of the non-phenolic moieties and the oxidation of aromatic rings because the rate of nitrogen incorporation is directly related to these steps and directly proportional to oxygen pressure [56].

The fertilizing effects of these N-ALH were also studied earlier. In one study, up to 14% nitrogen was incorporated into the lignin and used as fertilizer in the pot-experiments [167]. The earlier studies on the OA process showed that the C/N ratio could be decreased to 3-7 (Table 1 and Table 3). Meier et al. Studied the effects of N-lignin (modified by OA, C/N 4-7) on Sorghum

plants at the dose rate of 1385 kg/ha (180 kg/ha of nitrogen content), and the results showed a crop yield increase of 82%. Another study showed that applying artificial lignohumates (N-enriched, total N content 10-24%) on different woody plants increased the green mass of the plants by more than 50% and decreased the nitrogen leaching by nearly 75% compared to commercial urea [142]. Therefore, transforming technical lignin into nitrogen fertilizer through the OA could be a promising route in the agricultural field due to the available organic carbon and nitrogen. In addition, the N-lignin's oxygenated part (i.e., carboxylic ends) would participate in mineral transportation.

Table 2.4: Different approaches for the modification of lignins by OA towards N-ALH.

Raw materials	**Chemicals/reagents**	**Temperature (^{o}C), time (min)**	**C/N**	**Application remarks**	**Ref.**
KL, LS, OL	NH_4OH, O_2	150, 120	4-7	Increased Sorghum productivity by 3 times	[167]
OL	NH_4OH, O_2	130, 15-1455	3-5	Increased 63% nitrogen incorporation	[56, 57]
OL	NH_4OH, O_2	100, 15-180	NA	Increased 67% nitrogen incorporation at pH 11.	[169]

2.9. Potential applications of humified lignin

2.9.1. Soil treatment

Although natural HS are used mainly as soil conditioners, there are other potential applications for HS in soil. HS helps to segregate the compactness of soil structures, reduces water evaporation from the soil surface, and has a role in transporting micronutrients from soil to plants [170]. Artificial humified lignin derivatives may have these unique properties too. The ALH with similar physicochemical properties will be an excellent alternative as a soil stimulator [58, 147,

161, 162, 170]. As controlled alkaline oxidation of lignin results in increased aromatic/aliphatic-OH and carboxylic-OH contents (Table 2.3) in the products, they should function similarly to natural HS [59, 147]. In this context, ALH may have potential applications for soil loosening, decreasing the bound water evaporation rate, and transporting essential nutrients to plants.

Figure 2.11 demonstrates a model mechanism of ALH in soil. Route A describes that the carboxylic and hydroxyl groups of ALH will dissociate into their ions, and the hydrophilic ends will exhibit the chelating behavior. The anionic hydrophilic ends will form unstable complexes with the essential minerals available in the soil, such as Na^{+}, K^{+}, Ca^{2+}, M^{2+}, Fe^{2+}, and Fe^{3+}, by electrostatic attraction [171]. It was reported that the mineral transportation by natural HS would occur differently by low molecular weight (LMW, <3500 g/mol) and high molecular weight (HMW, >3500 g/mol) fractions[172]. The HMW fractions (HA) of HS stimulate the root plasma membrane, enzyme activity and increase plant growth while LMW fractions (FA) are directly co-transferred into the plant's roots [172-174]. In addition, the LMW fractions were greatly responsible for NO_3^- uptake and nitrogen metabolism[175, 176]. The LMW fractions of HS have better mineral binding capacity than HMW, resulting improved nutrient absorption by roots which is due to the relative abundances of oxygenated functional groups (carboxylic and phenolic-OH groups)[172, 177, 178]. Nardi and co-authors reported that the LMW fractions stimulate hormonal activity (i.e., auxin, gibberellin and cytokinin), however, the HMW fractions controlled the availability and activity of LMW on plant metabolism[175]. Therefore, the ALH that are obtained from AAO can be fractionated as LMW fractions and HMW fractions for specific applications.

Route B demonstrates the dispersion ability of ALH on the soil. Generally, ideal soil contains 45, 5, 25% of minerals, organic matter, and air, respectively; and the rest is water [179]. If the soil

minerals increase to 69%, it will decrease the organic matter and air to 1 and 5%, respectively, resulting in a compact soil structure [179]. As a result, water penetration into the soil would be hampered. Therefore, the dissociated minerals (positive and negative mineral ions) would attract each other to form salts. In this case, when ALH are used, the organic content would be increased, which would help to interact with the positive mineral ions and possibly adsorb them due to the presence of strong anionic hydrophilic groups. In this way, ALH would restore the negative ions into the soil. Moreover, the ALH would create electrostatic repulsion due to the anionic hydrophilic ends, and phenolic ends would enhance the steric hindrance to disperse the soil particles resulting in untied soil [180]. The ALH derived from AAO should have more negative charge density due to having higher carboxylic acid groups (Table 2.3) than ALH from AOD. Therefore, AAO-derived ALH should exhibit higher dispersibility in soil.

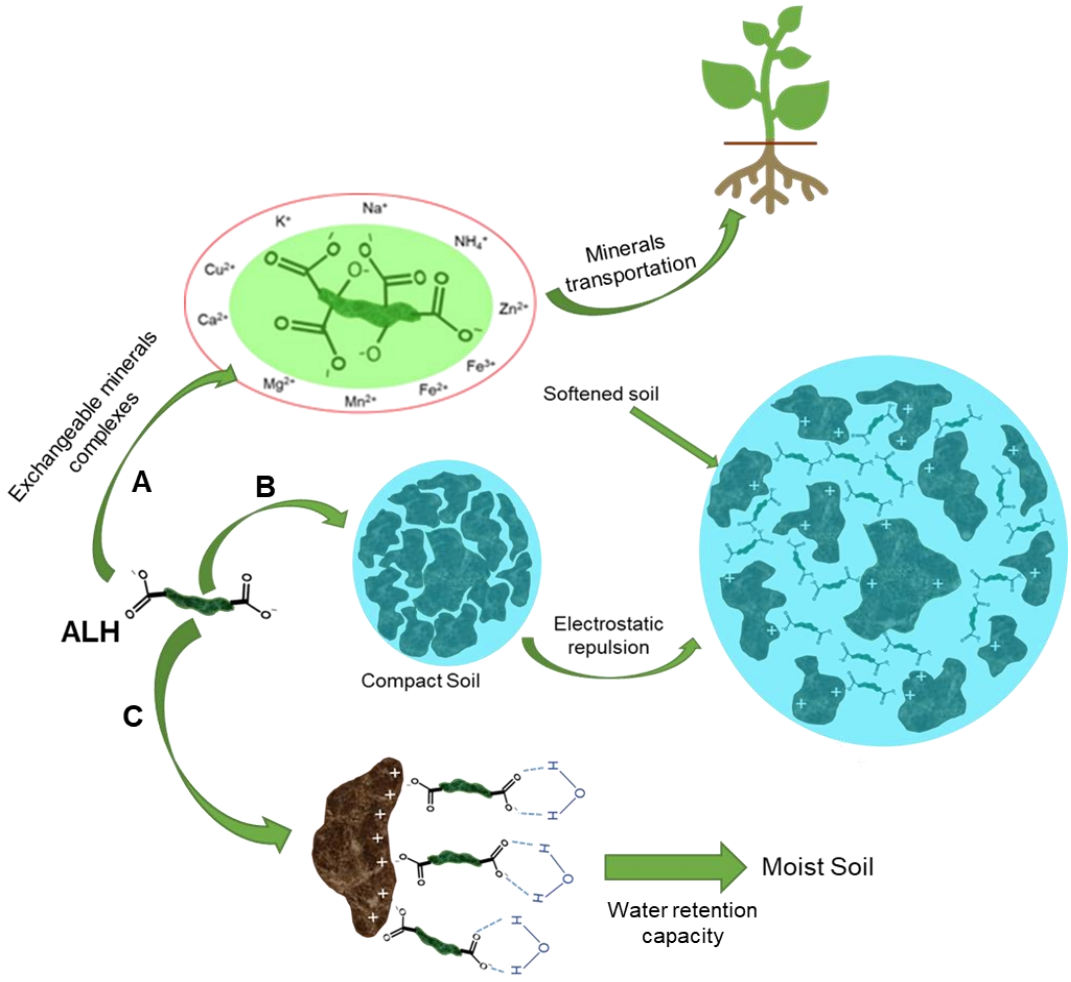

Figure 2.11: A schematic representation of mineral transportation, soil conditioning, and water retention capabilities of ALH; adapted and modified from[171, 181].

Route C represents the water retention capacity of ALH. Due to the hydrophilic anionic functional groups (i.e., carboxylic groups) (Table 2.3), the ALH would be adsorbed by the positively charged minerals in the soil, and the other ends would hold the water molecules because of the electrical attraction [181, 182]. Therefore, the ALH derived from AAO and AOD would be suitable for increasing the soil's water retention capacity.

On the other hand, the N-ALH derived from the OA process may be appropriate as a fertilizer since it contains a lower C/N ratio (Table 3). The direct application of N-ALH has been studied

for crop productivity and slow-release fertilizing ability [142, 167]. However, other effects on soil, such as mineral transportation, soil texture, and water retention capacity, were not yet studied for the N-ALH.

2.9.2. Medicinal application

Due to their antiviral [183, 184], anticarcinogenic [185], antibacterial, antioxidant, anti-inflammatory, and antiseptic properties [170, 186], the medicinal usages of HS have been practiced for centuries [170]. The antioxidant properties of lignin-derived materials have also been reported due to the availability of phenolic and acidic (aliphatic and aromatic) groups, which have chelating and radical-scavenging properties [32, 187]. On the other hand, low molecular weight (i.e., 1500 g/mol) fractions of HS show inhibiting effects against HIV-1 in vitro [170]. The anticarcinogenic properties of FA fractions were also reported earlier [188]. In addition, an earlier study reported that the oral consumption of HA by domestic animals could reduce the cholesterol, lipids, and glucose content and increase the red blood cells and hemoglobin in the animal bodies [189]. One recent study also reported the potential antiviral effects of natural HS against the recent COVID-19 virus [190].

In this context, the smaller molecular weight fractions of the ALH that are generated from the direct alkaline oxidation (both AAO and AOD) of lignin products (i.e., mostly oligomeric phenolic derivatives) can be utilized for medicinal applications. As stated above, the ALH is capable of complexation with metals, such as iron, due to the abundant of phenolic and carboxylic acid groups [133]. Similar to FA, ALH can be a novel compound to improve the rate of iron adsorption in blood and increase the number of red blood cells [170]. Antioxidant medications reduce the risk of several diseases caused by oxidative stress, typically brought on

by free radicals like reactive oxygen species (ROS), such as superoxide anion, hydroxyl free radical, hydrogen peroxide, etc. [191]. ALH can be a potential substance as an antioxidant by neutralizing these ROS due to their heterogeneous aromatic compositions (i.e., phenolics and quinones) and supramolecular structure [32, 187, 191]. The reactive phenolic moieties of oxidized lignin might cause bacterial and microbial cell death [191]. Moreover, the acidic functional groups (aliphatic or aromatic) of the ALH would reduce the cell binding of different viruses (i.e., HIV) [192]. Although the chemical properties between natural HA and AAO/AOD-derived ALH are comparable, extensive studies are needed to examine the medicinal effects the ALH materials. Finally, for medical applications, the post-purification of the ALH is highly recommended for removing the excess alkali and other toxic chemicals (i.e., phenol) generated from the reactions [193].

2.9.3. Wastewater treatment

Wastewater treatment by HA has been studied extensively [194-198]. Similar to its action in soil, it can develop complexes with heavy metal ions in solution systems, reducing the toxicity of drinking water, industrial wastewater, and surface water. The mechanisms of HS for wastewater treatment depend on factors such as the nature of the HS (particularly the fulvic and humic acid content), soil chemistry, and water's chemical properties, such as acidic or alkaline. Like HS, ALH can be an alternative product to remove these heavy metals and other suspended particles, such as oil, grease, and certain organic compounds from water. The long lipophilic aliphatic chain and hydrophilic ends should have excellent surfactant properties that help remove oil and greases [199, 200]. The anionic characteristics of the carboxylic acid groups on ALH should demonstrate their high cationic exchange capacity, enhancing the formation of insoluble

complexes with the polyvalent metal cations. The complexation with heavy metals such as lead (Pb), copper (Cu), cadmium (Cd), nickel (Ni), cobalt (Co) zinc (Zn), iron (Fe), aluminum (Al) with the ALH is possible if the ALH has a desired carboxylic content. The metal complexation is highly pH (pH 4-8) dependent and forms strong chelates with the metal ions having oxidation states of +2 [201]. In addition, a high molecular weight (14,000-33,700 g/mol) ALH would be more effective for wastewater treatment [202, 203]. Although the current approaches (i.e., aerobic oxidations) of transforming lignin to ALH attain sufficient anionic functional groups, the molecular weights are significantly reduced (Table 2.3), making them less effective for heavy metal removal applications. However, extensive research on new method development is necessary for the scope in wastewater treatment by ALH.

2.10. Challenges and future directions of lignin modification towards humification

Generally, the main drawback of lignin valorizations is claimed to be its complex heterogeneous aromatic structures, while it is a blessing in terms of its transformation towards humification. In the direct oxidative process of lignin, a high temperature (170-195 ºC) is required to break down the lignin skeleton and reduce the molecular weight of lignin significantly, which may limit the application of the produced materials. This is attributed to the high molecular weights fraction of HS are known to have higher performance for heavy metal removal and soil softening (dispersibility) [204]. Therefore, a milder reaction condition maintaining the lignin structure more intact would be preferred to help protect the linkages and oxidize the lignin structure selectively.

It was reported that the oxidation of lignin would produce phenolic monomers, such as protocatechuic acid, hydroxybenzoic acid, and p-coumaric acid. Those phenolic compounds are known as potential allelopathic agents (phytotoxic chemicals) and inhibit plant growth [152, 157, 205-208]. The negative effects of those phenolic compounds depend on not only their used concentrations but also their chemical structure and specific plant species[156, 209] . The direct oxidation methods of lignin for humification may require a separation process to remove the phytotoxic compounds (Figures 2.7 and 2.8), which may be costly. Therefore, introducing new selective oxidizing catalysts or technological advances in the oxidation process may be required to reduce the production cost of such chemicals in converting lignin to HS.

Nonetheless, naturally occurring HS are enriched in carbon and nitrogen [142, 210]. Few studies claim that natural sources of HS, such as lignite, i.e., one of the major coal sources for commercial HA, contains significant amounts of iron in polyphenol−Fe complexes [211-214]. A past study revealed that HS and lignin-derived HS have similar levels of carbon [147]. However, none of the other plant essential nutrients (K, Fe, Ca, N, P, etc.) are present in ALH, which is one of the main limitations of using artificial HS as organic fertilizers and soil stimulators. Incorporating inorganic minerals into ALH is another critical stage to transforming lignin into HS-like materials. Natural HS are found in complexes with different transitional metals, like Fe [215]. Learning from this, Fenton-based single-staged oxidation under mild conditions can be an example of converting lignin into artificial HS with Fe-complexes. In this context, Jeong et al. reported that a Fenton-based one-pot advanced oxidation was employed to mimic fungus-driven lignin humification and incorporate iron into the oxidized lignin samples [133]. In addition, Fenton reagent-based alkaline (KOH) oxidation can be performed to enhance the lignin reactivity and conversion to the HS-derived product.

Currently, there are some challenges with lignin reactivity in the OA processes. Meier et al. reported that lignosulphonates and kraft lignin showed higher reactivity than any other lignins for OA, while the ASAM (Alkaline Sulfite Anthraquinone and Methanol) lignin was not suitable for this process due to its high degree of sulfonation, low molecular weight, and high ash content. Moreover, current approaches of OA were carried out with NH_4OH along with an oxidant, such as air/oxygen [167]. Due to their available nitrogen, OA-modified lignins are generally limited to fertilizing applications. In addition to NH_4OH, KOH and other alkalis can be used to improve the lignin dissolution and enhance lignin's oxidation reaction [59]. In this way, the modified lignin would be enriched with nitrogen in different forms, and KOH would facilitate the formation of carboxylic acid groups [147], which could make new routes for producing HS-like lignin. Moreover, the global HA market is expanding day by day, mainly in the agricultural sector. It was reported that the market value of HA in the agricultural field was around USD 365 million, and it is projected to reach up to USD 934 million by 2030 [216]. Currently, the production of HA mainly depend on natural sources (i.e., coal, peat, lignite river sediments, etc.), which is neither a sustainable process nor environment friendly. Therefore, the chemical transformation of lignin materials towards artificial humification can be a potential route considering the current HA's renewability, sustainability, and environmental concerns.

2.11. Conclusion

Naturally produced HS contains insoluble humin, alkali-soluble HA, and water-soluble FA fractions. HA has been widely used as a soil conditioner due to its wide range of oxygenated functional groups, such as phenolic hydroxyl, quinones, and carboxylic acid. Past research showed that those functional groups might have originated from lignin decomposition in HA in

nature. As several physicochemical properties, such as solubility, phenolic hydroxyl, and carboxylic acid groups, of lignin and HA are similar, the chemical transformation of lignin to HS is possible. The most popular method to transform lignin/lignocellulosic biomass into HS is alkaline oxidation (AAO and AOD). These processes' primary goal is to increase the lignin materials' hydrophilicity by converting aliphatic/phenolic hydroxyl groups to carboxylic acid groups. On the other hand, OA aims to incorporate nitrogen into the main lignin structure in different forms, such as ammonium ion, amide, and nitrile. Although the AAO can be readily applied for lignin conversion, the costs associated with the post-purification of the product for eliminating phytotoxic chemicals generated during the oxidation process are challenging. Finally, to meet the demand for generating high-quality lignin-derived HS for applications in soil, wastewater treatment, and medicine, more research is needed to mitigate the challenges of incorporating other inorganic mineral nutrients (i.e., K, Fe, N, etc.) into lignin-based HS, and the post-purification of lignin-derived HS for eliminating toxic chemicals while maintaining desired characteristics, such as molecular weight and carboxylic acid groups.

References

[1] D. Fróna, J. Szenderák, M. Harangi-Rákos, The challenge of feeding the world, Sustainability 11(20) (2019) 5816.

[2] R. Putri, M. Naufal, M. Nandini, D. Dwiputra, S. Wibirama, J. Sumantyo, The Impact of Population Pressure on Agricultural Land towards Food Sufficiency (Case in West Kalimantan Province, Indonesia), IOP Conference Series: Earth and Environmental Science, IOP Publishing, 2019, p. 012050.

[3] H. Khaled, H.A. Fawy, Effect of different levels of humic acids on the nutrient content, plant growth, and soil properties under conditions of salinity, Soil and Water Research 6(1) (2011) 21-29.

[4] F.J. Stevenson, Humus chemistry: genesis, composition, reactions, John Wiley & Sons1994.

[5] A. Zularisam, A. Ismail, M. Salim, M. Sakinah, H. Ozaki, The effects of natural organic matter (NOM) fractions on fouling characteristics and flux recovery of ultrafiltration membranes, Desalination 212(1-3) (2007) 191-208.

[6] J. Andriesse, Nature and management of tropical peat soils, Food & Agriculture Org.1988.

[7] M. Schnitzer, Organic matter characterization, Methods of Soil Analysis: Part 2 Chemical and Microbiological Properties 9 (1983) 581-594.

[8] M. Filella, J. Buffle, N. Parthasarathy, HUMIC AND FULVIC COMPOUNDS, in: P. Worsfold, A. Townshend, C. Poole (Eds.), Encyclopedia of Analytical Science (Second Edition), Elsevier, Oxford, 2005, pp. 288-298. https://doi.org/https://doi.org/10.1016/B0-12-369397-7/00260-0.

[9] C. Niederer, R.P. Schwarzenbach, K.-U. Goss, Elucidating differences in the sorption properties of 10 humic and fulvic acids for polar and nonpolar organic chemicals, J Environmental Science & Technology 41(19) (2007) 6711-6717.

[10] R.E. Pettit, Organic matter, humus, humate, humic acid, fulvic acid and humin: their importance in soil fertility and plant health, CTI Research (2004) 1-17.

[11] E. Erhart, W. Hartl, Compost use in organic farming, Genetic engineering, biofertilisation, soil quality and organic farming, Springer2010, pp. 311-345.

[12] C. Clapp, An Organic Matter Trail: Polysaccharides to Waste Management to Nitrogen/Carbon to Humic Substances, Book chapter (2001).

[13] T. Mohd, H.A. Osumanu, M. Nik, Effect of mixing urea with humic acid and acid sulphate soil on ammonia loss, exchangeable ammonium and available nitrate, American Journal of Environmental Sciences 5(5) (2009) 588-591.

[14] G. Vallini, A. Pera, M. Agnolucci, M. Valdrighi, Humic acids stimulate growth and activity of in vitro tested axenic cultures of soil autotrophic nitrifying bacteria, Biology and Fertility of Soils 24(3) (1997) 243-248.

[15] J.F. Banfield, R.J. Hamers, Processes at minerals and surfaces with relevance to microorganisms and prebiotic synthesis, Geomicrobiology, De Gruyter2018, pp. 81-122.

[16] K. Day, R. Thornton, H. Kreeft, Humic acid products for improved phosphorus fertilizer management, Humic Substances, Elsevier2000, pp. 321-325.

[17] M. Schnitzer, Binding of humic substances by soil mineral colloids, Interactions of Soil Minerals with Natural Organics and Microbes 17 (1986) 77-101.

[18] K.H. Tan, Degradation of soil minerals by organic acids, Interactions of Soil Minerals with Natural Organics and Microbes 17 (1986) 1-27.

[19] C.N. Albers, G.T. Banta, P.E. Hansen, O.S. Jacobsen, Effect of different humic substances on the fate of diuron and its main metabolite 3, 4-dichloroaniline in soil, Environmental Science & Technology 42(23) (2008) 8687-8691.

[20] I. Cattani, H. Zhang, G.M. Beone, A.A.M. Del Re, R. Boccelli, M. Trevisan, The role of natural purified humic acids in modifying mercury accessibility in water and soil, Journal of environmental quality 38(2) (2009) 493-501.

[21] W. Luo, B. Gu, Dissolution and mobilization of uranium in a reduced sediment by natural humic substances under anaerobic conditions, Environmental Science & Technology 43(1) (2009) 152-156.

[22] S. Wang, C.N. Mulligan, Enhanced mobilization of arsenic and heavy metals from mine tailings by humic acid, Chemosphere 74(2) (2009) 274-279.

[23] N. Brosse, M.N. Mohamad Ibrahim, A. Abdul Rahim, Biomass to bioethanol: Initiatives of the future for lignin, ISRN Materials Science 2011 (2011).

[24] S.H. Lee, T.V. Doherty, R.J. Linhardt, J.S. Dordick, Ionic liquid- mediated selective extraction of lignin from wood leading to enhanced enzymatic cellulose hydrolysis, Biotechnology Bioengineering 102(5) (2009) 1368-1376.

[25] L. Hu, H. Pan, Y. Zhou, M. Zhang, Methods to improve lignin's reactivity as a phenol substitute and as replacement for other phenolic compounds: A brief review, BioResources 6(3) (2011) 3515-3525.

[26] R.C. Kuhad, A. Singh, Lignocellulose biotechnology: current and future prospects, Critical Reviews in Biotechnology 13(2) (1993) 151-172.

[27] D.-y. Min, S.W. Smith, H.-m. Chang, H. Jameel, Influence of isolation condition on structure of milled wood lignin characterized by quantitative 13C nuclear magnetic resonance spectroscopy, BioResources 8(2) (2013) 1790-1800.

[28] S. Mankar, A. Chaudhari, I. Soni, Lignin in phenol-formaldehyde adhesives, International Journal of Knowledge Engineering, ISSN (2012) 0976-5816.

[29] M. Wang, M. Leitch, C.C. Xu, Synthesis of phenol–formaldehyde resol resins using organosolv pine lignins, European Polymer Journal 45(12) (2009) 3380-3388.

[30] S. Sutradhar, K.M.Y. Arafat, J. Nayeem, M.S. Jahan, Organic acid lignin from rice straw in phenol-formaldehyde resin preparation for plywood, Cellulose Chemistry and Technology 54 (2020) 463-471.

[31] N. Alwadani, P. Fatehi, Synthetic and lignin-based surfactants: Challenges and opportunities, Carbon Resources Conversion 1(2) (2018) 126-138.

[32] T. Aro, P. Fatehi, Production and application of lignosulfonates and sulfonated lignin, ChemSusChem 10(9) (2017) 1861-1877.

[33] F. Kong, K. Parhiala, S. Wang, P. Fatehi, Preparation of cationic softwood kraft lignin and its application in dye removal, European Polymer Journal 67 (2015) 335-345.

[34] M.K. Konduri, F. Kong, P. Fatehi, Production of carboxymethylated lignin and its application as a dispersant, European Polymer Journal 70 (2015) 371-383.

[35] M. Brebu, C. Vasile, Thermal degradation of lignin—a review, J Cellulose Chemistry Technology 44(9) (2010) 353.

[36] D. Mohan, C.U. Pittman Jr, P.H. Steele, Pyrolysis of wood/biomass for bio-oil: a critical review, Energy fuels 20(3) (2006) 848-889.

[37] M.P. Pandey, C.S. Kim, Lignin depolymerization and conversion: a review of thermochemical methods, Chemical Engineering and Technology 34(1) (2011) 29-41.

[38] Y. Sun, J. Cheng, Hydrolysis of lignocellulosic materials for ethanol production: a review, Bioresource Technology 83(1) (2002) 1-11.

[39] J. Van Dyk, B. Pletschke, A review of lignocellulose bioconversion using enzymatic hydrolysis and synergistic cooperation between enzymes—factors affecting enzymes, conversion and synergy, Biotechnology Advances 30(6) (2012) 1458-1480.

[40] J.A. Lloyd, J. Ralph, Hydrogenation and hydrogenolysis of wood lignin: a review, Forest Products Division, Forest Research Institute1977.

[41] S. Son, F.D. Toste, Non- Oxidative Vanadium- Catalyzed C□ O Bond Cleavage: Application to Degradation of Lignin Model Compounds, Angewandte Chemie International Edition 49(22) (2010) 3791-3794.

[42] S. Eachus, C. Dence, Hydrogenation of lignin model compounds in the presence of a homogeneous catalyst, Wood Research and Technology (1975) 41-48.

[43] T. Furusawa, T. Sato, H. Sugito, Y. Miura, Y. Ishiyama, M. Sato, N. Itoh, N. Suzuki, Hydrogen production from the gasification of lignin with nickel catalysts in supercritical water, International Journal of Hydrogen Energy 32(6) (2007) 699-704.

[44] M. Osada, T. Sato, M. Watanabe, T. Adschiri, K. Arai, Low-temperature catalytic gasification of lignin and cellulose with a ruthenium catalyst in supercritical water, Energy and Fuels 18(2) (2004) 327-333.

[45] S. Kang, X. Li, J. Fan, J. Chang, Hydrothermal conversion of lignin: a review, Renewable Sustainable Energy Reviews 27 (2013) 546-558.

[46] D.S. Argyropoulos, D.S. Argyropoulos, Oxidative delignification chemistry, ACS Publications2001.

[47] H. Lange, S. Decina, C. Crestini, Oxidative upgrade of lignin–Recent routes reviewed, European polymer journal 49(6) (2013) 1151-1173.

[48] C. Crestini, M. Crucianelli, M. Orlandi, R. Saladino, Oxidative strategies in lignin chemistry: A new environmental friendly approach for the functionalisation of lignin and lignocellulosic fibers, Catalysis Today 156(1-2) (2010) 8-22.

[49] J.D. Araújo, C.A. Grande, A.E. Rodrigues, Design, Vanillin production from lignin oxidation in a batch reactor, J Chemical Engineering Research 88(8) (2010) 1024-1032.

[50] A.G. Demesa, A. Laari, I. Turunen, M. Sillanpää, Alkaline partial wet oxidation of lignin for the production of carboxylic acids, Chemical Engineering &Technology 38(12) (2015) 2270-2278.

[51] P. Figueiredo, K. Lintinen, J.T. Hirvonen, M.A. Kostiainen, H.A. Santos, Properties and chemical modifications of lignin: Towards lignin-based nanomaterials for biomedical applications, Progress in Materials Science 93 (2018) 233-269. https://doi.org/https://doi.org/10.1016/j.pmatsci.2017.12.001.

[52] J. Villar, A. Caperos, F. García-Ochoa, Oxidation of hardwood kraft-lignin to phenolic derivatives with oxygen as oxidant, Wood Science &Technology 35(3) (2001) 245-255.

[53] S. Laurichesse, L. Avérous, Chemical modification of lignins: Towards biobased polymers, Progress in polymer science 39(7) (2014) 1266-1290.

[54] F. Stevenson, M.M.H. Hayes, P. MacCarthy, RL Malcolm,, R.S. . Reductive cleavage of humic substances, Humic Substances II: In Search of Structure, Wiley, Chichester, UK (1989) 121-142.

[55] S.M. Shevchenko, G.W. Bailey, Life after death: Lignin- humic relationships reexamined, Critical Reviews in Environmental Science and Technology 26(2) (1996) 95-153.

[56] E.A. Capanema, M.Y. Balakshin, C.-L. Chen, J.S. Gratzl, A.G. Kirkman, Oxidative ammonolysis of technical lignins. Part 2. Effect of oxygen pressure, Holzforschung 55(4) (2001) 405-412.

[57] E.A. Capanema, M.Y. Balakshin, C.-L. Chen, J.S. Gratzl, A.G. Kirkman, Oxidative ammonolysis of technical lignins. Part 3. Effect of temperature on the reaction rate, Holzforschung 56(4) (2002) 402-415.

[58] A. Ertani, O. Francioso, V. Tugnoli, V. Righi, S.J.J.o.a. Nardi, f. chemistry, Effect of commercial lignosulfonate-humate on Zea mays L. metabolism, 59(22) (2011) 11940-11948.

[59] O.A. Gladkov, R.B. Poloskin, Y.J. Polyakov, I.V. Sokolova, N.I. Sorokin, A.V. Glebov, Method for producing humic acid salts, Google Patents, 2007.

[60] D. Meier, V. Zúñiga-Partida, F. Ramírez-Cano, N.-C. Hahn, O. Faix, Conversion of technical lignins into slow-release nitrogenous fertilizers by ammoxidation in liquid phase, Bioresource Technology 49(2) (1994) 121-128.

[61] E.A. Capanema, M.Y. Balakshin, C.L. Chen, J.S. Gratzl, Oxidative ammonolysis of technical lignins. Part 4. Effects of the ammonium hydroxide concentration and pH, Journal of Wood Chemistry and Technology 26(1) (2006) 95-109.

[62] T. Senn, A.R. Kingman, A review of humus and humic acids, Research series 145 (1973) 1-5.

[63] A. Baglieri, A. Ioppolo, M. Negre, M. Gennari, A method for isolating soil organic matter after the extraction of humic and fulvic acids, Organic Geochemistry 38(1) (2007) 140-150.

[64] S. Dou, J. Shan, X. Song, R. Cao, M. Wu, C. Li, S. Guan, Are humic substances soil microbial residues or unique synthesized compounds? A perspective on their distinctiveness, Pedosphere 30(2) (2020) 159-167. https://doi.org/https://doi.org/10.1016/S1002-0160(20)60001-7.

[65] L. Maillard, Formation d'humus et de combustibles mineraux sans intervention de l'oxygene atmospherique, des microorganismes des hautes temperatures ou des fortes pressions, J CR Acad. Sci. Paris 154 (1912) 66.

[66] W. Eller, Künstliche und natürliche Huminsäuren, Brennstoffchem 2 (1921) 129-133.

[67] D. Sen, S. Jun, S. Xiangyun, C. Rui, W. Meng, L. Chenglin, G. Song, Are humic substances soil microbial residues or unique synthesized compounds? A perspective on their distinctiveness, Pedosphere 30(2) (2020) 159-167.

[68] J. Weber, Definition of soil organic matter, Humintech: Humic acids based products (2002).

[69] W. Flaig, Generation of model chemical precursors."Humic Substances and their Role in the Environment"(FH Frimmel and RF Christman, Eds.), Wiley, Chichester1988.

[70] B.A.G. de Melo, F.L. Motta, M.H.A. Santana, Humic acids: Structural properties and multiple functionalities for novel technological developments, Materials Science and Engineering: C 62 (2016) 967-974. https://doi.org/https://doi.org/10.1016/j.msec.2015.12.001.

[71] R. Von Wandruszka, Humic acids: Their detergent qualities and potential uses in pollution remediation, Geochemical Transactions 1(1) (2000) 1-6.

[72] P. Boguta, Z. Sokolowska, Interactions of humic acids with metals, Acta Agrophysica. Monographiae 2 (2013).

[73] C.F. Mahler, N. Dal Santo Svierzoski, C.A.R. Bernardino, Chemical characteristics of humic substances in nature, Humic Substance (2021).

[74] B.K.G. Theng, Formation and properties of clay-polymer complexes, Elsevier2012.

[75] R. Sutton, G. Sposito, Molecular structure in soil humic substances: the new view, Environmental Science and Technology 39(23) (2005) 9009-9015.

[76] K.A. Thorn, D.W. Folan, P. MacCarthy, Characterization of the International Humic Substances Society standard and reference fulvic and humic acids by solution state carbon-13 (13C) and hydrogen-1 (1H) nuclear magnetic resonance spectrometry, Water-Resources Investigations Report 89(4196) (1989) 1-93.

[77] J. Kochany, W. Smith, Application of humic substances in environmental remediation, WM'01 Conference, 2001.

[78] J.S. Mun, J.A. Pe, 3rd, S.P. Mun, Chemical Characterization of Kraft Lignin Prepared from Mixed Hardwoods, Molecules 26(16) (2021). https://doi.org/10.3390/molecules26164861.

[79] I. Sumerskii, P. Korntner, G. Zinovyev, T. Rosenau, A. Potthast, Fast track for quantitative isolation of lignosulfonates from spent sulfite liquors, RSC advances 5(112) (2015) 92732-92742.

[80] J. Köhnke, N. Gierlinger, B. Prats-Mateu, C. Unterweger, P. Solt, A.K. Mahler, E. Schwaiger, F. Liebner, W. Gindl-Altmutter, Comparison of four technical lignins as a resource for electrically conductive carbon particles, BioResources 14(1) (2019) 1091-1109.

[81] A. Stücker, J. Podschun, B. Saake, R. Lehnen, A novel quantitative 31 P NMR spectroscopic analysis of hydroxyl groups in lignosulfonic acids, Analytical Methods 10(28) (2018) 3481-3488.

[82] P. Jõul, T.T. Ho, U. Kallavus, A. Konist, K. Leiman, O.-S. Salm, M. Kulp, M. Koel, T. Lukk, Characterization of Organosolv Lignins and Their Application in the Preparation of Aerogels, Materials 15(8) (2022) 2861.

[83] B. Ahvazi, O. Wojciechowicz, T.-M. Ton-That, J. Hawari, Preparation of lignopolyols from wheat straw soda lignin, Journal of Agricultural and Food Chemistry 59(19) (2011) 10505-10516.

[84] Y. Shao, M. Bao, W. Huo, R. Ye, Y. Liu, W. Lu, Production of artificial humic acid from biomass residues by a non-catalytic hydrothermal process, Journal of Cleaner Production 335 (2022) 130302. https://doi.org/https://doi.org/10.1016/j.jclepro.2021.130302.

[85] F. Yang, S. Zhang, K. Cheng, M. Antonietti, A hydrothermal process to turn waste biomass into artificial fulvic and humic acids for soil remediation, Science of The Total Environment 686 (2019) 1140-1151. https://doi.org/https://doi.org/10.1016/j.scitotenv.2019.06.045.

[86] Y. Zhang, G. Cui, G. Zhang, Y. Dou, Study on extraction of biological humic acids from fermented furfural residue, Agricultural Science & Technology 17(6) (2016) 1442.

[87] M.-Y. Chang, W.-J. Huang, Hydrothermal biorefinery of spent agricultural biomass into value-added bio-nutrient solution: Comparison between greenhouse and field cropping data, Industrial Crops and Products 126 (2018) 186-189.

[88] W. Junzhe, T. Lihua, G. Jianxin, Alkali catalysis hydrothermal conversion of cabbage leaf in kitchen waste, Chinese Journal of Environmental Engineering 11(1) (2017) 578-581.

[89] M. Klavins, L. Ansone-Bertina, L. Arbidans, L. Klavins, Biomass waste processing into artificial humic substances, Environmental and Climate Technologies 25(1) (2021) 631-639.

[90] W. Sui, S. Li, X. Zhou, Z. Dou, R. Liu, T. Wu, H. Jia, G. Wang, M. Zhang, Potential hydrothermal-humification of vegetable wastes by steam explosion and structural characteristics of humified fractions, Molecules 26(13) (2021) 3841.

[91] Z.-T. Hu, W. Huo, Y. Chen, Q. Zhang, M. Hu, W. Zheng, Y. Shao, Z. Pan, X. Li, J. Zhao, Humic substances derived from biomass waste during aerobic composting and hydrothermal treatment: A review, Frontiers in Bioengineering and Biotechnology 10 (2022).

[92] P. Chen, R. Yang, Y. Pei, Y. Yang, J. Cheng, D. He, Q. Huang, H. Zhong, F. Jin, Hydrothermal synthesis of similar mineral-sourced humic acid from food waste and the role of protein, Science of The Total Environment 828 (2022) 154440. https://doi.org/https://doi.org/10.1016/j.scitotenv.2022.154440.

[93] Z. Xu, Y. Yang, P. Yan, Z. Xia, X. Liu, Z.C. Zhang, Mechanistic understanding of humin formation in the conversion of glucose and fructose to 5-hydroxymethylfurfural in [BMIM] Cl ionic liquid, RSC advances 10(57) (2020) 34732-34737.

[94] C. Moretti, B. Corona, R. Hoefnagels, I. Vural-Gürsel, R. Gosselink, M. Junginger, Review of life cycle assessments of lignin and derived products: Lessons learned, Science of The Total Environment 770 (2021) 144656. https://doi.org/https://doi.org/10.1016/j.scitotenv.2020.144656.

[95] D. Kai, M.J. Tan, P.L. Chee, Y.K. Chua, Y.L. Yap, X.J. Loh, Towards lignin-based functional materials in a sustainable world, Green Chemistry 18(5) (2016) 1175-1200.

[96] W. Boerjan, J. Ralph, M. Baucher, Lignin Biosynthesis, Annual Review of Plant Biology 54(1) (2003) 519-546. https://doi.org/10.1146/annurev.arplant.54.031902.134938.

[97] S. Imman, P. Khongchamnan, W. Wanmolee, N. Laosiripojana, T. Kreetachat, C. Sakulthaew, C. Chokejaroenrat, N. Suriyachai, Fractionation and characterization of lignin from sugarcane bagasse using a sulfuric acid catalyzed solvothermal process, RSC Adv 11(43) (2021) 26773-26784. https://doi.org/10.1039/d1ra03237b.

[98] Z. Chen, C. Wan, Biological valorization strategies for converting lignin into fuels and chemicals, Renewable and Sustainable Energy Reviews 73 (2017) 610-621.

[99] Y. Lu, Y.-C. Lu, H.-Q. Hu, F.-J. Xie, X.-Y. Wei, X. Fan, Structural characterization of lignin and its degradation products with spectroscopic methods, Journal of Spectroscopy 2017 (2017).

[100] N. Zhou, W. Thilakarathna, Q. He, H. Rupasinghe, A Review: Depolymerization of Lignin to Generate High-Value Bio-Products: Opportunities, Challenges, and Prospects. Front, Energy Res 9 (2022) 758744.

[101] J. Luterbacher, D.M. Alonso, J. Dumesic, Targeted chemical upgrading of lignocellulosic biomass to platform molecules, Green Chemistry 16(12) (2014) 4816-4838.

[102] B.M. Upton, A.M. Kasko, Strategies for the conversion of lignin to high-value polymeric materials: review and perspective, Chemical reviews 116(4) (2016) 2275-2306.

[103] A. Tejado, C. Pena, J. Labidi, J. Echeverria, I. Mondragon, Physico-chemical characterization of lignins from different sources for use in phenol–formaldehyde resin synthesis, Bioresource Technology 98(8) (2007) 1655-1663.

[104] S. Sutradhar, W. Gao, P. Fatehi, A Green Cement Plasticizer from Softwood Kraft Lignin, Industrial & Engineering Chemistry Research 62(3) (2023) 1676-1687. https://doi.org/10.1021/acs.iecr.2c03970.

[105] F.S. Chakar, A.J. Ragauskas, Review of current and future softwood kraft lignin process chemistry, Industrial Crops and Products 20(2) (2004) 131-141.

[106] J. Zakzeski, P.C. Bruijnincx, A.L. Jongerius, B.M. Weckhuysen, The catalytic valorization of lignin for the production of renewable chemicals, Chemical reviews 110(6) (2010) 3552-3599.

[107] D. Areskogh, J. Li, G.r. Gellerstedt, G.J.B. Henriksson, Investigation of the molecular weight increase of commercial lignosulfonates by laccase catalysis, 11(4) (2010) 904-910.

[108] M.N. Belgacem, A. Blayo, A. Gandini, Organosolv lignin as a filler in inks, varnishes and paints, Industrial Crops and Products 18(2) (2003) 145-153.

[109] F. Juan, Z. Huaiyu, Optimization of synthesis of spherical lignosulphonate resin and its structure characterization, J Chinese Journal of Chemical Engineering 16(3) (2008) 407-410.

[110] H. Byman-Fagerholm, P. Mikkola, J.B. Rosenholm, E. Lidén, R. Carlsson, The influence of lignosulphonate on the properties of single and mixed Si3N4 and ZrO2 suspensions, European Ceramic Society 19(1) (1999) 41-48.

[111] J. Lora, Industrial commercial lignins: sources, properties and applications, Monomers, polymers and composites from renewable resources, Elsevier2008, pp. 225-241.

[112] G. Shulga, F. Rekner, J. Varslavan, SW—soil and water: Lignin-based interpolymer complexes as a novel adhesive for protection against erosion of sandy soil, Journal of Agricultural Engineering Research 78(3) (2001) 309-316.

[113] A. Ansari, M. Pawlik, Floatability of chalcopyrite and molybdenite in the presence of lignosulfonates. Part I. Adsorption studies, J Minerals Engineering 20(6) (2007) 600-608.

[114] L. Grierson, J. Knight, R.J.C. Maharaj, C. Research, The role of calcium ions and lignosulphonate plasticiser in the hydration of cement, 35(4) (2005) 631-636.

[115] S. Kumar, A. Mohanty, L. Erickson, M. Misra, Lignin and its applications with polymers, Journal of Biobased Materials

Bioenergy 3(1) (2009) 1-24.

[116] D. Stewart, Lignin as a base material for materials applications: Chemistry, application and economics, Industrial Crops and Products 27(2) (2008) 202-207.

[117] S. González-García, M.T. Moreira, G. Artal, L. Maldonado, G. Feijoo, Environmental impact assessment of non-wood based pulp production by soda-anthraquinone pulping process, Journal of Cleaner Production 18(2) (2010) 137-145.

[118] A. Rodríguez, R. Sánchez, A. Requejo, A. Ferrer, Feasibility of rice straw as a raw material for the production of soda cellulose pulp, Journal of Cleaner Production 18(10-11) (2010) 1084-1091.

[119] B. Saake, R. Lehnen, Lignin, Ullmann's Encyclopedia of Industrial Chemistry, Wiley-VCH, Weinheim, 2007.

[120] B. Baurhoo, C. Ruiz-Feria, X. Zhao, Purified lignin: Nutritional and health impacts on farm animals—A review, Animal Feed Science Technology 144(3-4) (2008) 175-184.

[121] R. Gosselink, E. de Jong, A. Abächerli, B. Guran, Activities and results of the thematic network EUROLIGNIN, Proceedings of the 7th ILI Forum, Barcelona, Spain, 2005, pp. 25-30.

[122] K. Wörmeyer, T. Ingram, B. Saake, G. Brunner, I. Smirnova, Comparison of different pretreatment methods for lignocellulosic materials. Part II: Influence of pretreatment on the properties of rye straw lignin, Bioresource Technology 102(5) (2011) 4157-4164.

[123] M.S. Jahan, M.M. Rahman, S. Sutradhar, M. Quaiyyum, Fractionation of rice straw for producing dissolving pulp in biorefinery concept, Nordic Pulp & Paper Research Journal 30(4) (2015) 562-567.

[124] J.H. Lora, W.G. Glasser, Recent industrial applications of lignin: a sustainable alternative to nonrenewable materials, Journal of Polymers the Environment 10(1-2) (2002) 39-48.

[125] J.J. Meister, Modification of lignin, Journal of Macromolecular Science, Part C: Polymer Reviews 42(2) (2002) 235-289.

[126] S. SUTRADHAR, K.M.Y. Arafat, J. NAYEEM, M.S. JAHAN, Organic acid lignin from rice straw in phenol-formaldehyde resin preparation for plywood, Cellulose Chemistry and Technology. 54(56) (2020) 463-471.

[127] J. Ralph, C. Lapierre, W. Boerjan, Lignin structure and its engineering, Current Opinion in Biotechnology 56 (2019) 240-249. https://doi.org/https://doi.org/10.1016/j.copbio.2019.02.019.

[128] X. Cao, M. Drosos, J.A. Leenheer, J. Mao, Secondary structures in a freeze-dried lignite humic acid fraction caused by hydrogen-bonding of acidic protons with aromatic rings, Environmental science & technology 50(4) (2016) 1663-1669.

[129] C. Guignard, L. Lemée, A. Amblès, Structural characterization of humic substances from an acidic peat using thermochemolysis techniques, (2000).

[130] J. Gerke, Concepts and misconceptions of humic substances as the stable part of soil organic matter: A review, Agronomy 8(5) (2018) 76.

[131] J.G. Lee, H.Y. Yoon, J.-Y. Cha, W.-Y. Kim, P.J. Kim, J.-R. Jeon, Artificial humification of lignin architecture: Top-down and bottom-up approaches, Biotechnology Advances (2019) 107416.

[132] F. de Souza, S.R. Bragança, Extraction and characterization of humic acid from coal for the application as dispersant of ceramic powders, Journal of Materials Research and Technology 7(3) (2018) 254-260. https://doi.org/https://doi.org/10.1016/j.jmrt.2017.08.008.

[133] H.J. Jeong, J.-Y. Cha, J.H. Choi, K.-S. Jang, J. Lim, W.-Y. Kim, D.-C. Seo, J.-R. Jeon, One-pot transformation of technical lignins into humic-like plant stimulants through Fenton-based advanced oxidation: accelerating natural fungus-driven humification, ACS omega 3(7) (2018) 7441-7453.

[134] C. Guignard, L. Lemée, A. Amblès, Structural characterization of humic substances from an acidic peat using thermochemolysis techniques, 20(5) (2000) 465-475. https://doi.org/10.1051/agro:2000142.

[135] M. Schnitzer, M.I.O.d. Serra, The chemical degradation of a humic acid, Canadian Journal of Chemistry 51(10) (1973) 1554-1566.

[136] L.B. Sonnenberg, J.D. Johnson, R.F. Christman, Chemical Degradation of Humic Substances for Structural Characterization, Aquatic Humic Substances, American Chemical Society1988, pp. 3-23. https://doi.org/doi:10.1021/ba-1988-0219.ch001

10.1021/ba-1988-0219.ch001.

[137] S. Yan, N. Zhang, J. Li, Y. Wang, Y. Liu, M. Cao, Q. Yan, Characterization of humic acids from original coal and its oxidization production, Scientific Reports 11(1) (2021) 15381. https://doi.org/10.1038/s41598-021-94949-0.

[138] B. Mycke, W. Michaelis, Molecular fossils from chemical degradation of macromolecular organic matter, Organic Geochemistry 10(4-6) (1986) 847-858.

[139] C. Chen, Lignins: Occurrence in wood tissues, isolation, reactions and structures, Wood Structures Composition (1991).

[140] D. Fengel, G. Wegener, Wood: chemistry, ultrastructure, Reactions 613 (1984) 1960-1982.

[141] O. Bikovens, G. Telysheva, K. Iiyama, Comparative studies of grass compost lignin and the lignin component of compost humic substances, Chemistry and Ecology 26(S2) (2010) 67-75.

[142] K. Fischer, R. Schiene, Nitrogenous fertilizers from lignins—A review, Chemical modification, properties, and usage of lignin, Springer2002, pp. 167-198.

[143] M.J. Galetakis, F.F. Pavloudakis, The effect of lignite quality variation on the efficiency of on-line ash analyzers, International Journal of Coal Geology 80(3-4) (2009) 145-156.

[144] D. Nieweś, M. Huculak-Mączka, M. Braun-Giwerska, K. Marecka, A. Tyc, M. Biegun, K. Hoffmann, J. Hoffmann, Ultrasound-Assisted Extraction of Humic Substances from Peat: Assessment of Process Efficiency and Products' Quality, Molecules 27(11) (2022) 3413.

[145] R.B. Finkelman, A. Wolfe, M.S. Hendryx, The future environmental and health impacts of coal, Energy Geoscience 2(2) (2021) 99-112. https://doi.org/https://doi.org/10.1016/j.engeos.2020.11.001.

[146] T.C. Drage, C.H. Vane, G.D.J.O.g. Abbott, The closed system pyrolysis of β-O-4 lignin substructure model compounds, 33(12) (2002) 1523-1531.

[147] S. Sutradhar, N. Alam, L.P. Christopher, P. Fatehi, KOH catalyzed oxidation of kraft lignin to produce green fertilizer, Catalysis Today 404 (2022) 49-62.

[148] U. Junghans, J.J. Bernhardt, R. Wollnik, D. Triebert, G. Unkelbach, D. Pufky-Heinrich, Valorization of Lignin via Oxidative Depolymerization with Hydrogen Peroxide: Towards Carboxyl-Rich Oligomeric Lignin Fragments, Molecules 25(11) (2020) 2717.

[149] G. Neri, A. Pistone, C. Milone, S. Galvagno, Wet air oxidation of p-coumaric acid over promoted ceria catalysts, Applied Catalysis B: Environmental 38(4) (2002) 321-329.

[150] A. Kalliola, Chemical and enzymatic oxidation using molecular oxygen as a means to valorize technical lignins for material applications, (2015).

[151] Y. Ji, E. Vanska, A. Van Heiningen, Rate determining step and kinetics of oxygen delignification, Pulp Pap-Canada 110(3) (2009) 29-35.

[152] A. Ertani, O. Francioso, V. Tugnoli, V. Righi, S. Nardi, Effect of commercial lignosulfonate-humate on Zea mays L. metabolism, Journal of agricultural and food chemistry 59(22) (2011) 11940-11948.

[153] W. Schutyser, J.S. Kruger, A.M. Robinson, R. Katahira, D.G. Brandner, N.S. Cleveland, A. Mittal, D.J. Peterson, R. Meilan, Y. Román-Leshkov, Revisiting alkaline aerobic lignin oxidation, Green chemistry 20(16) (2018) 3828-3844.

[154] H. Paananen, E. Eronen, M. Mäkinen, J. Jänis, M. Suvanto, T.T. Pakkanen, Base-catalyzed oxidative depolymerization of softwood kraft lignin, Industrial Crops and Products 152 (2020) 112473. https://doi.org/https://doi.org/10.1016/j.indcrop.2020.112473.

[155] J.J. Bernhardt, B. Rößiger, T. Hahn, D. Pufky-Heinrich, Kinetic modeling of the continuous hydrothermal base catalyzed depolymerization of pine wood based kraft lignin in

pilot scale, Industrial Crops and Products 159 (2021) 113119. https://doi.org/https://doi.org/10.1016/j.indcrop.2020.113119.

[156] O.A. Almaghrabi, Control of wild oat (Avena fatua) using some phenolic compounds I–Germination and some growth parameters, Saudi Journal of Biological Sciences 19(1) (2012) 17-24.

[157] N. Chaves, T. Sosa, J. Alías, J. Escudero, Identification and effects of interaction phytotoxic compounds from exudate of Cistus ladanifer leaves, Journal of Chemical Ecology 27(3) (2001) 611-621.

[158] D. Savy, V. Cozzolino, A. Nebbioso, M. Drosos, A. Nuzzo, P. Mazzei, A. Piccolo, Humic-like bioactivity on emergence and early growth of maize (Zea mays L.) of water-soluble lignins isolated from biomass for energy, Plant Soil 402(1-2) (2016) 221-233.

[159] H. Chang, J. Gratzl, Ring cleavage reactions of lignin models with oxygen and alkali, Chemistry of Delignification with Oxygen, Ozone Peroxide (1980) 151-163.

[160] F. Jin, J. Leitich, C. von Sonntag, The superoxide radical reacts with tyrosine-derived phenoxyl radicals by addition rather than by electron transfer, Journal of the Chemical Society, Perkin Transactions 2 (9) (1993) 1583-1588.

[161] D. Savy, L. Canellas, G. Vinci, V. Cozzolino, A. Piccolo, Humic-Like Water-Soluble Lignins from Giant Reed (Arundo donax L.) Display Hormone-Like Activity on Plant Growth, Journal of Plant Growth Regulation 36(4) (2017) 995-1001. https://doi.org/10.1007/s00344-017-9696-4.

[162] D. Savy, V. Cozzolino, G. Vinci, A. Nebbioso, A. Piccolo, Water-soluble lignins from different bioenergy crops stimulate the early development of maize (Zea mays, L.), Molecules 20(11) (2015) 19958-19970.

[163] D. Savy, P. Mazzei, M. Drosos, V. Cozzolino, L. Lama, A. Piccolo, Molecular characterization of extracts from biorefinery wastes and evaluation of their plant biostimulation, ACS Sustainable Chemistry and Engineering 5(10) (2017) 9023-9031.

[164] J. Zazo, J. Casas, A. Mohedano, M. Gilarranz, J. Rodriguez, Chemical pathway and kinetics of phenol oxidation by Fenton's reagent, Environmental science & technology 39(23) (2005) 9295-9302.

[165] J. Zeng, C.G. Yoo, F. Wang, X. Pan, W. Vermerris, Z. Tong, Biomimetic fenton-catalyzed lignin depolymerization to high- value aromatics and dicarboxylic acids, ChemSusChem 8(5) (2015) 861-871.

[166] S. Anita, K. Bhandari, Oxidative ammonolysis of commercial lignin-a new concept to produce N-modified lignin, Indian Forester 126(6) (2000) 643-646.

[167] D. Meier, V. Zúñiga-Partida, F. Ramírez-Cano, N.-C. Hahn, O. Faix, Conversion of technical lignins into slow-release nitrogenous fertilizers by ammoxidation in liquid phase, Bioresource technology 49(2) (1994) 121-128.

[168] E. Capanema, M.Y. Balakshin, C. Chen, J. Gratzl, A. Kirkman, H. Gracz, Effect of temperature on the rate of oxidative ammonolysis and structures of N- modified lignins, Proc. 10th ISWPC 3 (1999) 404-409.

[169] E.A. Capanema, M.Y. Balakshin, C.L. Chen, J.S. Gratzl, Oxidative ammonolysis of technical lignins. Part 4. Effects of the ammonium hydroxide concentration and pH, Wood Chemistry and Technology 26(1) (2006) 95-109.

[170] P. Goel, M. Dhingra, Humic substances: prospects for use in agriculture and medicine, Humic Substances, IntechOpen2021.

[171] K. Ampong, M.S. Thilakaranthna, L.Y. Gorim, Understanding the role of humic acids on crop performance and soil health, Frontiers in Agronomy 4 (2022).

[172] A. Muscolo, M. Sidari, S. Nardi, Humic substance: Relationship between structure and activity. Deeper information suggests univocal findings, Journal of Geochemical Exploration 129 (2013) 57-63. https://doi.org/https://doi.org/10.1016/j.gexplo.2012.10.012.

[173] J. Guo, J. Zhou, S. Liu, L. Shen, X. Liang, T. Wang, L. Zhu, Underlying Mechanisms for Low-Molecular-Weight Dissolved Organic Matter to Promote Translocation and Transformation of Chlorinated Polyfluoroalkyl Ether Sulfonate in Wheat, Environmental Science & Technology (2022). https://doi.org/10.1021/acs.est.2c04356.

[174] Z. Varanini, R. Pinton, M.G. De Biasi, S. Astolfi, A. Maggioni, Low molecular weight humic substances stimulate H^+ -ATPase activity of plasma membrane vesicles isolated from oat (Avena sativa L.) roots, Plant and Soil 153(1) (1993) 61-69.

[175] S. Nardi, G. Arnoldi, G. Dell'Agnola, Release of the hormone-like activities from Allolobophora rosea (Sav.) and Allolobophora caliginosa (Sav.) feces, Canadian Journal of Soil Science 68(3) (1988) 563-567.

[176] S. Nardi, D. Pizzeghello, C. Gessa, L. Ferrarese, L. Trainotti, G. Casadoro, A low molecular weight humic fraction on nitrate uptake and protein synthesis in maize seedlings, Soil Biology and Biochemistry 3(32) (2000) 415-419.

[177] A. Muscolo, F. Bovalo, F. Gionfriddo, S. Nardi, Earthworm humic matter produces auxin-like effects on Daucus carota cell growth and nitrate metabolism, Soil Biology and biochemistry 31(9) (1999) 1303-1311.

[178] S. Trevisan, O. Francioso, S. Quaggiotti, S. Nardi, Humic substances biological activity at the plant-soil interface: from environmental aspects to molecular factors, J Plant Signaling Behavior 5(6) (2010) 635-643.

[179] D. Crouse, North Carolina extension gardener handbook, Moore & LK Bradley, eds., Raleigh, NC: Published by NC State Extension, College of Agri and Life Sci., NC State University (2018).

[180] K. Billingham, Humic products: potential or presumption for agriculture, NSW Agriculture2015.

[181] F. Yang, C. Tang, M. Antonietti, Natural and artificial humic substances to manage minerals, ions, water, and soil microorganisms, Chemical Society Reviews 50(10) (2021) 6221-6239.

[182] Z. Cihlář, L. Vojtová, P. Conte, S. Nasir, J. Kučerík, Hydration and water holding properties of cross-linked lignite humic acids, Geoderma 230-231 (2014) 151-160. https://doi.org/https://doi.org/10.1016/j.geoderma.2014.04.018.

[183] R. Klöcking, B. Helbig, Medical aspects and applications of humic substances, Biopolymers for Medical and Pharmaceutical Applications. WILEY-VCH Verlag GmbH & C. KGaA. Weinheim (2005) 3-16.

[184] R. Klöcking, B. Helbig, G. Schötz, M. Schacke, P. Wutzler, Anti-HSV-1 activity of synthetic humic acid-like polymers derived from p-diphenolic starting compounds, Antiviral Chemistry and Chemotherapy 13(4) (2002) 241-249.

[185] G.K. Jooné, J. Dekker, C.E.J. van Rensburg, Investigation of the immunostimulatory properties of oxihumate, Zeitschrift für Naturforschung C 58(3-4) (2003) 263-267.

[186] E.M. Peña-Méndez, J. Havel, J. Patočka, Humic substances-compounds of still unknown structure: applications in agriculture, industry, environment, and biomedicine, J. Appl. Biomed 3(1) (2005) 13-24.

[187] K. Zhou, J.-J. Yin, L.L. Yu, ESR determination of the reactions between selected phenolic acids and free radicals or transition metals, Food Chemistry 95(3) (2006) 446-457.

[188] R.G.P.T. Jayasooriya, M.G. Dilshara, C.-H. Kang, S. Lee, Y.H. Choi, Y.K. Jeong, G.-Y. Kim, Fulvic acid promotes extracellular anti-cancer mediators from RAW 264.7 cells, causing to cancer cell death in vitro, International Immunopharmacology 36 (2016) 241-248. https://doi.org/https://doi.org/10.1016/j.intimp.2016.04.029.

[189] W. Banaszkiewicz, M. Drobnik, The influence of natural peat and isolated humic acid solution on certain indices of metabolism and of acid-base equilibrium in experimental animals, Roczniki Panstwowego Zakladu Higieny 45(4) (1994) 353-360.

[190] M. Hafez, A.I. Popov, V.N. Zelenkov, T.V. Teplyakova, M. Rashad, Humic substances as an environmental-friendly organic wastes potentially help as natural anti-virus to inhibit COVID-19, Sci. Arch 1 (2020) 53-60.

[191] M. Verrillo, M. Salzano, D. Savy, V. Di Meo, M. Valentini, V. Cozzolino, A. Piccolo, Antibacterial and antioxidant properties of humic substances from composted agricultural biomasses, Chemical and Biological Technologies in Agriculture 9(1) (2022) 28. https://doi.org/10.1186/s40538-022-00291-6.

[192] P. Hajdrik, B. Pályi, Z. Kis, N. Kovács, D.S. Veres, K. Szigeti, F. Budán, I. Hegedüs, T. Kovács, R. Bergmann, D. Máthé, In Vitro Determination of Inhibitory Effects of Humic Substances Complexing Zn and Se on SARS-CoV-2 Virus Replication, Foods 11(5) (2022). https://doi.org/10.3390/foods11050694.

[193] N. Panigrahy, A. Priyadarshini, M.M. Sahoo, A.K. Verma, A. Daverey, N.K. Sahoo, A comprehensive review on eco-toxicity and biodegradation of phenolics: Recent progress and future outlook, Environmental Technology & Innovation 27 (2022) 102423. https://doi.org/https://doi.org/10.1016/j.eti.2022.102423.

[194] C.-l. Li, F. Ji, S. Wang, J.-j. Zhang, Q. Gao, J.-g. Wu, L.-p. Zhao, L.-c. Wang, L.-r. Zheng, Adsorption of Cu(II) on humic acids derived from different organic materials, Journal of Integrative Agriculture 14(1) (2015) 168-177. https://doi.org/https://doi.org/10.1016/S2095-3119(13)60682-6.

[195] A. Piccolo, A. De Martino, F. Scognamiglio, R. Ricci, R. Spaccini, Efficient simultaneous removal of heavy metals and polychlorobiphenyls from a polluted industrial site by washing the soil with natural humic surfactants, Environmental Science and Pollution Research 28(20) (2021) 25748-25757. https://doi.org/10.1007/s11356-021-12484-x.

[196] S.J. Santosa, D. Siswanta, S. Sudiono, R. Utarianingrum, Chitin–humic acid hybrid as adsorbent for Cr (III) in effluent of tannery wastewater treatment, Applied Surface Science 254(23) (2008) 7846-7850.

[197] P. Stathi, Y. Deligiannakis, Humic acid-inspired hybrid materials as heavy metal absorbents, Journal of Colloid and Interface Science 351(1) (2010) 239-247.

[198] M. Wang, S.B. Chen, Removal of Cd, Pb and Cu from water using thiol and humic acid functionalized Fe2O3 nanoparticles, Advanced Materials Research, Trans Tech Publ, 2012, pp. 1956-1963.

[199] J. Avdalović, S. Miletić, V. Beškoski, M. Ilić, G. Gojgić-Cvijović, M. Vrvić, Humic Acid–ability to use as natural surfactants, (2012).

[200] C. Urdiales, M.P. Sandoval, M. Escudey, C. Pizarro, H. Knicker, L. Reyes-Bozo, M. Antilén, Surfactant properties of humic acids extracted from volcanic soils and their applicability in mineral flotation processes, Journal of Environmental Management 227 (2018) 117-123. https://doi.org/https://doi.org/10.1016/j.jenvman.2018.08.072.

[201] T. Das, M. Bora, J. Tamuly, S.M. Benoy, B.P. Baruah, P. Saikia, B.K. Saikia, Coal-derived humic acid for application in acid mine drainage (AMD) water treatment and electrochemical devices, International Journal of Coal Science & Technology 8(6) (2021) 1479-1490. https://doi.org/10.1007/s40789-021-00441-5.

[202] J.r. Novák, J. Kozler, P. Janoš, J. Čežíková, V. Tokarová, L. Madronová, Humic acids from coals of the North-Bohemian coal field: I. Preparation and characterisation, Reactive and Functional Polymers 47(2) (2001) 101-109. https://doi.org/https://doi.org/10.1016/S1381-5148(00)00076-6.

[203] L. Madronová, J. Kozler, J. Čežíková, J.r. Novák, P. Janoš, Humic acids from coal of the North-Bohemia coal field: III☆☆For Part II see Ref. [7].. Metal-binding properties of humic acids — measurements in a column arrangement, Reactive and Functional Polymers 47(2) (2001) 119-123. https://doi.org/https://doi.org/10.1016/S1381-5148(00)00077-8.

[204] W.-b. YAO, L. HUANG, Z.-h. YANG, F.-p. ZHAO, Effects of organic acids on heavy metal release or immobilization in contaminated soil, Transactions of Nonferrous Metals Society of China 32(4) (2022) 1277-1289.

[205] D. Pizzeghello, G. Nicolini, S. Nardi, Hormone- like activity of humic substances in Fagus sylvaticae forests, New Phytologist 151(3) (2001) 647-657.

[206] A. Muscolo, M. Panuccio, M. Sidari, The effect of phenols on respiratory enzymes in seed germination, Plant Growth Regulation 35(1) (2001) 31-35.

[207] L. Djurdjevic, A. Dinic, P. Pavlovic, M. Mitrovic, B. Karadzic, V. Tesevic, Allelopathic potential of Allium ursinum L, Biochemical Systematics and Ecology 32(6) (2004) 533-544.

[208] T.M. Gerig, U. Blum, Effects of mixtures of four phenolic acids on leaf area expansion of cucumber seedlings grown in Portsmouth B1 soil materials, Journal of Chemical Ecology 17(1) (1991) 29-40.

[209] R.D. Williams, R.E. Hoagland, The effects of naturally occurring phenolic compounds on seed germination, Weed Science 30(2) (1982) 206-212.

[210] N. Stern, J. Mejia, S. He, Y. Yang, M. Ginder-Vogel, E.E. Roden, Dual Role of Humic Substances As Electron Donor and Shuttle for Dissimilatory Iron Reduction, Environtan Science & Technology 52(10) (2018) 5691-5699. https://doi.org/10.1021/acs.est.7b06574.

[211] K.L. Haas, K.J. Franz, Application of metal coordination chemistry to explore and manipulate cell biology, Chemical Reviews 109(10) (2009) 4921-4960.

[212] S. Werneke, C. Swann, L. Farquharson, K. Hamilton, A. Smith, The role of metals in molluscan adhesive gels, Journal of Experimental Biology 210(12) (2007) 2137-2145.

[213] F. Zeng, S. Ali, H. Zhang, Y. Ouyang, B. Qiu, F. Wu, G.J. Zhang, The influence of pH and organic matter content in paddy soil on heavy metal availability and their uptake by rice plants, Environmental Pollution 159(1) (2011) 84-91.

[214] R. Kermer, S. Hedrich, S. Bellenberg, B. Brett, D. Schrader, P. Schoenherr, M. Koepcke, K. Siewert, N. Guenther, T. Gehrke, Lignite ash: Waste material or potential resource-Investigation of metal recovery and utilization options, Hydrometallurgy 168 (2017) 141-152.

[215] R. Pinton, S. Cesco, M. De Nobili, S. Santi, Z. Varanini, Water-and pyrophosphate-extractable humic substances fractions as a source of iron for Fe-deficient cucumber plants, Biology and Fertility of Soils 26(1) (1997) 23-27.

[216] Straits Research, Humic Acid Market is projected to reach USD 1.46 Billion by 2030, growing at a CAGR of 12%, Straits Research (2022).

Chapter 3

KOH catalyzed oxidation of kraft lignin to produce green fertilizer

*S. Sutradhar, N. Alam, L.P. Christopher, P. Fatehi, KOH catalyzed oxidation of kraft lignin to produce green fertilizer, Catalysis Today 404 (2022) 49-62.

Abstract

Due to the population growth, there is an urgent need for sustainable technologies and products to address the imbalance between the availability of arable land and growing food needs. Increasing crop productivity in a cost-efficient and environmentally-friendly pathway is one approach to address this issue. In this study, lignin, a low-cost and underutilized biomass

by-product of the pulping industry, was converted to a fertilizer via oxidation in the presence of KOH. The oxidation of lignin in water (15 wt.%) under the conditions of 195 °C temperature, 300 psi pressure, and KOH dosage of 30 wt.% (based on dried lignin) generated water-soluble lignin enriched with carboxylate groups. The X-ray photoelectron spectroscopy (XPS) and proton nuclear magnetic resonance (^{1}H NMR) analyses confirmed the introduction of carboxylate groups to lignin, while ^{31}P NMR and heteronuclear single quantum coherence (HSQC) NMR studies confirmed the alterations in the aliphatic and aromatic structures of lignin. The fertilizing effects of oxidized lignin were investigated on *Zea mays* (maize) plants. The results confirmed that the average length and dry weight of the plants grown in the presence of oxidized kraft lignin were 27% and 92% greater than those produced without lignin, and they were 12% and 81% higher than those grown in the presence of humic acid, respectively. After 30 days, the plants grown in the presence of oxidized kraft lignin contained 14% and 32% more chlorophyll than those generated in the presence of humic acid and control samples, respectively. Finally, the ash content analysis of the plants shows that applying oxidized kraft lignin as a fertilizer can reduce the ash content and increase the organic content of plants. These results confirmed that the oxidation of kraft lignin in the presence of KOH could be a strategy to induce a green fertilizer for crop cultivation.

Keywords: Biomass, lignin oxidation, catalytic reaction, humic substances, organic fertilizer, crop productivity

3.1. Introduction

Currently, NPK-based fertilizers are dominant for crop cultivations. However, the continual misuse of NPK-based chemical fertilizers has caused severe ecological problems, soil erosion,

and water contamination. The chemical fertilizers would deteriorate soil health and reduce crop quality and productivity due to nutrient imbalance between inorganic and organic substances [1, 2]. Inorganic fertilizers also cause soil compaction and organic reduction in agricultural land. Another disadvantage of these fertilizers is associated with the enhanced plant susceptibility to pathogens [3]. Furthermore, nitrogen and other inorganic fertilizers can seep through the soil into the groundwater, leading to oxygen deprivation that disrupts the aquatic microflora, fish, and ecosystem balance of crustaceans, followed by eutrophication [3, 4]. Moreover, the decomposition of N-containing substances in soil and contaminated waters would result in nitrous oxide, i.e., a potent greenhouse gas (GHG) [5]. If consumed by humans, chemical fertilizers may increase the risk of developing fatal diseases in human bodies due to their heavy metal contaminations [1, 6, 7].

As the damage of chemical fertilizers to the environment and human health is significant and cumulative, there is a growing need for developing alternative and eco-friendly fertilizers. According to projections from the food and agriculture organization (FAO) of the United Nations, the world's population will increase by 34%, and the food requirement will increase by 70% by 2050 [8]. This high-priority challenge calls for developing renewable and sustainable biofertilizers, plant stimulants, and soil conditioners to increase crop productivity, thereby addressing the growing food needs in a cost-efficient and environmentally friendly pathway.

Natural humic substances (HS) have been utilized as soil conditioners and fertilizers. Approximately 70% of HS is composed of humic acid (HA), which improves soil fertility and crop productivity [9-12]. Commercially, HA is extracted from coal-derived lignite and leonardite [13]. Natural HS resources are limited, and their quality varies in different places [14]. Furthermore, as the soil contains the maximum organic carbon on Earth, natural HS may release

more carbon into the atmosphere while they are extracted for HA production [15]. In this regard, renewable resources, such as agri-waste/compost [16-18], protein hydrolysates [19], biomass-derived phenolic extracts [20], and lignin [21, 22] could be the alternative resources for artificial HS production.

Lignin is the second most abundant biopolymer on Earth, but it has received little attention for green chemicals, specifically fertilizer productions. Kraft lignin (KL) is produced in the sulfate pulping process, which accounts for nearly 85% of the world's total lignin production [23]. Among technical lignin, KL has the highest phenolic hydroxyl groups and a significant amount of quinone, catechol, and carboxylate groups [24, 25]. KL can be functionalized for potential uses as fertilizers. However, there is a lack of information on converting KL to fertilizers.

The impact of aromatic compounds and lignin-derived materials on plant growth was studied in the past. Polymeric products obtained from the oxidative polymerization of natural phenols, such as catechol and vanillic acid, effectively enhanced the germination and salt tolerance of Arabidopsis plants (rockcress) [13]. Moreover, oxygenated functional groups, such as phenolic-OH carboxylic-OH, in HS were found to have beneficial effects on plant physiology [26, 27]. The carboxylic groups of HS can interact with the metal ions and enhance the mobility of the minerals in soil [28]. Several earlier studies reported that alkaline oxidation of lignin improves water solubility by increasing its carboxylic content [29-31]. Ertani and coworkers stated that applying potassium lignosulfonate-humate resulted in a notable increase in the leaves and roots, chlorophyll content, and enzyme activity of Zea mays L. plants. Savy and coworkers demonstrated that the soluble fractions of lignin from eucalyptus, poplar, cardoon, giant reed, and miscanthus exhibited bioactivity toward maize plants, such as gibberellin (GA) and the early plant (i.e., 8 days old) growth [22, 29, 30]. In one study, the Fenton reagent-based oxidized KL

(860 mg/L) was applied to *Arabidopsis thaliana* seeds to observe the germination, and the results showed that the chlorophyll content of the seedlings was increased by 15 % [27]. However, the Fenton based oxidized KL was not claimed to be water soluble. Savy and coworkers reported that the humic-like water-soluble lignin fractions would significantly enhance plant biostimulation activities [22]. In another study, lignin was isolated from cardoon and eucalyptus wood species via an alkaline oxidative hydrolysis process and oxidized with hydrogen peroxide to produce water-soluble lignin [30]. The use of the product on maize plants showed increased primary roots and early shoots by 42% and 46%, respectively [30]. Despite promising results, literature gaps exist in understanding the long-term effect of water-soluble oxidized kraft lignin on plants. Most studies were conducted for the early-stage germination, while in the current study, the impact of KOH oxidized KL was applied to maize seedlings to observe the physiological response of the plant in 40 days of growing. Also, the effects of chemical and structural properties of modified KLs (MKLs) on plants were assessed in this work. Based on our literature search, no other studies exploited the oxidation of KL in the presence of KOH and oxygen gas in a pot system to generate a product that is considered a ready-to-use fertilizer for maize seedlings. Moreover, such an oxidation process is considered green since green raw material (lignin) and solvent (water) were used in the process, and no other harmful chemicals were involved in the oxidation reaction [32]. This process generates only one product, which is a green fertilizer, and no other by-product is produced that needs to be disposed of or treated.

In the current study, kraft lignin was oxidized by oxygen gas in the presence of KOH. The objectives of this study were to 1) investigate the impact of oxidation on the chemical structures of kraft lignin, 2) generate oxidized water-soluble lignin with a desirable amount of carboxylate groups, and 3) assess the impact of oxidized lignin as a fertilizer on the growth of *Zea mays*. The

primary novelty of this work was the production of potassium-enriched water-soluble oxidized KL as a fertilizer for crop growth.

3.2. Materials and methods

3.2.1. Materials

Acid-washed softwood kraft lignin (KL) was obtained from a pulp mill in Alberta, Canada, which was produced via LignoForce technology. Potassium hydroxide (KOH), hydrochloric acid (HCl), and sodium nitrate ($NaNO_3$), all analytical grades, were purchased from Fisher Scientific. Humic acid (HA), ammonium dihydrogen phosphate ($NH_4H_2PO_4$), potassium nitrate (KNO_3), calcium nitrate ($Ca(NO_3)_2$), magnesium sulfate ($MgSO_4$), boric acid (H_3BO_3), manganese (II) chloride tetrahydrate ($MnCl_2{\cdot}4H_2O$), zinc sulfate heptahydrate ($ZnSO_4{\cdot}7H_2O$), copper sulfate pentahydrate ($CuSO_4{\cdot}5H_2O$), molybdic acid ($H_2MoO_4{\cdot}H_2O$), ferric ethylenediaminetetraacetic acid (EDTA), 2-chloro-4,4,5,5-tetramethyl-1,3,2-dioxaphospholane (TMDP), $CDCl_3$, pyridin, cyclohexanol, chromium (III) acetylacetonate, dimethylesulphoxide-d6 (DMSO-d6), deuterium oxide (D_2O), and p-hydroxy benzoic acid, DMSO, all analytical grades, were purchased from Sigma Aldrich and applied as received. Vermiculite (Holiday Vermiculite) was purchased from a local supplier in Northern Ontario.

3.2.2. Lignin oxidation

The oxidation of KL was conducted following the alkaline wet oxidation method. First, KL was mixed with 200 mL of 4.5 wt% potassium hydroxide solution. Then, the mixed solution was placed in a Parr reactor, 4848 (Illinois, USA), and oxidized with oxygen gas under different temperatures (130-260 °C) and pressures (200-640 psi). Oxidized lignin of MKL-1, MLK-2, and MKL-3 were produced under a continuous oxygen supply at a 7 mL/min flow rate, whereas

MKL-4 and MKL-5 were made under an initial 200 psi oxygen pressure in a closed environment. The initial pH of the experiment was 12.8-13, while the final pH of the reactions was 8.5-9.7. After the reaction, the oxidized lignin solution was transferred into a beaker. Then, one part of the samples was dried at 60°C for 48 h and used for plant growth. Another part of the sample was dialyzed for chemical analysis. After that, the solid content of the oxidized lignin solution was measured to identify the yield of oxidized lignin production. Detailed experimental conditions are shown in Table 3.1.

3.2.3. Elemental analysis

The organic elements of the samples were determined using an Elemental analyzer (Vario EL Cube, Germany) following the previously described combustion method [33]. The oxygen and hydrogen elements of the samples were determined to predict the methoxyl group of the samples following equation 1 [34].

OCH_3 (wt%) = -18.5769 + 4.0658 × (H wt%) + 0.34543 (O wt%) (1)

The inorganic elements of the samples were analyzed with a Varian Vista-PRO simultaneous Inductively coupled plasma - optical emission spectrometry (ICP-OES), Mulgrave, Australia. Briefly, 0.5 g of the samples were digested in a mixture of 4.5/1.5 mL/mL HNO_3/HCl ratio using a CEM MARS XPRESS microwave and closed perfluoroalkoxy (PFA) vessels. The microwave (1000 W) was set at 170 ºC for 20 minutes. After cooling, the samples were transferred to 50 mL polyethylene tubes, and their total volumes were fixed at 25 mL via adding deionized water. A 12 mL aliquot of these samples was filtered using 0.45 µm syringe filters. The inorganic elements of these samples were analyzed by the ICP-OES as stated above [35].

3.2.4. Carboxylic acid content analysis

According to the method described previously, the carboxylate group of the samples was determined by an automatic potentiometric titrator (785-DMP Titrino, Metrohm, Switzerland) [36]. Briefly, 1 mL of 0.8M standard KOH was mixed with 0.06 g of lignin sample. Then, 100 mL of deionized water was added to dissolve the sample. After that, 4 mL of 0.5 wt% p-hydroxy benzoic acid was added to the mixture, and the mixture was stirred for 15 min. Then, the titrator titrated the solution against 0.1 M standard HCl, and the endpoints were recorded. Equation 2 was used for analyzing the carboxylate group content of the products.

$$\textbf{Carboxylic group } \left(\frac{\textbf{mmol}}{\textbf{g}}\right) = \frac{\{(\textbf{Ep}'\textbf{3}-\textbf{Ep}'\textbf{2})-(\textbf{Ep3}-\textbf{Ep2})\} \times \textbf{C}}{\textbf{m}} \qquad (2)$$

Ep_3 and Ep_2 are the volume (mL) of HCl consumed at the second and third endpoints during the titration of blank, respectively, and Ep'_3 and Ep'_2 are the endpoints for the titration of MKLs. Also, C is the concentration (M) of standard HCl; m is the dry mass (g) of the sample used in the analysis.

3.2.5. Molecular weight analysis

The molecular weight of the MKL samples was determined using a Gel Permeation Chromatography (GPC), Malvern GPCmax VE2001 Module + Viscotek TDA305 (Malvern, UK) with multi-detectors (UV, RI, IV-DP, low angle, and right-angle laser detectors). The samples were dissolved in 0.1 mol/L $NaNO_3$ solutions, and their pH was adjusted to 7. A 0.2 µm nylon filter was used to filter the sample solutions, and the filtered solutions were used for the molecular weight analysis. The columns of PolyAnalytic PAA206 and PAA203 were used in the analysis. Also, 0.1 mol/L $NaNO_3$ solutions were used as solvent and eluent. The flow rate in the GPC instrument was set at 0.70 mL/min, while the column temperature was 35 °C, and poly (ethylene oxide) was used as standard samples for this aqueous GPC system [37]. The molecular weight of KL was determined according to previously described methods [38, 39]. Briefly, 100

mg sample was dissolved in 10 mL 1:1 (v/v) acetic anhydride and pyridine solution in a glass vial and stirred for 30 mins. Then, the vial was kept in the dark chamber at room temperature for 24 h. After that, the mixture was added dropwise to 200 mL of cold water to precipitate the KL and centrifuged three times to remove the solvents. Then, the acetylated KL was lyophilized and redissolved in 10 mL of DMSO. Then, the sample was analyzed by high-performance liquid chromatography (HPLC), Agilent model 1200 (USA) equipped with UV and a multi-angle laser light detector. Styragel HR4, HR4E and HR1 columns were used for the analysis. The analysis was carried out for 50 min at a 1 mL/min flow rate and the column temperature was set at 35 °C. HPLC grade DMSO was used as an eluent for this analysis.

3.2.6. Fourier Transform Infrared Spectroscopy (FTIR)

FTIR analysis was performed using a Bruker Tensor 37 (Bruker, Germany) with a PIKE MIRacle Diamond Attenuated Total Reflectance (ATR) accessory to observe the functional groups of lignin derivatives. Dried ground lignin derivatives (60-80 mg) were placed on the ATR crystal of this instrument. In this analysis, 32 scans were conducted at 500 and 4000 cm^{-1} with a resolution of 4 cm^{-1}.

3.2.7. X-ray photoelectron spectroscopy (XPS)

The XPS analysis of lignin samples was carried out according to the previously described method using Kratos AXIS Supra, Japan, with the monochromatic AL anode (1486.6 eV) [40]. In this set of experiments, 375 W of X-Ray was used to analyze the dried samples. The number of steps, dwell, and sweep times were 230 ms, 260 ms, and 60 s, respectively. ESCApe software (V1.2.0.1325) was used for analyzing the data points. Also, the elemental analysis of the ash of plants was determined following the previously described procedure [41].

3.2.8. NMR analysis

The ^{1}H-NMR, HSQC NMR, and ^{13}P-NMR spectra of the samples were recorded using a Bruker AVANCE Neo NMR-500 MHz instrument (Switzerland) and Topspin 4.02 version software. For H-NMR analysis, 40-45 mg of the samples were dissolved in 2 mL of DMSO-d_6 (for KL) and D_2O (for MKLs), respectively. Afterward, 1 mL of each solution was transferred into the NMR tube for analysis. For HSQC NMR analysis, 0.08 g of KL and 0.05 g of MKLs were dissolved in 1 mL of DMSO-d_6 separately, and then the solutions were taken to NMR tubes for analysis. Sixty-four scans were recorded, and the pulse width was 90° in the NMR analysis for both ^{1}H-NMR and HSQC NMR.

The ^{13}P-NMR analysis was performed to measure the phenolic and aliphatic hydroxyl groups of KL and MKLs. Briefly, around 20 mg of dried lignin samples were dissolved in 500 µL of a mixture of $CDCl_3$ and pyridine (1:1.6 vol/vol). The phosphitylation of the lignin samples was carried out with 100 µL of 2-chloro-4,4,5,5-tetramethyl-1,3,2-dioxaphospholane (TMDP). Then, 50 µL (20 g/L) of cyclohexanol, as an internal standard, and 52 µL (5 g/L) of chromium (III) acetylacetonate, as a relaxation agent, were individually mixed with $CDCl_3$/Pyridine mixture and added to the sample. Two hundred fifty-six scans were recorded with 90° pulse width and 5s relaxation delay. The quantification of the hydroxyl groups of the samples was carried out as reported previously in the literature [42]. Due to the poor solubility of MKL-5 in the solvents, the P-NMR of this sample could not be carried out.

3.2.9. Hoagland solution preparation

According to the procedure described previously, Hoagland solution (i.e., plant essential micro and macronutrient solution) was prepared and used as plant nutrient supply [43]. Briefly, 1, 6, 2, and 4 mL of $NH_4H_2PO_4$, KNO_3, $Ca(NO_3)_2$, and $MgSO_4$ solutions (all in 1 mol/L concentration) were added to 1 L of water (denoted as a nutrient solution), respectively. Another stock solution

(denoted as micronutrient stock) was prepared by dissolving 2.86 g of H_3BO_3, 1.81 g of $MnCl_2.4H_2O$, 0.22 g of $ZnSO_4.7H_2O$, 0.08 g of $CuSO_4.5H_2O$, and 0.02 g of $H_2MoO_4.H_2O$ in 1 L of deionized water. Then, 1 mL of the mixture was mixed with the nutrient solution. An iron stock solution was also prepared by adding 5 wt.% of $FeSO_4.7H_2O$ and 9.1wt.% of EDTA in water. Then, 0.25 mL of this stock solution was added to the previously mentioned 1 L nutrient solution. This final nutrient solution mixture was called the Hoagland solution and was considered the blank solution for crop cultivation in the study.

3.2.10. Pot test with vermiculite

In this set of experiments, 5-inch square pots were filled with vermiculite and seven Zea mays (corn) seeds. Then, 200 mL of the nutrient solution was added to the pots every 60 hours. The pots were placed in a dark room with 600W indoor LED UV grow light (as a light source for plants) and a temperature of 22-25 °C. The UV light was maintained for 14 h of continuous light and 10 h of darkness. Plants were allowed to grow in the first 15 days with only Hoagland solution. Then, 10 mg of carbon/liter (C/L) of MKLs and HA were dissolved in the Hoagland solution separately and added to the assigned pots. One set of experiments was conducted with the Hoagland solution as the blank sample. The plants were collected after 20, 30, and 40 days. The length of fresh plants was measured, and then the plants were dried for 72 h at 70°C to determine the dried weight of each plant. The roots' weights were not measured in this experiment because of the contamination from the attached vermiculite. Two pots for each set of experiments were used, and seven plants were in every pot.

3.2.11. Chlorophyll content determination

For the chlorophyll content determination, 100 mg of a fresh leaf of the grown plants (collected after 20, 30, and 40 days) was placed in a 12 mL vial containing 7 mL of dimethyl sulfoxide (DMSO). The mixtures were incubated at 65°C for 30 min, and then incubated extracts were diluted with DMSO to 10 mL. Produced extracts were transferred to a cuvette, and the absorbance at 645 nm for chlorophyll A (Chl A) and at 663 nm for chlorophyll B (Chl B) was measured against DMSO according to the literature [44]. The sum of the Chl A and Chl B concentrations represents the total chlorophyll content of the plants. The chlorophyll content was measured by taking different parts of leaf samples, and each experiment was carried out three times, and the average values were reported in this work.

3.2.12. Ash content analysis of plants

The ash content of the plants was determined according to the Tappi standard method T-211 om-02 [45]. Briefly, 2-3 g of the dry plant (previously cut) was taken in a percaline crucible and carbonized in a muffle furnace at 525±25 °C until no black char was observed. After the ignition, their ash content was determined according to the standard method.

3.3. Results and discussion

3.3.1. Effect of reaction parameters on MKL properties

The impacts of reaction time (20-180 min), temperature (130-260 °C), and initial pressure (200-300 psi) on MKL properties were studied, and the results are reported in Table 3.1. With

increasing the reaction temperature and oxygen pressure, the pH dropped from 13 to 8.6 (for MKL-3), indicating the increased concentration of acids in the solution, which may originate from carboxylate groups introduced to lignin. In a previous study, the oxidation of alkali lignin (4 wt.% concentration) at 225°C and 15 bar oxygen pressure for 60 min at pH 6 converted 20% of lignin to organic acids (e.g., formic acid, acetic acid, oxalic acid) [46]. In the current experiments, the final pH was kept in the range of 8.5-9.5 so that the degradation of lignin to aliphatic acids could be limited while carboxylate groups could be introduced to lignin [21]. In Table 3.1, it can be observed that the reaction time could drop from 180 to 20 minutes with increasing temperature from 130 to 260 °C while achieving the desired pH. Table 1 also presents that the -COOH content of the MKLs was higher than that of KL. In this case, the -COOH content was increased to 2.26 mmol/g in MKL-3 at 195°C temperature and 300 psi constant oxygen pressure; however, upon increasing the reaction temperature to 260 °C and pressure to 640 psi (200 psi oxygen and 440 psi vapor pressure), the -COOH content decreased to 1.7 mmol/g in MKL-5. However, all the MKLs were completely soluble in deionized at pH 7.

Also, the M_w of the MKLs was approximately 2,000 g/mol with similar M_n and polydispersity (Table 3.1), but such molecular weights were lower than those of KL. It can be observed that Mn seemed to have increased after oxidation, which is most probably associated with experimental errors related to the difference in the molecular weight analysis. In other words, two different systems were used for determining the molecular weight of oxidized and water-insoluble lignin, and the systems had different columns, detectors, and other parts. Also, unmodified lignin was acetylated before its molecular weight analysis. These reasons might have contributed to the slight increase in the Mn of oxidized samples (compared with unmodified KL). Another possible reason for the increased molecular weight of lignin might be the repolymerization of lignin at a

higher oxidation temperature, as seen in the ^{31}P-NMR results [47]. Interestingly, the results indicated an improvement (from 6.7 to 1.5) in the polydispersity of the lignin via oxidation, which would be probably due to the cleavage of the β-O-4, β-β linkages, and some C-C breaking [31, 48]. The total yields of the oxidation reactions are also available in Table 3.1. It can be seen that the yield of oxidation dropped as the temperature increased. However, the MKL-3 had the highest yield of 90.8% and more carboxylic acid groups than the other MKLs. The minimum yield was found for MKL-5 due to the extensive depolymerization of the KL at a higher temperature. An earlier study reported that the alkaline oxidation of alkali lignin at 225 ºC would cause the decomposition of the carboxylate groups of lignin to CO_2 and water and other lower molecular weight acids [46]. Similar results were reported in another study where lignosulfonates were oxidized with hydrogen peroxide/air to produce humic salts [21].

In the current study, the oxygen consumption was not recorded in the first three experiments (MKL-1 to MKL-3) due to the continuous supply of oxygen. Still, approximately 60 psi oxygen was consumed for MKL-4 and MKL-5 productions. Considering the results of Table 3.1, it can be stated that the conditions for MKL-3 preparation were better than those for other samples.

It is also seen that HA had slightly higher M_w and M_n but similar COOH. In earlier studies, the COOH content of soil-based HA was 2.8 mmol/g [49] and its M_w was in the range of 3,500 to 20,000 g/mol [50].

Table 3.1**:** Experimental conditions for the KL oxidation and properties of KL and HA

Sample	**T, °C**	**P_i, psi**	**P_f, psi**	**Time, min**	**Final pH**	**Yield, %**	**M_w, g/mol**	**M_n, g/mol**	**M_w/M_n**	***COOH content,**

										mmol/g
KL	N/A	N/A	N/A	N/A	N/A	N/A	6970	1060	6.7	0.16
MKL-1	130	200	200	180	9.7	93.6	1940	1280	1.5	1.18
MKL-2	160	250	250	90	9.2	90.5	1970	1380	1.4	1.46
MKL-3	195	300	300	70	8.6	90.8	1970	1350	1.5	2.26
MKL-4	230	200	410	40	8.7	84.6	2050	1360	1.5	2.00
MKL-5	260	200	640	20	9.5	79.5	1960	1300	1.5	1.70
HA	N/A	N/A	N/A	N/A	N/A	N/A	3000	2030	1.5	2.04

T=Temperature; P_i=Initial oxygen pressure; P_f= Final pressure during reaction; *COOH content determined by potentiometric titration; N/A=Not applicable.

Table 3.2 provides the amounts of organic elements, potassium, sodium, and calculated methoxyl group of the samples. Interestingly, the potassium content of all samples was higher than that of KL as the reaction was carried out in the presence of KOH. In another study, lignosulfonate was converted to humates in the presence of NaOH, and a significant amount of sodium was detected in the product [21]. In our current study, the potassium ion may attach ionically with the carboxylic acid groups to form salts in MKLs.

Also, it can be observed that the carbon element and OCH_3 contents of the lignin derivatives decreased while their oxygen content increased. The results in Table 3.2 show that the C/O ratio in KL was 2.4, whereas the ratio was reduced to 1.5 in MKLs. In another study, it was observed that, after the oxidation of KL with H_2O_2, the C/O ratio was decreased from 3.2 to 2.6 [31]. As expected, the hydrogen content of KL dropped via oxidation, as also reported in another study on the oxidation of lignin with NaOCl [51]. Also, it can be observed that the S content, originating

from KL production from black liquor via LignoForce technology, decreased from 1.93 to 0.93 wt.% (in MKL-4). The sulfur element may convert to their oxides during oxidation. In the current study, lignin demethylation promoted di-hydroxyphenolic units (catechols), initiating aliphatic carboxylate end formation [21]. Gladkov and coworkers also observed a significant rise (two folds) in the COOH group (12-20 wt.%) when conducting alkaline oxidation of lignosulfonate with oxygen/air (0.5-3 MPa) at 170-210 ºC temperature [21].

In our current study, the primary objective was to increase the carboxylic acid group and potassium content of lignin. Among the five samples, MKL-3 had the highest amount of -COOH content, which was selected for further analysis. Also, HA had lower potassium, carbon, and methoxyl group but similar oxygen content. HA reported in another study had similar elemental compositions to that reported in the current study [52].

Table 3.2: Organic and primary inorganic elements (wt.%) of lignin derivatives and HA.

Sample	K, wt%	Na, wt%	C, wt%	H, wt%	S, wt%	O, wt%	OCH_3, wt%
KL	0.03	0.43	64.48	5.55	1.93	27.21	13.39
MKL-1	11.7	0.23	49.33	3.56	1.24	32.04	6.97
MKL-2	12	0.24	50.15	4.01	1.2	31.16	8.47
MKL-3	12	0.23	50.1	3.37	1.01	31.58	6.03
MKL-4	11.9	0.25	51.05	3.92	0.91	30.3	7.83
MKL-5	12.8	0.24	50.51	3.28	1.51	29.3	4.87
HA	1.72	3.67	43.42	1.9	0.34	33.05	0.56

3.3.2. FTIR analysis

Figure 3.1 represents the FTIR spectra of KL and MKL-3. The broadband at 3360 cm^{-1} in KL is

for phenolic and aliphatic hydroxyl groups, which became weaker in the MKL sample due to oxidation. The peaks at 2875 cm^{-1} represent the aromatic methoxyl groups and the methyl/methylene groups attached to the side chain of the aromatic ring of lignin. A significant change in the spectral band is observed near 1705 cm^{-1} and 1600 cm^{-1}, which is the characteristic peak of C=O stretching for aromatic ring vibration and deformation [36]. The pulse at 1480 cm^{-1} can be attributed to the aromatic structure deformation [53]. The degraded aromatic guaiacyl units can be observed from the peak regions between 1390 and 1375 cm^{-1} [36]. The FTIR spectra for the samples of MKL-1, MKL-2, MKL-4, and MKL-5 are available in the supplementary file (Figure A3.1).

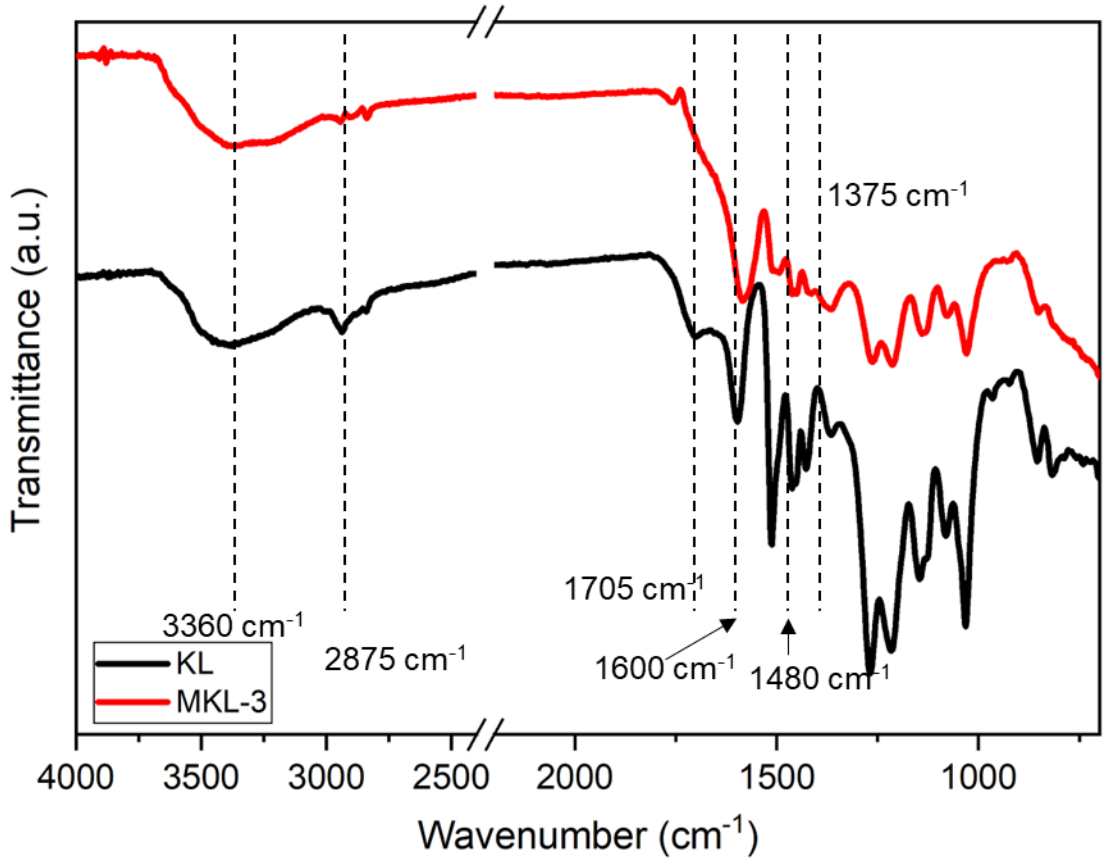

Figure 3.1: FTIR spectra of KL and MKL-3

3.3.3. XPS analysis

The XPS survey spectra and scan of C 1s for KL and MKL-3 are illustrated in Figure 3.2. In the survey spectra, the peaks that appeared at 285 and 532 eV are attributed to C1s and O1s, respectively. The only peak that appeared in MKL-3 at 378 eV corresponds to K1s that may come from the residual KOH or K^+ that are ionically attached to carboxylate ions. From the XPS scan, the primary binding energy at 285.4, 286.4, and 289.3 eV in KL are assigned to the C-C, -C-O- and C=O groups [54]. The results show that the alkaline oxidation significantly increased the C=O (289.2 eV) content in MKL-3 and decreased the C-C (284.3 eV) and -C-O- (286.8) contents of KL. These results are consistent with the FTIR and NMR results. The XPS spectrum and C1s scans for the samples of MKL-1, MKL-2, and MKL-4 are presented in the supplementary file (Figure A3.2).

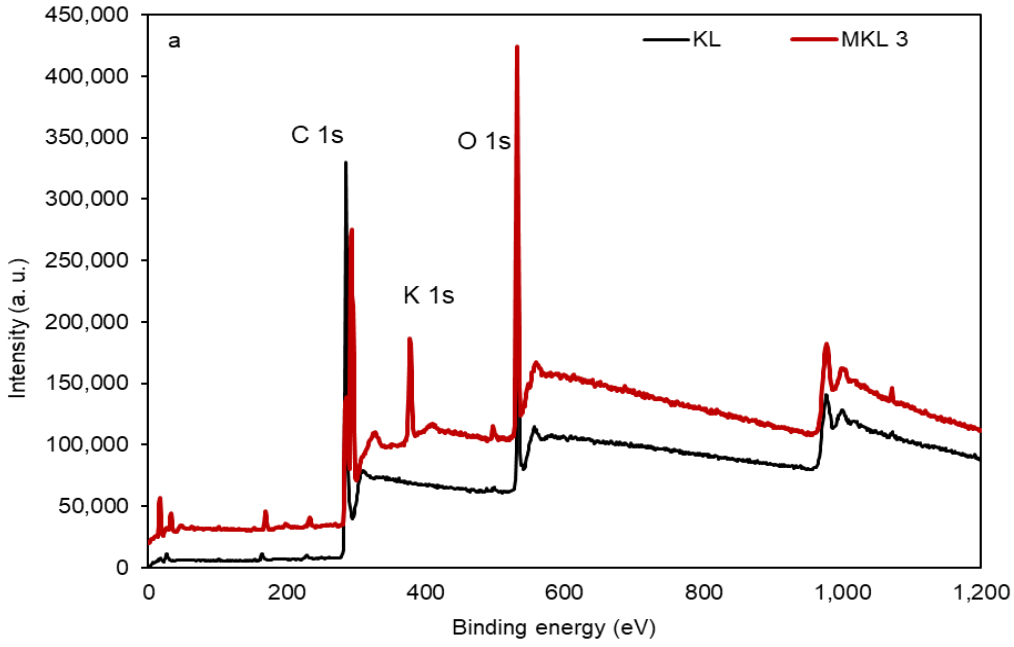

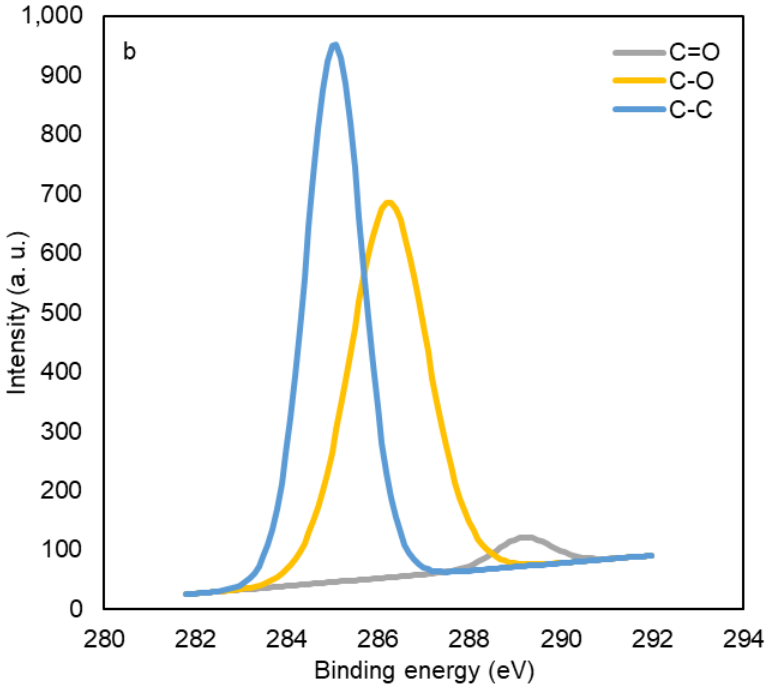
b
C=O
C-O
C-C
Intensity (a. u.)
Binding energy (eV)
1,000
900
800
700
600
500
400
300
200
100
0
280
282
284
286
288
290
292
294

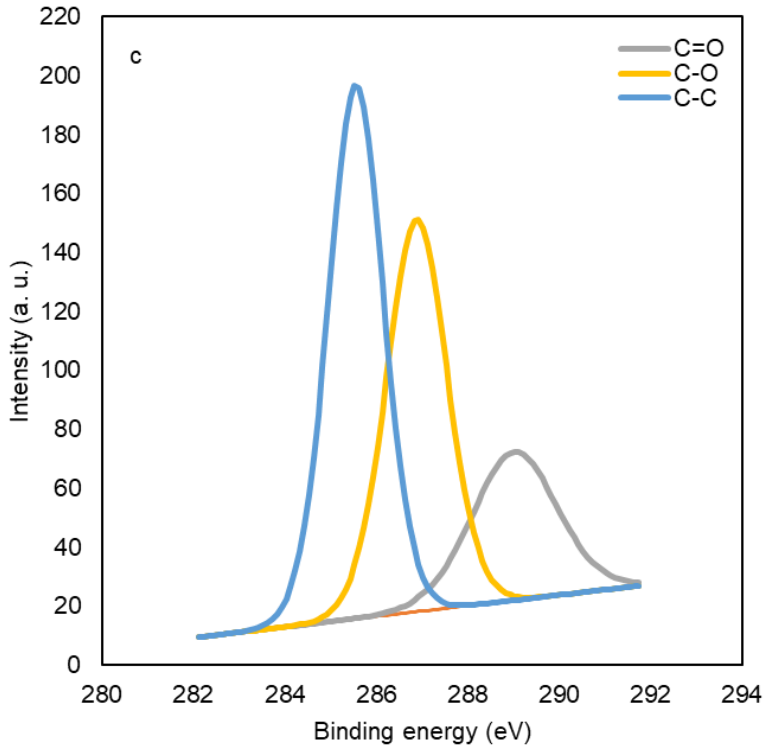
c
C=O
C-O
C-C
Intensity (a. u.)
Binding energy (eV)
220
200
180
160
140
120
100
80
60
40
20
0
280
282
284
286
288
290
292
294

Figure 3.2: a) XPS survey spectra of KL and MKL-3; b) XPS scan (C 1s) for the KL and c) for the MKL-3.

3.3.4. ^{1}H-NMR analysis

Figure 3.3 shows the H-NMR spectra of KL and MKL-3. The long sharp peaks at 2.5 ppm and 4.6 ppm are attributed to DMSO and D_2O in the KL and MKL-3 solutions, respectively [55]. The signals between 3.2 to 4.0 ppm are attributed to the methoxyl protons. The dramatically reduced peaks in the MKL suggest that the oxidation reaction degraded the methoxyl content in the MKL. Simultaneously, the large sharp peak at 8.6 ppm in the MKL represents the signal for the carboxylate group [56]. The peaks in the range of 6.4-7.5 ppm are attributed to the aromatic protons of lignin [57]. In the MKL spectrum, the peaks that appeared at 1-3 ppm are attributed to the aliphatic protons generated via cleaving the aromatic ring of KL [55, 57]. The ^{1}H-NMR spectra for the MKL-1, MKL-2, and MKL-4 are available in the supplementary file (Figure A3.3).

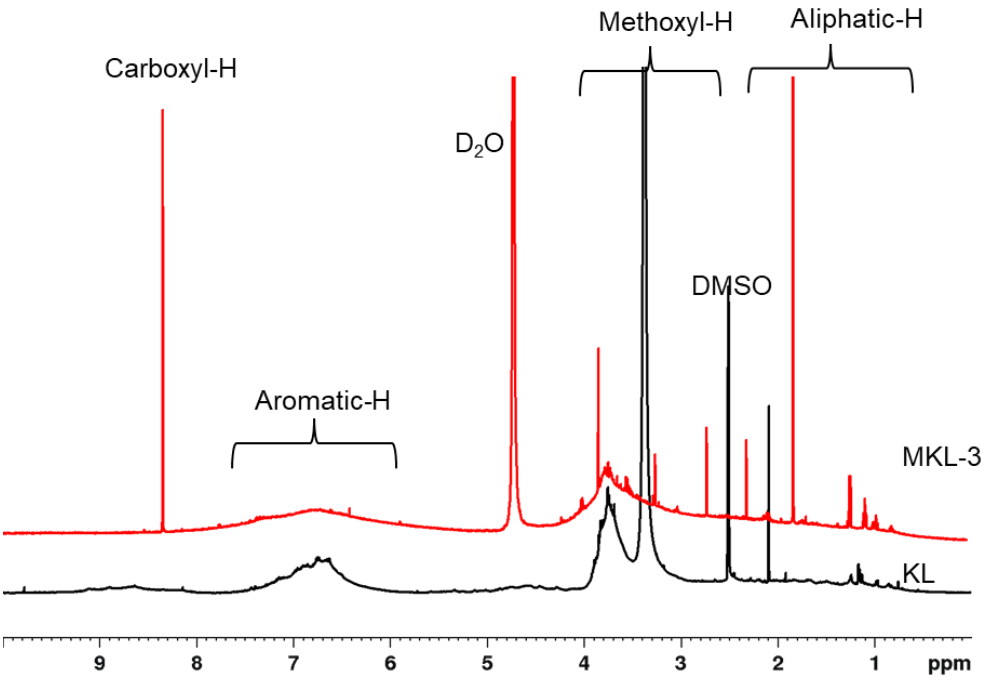

Figure 3.3: 1H-NMR spectra of KL and MKL-3.

3.3.5. ^{13}P-NMR analysis

Figure 3.4 exhibits the ^{13}P-NMR of KL and MKL-3. Based on these results, the concentration of the hydroxy groups of lignin derivatives was quantitatively determined, and the results are available in Table 3.3. As seen, a considerably higher carboxylate-OH (up to 2.07 mmol/g) was observed in MKL-3 than KL (0.43 mmol/g). The total aliphatic-OH, phenolic-OH, and carboxylate-OH of KL were found to be 2.45, 5.89, and 0.43 mmol/g, respectively, which is consistent with a previously reported study [58]. In another study, KL was oxidized with hydrogen peroxide, and the oxidized lignin had a carboxylate content of 0.4-0.7 mmol/g [59]. The oxidation of lignin reduced the aliphatic-OH (up to 46%) and phenolic-OH (up to 35%) of KL significantly (Table 3.3). Moreover, an approximately 57% reduction in the catechol content of KL was observed via oxidation (comparing KL and MKL-3), which can be attributed to the

cleavage of the aromatic ring of KL to produce muconic acid-like structure [60]. Also, the guaiacyl OH, and the C-5 substituted OH groups were decreased by 46% and 42% via oxidation, respectively, which is consistent with a previously reported study [61]. However, it can be seen that the condensed C-5 substituted -OH is significantly higher and the -COOH is lower in MKL-4 than in MKL-3. Gladkov and coworkers reported that the alkaline oxidation of lignosulfonate may re-polymerize to condensed phenolic structures at a temperature higher than 210 ºC [21]. ^{13}P-NMR spectra for the MKL-1, MKL-2 and MKL-4 are available in the supplementary file (Figure A3.4).

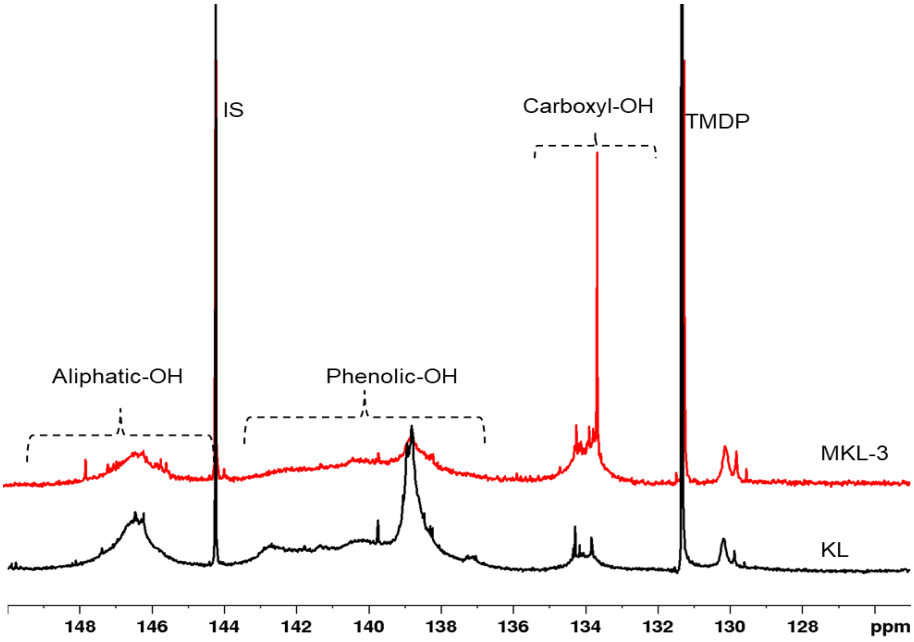

Figure 3.4: 13P-NMR spectra of KL and MKL-3.

Table 3.3: Hydroxyl contents of KL and MKLs determined from quantitative ^{13}P-NMR.

Samples	Aliphatic OH, mmol/g	Total Phenolic OH,	Syringyl OH, mmol/g	Guaiacyl OH, mmol/g	p-hydroxyphenyl OH, mmol/g	C-5 substituted OH,	Catechol, mmol/g	Carboxyl-OH, mmol/g

	mmol/g					mmol/g		
KL	2.45	5.89	0.54	1.10	0.17	1.83	2.36	0.43
MKL 1	1.94	4.40	0.45	0.85	0.11	1.63	1.44	1.06
MKL 2	1.75	4.27	0.41	0.69	0.08	1.51	1.42	1.41
MKL 3	1.34	3.87	0.35	0.60	0.10	1.06	1.01	2.07
MKL 4	1.83	3.68	0.39	0.50	0.10	1.63	0.87	1.76

3.3.6. HSQC NMR analysis

HSQC NMR analysis was conducted to reveal the detailed structures of the oxidized lignin. Figure 3.5 represents the aromatic (δ_C/δ_H 100-135) and C-O aliphatic (**(**δ_C/δ_H 50-90/ 2.5-6) regions of KL and MKL-3, and the appropriate signal assignments are displayed in Table 4 [62-64]. In the C-O aliphatic side chain region, the intense large peak areas at δ_C/δ_H of 56/3.6-3.9 is attributed to the C-H of methoxyl group and β-O-4' aryl ether linkages [63]. The C_α–H_α cross-signals in the β-O-4' structures are observed at δ_C/δ_H of 71.6/4.8 ppm (A_α). Moreover, the correlation signals for the β-O-4' of Cγ–Hγ were detected at 59.6-60/3.38-3.62 and C_β-H_β at 83.8/4.3 ppm. The intense cross signals for the C_α-H_α, C_β–H_β and C_γ–H_γ in phenylcoumaran substructures were observed at δ_C/δ_H, 86.8/5.5, 53.7/3.49, and 71.6/4.8, respectively. However, the S-type β-O-4' substructures were not significantly observed in the current study, which is ascribed to the abundance of G-type lignin and lack of S-type lignin in softwood kraft lignin [62].

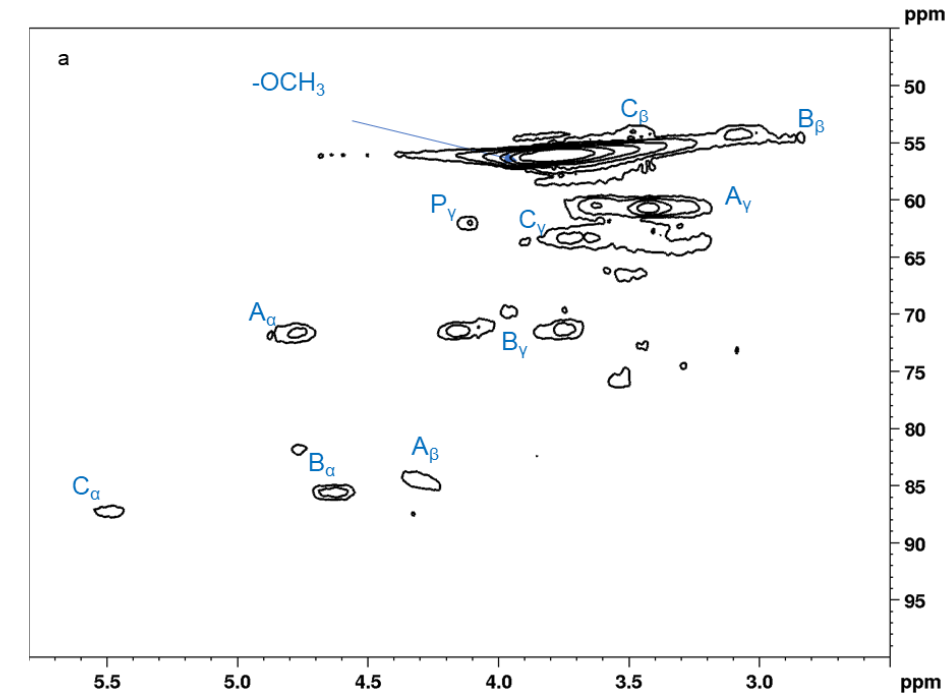
a
-OCH3
Cβ
Bβ
Pγ
Cγ
Aγ
Aα
Bγ
Bα
Aβ
Cα
ppm
50
55
60
65
70
75
80
85
90
95
5.5
5.0
4.5
4.0
3.5
3.0
ppm

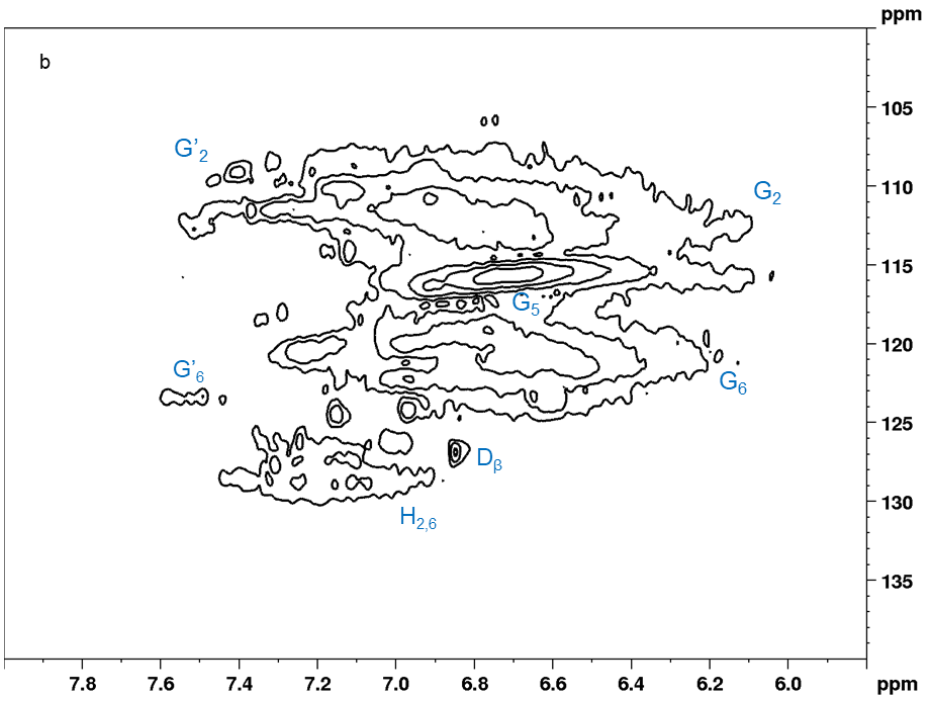
b
G'2
G2
G5
G'6
G6
Dβ
H2,6
ppm
105
110
115
120
125
130
135
7.8
7.6
7.4
7.2
7.0
6.8
6.6
6.4
6.2
6.0
ppm

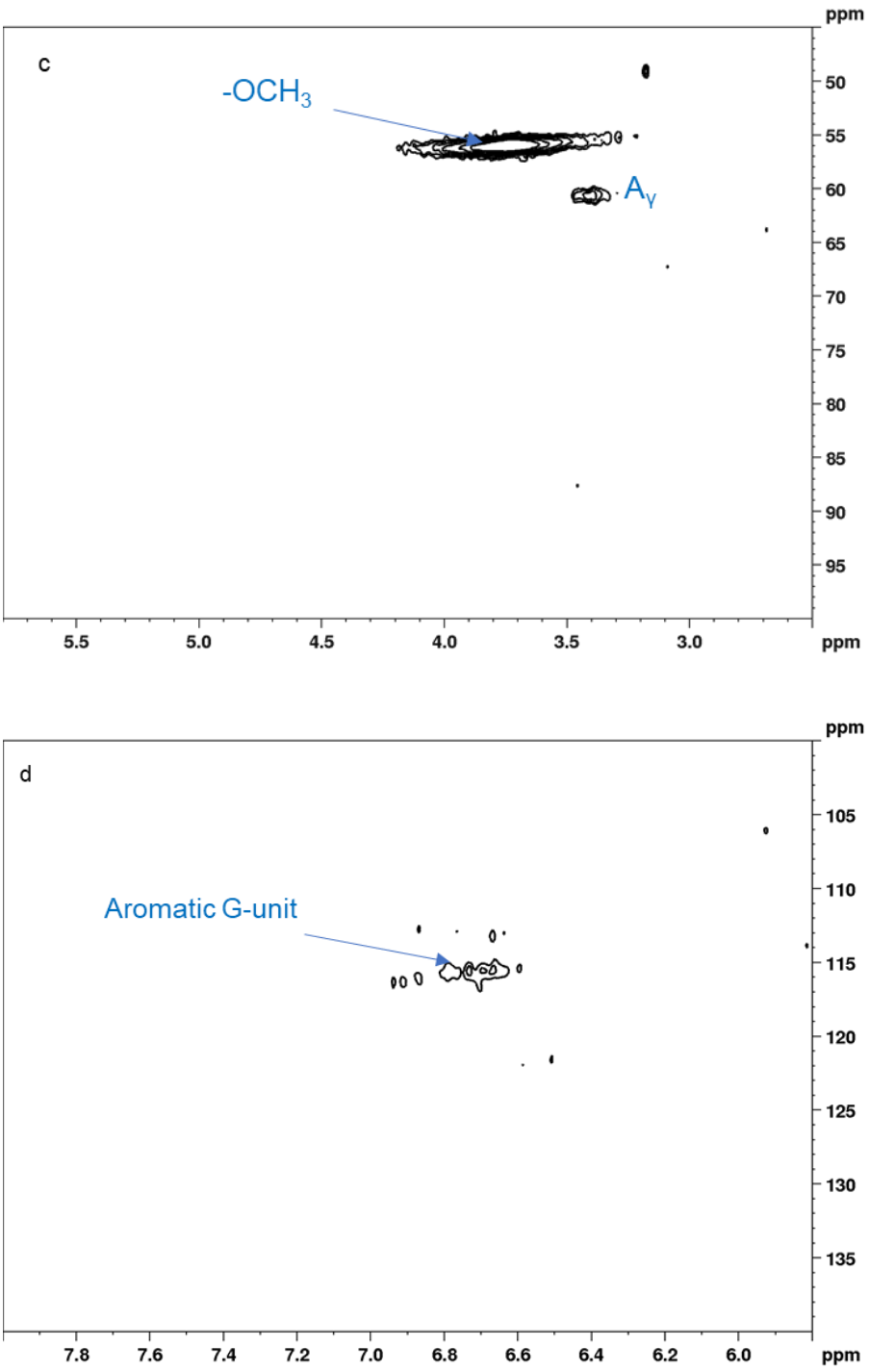

Figure 3.5: HSQC NMR spectra of KL and MKL-3; a) C-O aliphatic region (δ_C/δ_H 50-90/ 2.5-6) of KL, b) aromatic regions (δ_C/δ_H 100-135) of KL, c) C-O aliphatic region (δ_C/δ_H 50-90/ 2.5-6) of MKL-3 and d) aromatic regions (δ_C/δ_H 100-135) of MKL-3

The correlation signals at the δ_C/δ_H of 110.5/6.9, 114.9/6.76 and 119.1/6.7 could be attributed to C_2–H_2, C_5–H_5, and C_6–H_6 of guaiacyl unit, respectively [63]. Also, the cross signals at the δ_C/δ_H of 111.5/7.5 and 123.4/7.6 were related to the C_2-H_2 and C_6-H_6 in oxidized (Cα=O) guaiacyl units. Moreover, minor cross signals were detected at the δ_C/δ_H of 126.2/6.8 for C_β-H_β in cinnamaldehyde end groups (G-type) and at the δ_C/δ_H of 127/7.1 for $C_{2,6}$–$H_{2,6}$ in p-hydroxybenzoate units (H-type) [62]. The $C_{3,5}$–$H_{3,5}$ signals could be overlapped with the C_5–H_5 of the G-type lignin [64]. The HSQC spectra for the other samples (MKL-1, MKL-2, and MKL-4) are presented in the supplementary file (Figure A3.5), where a similar observation can be found.

In contrast, the intensity of C-H in methoxyl groups was smaller in MKL-3, confirming the oxidative degradation of lignin, which was also observed via ^{13}P-NMR analysis. It was also observed that the β-O-4' structures of C_α-H_α and C_β-H_β disappeared after the oxidation treatment. Most prominently, the β-β' and β-5' bonds in resinol and phenyl coumarane units degraded via oxidation. Moreover, a significant reduction in the aromatic region (Figure 3.5d for MKL-3) would show that the alkaline aerobic oxidation would lead to the aromatic ring cleavage to form muconic acid-like structures [65].

Table 3.4: The major assignments of the ^{13}C-^{1}H cross signals obtained from HSQC NMR spectra

Label	**δ_C/δ_H (ppm)**	**Assignments**
C_β	53.7/3.49	C_β-H_β in phenyl coumarane units
B_β	53.7/3.08	C_β-H_β in resinol units
-OCH_3	56/3.6-3.9	C-H in methoxyl group
A_γ	59.6-60/3.38-3.62	C_γ-H_γ in β-O-4' linkage

Pγ	61.8/4.12	C_γ-H_γ in p-hydroxycinnamyl alcohol end groups
Bγ	71/3.78, 4.15	C_γ-H_γ in resinol units
C_γ	62.8/3.73	C_γ-H_γ in phenyl coumarane
A_α	71.6/4.8	C_α-H_α in β-O-4' linkage
A_β	83.9/4.3	C_β–H_β in β-O-4 linked to G units
B_α	85.1/4.6	C_α-H_α in resinol units
Cα	86.8/5.5	C_α-H_α in phenylcoumaran substructures
G_2	110.5/6.9	C_2-H_2 in guaiacyl units
G'_2	111.5/7.5	C_2-H_2 in oxidized (Cα=O) guaiacyl units
G_5	114.9/6.76	C_5-H_5 in guaiacyl units
G_6	119.1/6.7	C_6-H_6 in guaiacyl units
G'_6	123.4/7.6	C_6-H_6 in oxidized (Cα=O) guaiacyl units
D_β	126.2/6.8	C_β-H_β in cinnamaldehyde end groups
$H_{2,6}$	127/7.1	$C_{2,6}$-$H_{2,6}$ in p-hydroxybenzoate units

3.3.7. Proposed reaction mechanism

Figure 6 demonstrates the proposed reaction scheme of KL oxidation with oxygen gas in the presence of KOH. The oxidative degradation of three major lignin inter-unit linkages (i.e., β-O-4, β-β and phenylcoumaran) were presented in the reaction scheme (Figure 6). Under alkaline conditions, O_2 converts to superoxide anion ($O_2^{\bullet -}$) and hydroxyl radical (HO•) and by further protonation, it converts to hydroperoxyl anion (HOO^-) [65]. Among these oxygen derivatives ($O_2^{\bullet -}$, HOO• and HOO^-), $O_2^{\bullet -}$ and HOO• act as electrophiles and attack lignin molecules at higher electron density sites, such as the phenoxyl ion (generated by deprotonation in presence of

KOH) and the aromatic ring [66]. On the other hand, HOO^- acts as a nucleophile that attacks low electron density sites, such as carbonyl carbons that may convert the quinones (**G**) into carboxylate structure by ring-opening [65]. Increased aliphatic protons and decreased phenolic-OH and aromatic G units shown in Figures 3.3, 3.4, and 3.5 can prove this observation. An earlier study reported that the phenolic intermediates could be attacked by the superoxide anion during the alkaline lignin oxidation to form phenoxyl radicals. As time elapses, these phenoxyl radicals would be converted and degraded to different depolymerized lignin fractions, including low molecular weight carboxylate groups [67, 68]. In terms of lignin reactivity towards oxygen, it is considered that syringyl type lignin units are more reactive than guaiacyl and p-hydroxyphenyl types [66, 69]. However, catechols that contain two hydroxyl groups are the most reactive lignin units for oxygen attack [65]. Thus, the catechol structures can readily be converted to quinones followed by opening the lignin ring to obtain the muconic acid-like forms (**H, L**) [70]. The significant increase in the carboxylate group content and decrease in the catechol content can be observed from the quantitative ^{31}P-NMR analysis (Figure 3.4). Also, the reduction of aromatic G-units was observed in the P-NMR and HSQC-NMR in Figures 3.4 and 3.5. The oxidative cleavage of resinol unit (β-β) can result in structure A, while further oxidation can transform it into carboxylic acid groups. Also, the alkaline oxidation can degrade the phenylcoumaran linkages (**P**) and break the C-C side chain to carbonyl structures (as shown in Figure 3.3), which may further oxidize to carboxylic acid groups (**E, K**) [65]. The resinol and phenylcoumaran units were not observed in the HSQC-NMR of oxidized KL, which supports the hypothesis on the degradation of β-β and phenylcoumaran sub-structures. The increased carboxylate group was evident in the XPS, H-NMR and P-NMR assessments in Figures 3.2, 3.3, and 3.4, respectively. Moreover, the alkaline oxidation would yield undesirable side reactions.

The phenoxyl radical (R) may form dimeric condensed product (**M**) of G-units that may not be observed from the HSQC aromatic regions [65, 68], but they were observed in the P-NMR analysis in Figure 3.4.

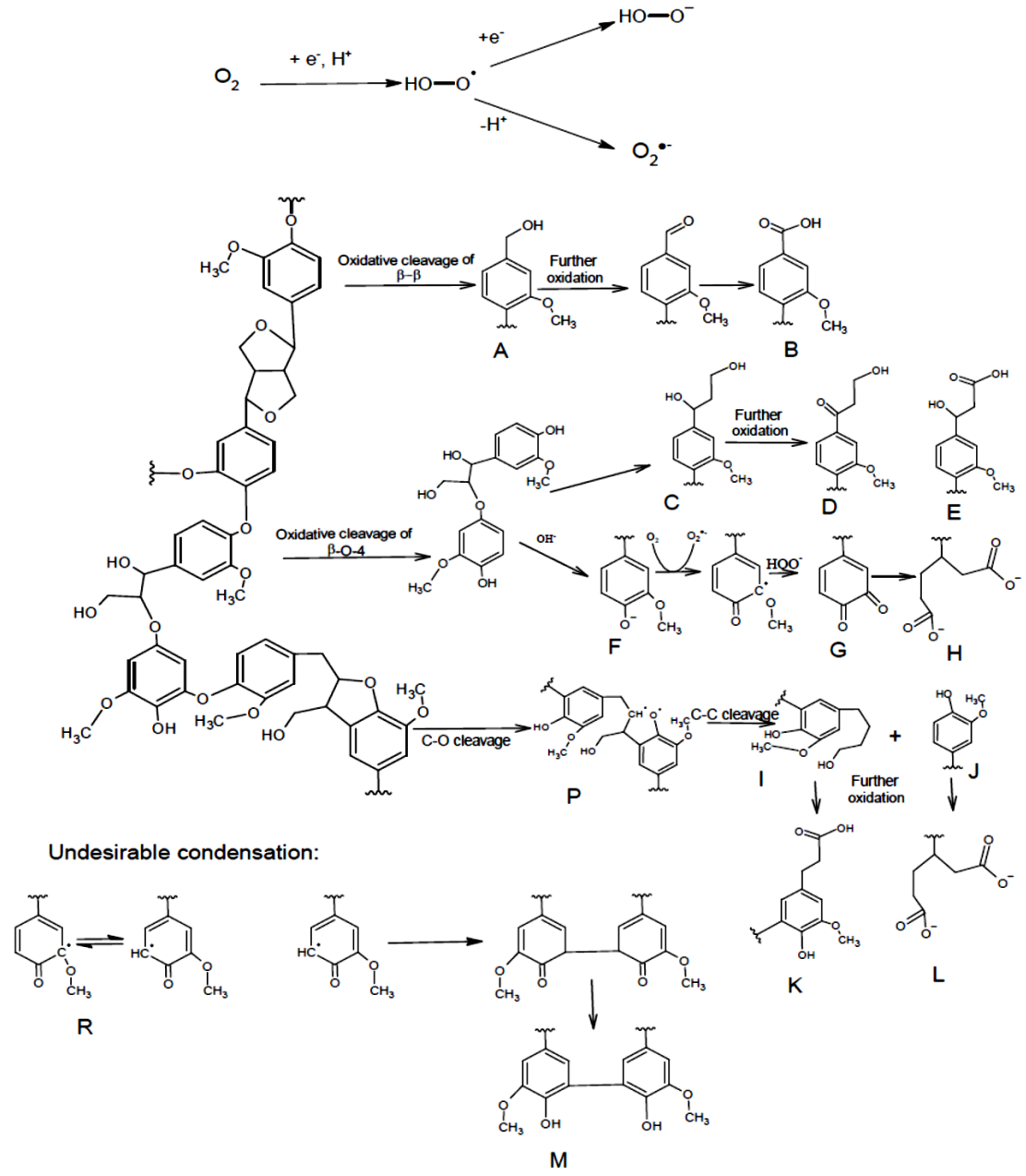

Figure 3.6: The oxygen reduction steps and possible reaction scheme pathway of KOH catalyzed KL oxidation with oxygen gas.

3.3.8. Effects of MKLs on Zea Mays plants

In this study, the MKLs were used directly at a dose of 10 mg C/L in plant cultivation. Even though the pH of the product was between 8.5 and 9.7, which originates from KOH used in the reaction, its use should not affect the soil pH. As the pH of the Hoagland solution is slightly acidic (pH ~5.5), after adding the small amount of MKLs, the pH would remain around 6.5. A previous study on KOH pulping of rice straw claimed that the neutralized potassium-enriched black liquor could be used in the agricultural field for irrigation [71]. Figure 3.7 presents the average length of the plants treated with different lignin derivatives and HA. It can be seen that after 20 days, the size of the plants was not significantly different. That is because the plants were grown only with Hoagland solution in the first 15 days. However, after 30 days, the difference in length was noticeable. After 40 days, the samples treated with MKL-3 had 12% and 27% increments in size compared with the HA and blank samples, respectively. Figure 3.8 demonstrates that the plants treated with MKLs had a much higher dry weight, especially those treated with MKL-3. These results might be attributed to the improved carboxylate content of MKLs (Table 3.3) that may participate in a cation exchange with proton and increase the mobility of the essential mineral ions (i.e., RCOOK, $R(COO)_2Ca$) in plants [28]. The roots of the plants would absorb the potassium of MKLs, thereby improving micronutrient transference [72]. A recent study also highlighted that KL with functional groups, such as carboxylic and phenolic hydroxyl groups, can stimulate plant growth [27].

Figure 3.8 shows that the average dry weight of biomass treated with MKL-3 was approximately 81% and 92% higher than those generated via treating with HA and blank samples, respectively.

The higher sodium content can explain these results on HA. It is evident in Table 3.2 that HA had 3.7% more sodium than MKLs did. Earlier studies reported that a high sodium content (100 mM of NaCl) harmed plant growth and photosynthesis because it would reduce the necessary amounts of N, P, and K uptake in plants [73-75].

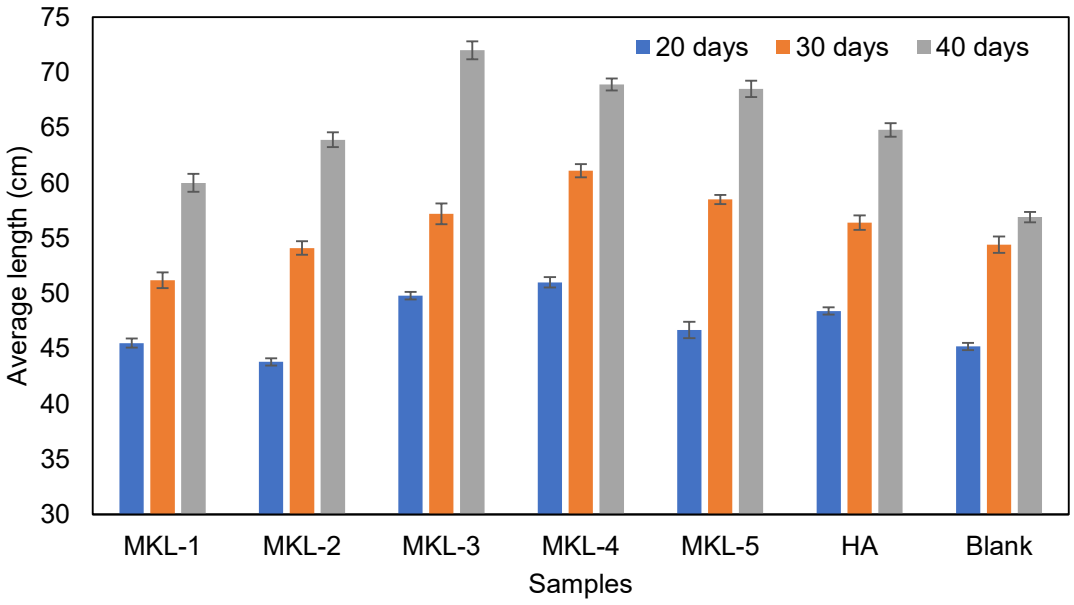

Figure 3.7: Average length of Zea mays plant after growing for 20, 30, and 40 days in vermiculite medium with sample doses of 10 mg C/L.

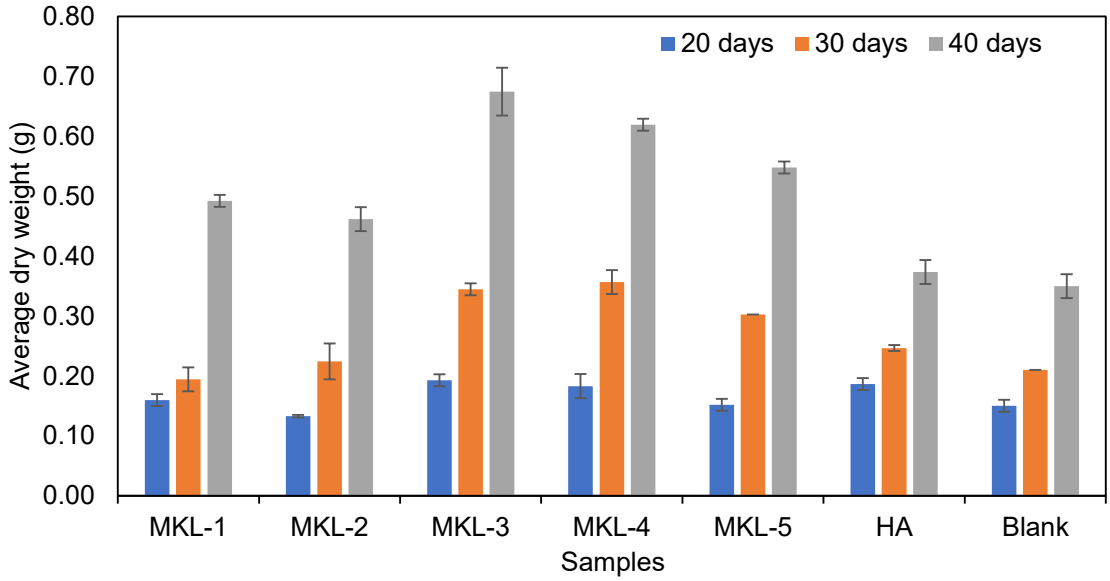

Figure 3.8: Average dry weight of Zea Mays plant after growing for 20, 30, and 40 days in vermiculite medium with the sample doses of 10 mg C/L.

The impact of MKL on the chlorophyll content of the leaves of plants is presented in Figure 3.9. At 10 mg C/L sample dose, the chlorophyll content of plants was insignificantly changed after 20 days, while the change was more remarkable after 30 days. Interestingly, the chlorophyll content of the sample treated with MKL-3 was 14% and 32% higher than those treated with HA and blank, respectively. After 40 days, however, the chlorophyll content of the samples dropped significantly in all samples due to the root-bound and the increased salinity in the pots [76, 77]. Poorter and coworkers reported that small pots hamper photosynthesis and reduce plant growth [77]. It was also reported that soil salinity would decrease agricultural crop productivity and would significantly damage the soil ecosystem [78]. Some elements, such as sodium, chlorine, and boron, have toxic effects on plants. It was stated that the excessive accumulation of sodium in cell walls could rapidly lead to osmotic stress and cell death [79]. Moreover, the adverse

effects of salinity on plant growth may hamper the supply of photosynthetic hormones to the growing tissues [80]. The study also reported that salinity would affect photosynthesis mainly through reducing leaf area and chlorophyll content.

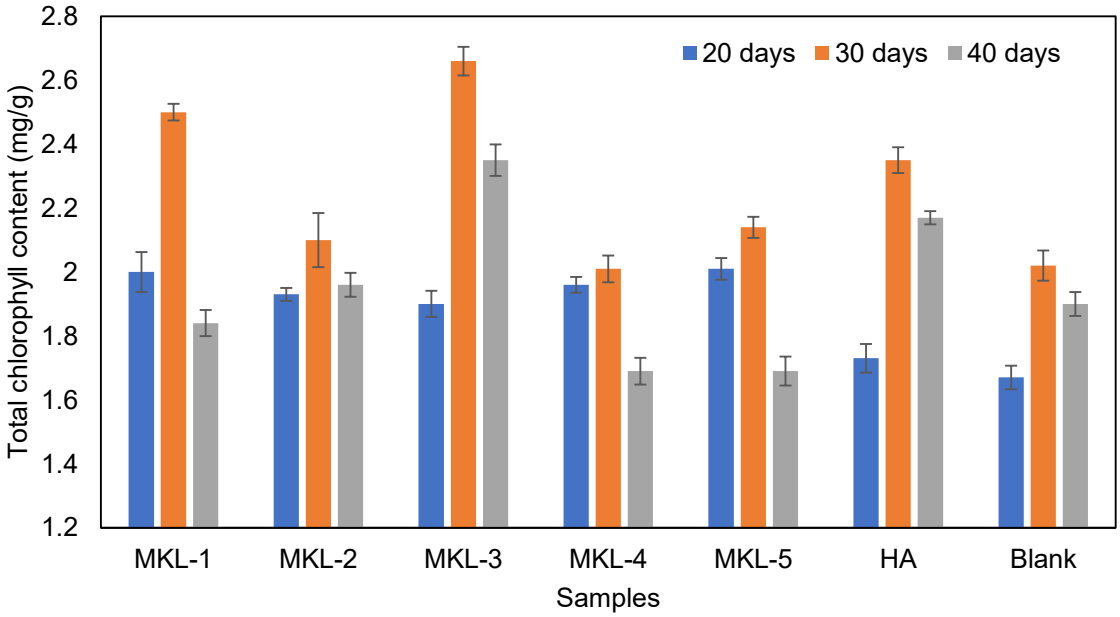

Figure 3.9: Average total chlorophyll content of leaves after 20, 30 and 40 days when treated with MKLs and HA dosage of 10 mg C/L and blank.

3.3.9. Effects of MKLs on the ash contents of Zea Mays plants

Table 3.5 presents the ash content of the plants after 30 and 40 days of growth. It is seen that the plants treated with HA samples and the plants treated with the blank sample contained higher ash than that treated with the MKL-3, implying that the organic proportion of biomass was increased in the plants via treating with MKL-3. Earlier research suggested that corn plants treated with lignosulfonate humate (1 mg C/L) had higher carbohydrates (increase from 29.24 to 96.97 mg/g dry weight) and protein (an increase from 2.9 to 3.53 mg/g) compared to the untreated sample

[81]. Thus, it may be assumed that MKL-3, similar to HA, could regulate the hormonal activity of carbohydrate metabolism.

Also, the ashes were analyzed by XPS to observe their elemental mineral content. Figure 3.10 represents that the blank contains higher amounts of minerals (e.g., Si, K, Ca, Mg, P) than the plants treated with HA and MKL-3. Also, the ash of the blank sample contained around 44% more oxygen than the MKL-3 and HA-treated ones, mainly from the elements' oxides (e.g., SiO_2, K_2O, CaO, MgO, $PO4^{3-}$) [82]. However, only 3.7% carbon was recorded in the ash of blank samples. In comparison, 33.7 and 36% carbon contents were observed in the HA and MKL-3 treated plants, respectively (Figure 3.10), which may come from the inorganic carbonates, such as $CaCO_3$ and $MgCO_3$ [83]. Also, it can be observed from the study that the elemental minerals (e.g., Mg, Ca, K) are lower in MKL-3 than in other samples because of the higher relative percentages of carbon (organic and inorganic) in this sample.

To identify the major elements of the ash, the XPS spectra for these samples are presented in the supplementary file (Figure A3.6). Interestingly, the plants treated with MKL-3 contain 27% and 50% less Si than HA and blank, respectively. Such results are attributed to the available Si in soil that could form an unstable complex with carboxylate groups of MKL-3 and HA. A previous study reported that semimetals, such as Si and Ge, could form complexes with HA's carboxyl, phenolic/aliphatic hydroxyl groups [84]. It can be suggested that since the overall ash and silicon contents were low in the samples treated with MKL-3, this treatment could induce the corn plants that are suitable for pulping [85].

Table 3.5: Ash content of plants after 30 and 40 days of growing.

Sample	**Time**	**Ash content, %**

MKL-3	30 days	14.74±0.39
	40 days	11.01±0.50
HA	30 days	14.63±0.20
	40 days	12.46±0.40
Blank	30 days	15.64±0.07
	40 days	12.62±0.20

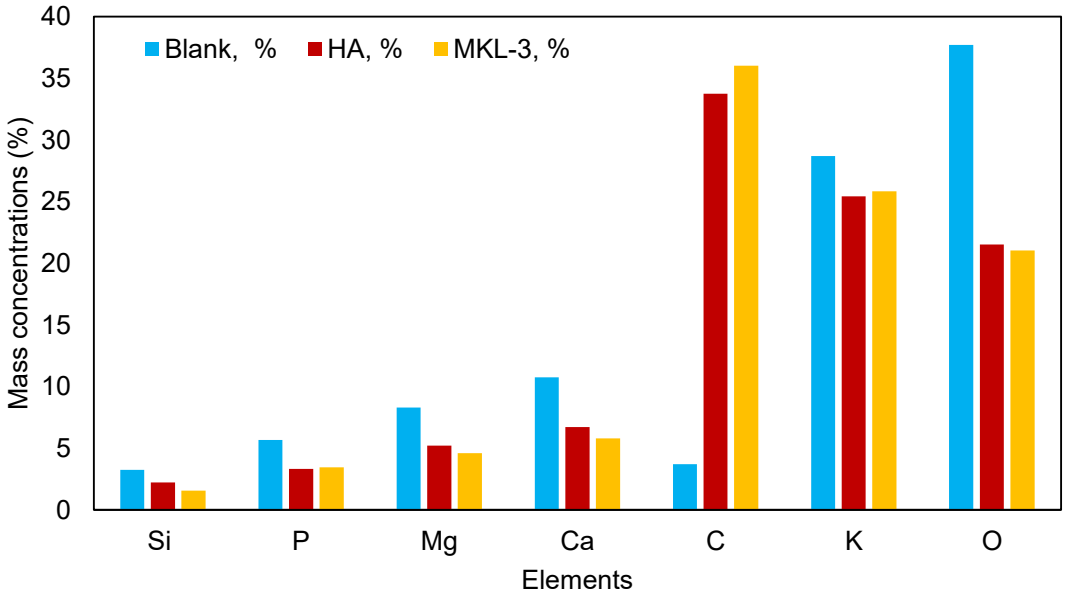

Figure 3.10: The mass concentrations of the major elements in the ash after 40 days.

It should be stated that there are some advantages of this approach: 1) under KOH aerobic oxidation at 195 °C, the highest carboxylic content was achieved; 2) the product was water-soluble, which would help its interaction with soil minerals, and 3) the reaction products could be used without any purification step.

The average price of kraft lignin varies between $250 and $500 [86], and the price of potash fertilizer in the USA (Illinois) is $600 in 2021 [87]. However, as a lower dosage of MKL than

regular fertilizer would be required for obtaining a similar plant growth (Figure 3.7), farms might need to use less MKL to achieve similar plant growth but still benefit from soil preservation, etc. Therefore, if MKL were priced higher than regular fertilizers, its price and use might still be justified and attractive to farmers. However, further research is needed to evaluate the detailed economic aspects of using MKL in the farm field.

3.4. Conclusion

In this study, KL was successfully oxidized with oxygen gas under an alkaline environment to induce a green fertilizer for crop cultivations. Also, ^{1}H-NMR and XPS analyses confirmed the presence of the carboxylate group on MKL, while ^{31}P NMR analysis confirmed the reduction in the aliphatic, phenolic, and catechol -OH groups of lignin via oxidation. The HSQC NMR analysis confirmed that the oxidation degraded the Cα-Cβ, β-O-4, and β-β linkages of the KL. The oxidation of lignin at 195 °C temperature and 300 psi continuous oxygen pressure generated MKL-3 with 2.26 mmol/g of COOH content and M_w of 1,970 g/mol. The present study showed that the C/O ratio of KL decreased from 2.4 to 1.6 via oxidation (for MKL-3 production), which was attributed to the attachment of the carboxylate group to KL. A significant amount of potassium was detected in MKLs as potassium could be attached to MKL in $–COO^{-}K^{+}$ form. Moreover, about 55% of the methoxyl group of KL was cleaved via oxidation for the MKL-3 production.

The plant growth analysis confirmed that the length of plants was 12% and 27% higher in MKL-3 treated plants compared to the plants treated with HA and blank, respectively. Also, the dry weight of plants treated with MKL-3 was increased by 81% and 92% compared to those treated by HA and blank samples, respectively. After 30 days of cultivation, the chlorophyll content of plant leaves treated with MKL-3 was 14% and 32% higher than that of plants treated with HA

and blank, respectively. Finally, the ash contents of the plants treated with MKL-3 were lower than those treated with HA and blank.

References

[1] K.R. Chandini, R. Kumar, O. Prakash, The impact of chemical fertilizers on our environment and ecosystem, Research trends in environmental sciences (2019) 69-86.

[2] R. Hijbeek, H. Ten Berge, A. Whitmore, D. Barkusky, J. Schröder, M. Van Ittersum, Nitrogen fertiliser replacement values for organic amendments appear to increase with N application rates, Nutrient cycling in agroecosystems 110(1) (2018) 105-115.

[3] M.T. Bashir, S. Ali, M. Ghauri, A. Adris, R. Harun, Impact of excessive nitrogen fertilizers on the environment and associated mitigation strategies, Asian Journal of Microbiology, Biotechnology and Environmental Sciences 15(2) (2013) 213-221.

[4] C.H. Stark, K.G. Richards, The continuing challenge of nitrogen loss to the environment: Environmental consequences and mitigation strategies, Dynamic Soil, Dynamic Plant 2(2) (2008) 41-55.

[5] C.A. de Klein, R.M. Monaghan, The effect of farm and catchment management on nitrogen transformations and N2O losses from pastoral systems—can we offset the effects of future intensification?, Current Opinion in Environmental Sustainability 3(5) (2011) 396-406.

[6] X.-X. Chen, Y.-M. Liu, Q.-Y. Zhao, W.-Q. Cao, X.-P. Chen, C.-Q. Zou, Health risk assessment associated with heavy metal accumulation in wheat after long-term phosphorus fertilizer application, Environmental Pollution 262 (2020) 114348.

[7] N. Sharma, R. Singhvi, Effects of chemical fertilizers and pesticides on human health and environment: a review, International journal of agriculture, environment and biotechnology 10(6) (2017) 675-679.

[8] T.A. Wise, Can we feed the world in 2050, A scoping paper to assess the evidence. Global Development and Environment Institute Working Paper (13-04) (2013).

[9] L. Fernández, R. Baigorri, O. Urrutia, J. Erro, P.M. Aparicio-Tejo, J. Yvin, J.M. García-Mina, Improving the short-term efficiency of rock phosphate-based fertilizers in pastures by using edaphic biostimulants, Chemical and Biological Technologies in Agriculture 3(1) (2016) 1-9.

[10] Y. Li, F. Fang, J. Wei, X. Wu, R. Cui, G. Li, F. Zheng, D. Tan, Humic Acid Fertilizer Improved Soil Properties and Soil Microbial Diversity of Continuous Cropping Peanut: A Three-Year Experiment, Scientific Reports 9(1) (2019) 12014. https://doi.org/10.1038/s41598-019-48620-4.

[11] J.D.L. Martins, R.P. Soratto, A.M. Fernandes, The Effect of Humic Substances and Phosphate Fertilizer on Growth and Nutrient Uptake of the Potato, Communications in Soil Science and Plant Analysis 51(11) (2020) 1525-1544. https://doi.org/10.1080/00103624.2020.1781154.

[12] J. Zhang, J. Wang, T. An, D. Wei, F. Chi, B. Zhou, Effects of long-term fertilization on soil humic acid composition and structure in Black Soil, PLoS One 12(11) (2017) e0186918-e0186918. https://doi.org/10.1371/journal.pone.0186918.

[13] J.-Y. Cha, T.-W. Kim, J.H. Choi, K.-S. Jang, L. Khaleda, W.-Y. Kim, J.-R.J.J.o.a. Jeon, f. chemistry, Fungal laccase-catalyzed oxidation of naturally occurring phenols for enhanced germination and salt tolerance of Arabidopsis thaliana: A green route for synthesizing humic-like fertilizers, 65(6) (2017) 1167-1177.

[14] J.G. Lee, H.Y. Yoon, J.-Y. Cha, W.-Y. Kim, P.J. Kim, J.-R.J.B.a. Jeon, Artificial humification of lignin architecture: Top-down and bottom-up approaches, (2019) 107416.

[15] J. Weber, Y. Chen, E. Jamroz, T. Miano, Preface: humic substances in the environment, Journal of Soils and Sediments 18(8) (2018) 2665-2667.

[16] O. Ahmed, M. Husni, A. Anuar, M. Hanafi, Effects of extraction and fractionation time on the yield of compost humic acids, New Zealand Journal of Crop and Horticultural Science 33(2) (2005) 107-110.

[17] Y. Chen, B. Chefetz, Y. Hadar, Formation and properties of humic substance originating from composts, The science of composting, Springer1996, pp. 382-393.

[18] P. Palanivell, K. Susilawati, O.H. Ahmed, N.M. Majid, Compost and Crude Humic Substances Produced from Selected Wastes and Their Effects on Zea mays L. Nutrient Uptake and Growth, The Scientific World Journal 2013 (2013) 276235. https://doi.org/10.1155/2013/276235.

[19] J. Pecha, T. Fürst, K. Kolomazník, V. Friebrová, P. Svoboda, Protein biostimulant foliar uptake modeling: the impact of climatic conditions, AIChE journal 58(7) (2012) 2010-2019.

[20] A. Ertani, P. Sambo, C. Nicoletto, S. Santagata, M. Schiavon, S. Nardi, The use of organic biostimulants in hot pepper plants to help low input sustainable agriculture, Chemical and Biological Technologies in Agriculture 2(1) (2015) 11.

[21] O.A. Gladkov, R.B. Poloskin, Y.J. Polyakov, I.V. Sokolova, N.I. Sorokin, A.V. Glebov, Method for producing humic acid salts, Google Patents, 2007.

[22] D. Savy, L. Canellas, G. Vinci, V. Cozzolino, A. Piccolo, Humic-Like Water-Soluble Lignins from Giant Reed (Arundo donax L.) Display Hormone-Like Activity on Plant Growth, Journal of Plant Growth Regulation 36(4) (2017) 995-1001. https://doi.org/10.1007/s00344-017-9696-4.

[23] A. Tejado, C. Pena, J. Labidi, J. Echeverria, I. Mondragon, Physico-chemical characterization of lignins from different sources for use in phenol–formaldehyde resin synthesis, Bioresource Technology 98(8) (2007) 1655-1663.

[24] F.S. Chakar, A.J. Ragauskas, Review of current and future softwood kraft lignin process chemistry, Industrial Crops and Products 20(2) (2004) 131-141.

[25] E.I. Evstigneyev, S.M. Shevchenko, Structure, chemical reactivity and solubility of lignin: a fresh look, Wood Science and Technology 53(1) (2019) 7-47.

[26] S. Nardi, M. Schiavon, O. Francioso, Chemical structure and biological activity of humic substances define their role as plant growth promoters, Molecules 26(8) (2021) 2256.

[27] H.J. Jeong, J.-Y. Cha, J.H. Choi, K.-S. Jang, J. Lim, W.-Y. Kim, D.-C. Seo, J.-R. Jeon, One-pot transformation of technical lignins into humic-like plant stimulants through Fenton-based advanced oxidation: accelerating natural fungus-driven humification, ACS omega 3(7) (2018) 7441-7453.

[28] W.-Z. Zhang, C. Xiao-Qin, Z. Jian-Min, L. Dai-Huan, W. Huo-Yan, D. Chang-Wen, Influence of humic acid on interaction of ammonium and potassium ions on clay minerals, Pedosphere 23(4) (2013) 493-502.

[29] D. Savy, V. Cozzolino, A. Nebbioso, M. Drosos, A. Nuzzo, P. Mazzei, A. Piccolo, Humic-like bioactivity on emergence and early growth of maize (Zea mays L.) of water-soluble lignins isolated from biomass for energy, Plant Soil 402(1-2) (2016) 221-233.

[30] D. Savy, V. Cozzolino, G. Vinci, A. Nebbioso, A. Piccolo, Water-soluble lignins from different bioenergy crops stimulate the early development of maize (Zea mays, L.), Molecules 20(11) (2015) 19958-19970.

[31] U. Junghans, J.J. Bernhardt, R. Wollnik, D. Triebert, G. Unkelbach, D. Pufky-Heinrich, Valorization of Lignin via Oxidative Depolymerization with Hydrogen Peroxide: Towards Carboxyl-Rich Oligomeric Lignin Fragments, Molecules 25(11) (2020) 2717.

[32] A. Ivanković, A. Dronjić, A.M. Bevanda, S. Talić, Review of 12 principles of green chemistry in practice, International Journal of Sustainable and Green Energy 6(3) (2017) 39-48.

[33] S. Sabaghi, N. Alipoormazandarani, P. Fatehi, Production and Application of Triblock Hydrolysis Lignin-Based Anionic Copolymers in Aqueous Systems, ACS omega 6(9) (2021) 6393-6403.

[34] M. Jablonsky, M. Botkova, J.J.C.C. Kosinkova, Technology, Prediction of methoxyl groups content in lignin based on ultimate analysis, 49(2) (2015) 165-168.

[35] F.C. Bressy, G.B. Brito, I.S. Barbosa, L.S. Teixeira, M.G.A. Korn, Determination of trace element concentrations in tomato samples at different stages of maturation by ICP OES and ICP-MS following microwave-assisted digestion, Microchemical Journal 109 (2013) 145-149.

[36] W. He, W. Gao, P. Fatehi, Engineering, Oxidation of kraft lignin with hydrogen peroxide and its application as a dispersant for kaolin suspensions, ACS Sustainable Chemistry & Engineering. 5(11) (2017) 10597-10605.

[37] P. Fatehi, W. Gao, Y. Sun, M. Dashtban, Acidification of prehydrolysis liquor and spent liquor of neutral sulfite semichemical pulping process, Bioresource Technology. 218 (2016) 518-525.

[38] W. Schutyser, J.S. Kruger, A.M. Robinson, R. Katahira, D.G. Brandner, N.S. Cleveland, A. Mittal, D.J. Peterson, R. Meilan, Y. Román-Leshkov, Revisiting alkaline aerobic lignin oxidation, Green chemistry 20(16) (2018) 3828-3844.

[39] S. Sutradhar, K.M.Y. Arafat, J. Nayeem, M.S. Jahan, Organic acid lignin from rice straw in phenol-formaldehyde resin preparation for plywood, Cellulose Chemistry and Technology. 54(5-6) (2020) 463-471.

[40] S. Sabaghi, N. Alipoormazandarani, W. Gao, P. Fatehi, Dual lignin-derived polymeric systems for hazardous ion removals, Journal of Hazardous Materials 417 (2021) 125970.

[41] B. Fu, J.C. Hower, S. Dai, S.M. Mardon, G. Liu, Determination of chemical speciation of arsenic and selenium in high-as coal combustion ash by X-ray photoelectron spectroscopy: Examples from a Kentucky stoker ash, ACS omega 3(12) (2018) 17637-17645.

[42] X. Meng, C. Crestini, H. Ben, N. Hao, Y. Pu, A.J. Ragauskas, D.S. Argyropoulos, Determination of hydroxyl groups in biorefinery resources via quantitative 31 P NMR spectroscopy, Nature Protocols 14(9) (2019) 2627-2647.

[43] D.R. Hoagland, D.I.J.C.C.a.e.s. Arnon, The water-culture method for growing plants without soil, 347(2nd edit) (1950).

[44] JD. Hiscox, GF. Israelstam, A method for the extraction of chlorophyll from leaf tissue without maceration, Canadian J of Botany 57(12) (1979) 1332-1334.

[45] T. Tappi, 211 om-02. Ash in wood, pulp, paper and paperboard: Combustion at 525◦ C, USA: TAPPI (2006).

[46] A.G. Demesa, A. Laari, I. Turunen, M. Sillanpää, Alkaline partial wet oxidation of lignin for the production of carboxylic acids, Chemical Engineering &Technology 38(12) (2015) 2270-2278.

[47] A. Shrivastava, 2 - Polymerization, in: A. Shrivastava (Ed.), Introduction to Plastics Engineering, William Andrew Publishing2018, pp. 17-48. https://doi.org/https://doi.org/10.1016/B978-0-323-39500-7.00002-2.

[48] W. Jeon, I.-H. Choi, J.-Y. Park, J.-S. Lee, K.-R. Hwang, Alkaline wet oxidation of lignin over Cu-Mn mixed oxide catalysts for production of vanillin, Catalysis Today 352 (2020) 95-103.

[49] T. Anđelković, R. Nikolić, A. Bojić, D. Anđelković, G. Nikolić, Binding of cadmium to soil humic acid as a function of carboxyl group content, Macedonian Journal of Chemistry and Chemical Engineering 29(2) (2010) 215-224.

[50] A. Violante, M. Ricciardella, M. Pigna, R. Capasso, Chapter 5 - Effects of organic ligands on the adsorption of trace elements onto metal oxides and organo-mineral complexes, in: P.M. Huang, G.R. Gobran (Eds.), Biogeochemistry of Trace Elements in the Rhizosphere, Elsevier, Amsterdam, 2005, pp. 157-182. https://doi.org/https://doi.org/10.1016/B978-044451997-9/50007-6.

[51] R. Wang, B. Zhou, Z. Wang, Study on the Preparation and Application of Lignin-Derived Polycarboxylic Acids, Journal of Chemistry 2019 (2019) 5493745. https://doi.org/10.1155/2019/5493745.

[52] L. Zhou, L. Yuan, B. Zhao, Y. Li, Z. Lin, Structural characteristics of humic acids derived from Chinese weathered coal under different oxidizing conditions, PLoS One 14(5) (2019) e0217469.

[53] P.S. dos Santosa, S.H. da Silvab, X. Erdociaa, D.A. Gattob, J.J.C.E.T. Labidi, Characterization of Kraft Lignin Precipitated with Different Alcohols, 43 (2015) 469-474.

[54] A.A. Myint, H.W. Lee, B. Seo, W.-S. Son, J. Yoon, T.J. Yoon, H.J. Park, J. Yu, J. Yoon, Y.-W. Lee, One pot synthesis of environmentally friendly lignin nanoparticles with compressed liquid carbon dioxide as an antisolvent, Green Chemistry 18(7) (2016) 2129-2146.

[55] S. Gharehkhani, N. Ghavidel, P. Fatehi, Kraft Lignin–Tannic Acid as a Green Stabilizer for Oil/Water Emulsion, ACS Sustainable Chemistry & Engineering 7(2) (2018) 2370-2379.

[56] G.-J. Jiao, Q. Xu, S.-L. Cao, P. Peng, D. She, Controlled-release fertilizer with lignin used to trap urea/hydroxymethylurea/urea-formaldehyde polymers, BioResources 13(1) (2018) 1711-1728.

[57] K. Bahrpaima, P. Fatehi, Synthesis and characterization of carboxyethylated lignosulfonate, ChemSusChem 11(17) (2018) 2967-2980.

[58] M. Wang, Y. Zhao, J. Li, Demethylation and other modifications of industrial softwood kraft lignin by laccase-mediators, Holzforschung 72(5) (2018) 357-365. https://doi.org/doi:10.1515/hf-2017-0096.

[59] T.M. Budnyak, I.V. Pylypchuk, M.E. Lindstro¨ , O. Sevastyanova, Electrostatic deposition of the oxidized kraft lignin onto the surface of aminosilicas: thermal and structural characteristics of hybrid materials, ACS omega 4(27) (2019) 22530-22539.

[60] F. Coupé, L. Petitjean, P.T. Anastas, F. Caijo, V. Escande, C. Darcel, Sustainable oxidative cleavage of catechols for the synthesis of muconic acid and muconolactones including lignin upgrading, Green Chemistry (2020).

[61] C. Crestini, M. Crucianelli, M. Orlandi, R. Saladino, Oxidative strategies in lignin chemistry: A new environmental friendly approach for the functionalisation of lignin and lignocellulosic fibers, Catalysis Today 156(1) (2010) 8-22. https://doi.org/https://doi.org/10.1016/j.cattod.2010.03.057.

[62] C. Crestini, H. Lange, M. Sette, D.S. Argyropoulos, On the structure of softwood kraft lignin, Green Chemistry 19(17) (2017) 4104-4121.

[63] J. Feng, J. Jiang, Z. Yang, Q. Su, K. Wang, J. Xu, Characterization of depolymerized lignin and renewable phenolic compounds from liquefied waste biomass, RSC advances 6(98) (2016) 95698-95707.

[64] T.-Q. Yuan, S.-N. Sun, F. Xu, R.-C. Sun, Characterization of lignin structures and lignin–carbohydrate complex (LCC) linkages by quantitative 13C and 2D HSQC NMR spectroscopy, Journal of agricultural and food chemistry 59(19) (2011) 10604-10614.

[65] A. Kalliola, Chemical and enzymatic oxidation using molecular oxygen as a means to valorize technical lignins for material applications, (2015).

[66] H. Sixta, Handbook of Pulp, Volume 2, (2006).

[67] Y. Ji, E. Vanska, A. Van Heiningen, Rate determining step and kinetics of oxygen delignification, Pulp Pap-Canada 110(3) (2009) 29-35.

[68] Y. Ji, E. Vanska, A. van Heiningen, New kinetics and mechanisms of oxygen delignification observed in a continuous stirred tank reactor, Holzforschung 63(3) (2009) 264-271.

[69] R.A. Northey, A review of lignin model compound reactions under oxygen bleaching conditions, (2001).

[70] R. Ma, M. Guo, X. Zhang, Recent advances in oxidative valorization of lignin, Catalysis Today 302 (2018) 50-60. https://doi.org/https://doi.org/10.1016/j.cattod.2017.05.101.

[71] M.S. Jahan, F. Haris, M.M. Rahman, P.R. Samaddar, S. Sutradhar, Potassium hydroxide pulping of rice straw in biorefinery initiatives, Bioresource technology 219 (2016) 445-450.

[72] S. Trevisan, O. Francioso, S. Quaggiotti, S. Nardi, Humic substances biological activity at the plant-soil interface: from environmental aspects to molecular factors, Journal of Plant Signaling Behavior 5(6) (2010) 635-643.

[73] B.B. Aşık, M.A. Turan, H. Çelik, A.V. Katkat, Uptake of wheat (Triticum durun cv. Salihli) under conditions of salinity, Asian J. Crop Sci. 1 (2009) 87-95.

[74] M.A. Khan, I.A. Ungar, A.M. Showalter, Effects of salinity on growth, water relations and ion accumulation of the subtropical perennial halophyte, Atriplex griffithii var. stocksii, Annals of Botany 85(2) (2000) 225-232.

[75] H. Kurban, H. Saneoka, K. Nehira, R. Adilla, G.S. Premachandra, K. Fujita, Effect of salinity on growth, photosynthesis and mineral composition in leguminous plant Alhagi pseudoalhagi (Bieb.), Soil science and plant nutrition 45(4) (1999) 851-862.

[76] S.H. Shah, R. Houborg, M.F.J.A. McCabe, Response of chlorophyll, carotenoid and SPAD-502 measurement to salinity and nutrient stress in wheat (Triticum aestivum L.), 7(3) (2017) 61.

[77] H. Poorter, J. Bühler, D. van Dusschoten, J. Climent, J.A. Postma, Pot size matters: a meta-analysis of the effects of rooting volume on plant growth, Functional Plant Biology 39(11) (2012) 839-850.

[78] P. Shrivastava, R.J.S.j.o.b.s. Kumar, Soil salinity: a serious environmental issue and plant growth promoting bacteria as one of the tools for its alleviation, 22(2) (2015) 123-131.

[79] R.J.P. Munns, cell, environment, Comparative physiology of salt and water stress, 25(2) (2002) 239-250.

[80] M.J.F.-M. Ashraf, Distribution, Functional Ecology of Plants, Some important physiological selection criteria for salt tolerance in plants, 199(5) (2004) 361-376.

[81] A. Ertani, O. Francioso, V. Tugnoli, V. Righi, S.J.J.o.a. Nardi, f. chemistry, Effect of commercial lignosulfonate-humate on Zea mays L. metabolism, 59(22) (2011) 11940-11948.

[82] S. Chowdhury, M. Mishra, O. Suganya, The incorporation of wood waste ash as a partial cement replacement material for making structural grade concrete: An overview, Ain Shams Engineering Journal 6(2) (2015) 429-437.

[83] L. Etiegni, A. Campbell, Physical and chemical characteristics of wood ash, Bioresource technology 37(2) (1991) 173-178.

[84] G.S. Pokrovski, J. Schott, Experimental study of the complexation of silicon and germanium with aqueous organic species: implications for germanium and silicon transport and Ge/Si ratio in natural waters, Geochimica et Cosmochimica Acta 62(21-22) (1998) 3413-3428.

[85] H. Cheng, H. Zhan, S. Fu, L.A. Lucia, Alkali extraction of hemicellulose from depithed corn stover and effects on soda-AQ pulping, BioResources 6(1) (2011) 196-206.

Chapter 4

A green cement plasticizer from softwood kraft lignin

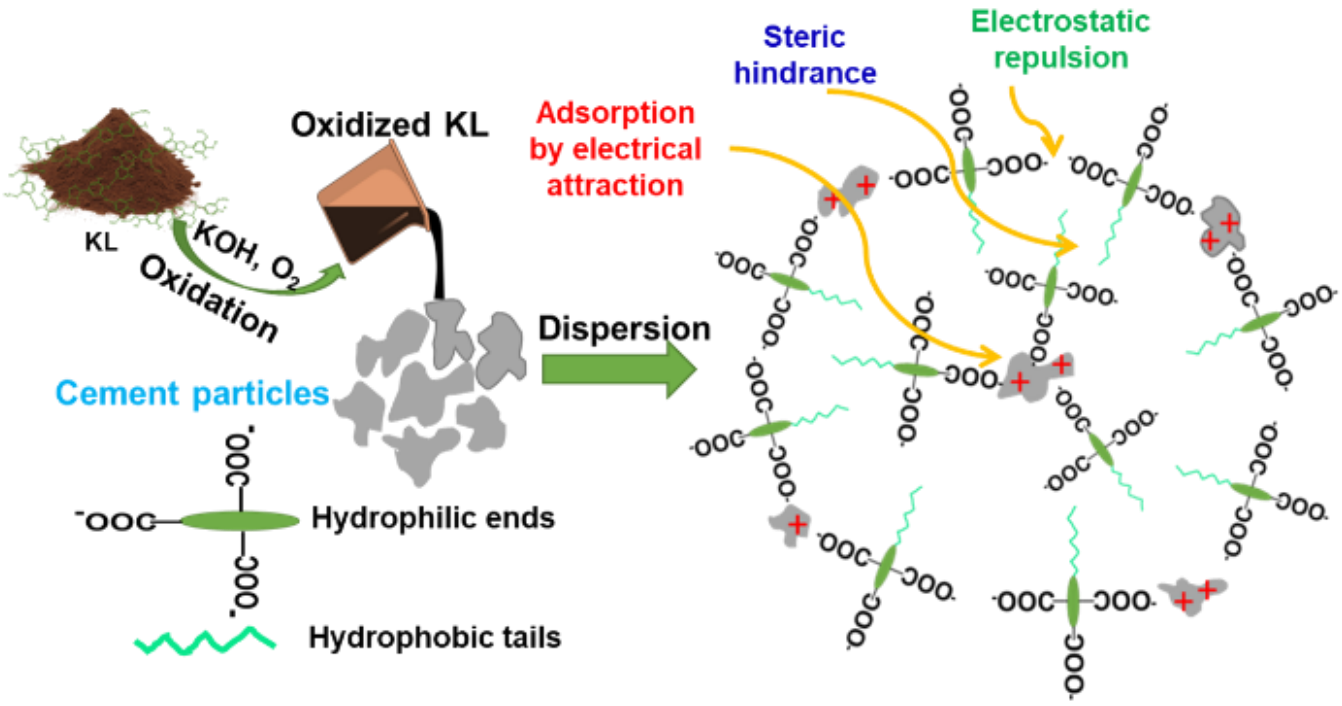

* S. Sutradhar, W. Gao, P. Fatehi, A Green Cement Plasticizer from Softwood Kraft Lignin, Industrial & Engineering Chemistry Research 62(3) (2023) 1676-1687. https://doi.org/10.1021/acs.iecr.2c03970.

Abstract

A green cement plasticizer was produced in one-step aerobic oxidation of kraft lignin (KL) in the presence of KOH. In this study, optimizing the reaction conditions led to the maximum carboxylic acid group and charge density of 2.6 mmol/g and 1.9 meq/g for oxidized lignin,

respectively. The NMR, FTIR, and XPS analyses quantified the alterations in the structure of KL after the oxidation reaction. The molecular weight analysis revealed that lignin depolymerization would depend on the temperature, lignin amount, and KOH concentrations. The oxidized lignin with a higher carboxylic acid group adsorbed on the cement particles more readily than a commercial plasticizer, which increased the flowability of the pastes. The compressive strength of cement was improved much more by using oxidized lignin than a commercial plasticizer and lignosulfonate. The current study suggested that the one-pot KOH-mediated oxidation of kraft lignin is a promising approach to producing a green plasticizer for cement application.

4.1. Introduction

Plasticizers are commonly used in cement pastes to improve concrete strength, durability, and flowability [1]. They are used in the concrete admixture to increase its dispersibility by decreasing the agglomeration of the hydrating cement materials [2, 3] and reduce its water requirement by maintaining its strength [4]. Commercial plasticizers, such as hydroxycarboxylic acid, and sulphonic naphthalene acid, have carboxylate and sulfonate groups that create electrostatic repulsions in the cement paste and increase the fluidity of the cement paste [5-7]. However, these plasticizers are mostly petroleum-based and thus environmentally unfriendly [8]. Alternatively, lignosulfonate (LS) has been used commercially as a bio-based cement plasticizer [9]. The LS is the by-product of the sulfite pulping process. It has been used as a dispersant in various fields (i.e., oil-well, cement admixtures, coal-water slurry) for its excellent water solubility and negative charges [2, 9-12]. However, the production of LS is in decline and cannot meet the demand of the industry [13]. On the other hand, 90% of the lignin available in the market originates from the Kraft pulping operation [14]. Despite its vast potential, most kraft

lignin (KL) is burnt for energy generation, and only 2% of its production is utilized for value-added products [15]. Therefore, there is a strong incentive for valorizing kraft lignin in different markets.

KL can be modified following different methods, such as polymerization, sulfonation, oxidation, and sulfomethylation, for various applications [16-18]. Studies on concrete research suggest that sulfonate groups attached to plasticizers can cause early shrinkages [19]. He and coworkers modified KL in two stages involving oxidation by nitric acid followed by sulfomethylation in the presence of formaldehyde and used the product as a cement plasticizer [13]. However, nitric acid is not environmentally friendly, and formaldehyde may cause serious health issues [20]. Therefore, it may not be the best approach to produce lignin-derived plasticizers for concrete applications. In another work, wheat straw soda lignin was oxidized by oxygen gas, and the product was used as a cement plasticizer [1]. Interestingly, potassium ion was reported to interact with the active minerals of cement, such as aluminum oxide and silica, to form poly calcium potassium gypsum and feldspar, which would improve the strength of concrete [21]. In another study, it was reported that, compared to sodium ions, potassium ions would help to decrease the formation of capillary porosity but increase the gel porosity in the concrete structure, which enhances the concrete strength [22]. However, no study was conducted on the KOH-mediated oxidation of softwood KL to produce a plasticizer for cement pastes.

In the current study, potassium-enriched oxidized KL with the carboxylic acid group was produced and used as a cement plasticizer. First, softwood KL was oxidized by oxygen gas in the presence of KOH. The reaction parameters were optimized to obtain oxidized lignin with the highest carboxylate group. In addition to characterizing the products with advanced tools, the performance of the oxidized KL as a green plasticizer was assessed in a cement paste in detail.

The primary novelty of this research was the introduction of a ready-to-use cement plasticizer from kraft lignin in a single-batch reactor without extra purification steps.

4.2. Materials and Methods

4.2.1. Materials

Acid-washed softwood kraft lignin (KL) was supplied by FPInnovations. Potassium hydroxide (KOH), potassium chloride (KCl), hydrochloric acid (HCl), $NaNO_3$, poly diallyl dimethylammonium chloride (PolyDADMAC), acetic anhydride, lignosulfonate, pyridine, sodium nitrate, HPLC grade dimethyl sulfoxide (DMSO) and DMSO-d_6 were purchased from Sigma-Aldrich. Commercial Quikrete cement (type 10) was purchased locally. MasterPozzolith 210 (Commercial plasticizer, CP) was purchased from BASF, Canada.

4.2.2. Oxidation of KL

KL was oxidized with oxygen gas as an oxidizing agent in the presence of KOH. Different amounts of KL (5-15 wt% in water) were dissolved in different KOH solutions (30% of lignin weight). Then, the mixture was poured into a 600 mL Parr reactor for the oxidation reaction (Table 4.1 in supplementary material). In this experiment, an initial 100 psi oxygen pressure was supplied, and oxidation was carried out at various temperatures (180-260 °C) for 30 minutes. Oxygen gas was consumed during the reaction. After 30 minutes, the reactor was allowed to cool down to room temperature, and the final pressure inside the reactor was recorded. The required oxygen gas for each reaction was determined considering the difference in the pressure of the

reactor before (100 psi) and after the reaction. Also, the pH of the reaction mixture was measured before and after the oxidation reaction. The modified samples were denoted as oxidized KL (OKL). The OKL samples generated with 5 wt%, 10 wt%, and 15 wt% lignin in water were named OKLA, OKLB, and OKLC, respectively. The overall yield (OY) of the liquid reaction product was measured by drying the sample at 50 °C for 72 hours and comparing the mass of the generated products with the original KL mass. The performance analyses (i.e., adsorption, zeta potential, flowability, and compression strength tests) of these samples were conducted without any purification step. To eliminate the impact of impurity on the characterization of the product, part of the generated oxidized samples was dialyzed by membrane dialysis with the molecular weight cut-off of 1000 g/mol for 72 hours and dried at 50 °C, and the purified samples were used for characterization (i.e., titration, charge density, GPC, FTIR, NMR, XPS, and TGA). Detailed experimental conditions and sample names can be found in Table S1 in the supplementary material.

4.2.3. Characterizations

The carboxylic acid group content of the lignin derivatives was analyzed following a previously described procedure.[23] Briefly, 0.06 g of lignin samples and 1 mL of 0.8M KOH solution were added to a 250 mL beaker. After that, 100 mL of deionized water was added to dissolve the samples, and 4 mL of 0.05 wt% p-hydroxybenzoic acid was added as an internal standard. The solution was titrated against 0.1 M standard HCl solution, and the endpoints were recorded by an automatic potentiometric titrator (785-DMP Titrino, Metrohm, Switzerland). The following equation was used to determine the carboxylic acid group content of the samples.

$$\text{Carboxylic acid group } \left(\frac{\text{mmol}}{\text{g}}\right) = \frac{\{(\text{Ep}'2 - \text{Ep}'1) - (\text{Ep}2 - \text{Ep}1)\} \times \text{C}}{\text{m}}$$

Where Ep_2 and Ep_1 are the volumes of HCl consumed at the second and third endpoints during the titration of blank, respectively, and the Ep'_2 and Ep'_1 are the endpoints for the OKLs. Also, C is the concentration of standard HCl; m is the dry mass of the sample used for the analysis.

The charge density of the samples was determined following a previously described method by the Mutek Particle Charge Detector (PCD-4) [24]. Briefly, 1 wt.% of the sample solutions was prepared, and 1 mL of the solution was taken for analysis. Then, 10 mL of deionized water was added to the cell and titrated against a poly diallyl dimethylammonium chloride (PolyDADMAC) standard solution (0.05M). Finally, the charge density of the samples was determined according to the literature [24].

To measure the molecular weight of KL, it was initially acetylated following the previously described method [24]. First, 500 mg of KL was dissolved in 20 mL of 1:1 (v/v) acetic anhydride and pyridine solution in a glass vial and stirred for 30 mins. Then, the vial was kept in the dark chamber at room temperature for 24 hours. After that, the mixture was added to 200 mL of ice-cool water dropwise to precipitate KL and centrifuged 3 times to remove the solvents. After that, the lignin was lyophilized. Then, 100 mg of the dry acetylated KL was dissolved in 10 mL of DMSO and analyzed by an HPLC, Agilent Technologies (model 1200, USA) equipped with an RI detector. The HPLC was equipped with Styragel HR4, HR4E, and HR1 columns, and the total retention time was 50 min. HPLC grade DMSO was used as the eluent, and the flow rate was set to 1 mL/min. The column temperature was set at 35 °C for the molecular weight analysis.

The molecular weights of OKLs, LS, and CP were determined by Gel Permeation Chromatography (Viscotek GPC max, Malvern, UK). In this experiment, 0.05 g of OKL was dissolved in 10 mL of 0.1N $NaNO_3$, and the pH of the solution was adjusted to 7. The solution was then filtered by a 0.2 μm filter and analyzed by a standard method. The detector and column

temperatures were set at 35 °C. At a 0.7 ml/min flow rate, 70 µL of each sample solution was injected into the column. Finally, the molecular weights were detected by an RI detector (Figure S2 in supplementary material).

4.2.4. Fourier-Transform Infrared Spectroscopy (FTIR)

The structure of KL and OKLs were analyzed by a Bruker Tensor 37 FTIR instrument (Bruker, Germany), which was equipped with a PIKE MIRacle Diamond Attenuated Total Reflectance (ATR) accessory. Around 1.5-2 mg of dried powdered samples were placed on the ATR crystal of the instrument, and the transmittance (a.u.) of the samples was analyzed. For all samples, 64 scans were conducted in the wavenumber range of 500-4000 cm^{-1}. The resolution of the spectra was 4 cm^{-1}.

4.2.5. X-Ray Photoelectron Spectroscopy (XPS)

The chemical structure of the samples was analyzed by an X-ray photoelectron spectroscopy (XPS) using a Kratos AXIS Supra, Japan, with the monochromatic AL anode. A previously described method was followed to analyze the lignin samples [25]. The dried samples were analyzed by a 375 W X-ray. In this experiment, the number of steps, sweep and dwell time were 230, 60 s, and 260 ms, respectively. Data analysis was performed using ESCApe software (V1.2.0.1325).

4.2.6. Heteronuclear Single Quantum Coherence (HSQC) NMR

The HSQC NMR spectra of the samples were recorded using a Bruker AVANCE Neo NMR-500 MHz instrument (Switzerland) and Topspin 4.02 software. Briefly, 80 mg of lignin samples were dissolved in 1 mL of DMSO-d_6 in small glass vials and stirred overnight at room temperature for

complete dissolution. Then, the solutions were transferred to NMR tubes and analyzed. For ^{1}H NMR, 2048 data points were collected from 16 to 0 ppm, and 64 scans were recorded with 256 increments at 25 °C. For the ^{13}C NMR, 1024 data points were collected from 160 to 0 ppm at the same instrument settings. The recycling delay was 1.00s, and the pulse width was set to 90°.

4.2.7. Thermogravimetric (TGA) Analysis

The thermal stability of the lignin samples was studied following the previously described method using a TGA-i1000 series (Instrument specialist Inc.) [26]. First, all the samples were freeze-dried. After that, each sample was heated by the instrument in the presence of nitrogen gas at 30 mL/min. The temperature was increased at a rate of 10 °C/min in the range of 25 and 800 °C.

4.2.8. Adsorption Analysis

Adsorption analysis was carried out by mixing 1.8 g of cement and specific amounts of plasticizers (0.1-0.5 wt.% of cement) to 30 mL of water in a falcon tube. The tubes were stirred for 3 hours at room temperature. After that, the mixtures were centrifuged at 4000 rpm for 8 minutes, and the supernatants were separated from the samples and kept in a clear glass vial. Then, they were analyzed using a UV-vis spectrometer (Varian Cary 50 Scan UV Visible Spectrophotometer) at 280 nm, and their absorbance was recorded. The concentration of OKL that remained in the solutions was calculated from the calibration curve, which was made of different diluted solutions of OKL. Finally, the adsorbed amount of OKLs on the cement surface was computed considering the initial amount of OKL in solutions that remained in the supernatants after mixing with cement.

4.2.9. Zeta Potential Analysis

A NanoBrook ZetaPALS (Brookhaven Instruments, Holtsville, New York, USA) determined the zeta potential of solutions containing the samples. The zeta potential was measured after the adsorption analysis. Briefly, specific amounts of OKL, LS, and CP (0.1-0.5 wt% doses of cement) were dissolved in 30 mL of deionized water, and its pH was adjusted to 11 using 0.1 M KOH solution (i.e., similar pH of the supernatants after the adsorption analysis). The supernatants of the cement mixture and the samples were collected after the adsorption analysis and used for the zeta potential analysis.

4.2.10. Flowability Analysis

The flowability of cement pastes was measured following the method described earlier [13]. Briefly, 80 g of water was added to 200 g of cement (water-to-cement weight ratio of 0.4), stirred manually in a beaker for 5 minutes, and poured into a metal flow cone (bottom diameter 6 cm, top diameter 3 cm, and height 6 cm). As the cone was lifted, the cement pastes were allowed to spread for 30 seconds, and the diameters of the spread pastes were recorded from four different positions, and the average diameters were reported. To investigate the effects of OKLs, LS, and CP; different doses (0.15- 0.5 wt% of cement) of these chemicals were dissolved in water, they were added to the cement pastes, and the flowability of the admixtures was determined as stated above.

The water reducibility of the OKLB2 was measured following the same flowability analysis. In this set of experiments, the flowability of the OKL2 at different doses (0.25 and 0.35 wt% of cement) at the water/cement (W/C) ratio of 0.4 was tested and compared with blank cement

samples. The blank samples were prepared at different W/C ratios (0.4, 0.5, and 0.6) following the same procedure stated above.

4.2.11. Compressive Strength Analysis

Briefly, cement pastes were prepared at different lignin derivative dosages (0-0.5 wt%) and poured into the cube molds (50 × 50 × 50 mm). The W/C mass ratio was kept at 0.4 in all the test specimens. The molds were left for 24 hours to settle, and the molds were removed the next day. After that, the cubes were cured in water at 20-24 °C for 28 days and tested. The compressive strength of the cement samples was measured by the MTS (Systems corporation), Model No. 311.21, compression strength machine, Minneapolis, Minnesota, USA, according to ASTM C109/C109M [27]. Each specimen was placed in the compression test instrument, and a constant displacement rate of 0.5 mm/min was applied until the cubes were completely deformed. Multiple cubes were prepared for each set of samples, and the average values were reported.

4.3. Results and Discussion

4.3.1. Optimization of the KL Oxidation

The effect of the temperature of the reaction on the KOH-assisted oxidation of SKL is reported in Figure 4.1. It is observable that the total yield decreased as the temperature increased. It was reported earlier that the alkaline oxidation of lignin might generate gaseous products, such as methane, ethane, and the oxides of carbon [28]. It can also be noticed that the overall yield of the final products decreased even though the lignin concentrations were increased from 5 wt.% (OKLA) to 15 wt.% (OKLC) in the reaction mixture. This may be due to the higher concentration of KOH in the solution. As mentioned above, the concentration of KOH was

increased (30 wt.% of lignin) based on total lignin content. The higher alkali concentration in the solution facilitated the depolymerization of the lignin units [29, 30]. All experimental conditions and other properties and characterizations can be found in Table A4.1 in the supplementary material.

The consumption of oxygen is shown in Figure 4.1b. It is seen that oxygen consumption peaked at 240 °C for all samples. Generally, two competing reactions occur in the alkaline oxidation of lignin: lignin decomposition and repolymerization. It was reported that the interunit linkages would be cleaved during the alkaline oxidation of lignin. During alkaline aerobic oxidation, the molecular oxygen would convert to superoxide anion ($O_2\bullet^-$) and hydroperoxyl anion (HOO^-), which would attack different active sites and linkages of lignin [31, 32]. A specific activation energy is needed to initiate the reaction [32]. Therefore, upon increasing the temperature, the phenolic hydroxyl groups are ionized by facilitating the electron transfer to oxygen [31]. Therefore, the increased temperature elevated the consumption of oxygen. It can also be seen from Figure 4.1b that the consumption of oxygen was increased by increasing the lignin concentrations and started to decrease upon increasing temperature from 240 °C. At a higher temperature of 270 °C, the competing lignin repolymerization dominated, and the Mw and Mn increased (Figure 4.1d and 1e), which is not oxygen dependent, and thus reduced the oxygen consumption. It was reported in an earlier study that some C-C linkages of lignin are broken during oxidation reactions, which generate heat and act as an exothermic reaction [33]. Upon increasing temperature, the equilibrium position of the reaction may proceed backward; thus the required oxygen is less for the oxidation reaction.

In alkaline aerobic oxidation of lignin, the final pH of the reaction mixture reveals essential information. As the oxidation of lignin proceeds, more carboxylic acid groups are introduced to

lignin dropping the pH of the solution [28]. As we can see in Figure 4.1c, the final pH dropped (pH 7.4) significantly in OKLA samples when the temperature was increased to 240 °C. Demesa et al. reported that when lignin concentration was decreased (4 wt.% to 0.4 wt.%), the conversion of lignin to organic acids increased [28]. From the current study, it can also be seen that OKLA (5 wt.%) had the lowest pH compared to OKLB (10 wt.%) and OKLC (15 wt.%) samples.

Figure 4.1 (d, e) represents the molecular weight analysis of the OKLs at different temperature ranges and lignin concentrations. The molecular weights of KL can be found in Table 2. It can be seen that the molecular weight decreased significantly from 7000 g/mol (KL) to around 3600 g/mol and continued to decrease until the temperature was increased to 240 °C for all OKLs. Afterward, a sharp increase in molecular weight can be noticed. This may be attributed to the repolymerization of oxidized lignin units occurring on the condensed phenolic structure at a higher temperature, as stated earlier [28]. These undesirable side reactions transform lignin into a bi-phenyl condensed format that is stable and difficult to cleave even at higher temperatures [32, 34]. To prove the repolymerization products, XPS for OKLC samples (supplementary file, Table A4.2, and Figure A4.2) were conducted.

The results showed that the relative percentages of C-C bonds increased in OKLC4 by around 11% when compared with OKLC3. Our recent study also observed the condensed phenolic structures during the alkaline oxidation in P-NMR [34]. It can also be observed that even though the Mw decreased initially, the Mn seemed to be increased with increasing temperatures in all OKLs when compared to KL (Mn of 1200 g/mol). The increased Mn during lignin oxidation was also observed in an earlier study [35]. The variation in the RI responses for all samples at 240 and 270 °C can be observed as a function of time in Figure 4.1 (f, g) and for all the samples in all reaction parameters can be found in Figure S1 in the supplementary material. The effects of

lignin concentrations and reaction temperatures on carboxylic acid and charge density were also assessed in our study and represented in Figure 4.1(h, i). It is seen that OKLB2 achieved a maximum carboxylic acid group and charge density. Recent studies also reported similar ranges of carboxylic acid groups (0.93-2.6 mmol/g) when lignin was oxidized in an alkaline medium [35, 36]. Demesa and the coworkers reported that the formation of carboxylic acids was the highest when alkali lignin (40 g/L in NaOH solution) was oxidized at 225 °C with 15 bar oxygen pressure for 20 min and started decreasing the yields when further increasing the temperature and reaction time [28]. Although the OKLA2 and OKLB2 samples show similar carboxylic acid groups and charge density ranges, OKLC2 samples contain significantly lower values of carboxylic acid groups and charge density. It can also be found that the carboxylic acid groups and charge density started decreasing with further increasing temperatures. This may be due to the decarboxylation and further lignin condensation, which led to lignin repolymerization. Considering the results, it can be concluded that the sample generated from 10 wt.% lignin concentrations at 210 °C temperature for 30 minutes, OKLB2, was the best sample as it contained 2.6 mmol/g of carboxylic acid group content, 1.89 meq/g of charge density and overall production yield of 75.4 %. Therefore, this sample was selected for further analysis.

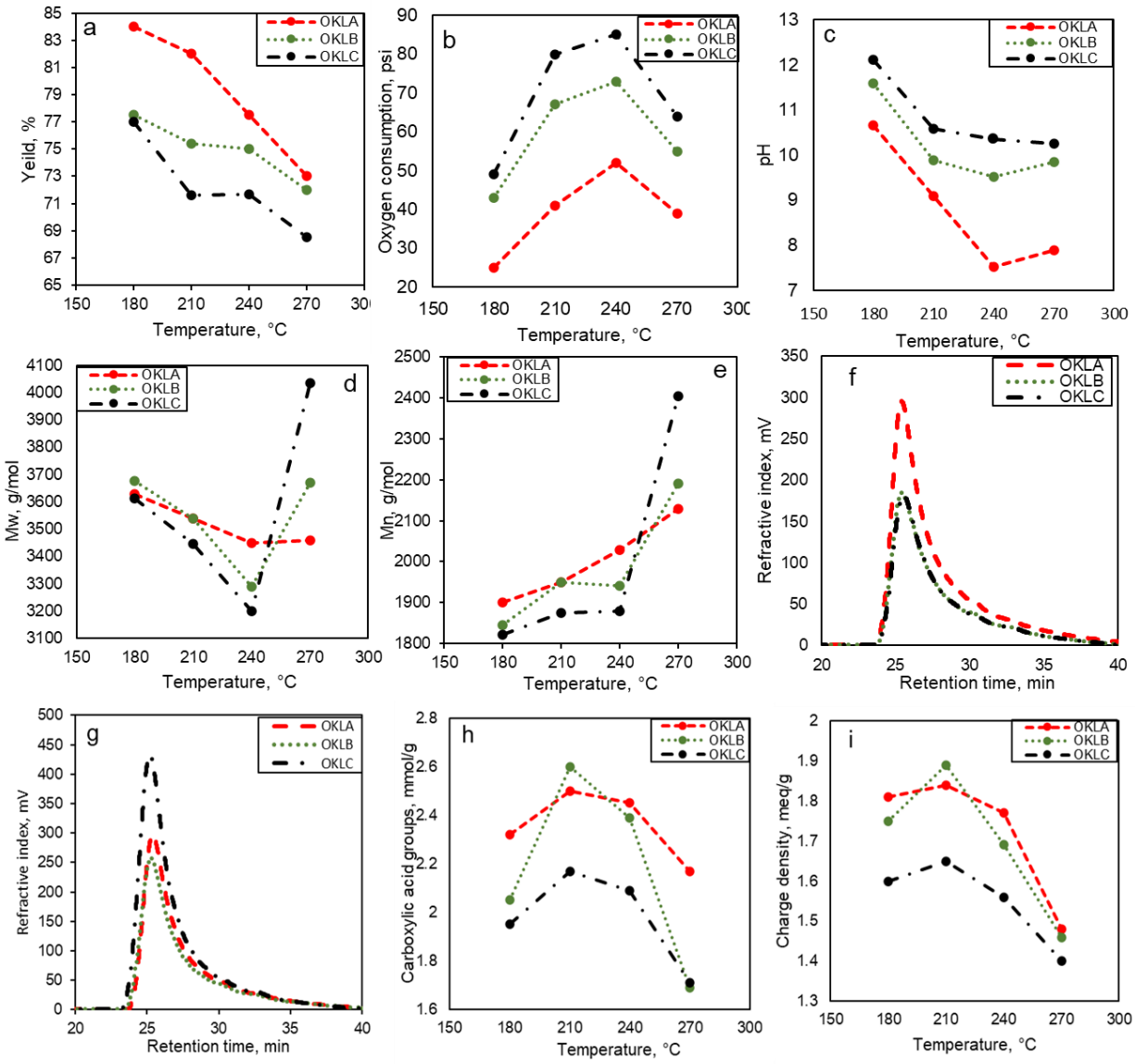

Figure 4.1: Effects of temperature on a) overall yields; b) consumption of oxygen gas (psi); c) variation of pH on the different reaction parameters; d) Mw; e) Mn; h) carboxylic acid; i) charge density of oxidized sample; f) GPC traces-RI responses as a function of retention time for the samples at 240 °C; and g) GPC traces-RI responses as a function of retention time for the samples at 270 °C

4.3.2. Structural Characterization of KL and Selected OKL

4.3.2.1. FTIR Analysis

Figure 4.2 shows the FTIR spectra of KL and OKLB2. It can be seen that, due to the abundance of G-units in softwood KL, the peaks at around 815 and 850 cm^{-1} are attributed to C-H out-of-plane vibration of guaiacyl units [37]. The spectra region around 1260 cm^{-1} is attributed to the C=O stretching for G-unit [37]. The disappearance of the peaks in OKLB2 may indicate the deformation of aromatic G-units during oxidation. Another characteristic peak at around 1360 cm^{-1} in KL shows intact aryl-ether bonds [37]. However, the shifting of this peak in OKLB2 may attribute to the aliphatic -OH and non-etherified phenolic-OH indicating the cleavage of β-O-4 and α-O-4 linkages during the oxidative depolymerization [37, 38]. The typical bands at 1590, 1540, and 1500 cm^{-1} are related to aromatic skeleton vibrations in KL, and their lower intensity in OKLB2 may suggest the opening of aromatic rings [37, 39]. The signal at 1700 cm^{-1} in OKLB2 is attributed to the C=O stretching for unconjugated carbonyl groups [39, 40]. The peaks at 2848 and 2934 cm^{-1} are assigned to the C-H stretching of methoxyl groups and CH_3/CH_2 groups, respectively [37]. Another specific peak at 3340 cm^{-1} is attributed to the aliphatic and phenolic OH stretching in KL [37]. The reduced intensity in the 1300-1100 cm^{-1} may suggest the extensive oxidative disruption in the aromatic region (G-units) that can be observed from HSQC NMR, which will be explained later[37].

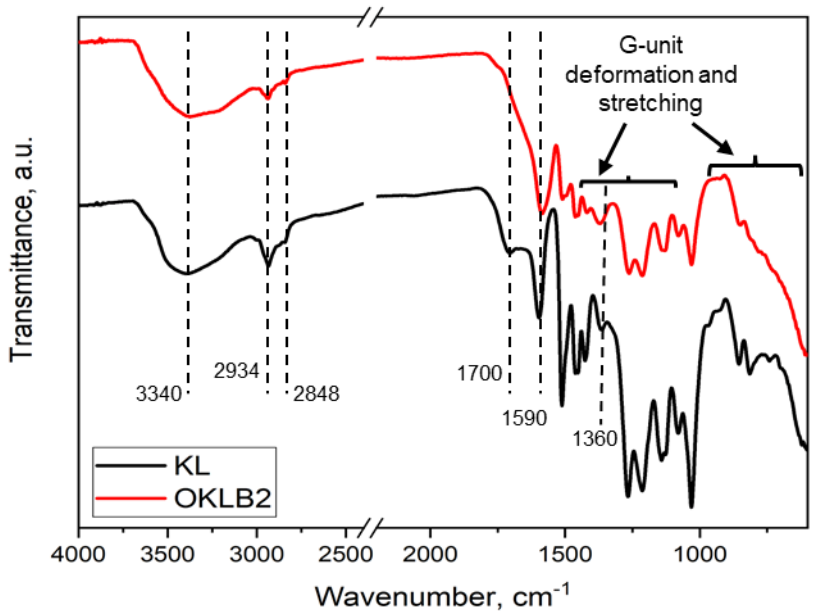

Figure 4.2: FTIR spectra analysis of KL and OKLB2

4.3.2.2. HSQC NMR Analysis

The HSQC NMR spectra of KL and OKLB2 are shown in Figure 4.3. Significant lignin interunit structures, such as β-aryl ether (A), resinol (B) and phenylcoumaran (C) structures, along with the aromatic monomers such as H, G, and cinnamaldehyde groups, were identified in KL [41]. In Figure 3 (a), the aliphatic C-C linkages in KL can be observed. The spectra region at ~ δ_C/δ_H 22/1.4 ppm is attributed to the guaiacyl hydroxyethyl ketone (E) [42]. The strong spectra for the Cα-Cβ side-chain linkages of guaiacyl propanol (F) can be located at δ_C/δ_H 33/2.5 ppm and 37/1.6 ppm [42]. The Cα-Cβ of secoisolariciresinol units (D) can also be identified at the δ_C/δ_H of 38/2.5 ppm and 42.5/2 ppm [42]. From Figure 4.3 (b), it can be observed that the relative intensity of these bonds becomes weaker after alkaline oxidation suggesting the decomposition. Moreover, the intense spectra at around δ_C/δ_H 50/3.5 ppm indicate the abundances of β-1 linkages in KL, whereas, after oxidative conversion, a significant reduction in the spectra can be

observed. The aliphatic side chain degradations were also observed in another study where corn stover lignin (50 mg) was oxidized by peracetic acid (250 mg) at 60 °C for 5 h, and the Cα-Cβ bonds were cleaved to form the phenolic compound [43]. Figure 4.3 (c) and 4.3 (d) represent the aliphatic C-O linkages in KL and OKLB2, respectively, where it can be observed that KL preserves all the β-O-4 (A), β-β (B) and β-5 (C) linkages. In contrast, alkaline oxidation cleaved them all, including the lignin carbohydrate complexes (LCC). The reduced intensity of the aliphatic C-O side chain linkages in OKLB2 in Figure 4.3(e) suggests the degradation of KL. This phenomenon was also reported for the alkaline oxidation of lignin [41]. An earlier study reported that, under alkaline oxidative conditions, the phenylpropane units would undergo Cβ-O and Cβ-Cβ (resinol unit) cleavage to transform into low molecular weight phenolic units, and further oxidation may lead to carboxylic end groups [34, 36]. The intensity of the methoxyl groups was also reduced significantly after the oxidation (Figure 4.3d). One earlier study on organosolv lignin (50 mg) oxidation under the microwave (80W) in the presence of 2.5 mL of water, 2.5 mL of acetonitrile, and 5 mg of copper sulfate in hydrogen peroxide (0.15 g) reported a similar observation.[36] Figure 4.3 (e) shows the abundance of the aromatic region in KL where the G-units dominate. The intense and overlapped cross signals from the δ_C/δ_H of 110-124/6.2-7.5 ppm can be attributed to C_2-H_2 (G_2), C_5-H_5 (G_5) and C_6-H_6 (G_6) of guaiacyl units in unmodified KL. The spectra region for the δ_C/δ_H of 127-128/7.1-7.5 ppm in Figure 4.3(e) is attributed to the H-units of lignin, and the region around δ_C/δ_H 126/6.8 ppm depicts the cinnamaldehyde end groups in KL. A significant decomposition of the aromatic regions can also be observed in Figure 4.3(f) in OKLB2. Previous research on alkaline aerobic corn stover lignin (15 wt.%) oxidation at 55-80 °C postulated that, during alkaline oxidation, first the phenolic-OH converted to quinone, later the methoxyl group (in C-3 position) is attacked by the oxygen

species ($O_2^{-\bullet}$) and finally the aromatic ring breaks in C3-C4 and transform into the aliphatic bi-carboxylic structure [32].

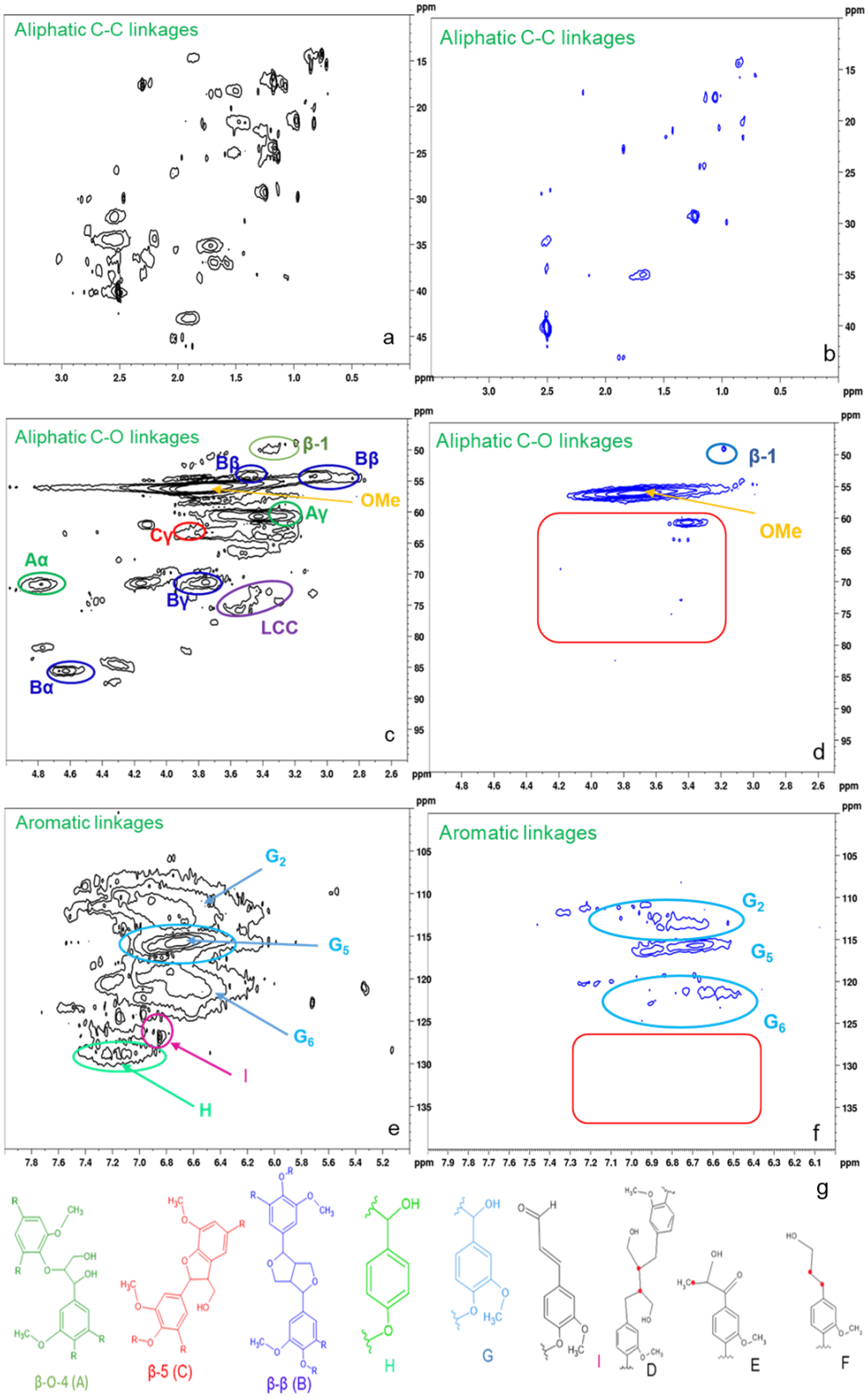
Aliphatic C-C linkages
a
Aliphatic C-C linkages
b
Aliphatic C-O linkages
β-1
Bβ
Bβ
OMe
Aγ
Cγ
Aα
Bγ
LCC
Bα
c
Aliphatic C-O linkages
β-1
OMe
d
Aromatic linkages
G2
G5
G6
I
H
e
Aromatic linkages
G2
G5
G6
f
g
β-O-4 (A)
β-5 (C)
β-β (B)
H
G
I
D
E
F

Figure 4.3: HSQC NMR spectra of KL and OKLB2. a) aliphatic C-C region of KL; b) aliphatic C-C region of OKLB2; c) aliphatic C-O region of KL; d) aliphatic C-O region of OKLB2; e) aromatic region of KL; f) aromatic region of OKLB2; g) lignin inter-unit linkages.

4.3.2.3. XPS Analysis

XPS was performed to observe the chemical and structural changes before and after oxidation. Figure 4.4 represents the XPS survey spectra and C1s and O1s scans of KL and OKLB2. Table 4.1 describes the relative mass concentrations of the different bonds of KL and OKLB2. Figure 4.4(a) confirms that OKLB2 contains potassium ions implying that the dialysis of the sample after oxidation did not remove all of the potassium used in the form of KOH during the oxidation reaction. In the wide spectrum, the peak at 378 eV is attributed to the K 2s,[44] which might be ionically attached to the COO^-. The larger sharp peak at 285 and 532 eV is attributed to the C1s and O1s, respectively [34, 45].

Figure 4.4 (b, c, d, e) represents the C1s and O1s scans for different bond types. In this Figure, the C1, C2, C3, and C4 bonds are attributed to C-C/C-H, C-OH, C=O (carbonyl), and C=O (carboxylic), respectively, whereas O1, O2, and O3 bonds are attributed to C=O (carboxyl/carbonyl), C-O-C and C-OH (phenolic), respectively [45, 46]. It can be seen that 1) the C1 bond types (C-H/C-C) relatively decreased by 6.3% due to the oxidative depolymerization, which was also confirmed in the HSQC NMR results in Figure 4.3; 2) C2 types (C-OH) increased by 6.6 % as a result of oxidation; 3) carbonyl bond types, C3 (C=O), decreased by 2.9%; and 4) the C4 bond types (carboxylic, C=O) increased by 3.3%. This phenomenon can be explained by the fact that the carbonyl groups were converted to carboxylic acid groups during oxidation. It can also be observed that the O1 bond types (C=O) increased by 3.1%. On the other

hand, the O2 (C-O-C) and O3 (C-OH, phenolic) decreased by 1.5 and 5.7%, respectively. The reduction in the O2-type bonds may be due to the cleavage of aryl ether linkages and methoxy groups. The O3 types (the aliphatic or phenolic-OH) may have decreased due to the conversion to O1(carboxylic, C=O).

Table 4.1: Binding energies and mass concentrations of carbon and oxygen species of KL and OKLB2

		Binding energy, eV		**Mass concentration, %**	
Bond types	Assignments	KL	OKLB2	KL	OKLB2
C1	C-H, C-C	284.9	284.7	63.1	56.8
C2	C-OH	286.3	286	24.3	30.9
C3	C=O, carbonyl	287.1	286.8	10.4	7.5
C4	C=O, carboxylic	288.5	288.3	1.5	4.8
O1	C=O	531.6	531.7	23.1	29.2
O2	C-O-C	533.3	533.4	62.2	60.7
O3	C-OH, phenolic	534.5	534.4	15.7	10

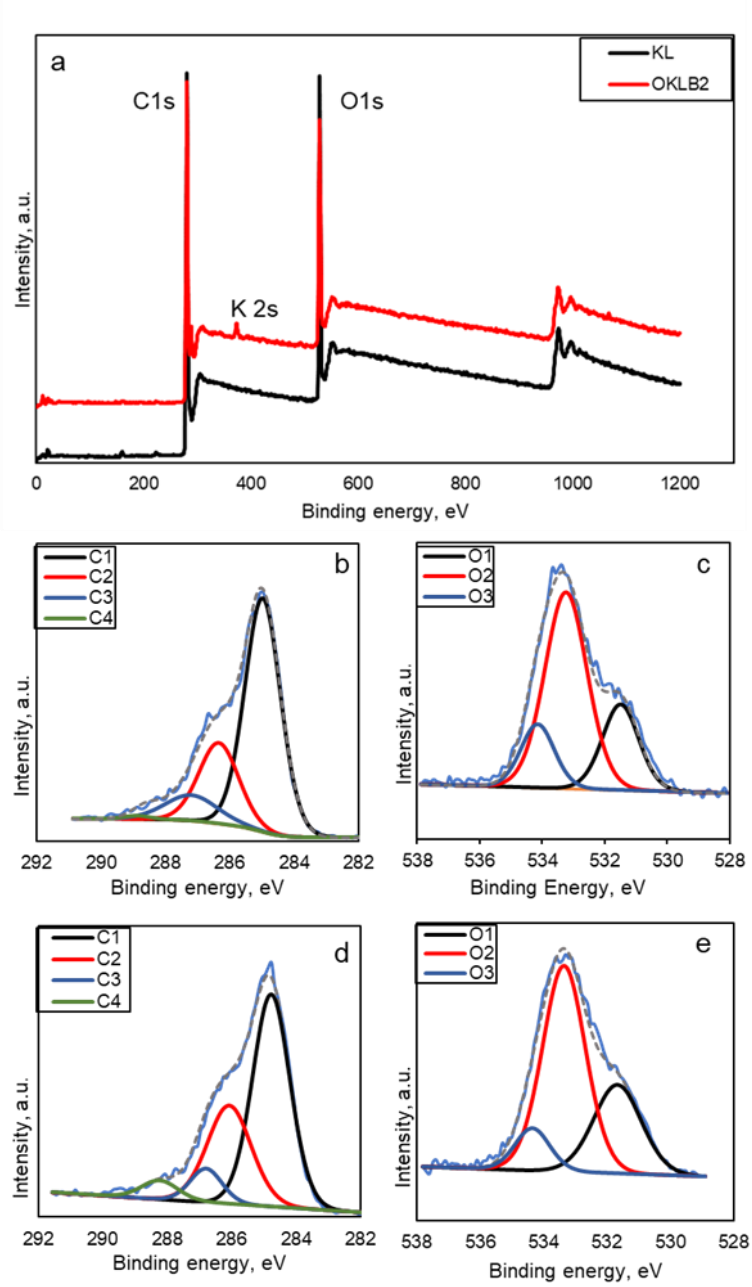

Figure 4.4: a) XPS broad spectra of KL and OKLB2; b) C1 scan of KL; c) O1 scan of KL; d) C1 scan of OKLB2: e) O1 scan of OKLB2.

4.3.3. TGA Analysis

Figure 4.5 depicts the thermal decomposition of KL and OKLB2 under a nitrogen environment. Generally, the degradation of lignin is divided into three stages: 1) stage one (30-120 °C) indicates the weight loss due to the evaporation of moisture, 2) stage 2 (180-350 °C) is attributed to the degradation of the low molecular weight volatiles (e.g., phenolic monomers), and carbohydrate conversion to gases, such as carbon dioxide, carbon monoxide, methane, and 3) stage 3 (> 350 °C) is attributed to the decomposition of the phenolic compounds, alcohols, aldehydes, and acids [47]. From the TGA curves of KL and OKLB2, it can be observed that approximately 5% of weight losses were found due to moisture in stage one. In the next stage, no significant weight loss was observed in KL. However, OKLB2 had 7-8% decomposition, which may be due to the degradation of the COOH to CO_2. Further increasing temperature from 350 °C to 750 °C led to a significant weight loss (~83 wt.%) in KL, which could be attributed to the degradation of aromatic rings and other side-chain oxygenated functional groups [48]. Earlier studies also reported that about 3-5 wt.% of lignin could remain as residues if KL were pure, and more would remain as residues if KL were not pure [24, 48, 49]. However, OKLB2 did not degrade remarkably after 450 °C and remained undecomposed. The significant amount of ash in OKLB2 mainly comes from the potassium ions (2.2 wt.%) that may be ionically bound to COO^-. Another reason for having 54% residue may be related to the condensed aromatic structures with C-C and ether bond linkages because ether bonds remain unbroken even at a higher temperature than 600 °C [24]. The increased weight loss rate in OKLB2 after 700 °C may be due to the condensed aromatic structures, such as polycyclic aromatic hydrocarbons [50, 51]. The presence of potassium ion (2.2 wt.%) and the condensed aromatic structures (remaining around 52 wt.%) can be correlated (from the XPS and HSQC analysis). As stated earlier, the XPS showed (Table 4.1, Figure 4.4, and Figure A4.2) the relative abundances of the C-C (may come from condensed

aromatic structures) and remaining ether bonds, which were not broken during the oxidation. The HSQC also suggested that some aromatic structures remained un-disrupted, which may be due to the condensed structures.

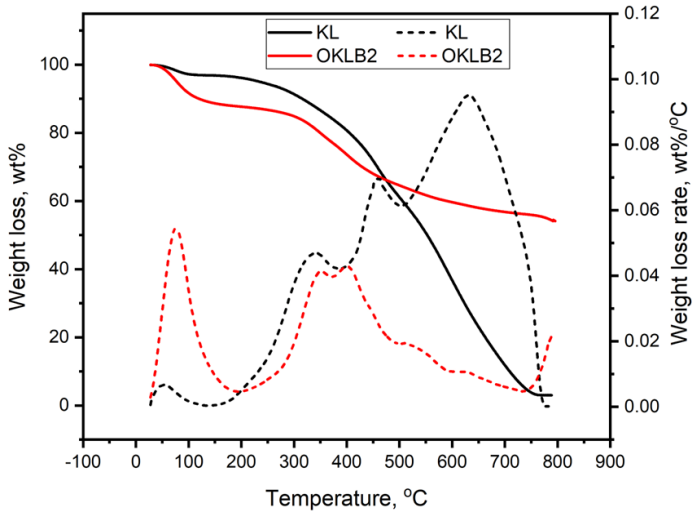

Figure 4.5: TGA and DTG curves of KL and OKLB2

4.3.4. Performance Analysis

4.3.4.1. Adsorption and Zeta Potential Analyses

When anionic plasticizers are added to cement pastes, they adsorb on the cement particles and create an electric repulsion among particles in the pastes. In this study, the adsorption of OKLs on the cement surface was investigated and compared with that of LS and CP in Figure 4.6a. As seen, OKLB2 showed higher adsorption than LS and CP did. This phenomenon can be directly related to the charge density of the samples [13]. Figure 4.6a concludes that increasing the dosages increased the adsorbed amounts. It was stated that the adsorption of anionic plasticizers is essential to generate electrostatic repulsion between the cement particles [52]. On the other hand, it was reported that polycarboxylate superplasticizers might develop complexation

between the COO^- groups and Ca^{2+} in cement surfaces [53]. Therefore, carboxylic acid groups may increase the adsorption rate of OKLB2 on cement particles.

The zeta potential of the supernatant after the adsorption analysis was investigated and presented in Figure 4.6b. As the dosages of OKLB2 and LS were increased, the negative zeta potential of the supernatants on these solutions increased. This can be due to the increased amount of un-adsorbed lignin samples remaining in the solutions. On the other hand, the zeta potential of CP did not change significantly. The zeta potential analysis for all samples before adsorption analysis (without adding cement) can be found in Figures A4.3 and A4.4 in the supplementary material.

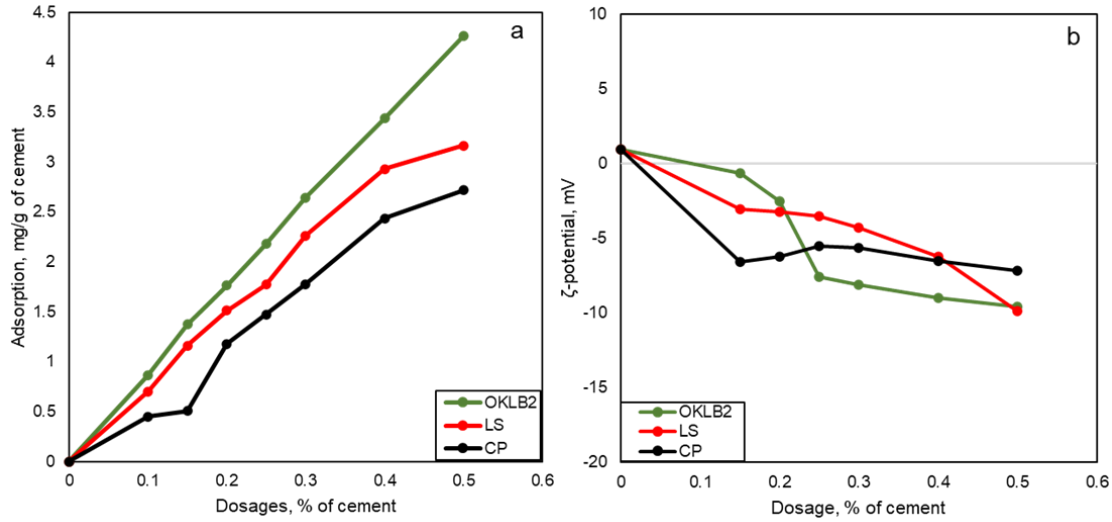

Figure 4.6: (a) Adsorption analysis of OKLB2, LS, and CP at different sample doses; (b) Zeta potential of the samples at pH 11.

Table 4.2: Molecular weights and charge density of KL, LS and CP

Samples	Mw, g/mol	Mn, g/mol	Mw/Mn	Charge density, meq/g
KL	7000	1200	5.83	0.3
OKLB2	3540	1950	1.8	1.9

LS	9380	3740	2.5	1.3
CP	4030	2300	1.75	0.1

4.3.4.2. Effect of Lignin Derivatives on the Flowability of Cement Paste

The effect of charge densities of OKL on the flowability of cement paste is illustrated in Figure 4.7a. Generally, when the attractive forces between the cement particles are dominant, the particles will exhibit more yield stress resulting in aggregations. Upon adding the plasticizer, the repulsion forces between the particles increase due to increasing the net negative charges, thus lowering the yield stress and enhancing the paste flowability. As seen, the highest flowability was observed for OKLB2 with the carboxylic acid group content of 2.6 mmol/g and charge density of 1.9 meq/g. A previous study reported that the flowability of cement paste would improve with increasing charge density of lignin derivatives [23], which is attributed to the enhanced electrostatic repulsion in the cement pastes. Also, when lignin is adsorbed on the cement particles, its phenolic hydroxyl groups may contribute to steric hindrance on the particles. As OKLB2 generated the highest flowability, the effect of the dosage of this sample, along with commercial lignosulfonate (LS) and plasticizer (CP), on cement pastes was tested, and the results are available in Figure 4.7b. As seen, the fluidity was improved by increasing their dosage in the cement pastes. This is because the higher dosage of anionic materials would increase the total negative charges, elevating the repulsion in the cement pastes. Earlier studies also reported comparable cement paste flowability with increasing plasticizer dosages [1, 9, 52]. It can also be observed that the fluidity performance of OKLB2 is around 18% better than LS at 0.25 wt.% dosage. Although the charge density of LS is less than OKLB2 (Table 4.2), its Mw

(9380 g/mol in Table 4.2) was higher, which played a role in enhancing the steric hindrance to achieve comparable flowability. In the case of CP, the flowability was not improved at the same level as OKLB2 and LS, which might be attributed to its low charge density (Table 4.2). Therefore, the un-adsorbed particles of CP may not contribute to increasing the electrostatic repulsion resulting in its poor flowability performance.

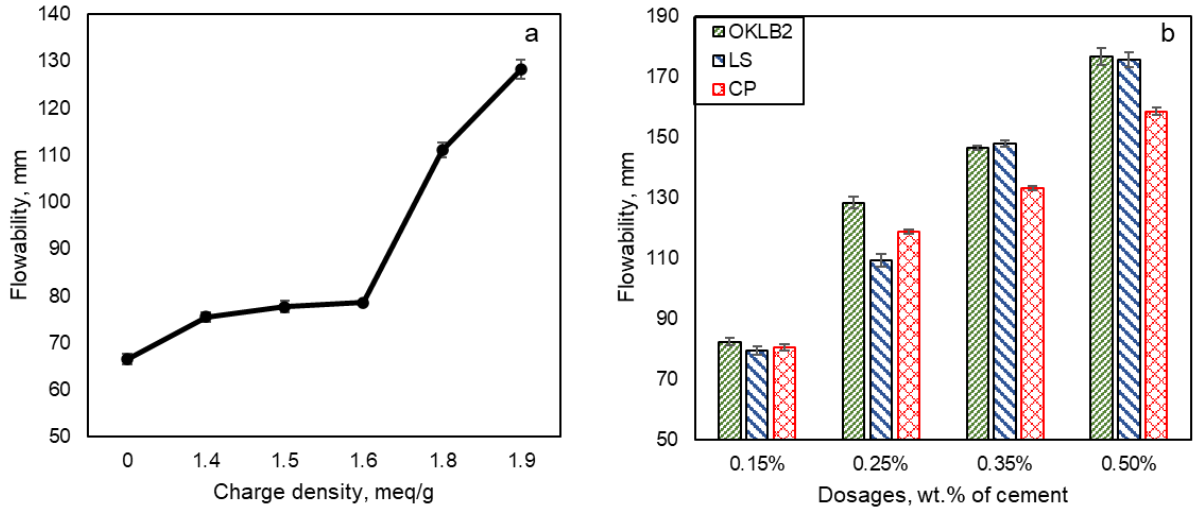

Figure 4.7: Effects of a) charge density of lignin derivatives (b) and dosage of samples on the flowability of cement paste W/C=0.4.

4.3.4.3. Impact on Compression Strength

The effect of sample dosage on the compression strength of cement is described in Figure 4.8. Evidently, the compression strength was increased by 45% at an OKLB2 dosage of 0.25 wt.% of cement. However, further increasing OKLB2 dosage (e.g., 0.5 wt.%) seems to decrease the strength. An earlier study reported that oxidized soda lignin (with a negative charge density of 6.9 mmol/g), produced in an alkaline (NaOH) aerobic oxidation, improved the compression

strength by 1.9% with adding 0.4 wt.% of the sample when compared with the blank [1]. One reason for the higher strength of OKLB2 might be attributed to the presence of carboxylic acid groups and its highest adsorption on the cement particles (Figure 4.6a). Carboxylate ions were reported to form complexes with calcium ions on the cement surface, and remaining un-adsorbed samples in the solution could enhance the interaction with cement particles during the hydration period, improving the cement compression strength [1, 54]. Another reason could be the presence of potassium ions in the sample. An earlier study articulated that K^+ would improve concrete formation by increasing gel porosity and decreasing capillary porosity [22]. It was reported that K^+ could interact with the alumina and silica in cement to improve microscopic strength in the hardened concrete [21].

Decreasing the compressive strength with further increasing OKLB2 dosages could be explained by the increased repulsion force in the cement paste. When OKLB2 is added at a low dosage (0.25 wt.%) to the cement paste, the negative charges of OKLB2 would create repulsion in the cement paste and improve the fluidity of the sample. However, the induced repulsion would not be so strong that it could negatively affect the cement particles from aggregation and bonding in the drying state. Thus, the compression strength of cement would not be negatively affected at a low OKLB2 dosage. At higher OKLB2 dosage, however, the repulsion force created between cement particles would be such high that, in addition to increasing the fluidity, OKLB2 would hinder cement particles from chemical bonding and aggregation upon drying, and thus they would negatively impact the compression strength of the cement paste.

In the case of LS and CP, the compression strength was lower and started to decrease at a lower dosage of 0.15 wt.%. At 0.5 wt.%, the compressive strength could not be measured for LS and CP due to very poor concrete structure. An earlier study reported that the dosage of 0.125 wt.%

LS improved concrete strength by 9%, and it decreased it by 25% at 0.5 wt.% dosages [55]. The results confirm that LS and CP were less effective than OKLB2. As discussed earlier, the adsorption of LS and CP was more limited than OKLB2 on cement particles; hence their interactions with cement particles were assumed poor. Moreover, LS has a higher molecular weight than OKLB2 (Table 4.2), which should create more steric hindrance, preventing cement particles from approaching for bonding development. Another possible reason can be explained by the reactivity of the sulfonate groups in LS and the carboxylic acid groups in OKLB2. Due to the more vigorous acidic nature of sulfonate groups than carboxylic acid groups [56], the LS may react with available lime in the cement and generate CO_2 bubbles that may entrap in the concrete and reduce the cement strength. On the other hand, the carboxylic acid group-rich OKLB2 may not readily interact with limes but adsorb on the cement particles.

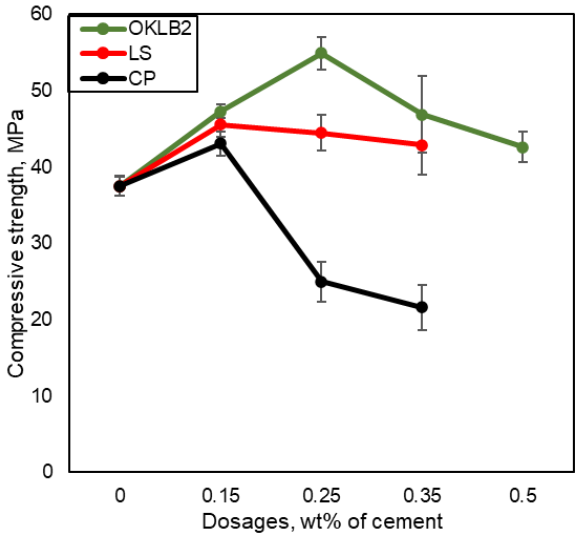

Figure 4.8: Effect of dosages of OKLB2, LS and CP on compressive strength of cement.

4.3.4.4. Water Reducibility

The water reducibility of OKLB2 as a green plasticizer was studied and reported in Figure 4.9. The results suggested that the OKLB2 at the dosages of 0.25 and 0.35 wt.% could reduce the water amount in the cement paste by 12% and 18%, respectively. It can also be determined that LS could reduce the water amount by 8% and 15%, respectively. In the same vein, CP could reduce the water content by 10 and 12% at the same dosages. However, LS and CP would decrease the concrete strength significantly at higher dosages (Figure 4.8). An earlier article reported that as a mid-range water reducer, the plasticizer should reduce water in the range of 8-18% and improve cement strength by 15% [57]. Considering the flowability and compressive strength analysis results, the current study depicts that OKLB2 can be used as a mid-range concrete plasticizer.

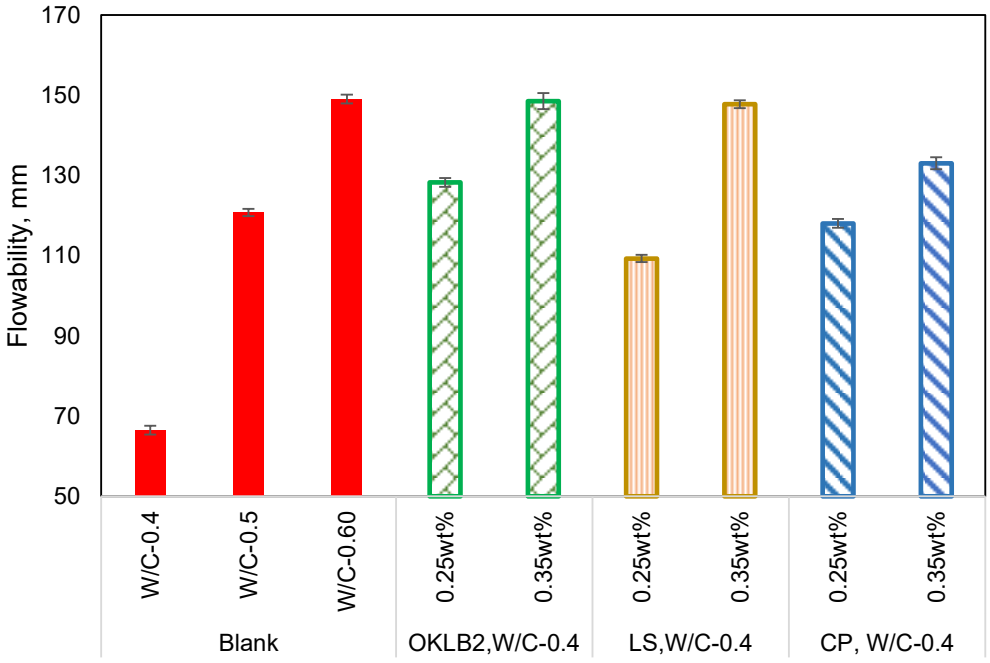

Figure 4.9: Water reducibility of lignin derivatives in cement pastes.

4.4. Conclusions

The oxidation of KL with oxygen gas in the presence of KOH was optimized to achieve water-soluble oxidized lignin with the maximum carboxylic acid content and charge density. The study showed that the oxidation reaction under the conditions of 10 wt.% lignin concentration in water, 100 psi initial oxygen gas pressure, and 210 °C generated oxidized lignin (OKLB2) with the highest amount (2.6 mmol/g) of the carboxylic acid group and charge density of 1.9 mmol/g. The FTIR analysis suggested structural modifications, such as the disruption of aromatic guaiacyl units and bond cleavage during the oxidation of lignin. The HSQC-NMR analysis of the samples confirmed the oxidative depolymerization of lignin linkages, and the disappearance of the aromatic guaiacyl units suggested the ring openings. The XPS analysis confirmed the presence of potassium ions and indicated that the relative abundances of the C-C bonds decreased and C=O bonds increased, which was attributed to the depolymerization and increasing carboxylic acid groups of lignin. The adsorption of OKLB2 was observed to be more than that of LS and CP on cement particles, which is attributed to the higher electrostatic attraction between the carboxylic acid groups and the cement particles. The results from zeta potential analysis revealed that the un-adsorbed OKLB2 might create electrical repulsion in the cement paste due to the available negative charges. The flowability performance of OKLB2 was much better than that of other samples, which was associated with its carboxylic acid group and steric hindrance. Furthermore, using OKLB2 in cement improved its strength by 45% compared with blank at 0.25 wt.% dosage. The improved compression strength is attributed to the enhanced cement bonding associated with the available carboxylic acid group and potassium ions originating from OKLB2. At higher OKLB2 dosage, the compression strength of cement was reduced due to the dominant

repulsion created between cement particles by surplus of carboxylic acid groups in the paste at a higher dosage of OKLB2. The water reducibility test suggested that the OKLB2 could reduce the water use in cement by 18% at a dosage of 0.35 wt.% with relatively higher compressive strength than blank. OKLB2 showed better adsorption, flowability, and strength than LS and CP did. The results confirmed that one-pot oxidation of lignin in the presence of KOH is a promising approach to generating a cement plasticizer. This oxidation process is green since the raw material (lignin) is completely bio-based, and the primary solvent of the oxidation process is water. Also, the process does not require any purification for products to be used as cement plasticizers, which would require production costs.

References

[1] A. Kalliola, T. Vehmas, T. Liitiä, T. Tamminen, Alkali-O2 oxidized lignin–A bio-based concrete plasticizer, Industrial Crops and Products 74 (2015) 150-157.

[2] S. Hanehara, K. Yamada, Interaction between cement and chemical admixture from the point of cement hydration, absorption behaviour of admixture, and paste rheology, Cement and Concrete Research 29(8) (1999) 1159-1165.

[3] X. Liu, Z. Wang, J. Zhu, Y. Zheng, S. Cui, M. Lan, H. Li, Synthesis, characterization and performance of a polycarboxylate superplasticizer with amide structure, Colloids and Surfaces A: Physicochemical and Engineering Aspects 448 (2014) 119-129.

[4] D.S. Shah, M.P. Shah, J. Pitroda, Chemical admixtures: a major role in modern concrete materials and technologies, National conference on trends and challenges of civil engineering in today's transforming world, 2014.

[5] O. Boukendakdji, E.-H. Kadri, S. Kenai, Effects of granulated blast furnace slag and superplasticizer type on the fresh properties and compressive strength of self-compacting concrete, Cement and concrete composites 34(4) (2012) 583-590.

[6] L. Grierson, J. Knight, R. Maharaj, The role of calcium ions and lignosulphonate plasticiser in the hydration of cement, Cement and Concrete Research 35(4) (2005) 631-636.

[7] B.-G. Kim, S. Jiang, C. Jolicoeur, P.-C. Aïtcin, The adsorption behavior of PNS superplasticizer and its relation to fluidity of cement paste, Cement and Concrete research 30(6) (2000) 887-893.

[8] S. Magina, A. Barros-Timmons, D.V. Evtuguin, Synthesis of Lignosulfonate-Based Dispersants for Application in Concrete Formulations, Materials (Basel) 14(23) (2021). https://doi.org/10.3390/ma14237388.

[9] İ.B. Topçu, Ö. Ateşin, Effect of high dosage lignosulphonate and naphthalene sulphonate based plasticizer usage on micro concrete properties, Construction and Building Materials 120 (2016) 189-197.

[10] G. Telysheva, T. Dizhbite, E. Paegle, A. Shapatin, I. Demidov, Surface- active properties of hydrophobized derivatives of lignosulfonates: effect of structure of organosilicon modifier, Journal of Applied Polymer Science 82(4) (2001) 1013-1020.

[11] M. Zhou, X. Qiu, D. Yang, H. Lou, Properties of different molecular weight sodium lignosulfonate fractions as dispersant of coal- water slurry, Journal of dispersion science and technology 27(6) (2006) 851-856.

[12] C.M. Childs, K.M. Perkins, A. Menon, N.R. Washburn, Interplay of Anionic Functionality in Polymer-Grafted Lignin Superplasticizers for Portland Cement, Industrial & Engineering Chemistry Research 58(43) (2019) 19760-19766. https://doi.org/10.1021/acs.iecr.9b03973.

[13] W. He, P. Fatehi, Preparation of sulfomethylated softwood kraft lignin as a dispersant for cement admixture, Rsc Advances 5(58) (2015) 47031-47039.

[14] L. Dessbesell, M. Paleologou, M. Leitch, R. Pulkki, C.C. Xu, Global lignin supply overview and kraft lignin potential as an alternative for petroleum-based polymers, Renewable and Sustainable Energy Reviews 123 (2020) 109768.

[15] D. Bajwa, G. Pourhashem, A.H. Ullah, S. Bajwa, A concise review of current lignin production, applications, products and their environmental impact, Industrial Crops and Products 139 (2019) 111526.

[16] S. Laurichesse, L. Avérous, Chemical modification of lignins: Towards biobased polymers, J Progress in Polymer Science 39(7) (2014) 1266-1290.

[17] S. Wang, F. Kong, W. Gao, P. Fatehi, Novel Process for Generating Cationic Lignin Based Flocculant, Industrial & Engineering Chemistry Research 57(19) (2018) 6595-6608. https://doi.org/10.1021/acs.iecr.7b05381.

[18] C. Fargues, Á. Mathias, A. Rodrigues, Kinetics of Vanillin Production from Kraft Lignin Oxidation, Industrial & Engineering Chemistry Research 35(1) (1996) 28-36. https://doi.org/10.1021/ie950267k.

[19] Y. Ma, J. Qian, Influence of alkali sulfates in clinker on the hydration and hardening of Portland cement, Construction and Building Materials 180 (2018) 351-363. https://doi.org/https://doi.org/10.1016/j.conbuildmat.2018.05.196.

[20] T. Salthammer, S. Mentese, R. Marutzky, Formaldehyde in the indoor environment, Chemical reviews 110(4) (2010) 2536-2572.

[21] Z. Yu, Z. Xie, T. Zhang, G. Yue, H. Liu, Q. Li, L. Wang, Influence of Potassium-Based Alkaline Electrolyzed Water on Hydration Process and the Properties of Cement-Based Materials with Fly Ash, Materials 14(22) (2021) 6956.

[22] V. Sopov, L. Pershina, L. Butskaya, E. Latorets, O. Makarenko, The role of chemical admixtures in the formation of the structure of cement stone, MATEC Web of Conferences, EDP Sciences, 2017, p. 01018.

[23] W. He, W. Gao, P.J.A.S.C. Fatehi, Engineering, Oxidation of kraft lignin with hydrogen peroxide and its application as a dispersant for kaolin suspensions, 5(11) (2017) 10597-10605.

[24] M.K. Konduri, F. Kong, P. Fatehi, Production of carboxymethylated lignin and its application as a dispersant, European Polymer Journal 70 (2015) 371-383.

[25] S. Sabaghi, N. Alipoormazandarani, P. Fatehi, Production and Application of Triblock Hydrolysis Lignin-Based Anionic Copolymers in Aqueous Systems, ACS omega 6(9) (2021) 6393-6403.

[26] W. Gao, J.P. Inwood, P. Fatehi, Sulfonation of phenolated kraft lignin to produce water soluble products, Journal of Wood Chemistry and Technology 39(4) (2019) 225-241.

[27] ASTM, Annual book of ASTM standards, Standard test method for compressive strength of hydraulic cement mortars (using 2-in. or [50-mm] cube specimens);C 109/C 109M-98, ASTM International1998.

[28] A.G. Demesa, A. Laari, I. Turunen, M. Sillanpää, Alkaline partial wet oxidation of lignin for the production of carboxylic acids, Chemical Engineering &Technology 38(12) (2015) 2270-2278.

[29] W. Jung, D. Savithri, R. Sharma-Shivappa, P. Kolar, Changes in lignin chemistry of switchgrass due to delignification by sodium hydroxide pretreatment, Energies 11(2) (2018) 376.

[30] R. Katahira, A. Mittal, K. McKinney, X. Chen, M.P. Tucker, D.K. Johnson, G.T. Beckham, Base-catalyzed depolymerization of biorefinery lignins, ACS Sustainable Chemistry & Engineering 4(3) (2016) 1474-1486.

[31] H. Sixta, Handbook of Pulp, Volume 2, (2006).

[32] A. Kalliola, Chemical and enzymatic oxidation using molecular oxygen as a means to valorize technical lignins for material applications, (2015).

[33] L. Jurasek, L. Kri tofová, Y. Sun, D.S. Argyropoulos, Alkaline oxidative degradation of diphenylmethane structures Activation energy and computational analysis of the reaction mechanism, Canadian Journal of Chemistry 79(9) (2001) 1394-1401.

[34] S. Sutradhar, N. Alam, L.P. Christopher, P. Fatehi, KOH catalyzed oxidation of kraft lignin to produce green fertilizer, Catalysis Today 404 (2022) 49-62.

[35] U. Junghans, J.J. Bernhardt, R. Wollnik, D. Triebert, G. Unkelbach, D. Pufky-Heinrich, Valorization of Lignin via Oxidative Depolymerization with Hydrogen Peroxide: Towards Carboxyl-Rich Oligomeric Lignin Fragments, Molecules 25(11) (2020) 2717.

[36] M. Camus, O. Condassamy, F. Ham-Pichavant, C. Michaud, S. Mastroianni, G. Mignani, E. Grau, H. Cramail, S. Grelier, Oxidative Depolymerization of Alkaline Lignin from Pinus Pinaster by Oxygen and Air for Value-Added Bio-Sourced Synthons, Polymers 13(21) (2021) 3725.

[37] T.A. Amit, R. Roy, D.E. Raynie, Thermal and structural characterization of two commercially available technical lignins for potential depolymerization via hydrothermal liquefaction, Current Research in Green and Sustainable Chemistry 4 (2021) 100106.

[38] S. SUTRADHAR, K.M.Y. Arafat, J. NAYEEM, M.S. JAHAN, Organic acid lignin from rice straw in phenol-formaldehyde resin preparation for plywood, Cellulose Chemistry and Technology. 54(56) (2020) 463-471.

[39] G. Rocha, L. Andrade, C. Martin, G. Araujo, V.E. Mouchrek Filho, A.A.d.S. Curvelo, Simultaneous obtaining of oxidized lignin and cellulosic pulp from steam-exploded sugarcane bagasse, Industrial Crops and Products 147 (2020) 112227.

[40] M. Fodil Cherif, D. Trache, N. Brosse, F. Benaliouche, A.F. Tarchoun, Comparison of the physicochemical properties and thermal stability of organosolv and kraft lignins from hardwood and softwood biomass for their potential valorization, Waste and Biomass Valorization 11(12) (2020) 6541-6553.

[41] W. Schutyser, J.S. Kruger, A.M. Robinson, R. Katahira, D.G. Brandner, N.S. Cleveland, A. Mittal, D.J. Peterson, R. Meilan, Y. Román-Leshkov, Revisiting alkaline aerobic lignin oxidation, Green chemistry 20(16) (2018) 3828-3844.

[42] C. Crestini, H. Lange, M. Sette, D.S. Argyropoulos, On the structure of softwood kraft lignin, Green Chemistry 19(17) (2017) 4104-4121.

[43] R. Ma, U. Sanyal, M.V. Olarte, H.M. Job, M.S. Swita, S.B. Jones, P.A. Meyer, S.D. Burton, J.R. Cort, M.E. Bowden, Role of peracetic acid on the disruption of lignin packing structure and its consequence on lignin depolymerisation, Green Chemistry 23(21) (2021) 8468-8479.

[44] F. Qian, X. Li, L. Tang, S.K. Lai, C. Lu, S.P. Lau, Potassium doping: Tuning the optical properties of graphene quantum dots, AIP Advances 6(7) (2016) 075116.

[45] Y. Wang, S. Liu, Q. Wang, X. Fu, P. Fatehi, Performance of polyvinyl alcohol hydrogel reinforced with lignin-containing cellulose nanocrystals, Cellulose 27(15) (2020) 8725-8743.

[46] Z. Tian, L. Zong, R. Niu, X. Wang, Y. Li, S. Ai, Recovery and characterization of lignin from alkaline straw pulping black liquor: As feedstock for bio- oil research, Journal of applied polymer science 132(25) (2015).

[47] D. Watkins, M. Nuruddin, M. Hosur, A. Tcherbi-Narteh, S. Jeelani, Extraction and characterization of lignin from different biomass resources, Journal of Materials Research and Technology 4(1) (2015) 26-32.

[48] L. Lazzari, E. Domingos, L. Silva, A. Kuznetsov, W. Romão, J. Araujo, Kraft lignin and polyethylene terephthalate blends: effect on thermal and mechanical properties, Polímeros 29 (2020).

[49] L.D. Duong, G.-Y. Nam, J.-S. Oh, I.-K. Park, N.D. Luong, H.K. Yoon, S.H. Lee, Y. Lee, J.-H. Yun, C.-G. Lee, S.H. Hwang, J. Nam, High Molecular-Weight Thermoplastic Polymerization of Kraft Lignin Macromers with Diisocyanate, Bioresources 9 (2014) 2359-2371.

[50] H. Kawamoto, Lignin pyrolysis reactions, Journal of Wood Science 63(2) (2017) 117-132. https://doi.org/10.1007/s10086-016-1606-z.

[51] M.E. Moustaqim, A.E. Kaihal, M.E. Marouani, S. Men-La-Yakhaf, M. Taibi, S. Sebbahi, S.E. Hajjaji, F. Kifani-Sahban, Thermal and thermomechanical analyses of lignin, Sustainable Chemistry and Pharmacy 9 (2018) 63-68. https://doi.org/https://doi.org/10.1016/j.scp.2018.06.002.

[52] M. Ilg, J. Plank, Synthesis and Properties of a Polycarboxylate Superplasticizer with a Jellyfish-Like Structure Comprising Hyperbranched Polyglycerols, Industrial & Engineering Chemistry Research 58(29) (2019) 12913-12926. https://doi.org/10.1021/acs.iecr.9b02077.

[53] B. Ma, H. Qi, H. Tan, Y. Su, X. Li, X. Liu, C. Li, T. Zhang, Effect of aliphatic-based superplasticizer on rheological performance of cement paste plasticized by polycarboxylate superplasticizer, Construction and Building Materials 233 (2020) 117181.

[54] X. Qiu, X. Peng, C. Yi, Y. Deng, Effect of Side Chains and Sulfonic Groups on the Performance of Polycarboxylate-Type Superplasticizers in Concentrated Cement Suspensions, Journal of Dispersion Science and Technology 32(2) (2011) 203-212. https://doi.org/10.1080/01932691003656888.

[55] Ł. Klapiszewski, I. Klapiszewska, A. Ślosarczyk, T. Jesionowski, Lignin-Based Hybrid Admixtures and their Role in Cement Composite Fabrication, Molecules 24(19) (2019). https://doi.org/10.3390/molecules24193544.

[56] J. DeRuiter, Carboxylic acid structure and chemistry: part 2, Principles of drug action 1 (2005) 1-10.

[57] G.E. Schaefer, How Mid-range Water Reducers Enhance Concrete Performance, Concrete Construction 40(7) (1995) 5599-602.

Chapter 5

Oxalic acid-mediated oxidative depolymerization of Kraft lignin for vanillin and vanillic acid production

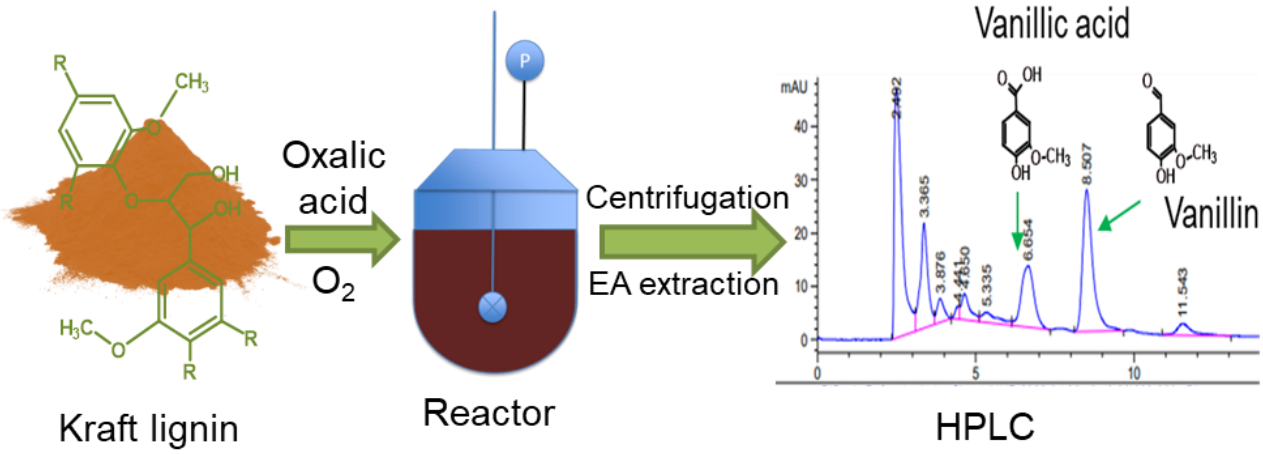

Abstract

In this work, kraft lignin (KL) was depolymerized in an oxalic acid-mediated aqueous solution to produce vanillin and vanillic acid. The findings showed that the depolymerization of KL (5 wt.%) in the presence of 1.25 M oxalic acid and 50 psi initial oxygen pressure at 125 °C for 60 min generated the maximum production yields of 15.7 wt.% and 11.7 wt.% for vanillin and vanillic acid, respectively. The phenolic compounds were quantified by high-performance liquid chromatography (HPLC) analysis. ^{13}C- and HSQC NMR analyses confirmed the presence of aromatic moieties and the absence of phenolic oligomers in the products. The ^{1}H-NMR and HSQC-NMR of KL and the partially depolymerized lignin (PDL) proved the cleavage of all β-O-4 linkages and disruption of aromatic regions. The recyclability, one-step aqueous reaction, relatively high production yield and recovery of oxalic acid (up to 78.6 %) could make this process industrially attractive for vanillin production.

5.1. Introduction

Lignin is the most abundant heterogeneous aromatic biomacromolecule consisting of three phenylpropanolic monomers, p-coumaryl, coniferyl, and sinapyl alcohols. These monomers are the precursors of the *p*-hydroxyphenyl (H), guaiacyl (G), and syringyl (S) units, respectively [1]. The significant interunit linkages in lignin macromolecules are commonly known as β-O-4, β-β, β-5, β-1 5-5′, α-O-4 units, where β-O-4 shares 40-60% in different wood species [2, 3]. Commercially, lignin is isolated from pulping industries as a by-product. About 85% of the total lignin is produced from the kraft process but is mostly burnt as a low-grade fuel for energy generation [4]. Despite the vast production, however, lignin is currently under-utilized.

The oxidation of lignin is one alternative to produce fine chemicals, such as aromatic aldehydes (vanillin, syringaldehyde) and acids [5-7]. Nitrobenzene, air/oxygen, metal oxides/hydroxides, and hydrogen peroxides are the commonly used oxidizing agents in lignin oxidation, depending on the desired end-used products [8]. Generally, the oxidative depolymerization of lignin can be categorized by base-catalyzed depolymerization (BCD) and acid-catalyzed depolymerization (ACD). The BCD of lignin is carried out with NaOH, KOH, Na_2CO_3, NH_4OH, Ca $(OH)_2$, and LiOH at temperatures ranging from 175-300°C in the presence of oxygen, air, or hydrogen peroxides. Moreover, BCD is performed at relatively high temperatures, which is one of the main limitations for the commercialization of this oxidation process for lignin depolymerization. Different transition metal oxides/salt catalysts, such as $CuSO_4$ [9], CuO [10], mixed salts (Cu^{2+} and Fe^{3+}) [11], Co^{2+}[12], and Mn^{2+} [13] have been used in alkaline oxidations to reduce the reaction time, temperature and enhance product yields of lignin depolymerization [14]. The yield

of phenolic compounds from oxidative BCD (including catalysts) was reported in the range of 6-30 wt.% [14, 15].

Lignin oxidation through ACD is also practiced producing phenolic compounds [16-20]. The ACD can be conducted by organic (i.e., peracetic acid, oxalic acid) and inorganic acids (H_2SO_4, HCl, H_3PO_4). ACD with inorganic acids requires high operating temperatures (150-350°C) [14, 16, 21]. Moreover, inorganic acids are hazardous and highly corrosive. The ACD of lignin by organic acids, such as peracetic acid (PAA), was recently studied at a relatively lower temperature (Lindsay et al., 2019; Ma et al., 2021). Due to strong oxidizing properties, PAA can selectively break down the ether and C-C bonds of lignin at low temperatures (~60°C) [18]. In this respect, Ma et al. (2021) effectively performed the oxidative depolymerization of corn stover lignin by PAA. This study reported around 28% of monomeric phenolic compound yields. However, PAA has a carcinogenic effect and can be a potential fire hazard [22]. Conversely, oxalic acid (OxA) is a safe, renewable, and potent reducing reagent [19]. In this context, Lindsay et al. conducted a series of experiments to study the cleavage of β-O-4 in phenoxyacetophenone in an OxA-mediated aqueous solution in the presence of air/oxygen and reported up to 73-80% of p-anisic acid yield [19]. Moreover, OxA can selectively depolymerize pre-oxidized *Pinus radiata* milled-wood lignin to produce vanillin [19]. Yet, no other study has reported the oxidative depolymerization of kraft lignin by OxA. As this method seems interesting, the OxA oxidation of KL was studied in this work comprehensively.

Niobium pentoxide is a heterogenous transitional metal oxide, and it has received attention in acid-based lignin depolymerization [18, 23]. This material has both Brønsted and Lewis acid sites, which make Nb_2O_5 a suitable catalyst for various chemical reactions, such as hydrolysis, esterification, and etherification of biomass [24]. In an aqueous OxA solution, Nb_2O_5 generates

niobium oxalate ionic species, such as $NbO(C_2O_4)_3^{3-}$, $NbO(C_2O_4)_2(H_2O)_2^-$ and $NbO(C_2O_4)(OH)_2(H_2O)_2^-$, which might play a role in lignin depolymerization [25]. In this context, earlier studies reported positive effects of ionic solutions on lignin conversion to other chemicals [26]. The ionic species would facilitate lignin dissolution, producing a high reactivity during oxidative depolymerization [27]. However, the catalytic activity of Nb_2O_5 on the OA-mediated lignin depolymerization was not investigated yet.

The primary objective of the current study was to investigate the OxA-mediated KL oxidation to produce phenolic compounds in the presence of molecular oxygen gas. The effects of reaction parameters on phenolic yields, vanillin, and vanillic acid were also assessed. The effect of niobium pentoxide on the OxA-mediated oxidative depolymerization of lignin was studied. The recyclability of the recovered OxA from the process was also studied. The primary novelty of the work is the detailed analysis on the high-yield generation of vanillin and vanillic acids in OxA-mediated oxidative depolymerization of KL.

5.2. Materials and Methods

5.2.1. Materials

Acid-washed softwood KL was supplied from a pulping company in Alberta, Canada, which was produced via LignoForce technology. Oxalic acid, niobium pentoxide, ethyl acetate, dimethylsulfoxide-d6 (DMSO-d_6), lignosulfonate, HPLC grade methanol, and acetic acid were all purchased from Sigma Aldrich and used as received. The standards of vanillin, vanillic acid, acetovanillone, and protocatechuic acid were also purchased from Sigma Aldrich. The dialysis tube (1000 g/mol cut-off) was purchased from Sigma Aldrich.

5.2.2. Process description

Figure 5.1 shows the experimental plan of the oxidation and separation processes. In this work, KL (5 wt%) was first dispersed in 100 mL of oxalic acid solution (0-2.5 M). The dispersed solution was poured into a 600 mL Parr reactor (Model 4575A) Illinois, USA. Oxygen gas was supplied in the reactor at an initial 50 psi pressure. The oxidation reactions were conducted at different temperatures (80-150 °C) for different time intervals (30-180 minutes). Afterward, the reaction mixture was centrifuged to separate the remaining lignin/residue, which was washed with deionized water several times to remove oxalic acids. Then, the solution (~100 mL) containing phenolic compounds was mixed with 160 mL of ethyl acetate (EA), which generated two phases of organic (OP) and aqueous (AP). The OP was collected and evaporated with a rotary vacuum evaporator at 40 °C. The generated solid material containing phenolic compounds was collected for further HPLC analysis. After that, the AP (containing OxA) was left to air dry, and the OxA crystals were collected, analyzed by HPLC, and utilized for reusability purposes. To study the recyclability of the collected oxalic acid, 45% of recovered oxalic acid was mixed with 55% fresh oxalic acid, and the oxidation reaction was conducted, as discussed in this section. This process was repeated four times to understand the recylceability performance of collected oxalic acid in 4 consequent cycles.

To evaluate the properties of partially depolymerized lignin, the remaining lignin residue of the reaciton (Figure 5.1) was suspended in 0.1 M NaOH solution and centrifuged to separate the insoluble residue/char from the soluble lignin fraction. Then, the alkali-soluble fraction was precipitated with 0.1N HCl and considered partially depolymerized lignin (PDL). For further characterization, PDL was dialyzed for 72 hours and dried in an oven at 50ºC.

The oxidation reaction was repeated on lignosulfonate, LS. In this experiment, 5 wt.% of LS was dissolved in 1.25 M oxalic acid solution, and the reaction was carried out at 125ºC for 60 mins with an initial oxygen pressure of 50 psi, i.e., optimum reaction conditions of KL. Due to its acidic nature, the unreacted LS did not produce precipitates. As stated above, the reaction mixture was extracted by EA, and HPLC analyzed the extracted products.

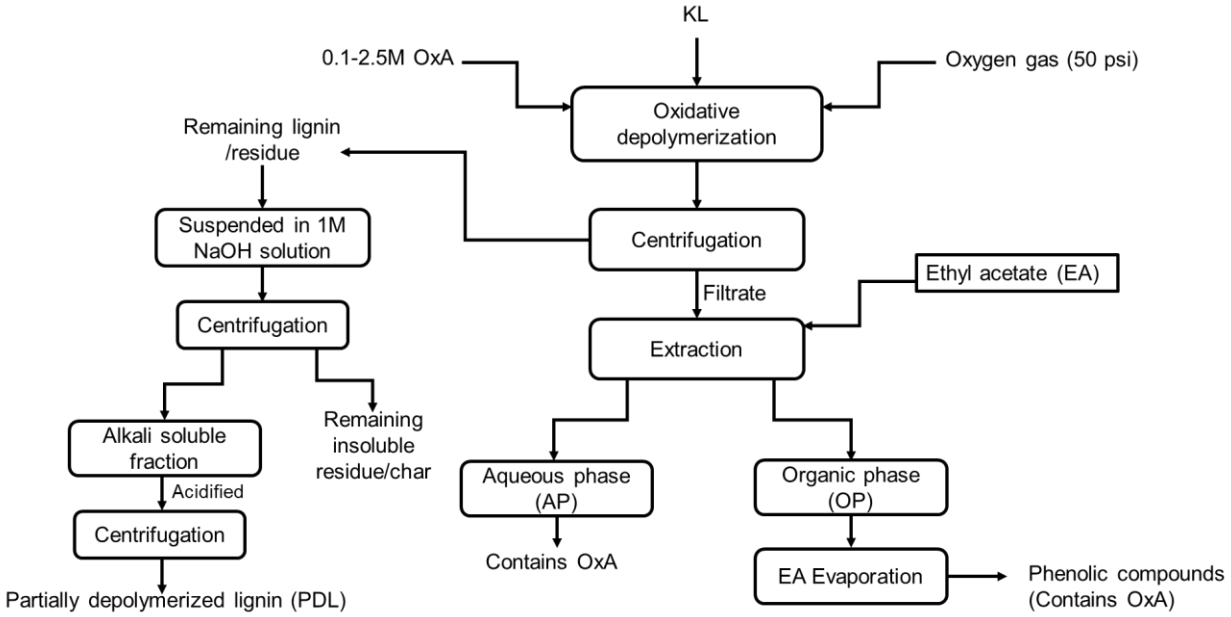

Figure 5.1: Schematic flow diagram of oxalic acid mediated KL oxidation.

5.2.3. High-performance liquid chromatography (HPLC) analysis

The phenolic compounds of KL and LS-based oxidation reactions were quantified by an HPLC instrument (Agilent Technologies Inc., USA). The analysis was adapted from a published paper [28]. For each sample, around 20 mg of dried extract was dissolved in 1 mL methanol and 3 mL

of 2% acetic acid solution and filtered by 0.45 μm cellulose acetate syringe filters. Then, 18:82 (v/v) methanol-aqueous acetic acid (2% v/v) was used as a mobile phase in this experiment. In this test, 20 μL of the sample was injected at a flow rate of 1 mL/min and 25°C. A reverse phase polar HPLC column (Beckman, ultrasphere ODS, 4.6 mm×25 cm, USA) was used for separating the phenolic compounds. Phenolic compounds were detected at 280 nm wavelength with an RI detector. The retention times of the detected compounds were compared with those of standard phenolic compounds to determine their concentrations. Three samples were run for each reaction, and the average result was reported with standard deviation.

5.2.4. Proton (^{1}H), carbon (^{13}C) and heteronuclear single quantum coherence (HSQC) NMR analysis

In this set of analyses, 75 mg of each sample (KL and PDL) were dissolved in 1 mL of DMSO-d_6 in a small vial and stirred overnight, and then the solution was transferred to NMR tubes for further analysis. The NMR spectra were recorded using a Bruker AVANCE Neo NMR-500 MHz instrument (Switzerland), and Topspin 4.02 software was used for analyzing the spectra. For the ^{1}H dimension, 64 scans with 256 increments at 25°C were recorded, and 2048 data points were collected from 0-16 ppm. For ^{13}C dimensions, 1024 data points were collected from 0-160 ppm, and 64 scans were recorded. Other instrument settings were kept the same. The pulse width and recycling delay were 90° and 1s for both dimensions. To confirm the presence of phenolic compounds in the OP, around ~100 mg of extract was dissolved in 1 mL of DMSO-d_6, and its ^{13}C and HSQC-NMR spectra were analyzed. The samples were run under the same conditions as mentioned above. In this analysis, the samples (PDL, and the extracted phenolic compounds) that were generated under the reaction conditions of 5 wt.% of KL at 125°C for 60 mins with an

initial oxygen pressure of 50 psi (without catalyst) were used since the concentration of undetected compounds were lower than other oxidation conditions.

5.2.5. Mass balance analysis

A preliminary mass balance was developed for the raw material and the products. After each reaction, the solid residue was separated, and its dried mass was recorded (Figure 1). The dry mass of the phenolic compounds in the filtrates was also recorded. The dried mass of the recovered OxA was measured from the AP after EA extraction (Figure 5.1), and the remaining OxA in phenolic compounds was determined in the HPLC analysis. The lignin conversion, the loss of lignin, and the OxA loss were calculated following equations 1 to 3.

$$Lignin\ conversion,\ wt.\% = \frac{\text{Initial lignin} - \text{PDL}}{\text{Initial lignin}} \times 100 \quad (1)$$

$$Lignin\ loss, wt.\% = \frac{Initial\ lignin - (\text{residual lignin} + \text{phenolic extracts})}{\text{Initial } lignin} \times 100 \quad (2)$$

$$OxA\ loss,\ wt.\% = \frac{\text{Initial OA} - (\text{Recovered from AP} + \text{remaining OA in OP})}{\text{Initial OxA}} \times 100 \quad (3)$$

5.3. Results and Discussion

5.3.1. Effects of reaction parameters on lignin depolymerization

5.3.1.1. Effects of oxygen and oxalic acid

Oxygen is one of the most commonly used oxidizing agents, while OxA is a reducing agent. To observe the effect of OxA and oxygen on lignin depolymerization, KL was depolymerized by oxygen and OxA in separate experiments, while the other reaction parameters remained constant.

The results of this analysis are available in Figure 5.2a. In the presence of oxygen, the total phenolic yield was less than 4 wt.%, among which 1.4 wt.% was vanillin. On the other hand, OxA facilitated 14 wt.% of total phenolic compound generation containing 4% vanillin. Also, because of the oxidizing effect of oxygen, trace amounts (0.7 wt.%) of vanillic acid were produced in the O_2 containing reaction.

In contrast, because of the reducing environment of OxA-containing systems, no vanillic acid was formed in the depolymerization by oxalic acid. Previous studies reported that the acid would initiate lignin depolymerization by cleaving the β-O-4 linkages [17, 29]. Generally, the protons of the acids attack the oxygen atom in the ether links on the lignin structure and break down the C-O bonds of lignin to produce phenolic monomers [29]. Therefore, without OxA, the lignin depolymerization process becomes slow. However, because of the amphoteric properties of water, it may generate some protons that could initiate the depolymerization of lignin. The HPLC analysis of the standard compounds and the extracted phenolic compounds can be found in the supplementary file (Figures A5.1 and A5.2).

5.3.1.2. Effects of temperature

The effect of temperatures were analyzed under the conditions of 5 wt.% lignin, 0.5M oxalic acid concentraiton, 60 min reaciton time and 50 psi oxygen pressure, and the results are summarized in Figure 5.2b. By increasing the reaction temperature from 80 to 125°C, the yield of phenolic compounds increased from 11% to around 18%. Interestingly, the yield of vanillin production increased from 4.5 to 9.7 wt.%. A recent study reported that preoxidized *Pinus radiata* (36 mg) was depolymerized by oxalic acid (360 mg in 0.25 mL water) in the presence of oxygen at 100°C and reported the total phenolic yields of 14 wt.% with the main product as vanillin [19]. It can

also be observed that vanillic acid did not form at 80°C. As the temperature increased to 125°C, the vanillic acid increased to 4.9 wt.% along with other phenolic compounds, such as apocynin and protocatechuic acids. However, upon increasing the temperature to 150°C, the phenolic compound yield significantly decreased to around 5.3 wt.%, which may be attributed to the decomposition of the OxA. Earlier studies reported that dehydrated oxalic acid would start to decompose at 140°C, it would begin to deteriorate at a low temperature in the presence of water, and the major decomposition products would be formic acid, CO_2, CO, and water [30]. Therefore, because of the decomposition of the OxA, the depolymerization of lignin was hampered, and hence a lower yield was obtained.

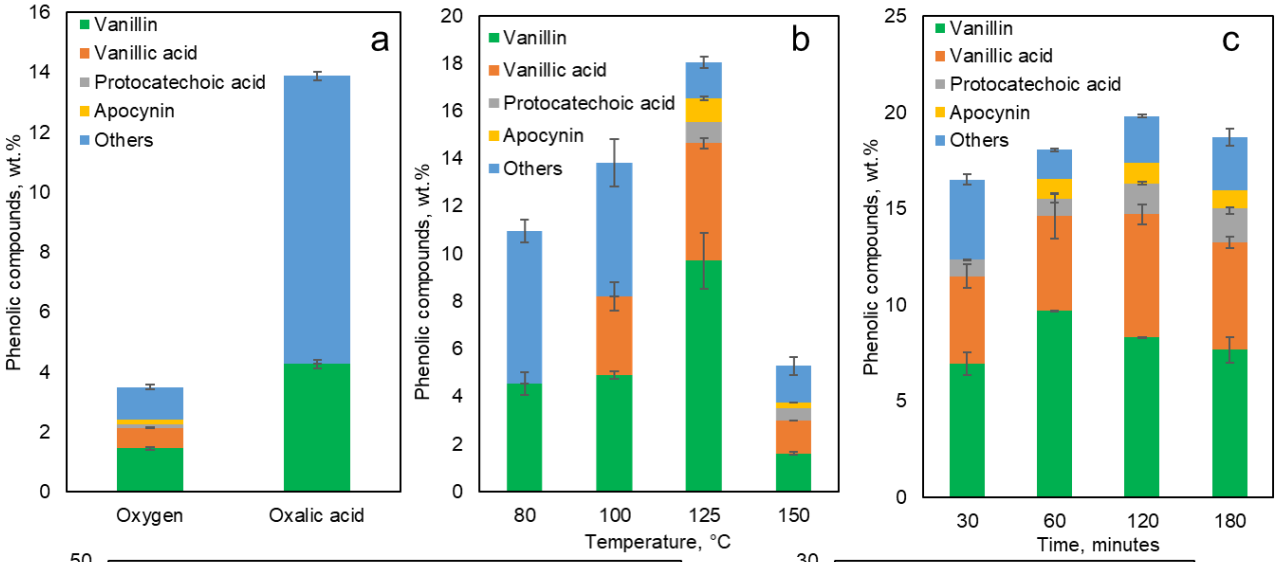
a
Vanillin
Vanillic acid
Protocatechoic acid
Apocynin
Others
Phenolic compounds, wt.%
Oxygen
Oxalic acid
b
Temperature, °C
c
Time, minutes

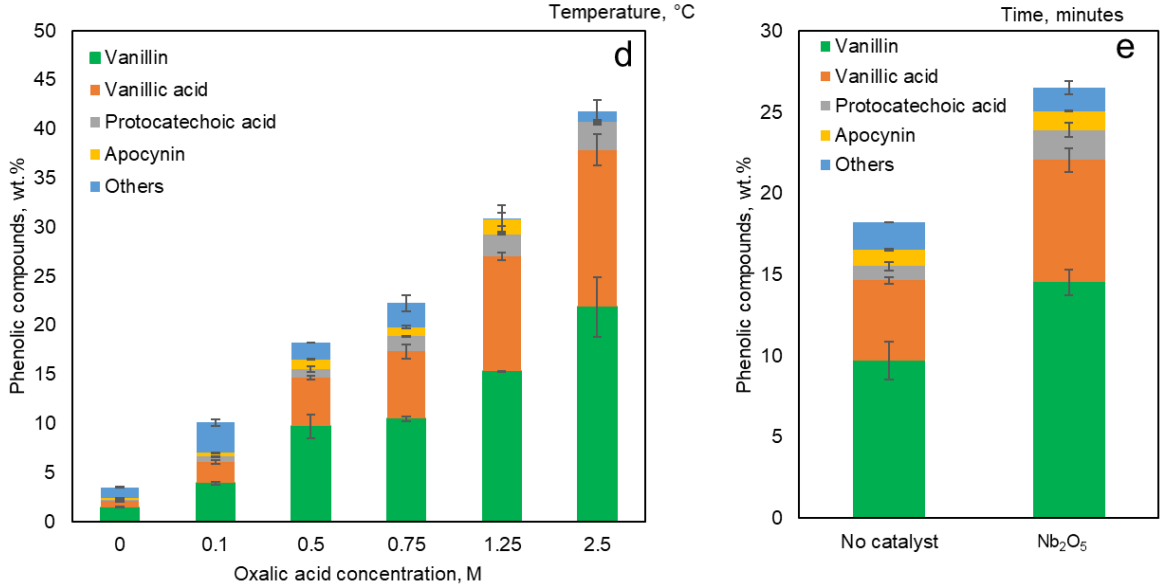
d
Oxalic acid concentration, M
e
No catalyst
Nb_2O_5

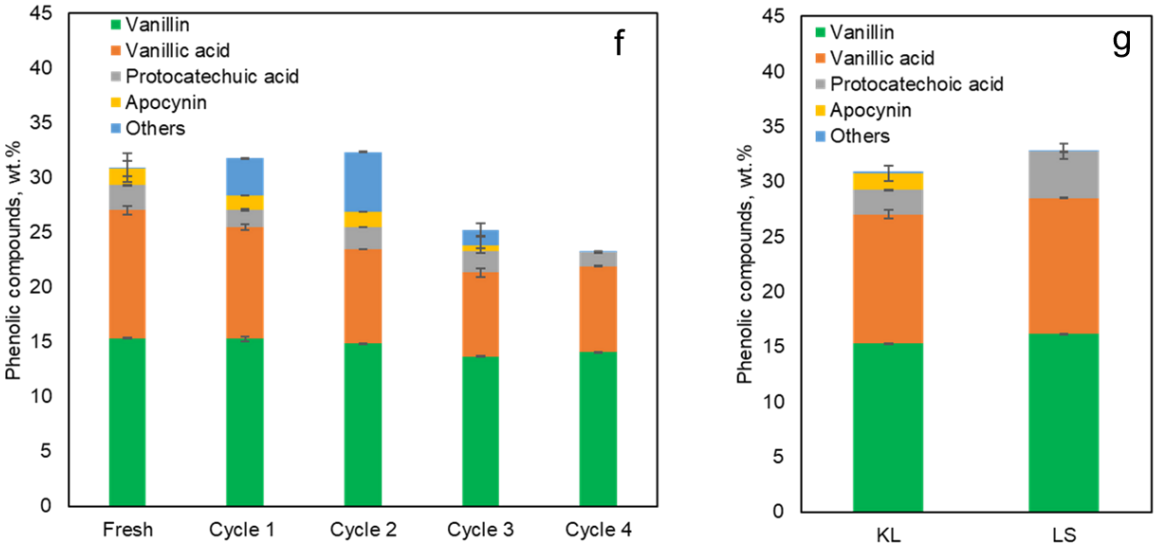
f
Protocatechuic acid
Fresh
Cycle 1
Cycle 2
Cycle 3
Cycle 4
g
KL
LS

Figure 5.2: Effects of different reaction parameters on yield of phenolic compounds. (a) Effects of oxygen and OxA, other reaction conditions: 5 g KL, 0/4.5 g OxA in 100 mL water (0.5 M), 125°C, 60 min, initial 50 psi oxygen; (b) Effects of temperatures, other reaction conditions: 5 g of KL, 4.5 g OxA in 100 mL of water (0.5 M), 60 min, initial 50 psi oxygen; (c) effects of time, other reaction conditions: 5 g KL, 4.5 g OxA in 100 ml water (0.5 M), 125°C, initial 50 psi oxygen; (d) effects of OxA concenration; other reaction conditions: 5 g KL, 125°C, 60 min, initial 50 psi oxygen; (e) effects of Nb_2O_5 catalyst; other reaction conditions: 5 g KL, 4.5 g OxA in 100 ml of water (0.5 M), 125°C, 60 min, initial 50 psi oxygen, Nb_2O_5-0.5 g; (f) Recyclability of recovered oxalic acid (45 wt.% recovered and 55 wt.% fresh); conducted under the conditions of 5 g of KL, 11.25 g OxA in 100 mL of water (1.25 M), 125°C, 60 min, O_2 pressure of 50 psi; g) Oxidative depolymerization of LS, reaction condition: 5 g LS, 11.25g OxA in 100 ml of water (1.25 M), 125°C, 60 min, initial 50 psi oxygen.

5.3.1.3. Effects of time

To investigate the effect of time on the yields, the KL was depolymerized at 125°C for different reaction periods, and the results are summarized in Figure 5.2c. It can be observed that, as the reaction time was extended from 30 to 120 mins, the total yields increased from around 16.5 to 19.8 wt.%. However, the vanillin yield was found to be at maximum (9.7 wt.%) in 60 mins. It can also be seen from Figure 2c that vanillin yields decreased from 9.7 wt.% (60 mins) to 7.7 wt.% (180 mins). Conversely, the total yield of vanillic acid and protocatechuic acid was increased from 5.8 (60 min) to 7.4 wt.% (180 min), which indicated that further time extension would convert vanillin to vanillic acid and protocatechuic acid (i.e., an increase in the vanillic

acid yield from 4.9 wt.% to 6.4 wt.%, and the protocatechuic acid yield increase from 0.9 wt.% to 1.8 wt.%).

5.3.1.4. Effects of OxA concentration

The effect of oxalic acid concentrations was investigated at 125°C for 60 mins in different concentrations of OxA (Figure 5.2d). As seen, by increasing the concentration of OxA from 0.1 M to 2.5 M, the total phenolic yields increased from 10 wt. % to 41.8 wt.%. Interestingly, the yields of vanillin, vanillic acid, and protocatechuic acid increased to 21.9, 16 wt.%, and 2.8 wt.%, respectively, at the highest OxA concentrations, which may be attributed to the available protons that attack the oxygen atoms in the ether linkages. Lindsay et al. (2019) reported that increasing the OxA concentration from 3 M to 16 M facilitated the lignin model compounds (Phenoxyacetophenone) cleavage and significantly increased the p-anisic acid (from 20% to 73%). Although the oxalic acid concentration is directly proportional to the yield of phenolic compounds, including vanillin and vanillic acid, using a higher concentration of oxalic acid may create some operational difficulties, such as solubility of oxalic acid in aqueous media. The solubility of oxalic acid in water at room temperature (25°C) is 11.7% (~1.3 M); however, with increasing temperature to 40°C, the solubility increases to 2.6 M [31]. Therefore, increasing the OxA concentration to 2.5 M might be problematic during separating the product solution, as the OxA may crystalize after the reaction mixture is cooled down.

5.3.1.5. Effects of Niobium pentoxide catalyst

Figure 5.2e describes the effect of the Nb_2O_5 catalyst in combination with OxA on the generation of the phenolic compound. In the presence of Nb_2O_5 (0.5 g), the phenolic yields were increased from 18.2 to 26.5 wt.%. Also, vanillin and vanillic acid yields increased from 9.7 to 14.5 wt.%

(49.5% higher) and 4.9 to 7.5 wt.% (i.e., 53% higher), respectively. However, a longer reaction time (120 min) did not provide a more effective conversion to phenolic compounds, which may be attributed to the degradation of the phenolic compounds due to over-oxidation. An earlier study on peracetic acid-mediated oxidative depolymerization of corn stover lignin (at 60°C for 5 h) in the presence of Nb_2O_5 (0.5 g) reported a 67% increase in phenolic compounds. The study reported that, among various transition metal oxide catalysts, Nb_2O_5 showed better catalytic activity [18]. However, an extended reaction time to 120 min did not increase the vanillin, but vanillic acid and protocatechuic acid increased from 4.9 to 5.8 wt.% and 0.9 to 1.9 wt.%, respectively (Figure A5.3a).

In addition, the effect of Nb_2O_5 on higher OxA concentration (1.25 M) was studied (Figure A3b). It was observed that, by increasing the OxA concentration, the total phenolic yields increased from 31 to 52.3 wt.% (71% increase). However, the yield of vanillic acid production dropped (21.4%). Interestingly, the yield of protocatechuic acid increased from 2.3 to 15.1 wt.%, which might be due to the over-oxidative conversion of the produced vanillin and vanillic acid. Another reason could be the possible demethylation of the vanillin and vanillic acid by the action of the Niobium-OxA ionic species, converting the carbonyl groups of vanillin to carboxylic groups [32]. Despite the promising catalytic effects of the Nb_2O_5 on the OxA-mediated KL oxidation at a low OxA concentration, the recovery of the catalyst was not possible since it was mixed and remained with the solid lignin residue (PDL) after the reaction. Considering the operational challenges with the recovery of the catalyst, we chose a higher OxA concentration (1.25 M) over Nb_2O_5 catalyst use, which provided a better yield of the products (Figure 5.2d) and doable recovery of OxA for recycling. Therefore, the recyclability of the OxA, structure of the material,

and the products' mass balance analysis were studied for the samles generated without the Nb_2O_5 catalyst.

5.3.1.6. Recyclability of oxalic acid

For industrial viability, the recyclability of the OxA is highly desired. The OxA crystals recovered from the aqueous phase (Figure 5.1) were analyzed by HPLC (Figure A5.2b), and it was observed that all the phenolic compounds were extracted. The recyclability of the OxA was performed for four consecutive cycles, and the results are presented in Figure 5.2f. The initial reaction was conducted with 5 wt.% lignin, 1.25 M fresh OA at 125°C for 60 mins in the presence of 50 psi O_2. After each reaction, the dry OxA crystals were collected (48-50 wt.% of initial OxA), used in the subsequent cycles, and continued for four cycles. Therefore, to be consistent, 45 wt.% of recovered OxA and 55 wt.% of fresh OxA were used in all the recycling tests. It can be observed that, after using 45 wt.% of recovered OxA, the total phenolic yields were almost similar (31%) in the first two cycles and decreased in the cycles 3 (26 wt.%) and 4 (24 wt.%). It can also be seen that the yields of vanillic acid fell slightly from 11.7 to 7.9 wt.%. Interestingly, the yields of vanillin did not decrease and remained almost similar (~15%). Lindsay et al. (2019) also reported no significant product (p-anisic acid and guaiacol) loss upon using a small portion of recovered OxA with the fresh OxA, where they cleaved β-O-4 model compounds. The total OxA might facilitate the cleavage of ether bonds. Thus, the vanillin yield was not hampered. On the other hand, the vanillic acid yield drop may be due to the production of formic acid (potent reducing agent) in the recovered OxA, which is one of the typical by-products in the thermal decomposition of OxA [20, 33]. Therefore, OxA can be reused twice, but its more recycling time crystals may retain some FA and hinder the oxidation process, reducing the oxidation of phenolic compounds, such as vanillic acid and protocatechuic acid.

5.3.1.7. Use of lignosulfonate

The OA-mediated oxidative depolymerization of lignosulfonates (LS) was also demonstrated under the best conditions of KL depolymerization (Figure 5.2g). It was noticed that, unlike KL, LS was completely soluble in OxA solution, which might be attributed to the presence of sulfonated groups on LS (1.25-2.5 mmol/g)[34]. Figure 2g shows that the yields of total phenolic compound, vanillin, and vanillic acid were comparable for the KL and LS (Figure 5.2g). Interestingly, no char-like by-products were observed after the reaction, indicating that Nb_2O_5 might be a suitable catalyst for the LS depolymerization since it can be recovered as the only solid product of the reaction via centrifugation or filtration, which will be studied in our future studies. Conventionally, vanillin is produced from LS under strong alkaline oxidative depolymerization [35]. The current study demonstrated one potential route for vanillin and vanillic acid production from LS by OxA-mediated oxidative depolymerization. However, our primary focus in this study was to valorize the underutilized KL. This is because the total production of LS and KL is 1.8 and 70 million tons annually, and a considerable portion of KL can be available for valorization [34, 36, 37].

5.3.2. ^{13}C-NMR and HSQC-NMR spectra analysis of OP

^{13}C-NMR and HSQC-NMR spectra of the OP were analyzed, and the results are reported in Figures 5.3a and 5.3b. In this NMR study, we analyzed the products obtained from the reaction condition of 5 wt.% of KL at 125°C for 60 min with an initial oxygen pressure of 50 psi (without catalyst) since other undetected compounds were significantly low. Figure 5.3a shows that the spectra in the region of 10-30 ppm is attributed to the C-atoms attached to the aliphatic side

chains [38]. Specifically, the peak that appeared at 25.1 ppm might be for the acetyl groups (-$COCH_3$) from the apocynin [39]. The sharp peak that occurred at 40 ppm is attributed to the DMSO-d6. The strong peak (1) at 56.6 ppm is attributed to the methoxyl-C, which can also be located in HSQC-NMR (Figure 5.3b) [40]. The peaks (2, 3) appearing at 110-130 ppm are ascribed to different C-atoms in the aromatic rings [38]. The small peaks that occurred at 175-185 ppm might be attributed to the aromatic carboxylic groups of vanillic acid and protocatechuic acid [41, 42]. The characteristic peak (4) at 191.2 ppm for carbonyl-C might be

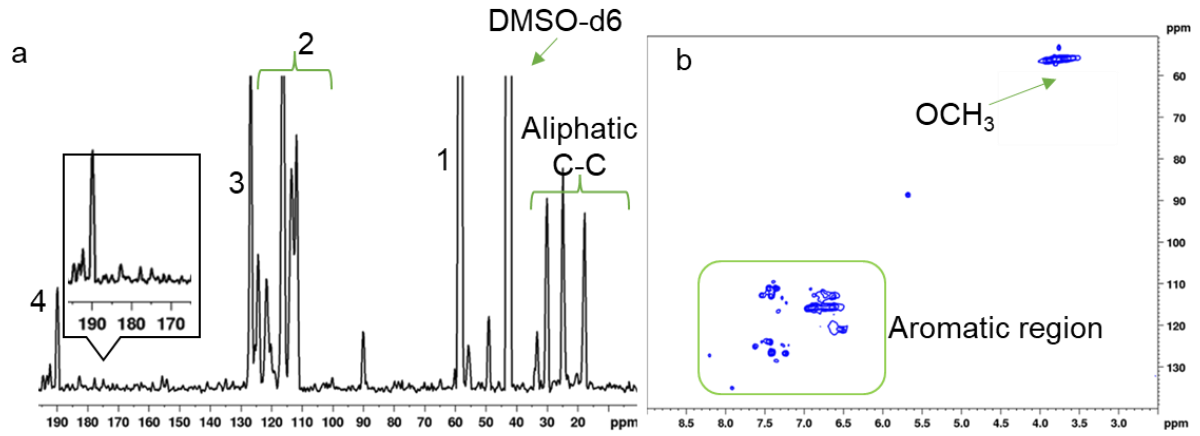

ascribed to vanillin [38]. Moreover, the abundance of the aromatic moieties and the methoxyl groups can be located in the HSQC-NMR spectra (Figure 3b), which confirmed the presence of phenolic compounds in the OP. Moreover, the absence of the lignin linkages (δ_C/δ_H 55-95/3-5.5 ppm) in the EA soluble fractions indicated that no oligomeric lignin fractions were available in the sample. The ^{13}C-NMR confirmed the presence of the characteristics of C-atoms of the aromatic rings and the functional groups (i.e., C=O) attached to the phenolic compounds. In contrast, the HSQC-NMR showed the aromatic portions of the extracted phenolic compounds (i.e., vanillin, vanillic acid, protocatechuic acid apocynin).

Figure 5.3: (a) ^{13}C-NMR and (b) HSQC-NMR spectra of EA soluble phenolic fractions produced under the conditions of 5 g of KL, 11.25 g OxA in 100 mL of water (1.25 M), 125°C, 60 mins, O_2 pressure of 50 psi.

5.3.3. Structural Characterisations of KL and PDL

5.3.3.1. ^{1}H-NMR analysis

Figure 5.4 describes the H-NMR spectra of KL and the PDL. The spectra in the 0.5-1.6 ppm region can be attributed to the non-oxygenated aliphatic side chain proton, whereas that in the 1.6-2.2 ppm region is ascribed to the oxygenated aliphatic side chain, such as acetyl groups (-$COCH_3$) [43]. The action of oxalic acid may reduce these oxygenated groups in PDL. The sharp peak at 2.51 ppm is the specific peak for DMSO-d6. The 3.55-3.9 ppm spectra are associated with the methoxyl proton [37]. The characteristic peaks in the 4.8-5.4 ppm are ascribed to β-O-4 and appeared in the KL spectrum. However, it did not exist in the spectrum of PDL, demonstrating the oxalic acid-mediated cleavage that can also be observed in HSQC-NMR in the later section [43, 44]. The strong proton signals in the 6-7.6 ppm region on the KL spectrum belong to the aromatic G-units, which was also observed on the spectrum of PDL, inferring that this unit was unaffected during the depolymerization [44]. However, the other phenolic-OH proton signals (8.4-9.2 ppm), such as from H-units, were partially decomposed during the reaction, as they could not be seen in the spectrum of PDL [44].

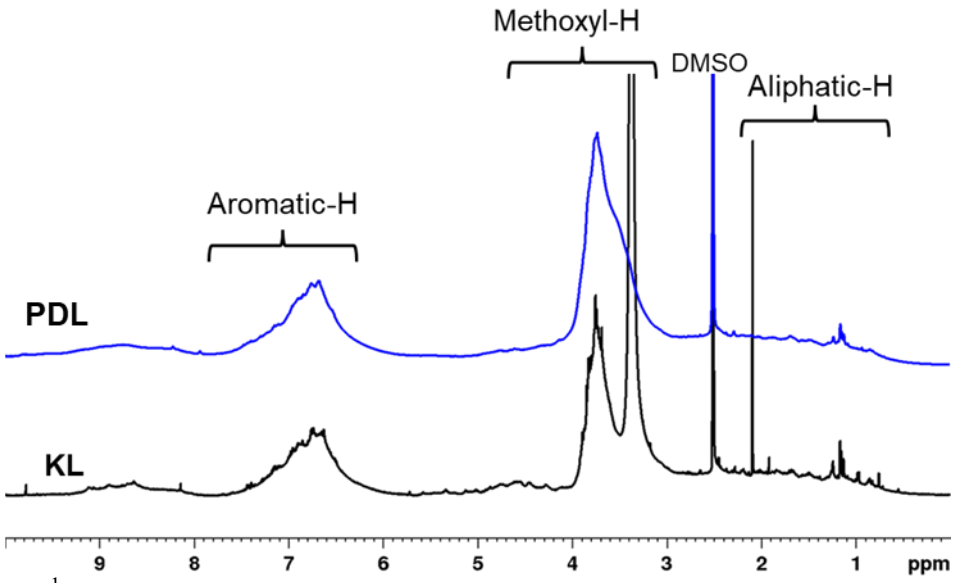

Figure 5.4: ^{1}H-NMR spectra of KL and PDL for the sample prepared under the conditions of 5 g of KL, 11.25 g oxalic acid in 100 ml of water (1.25 M), 125°C, 60 min and initial oxygen pressure of 50 psi.

5.3.3.2. HSQC-NMR analysis

HSQC-NMR analysis was conducted to observe the structural differences between KL and PDL. Figure 5.5 represents the different regions of the HSQC spectra and the central lignin units. The spectra region of δ_C/δ_H 5-50/0.5-3.0, 50-90/3-6 and 90-145/6-8.25 ppm are attributed to the C-C aliphatic side chain, C-O aliphatic side chain, and C-O aromatic regions, respectively [37, 39]. In the aliphatic region of KL (Figure 5.5a), the overlapped cross signals that appear at δ_C/δ_H 25.3/1.65-1.87 ppm are attributed to the acetyl groups (-$COCH_3$) [39]. The inexistence of these acetyl groups in PDL may suggest the degradation and transformation into apocynin. The spectra region at 22.1/1.4 ppm is a characteristic signal for guaiacyl hydroxy ethyl ketones [45]. The guaiacyl propanol (Cα-Cβ) and secoisolariciresinol (**D**) (Cβ-Cγ) linkages can be spotted at 33.1/2.5 and 42.1/1.87 ppm, and they can be observed in PDL [45]. However, the intensity of these spectra is reduced in PDL (Figure 5.5b). In Figure 5a, the correlation signals from δ_C/δ_H 53-

56.8/3.5-3.9 ppm are attributed to the intact methoxyl groups of KL and preserved in PDL (Figure 5.5b) [39, 45]. Most importantly, the cross signals at δ_C/δ_H 71.5/4.8, 83.7/4.4, and 60/3.5 ppm are attributed to the β-O-4 linkages (**A**) of Cα-Hα, Cβ-Hβ, and Cγ-Hγ positions, respectively [37, 39]. The disappearance of these signals in the PDL (from Figure 5.5b) confirmed the degradation of the β-O-4 linkages by the oxalic acid-mediated C-O cleavage. An earlier study also suggested that the singlet oxygen atom (generated from oxygen gas) might be responsible for the C-O ether bond cleavage [19]. However, the intensities of the other interunit linkages, such as resinol unit (**B**) (δ_C/δ_H 85.2/4.5 ppm) and phenylcoumaran (**C**) (δ_C/δ_H 62.7/3.7 ppm) are reduced, but they still can be spotted in the PDL. In Figure 5.5c, the abundance of guaiacyl units (**G**) and a portion of H units (**H**) can be attributed to the softwood KL. The cross-signal at δ_C/δ_H 126.5/6.9 ppm is ascribed for the Cβ-Hβ of cinnamaldehyde end groups (**E**), which can be located in both KL and PDL that could be suggested no C-C cleavage occurred during OxA depolymerization [37, 45]. The partial disruption of aromatic units can be observed in Figure 5.5d. Therefore, from the ^{1}H-NMR spectra (Figure 5.4), it can be clearly observed that the signals for β-O-4 linkages are absent in PDL, and the cleavage was also confirmed by the HSQC-NMR results in Figure 5.5d. Moreover, the partial disruption of aromatic moieties (G-units) suggested (Figure 5.5d) that OxA degraded the KL selectively where only β-O-4 inter unit linkages with G-units were broken (Figure 5.5 and Figure A5.2). In addition, the structural changes were also observed in the FTIR analysis of the KL, PDL and char, which can be found in Table A5.1 and Figure A5.4.

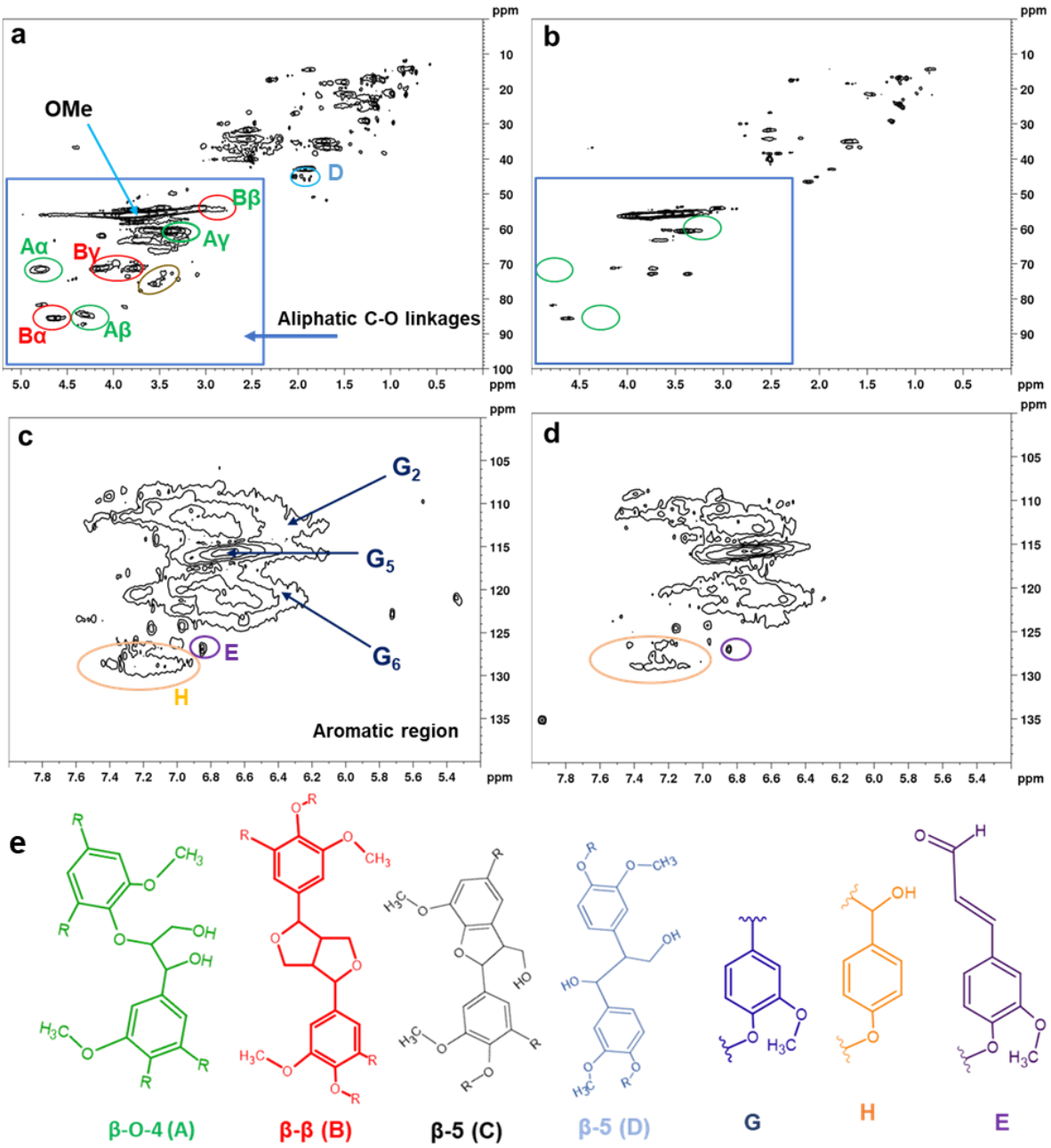

Figure 5.5: HSQC-NMR spectra of KL and PDL; aliphatic region of (a) KL and (b) PDL; Aromaic region of (c) KL and (d) PDL (e) inter-unit linkages of lignin. The spectrum of PDL is for the sample prepared under the conditions of 5 g of KL, 11.25 g oxalic acid in 100 mL of water (1.25 M), 125°C, 60 min, and initial oxygen pressure of 50 psi.

5.3.4. Proposed reaction scheme

The major products obtained from the OxA-mediated oxidative depolymerization of KL and the possible reaction pathways are presented in Figures 5.6A and 5.6B, respectively. The proposed reaction is described based on the product formation from the HPLC and the NMR analyses. Earlier studies suggested that β-O-4 linkages are very reactive in an acidic environment and cleave at the ether bonds [19, 20]. The current study also supports the statement, which was confirmed in the HSQC-NMR analysis (Figure 5.5). The depolymerization mechanism of KL occurs in two major pathways: the cleavage of ether linkage to phenolic monomers and further oxidation to the desired products. Due to the reducing properties of oxalic acid, it would first reduce hydroxyl groups of KL to methylene groups [19]. After that, the proton would attack the oxygen atom of the ether bonds and decompose KL into two phenolic monomers, such as p-cresol and the aromatic di-ketones compounds (**1**) [19, 29]. The oxidation of p-cresol (**2**) would generate vanillin, and its further oxidation would lead to vanillic acid. Under hydrolysis conditions, the aromatic di-ketone would break down to formic acid and vanillin at Cα-Cβ bonds [19]. The transformation of vanillic acid to protocatechuic acid would also occur by demethylation in its ortho position, which was identified by HPLC analysis (Figure 5.3). Previous studies reported that an acidic environment would facilitate the demethylation followed by catechol formation under oxidative conditions [46, 47]. The reason can be explained from the Figure 5.2c, where upon increasing the reaction time, the conversion of the protocatechuic acid increased and the vanillic acid decreased. In addition, the formation of apocynin started at 125°C (Figure 5.2b) may be attributed to the first intermediate product from the C-O cleavage of β-O-4 linkages and be only generated under pure oxygen atmosphere [19]. This statement can also be explained from the Figure 5.2a, where depolymerization did not generate any apocynin or

protocatechuic acid in the absence of oxygen, which suggested that their formation was likely to occur through the action of a singlet oxygen atom. A high temperature (125°C) would facilitate such a conversion.

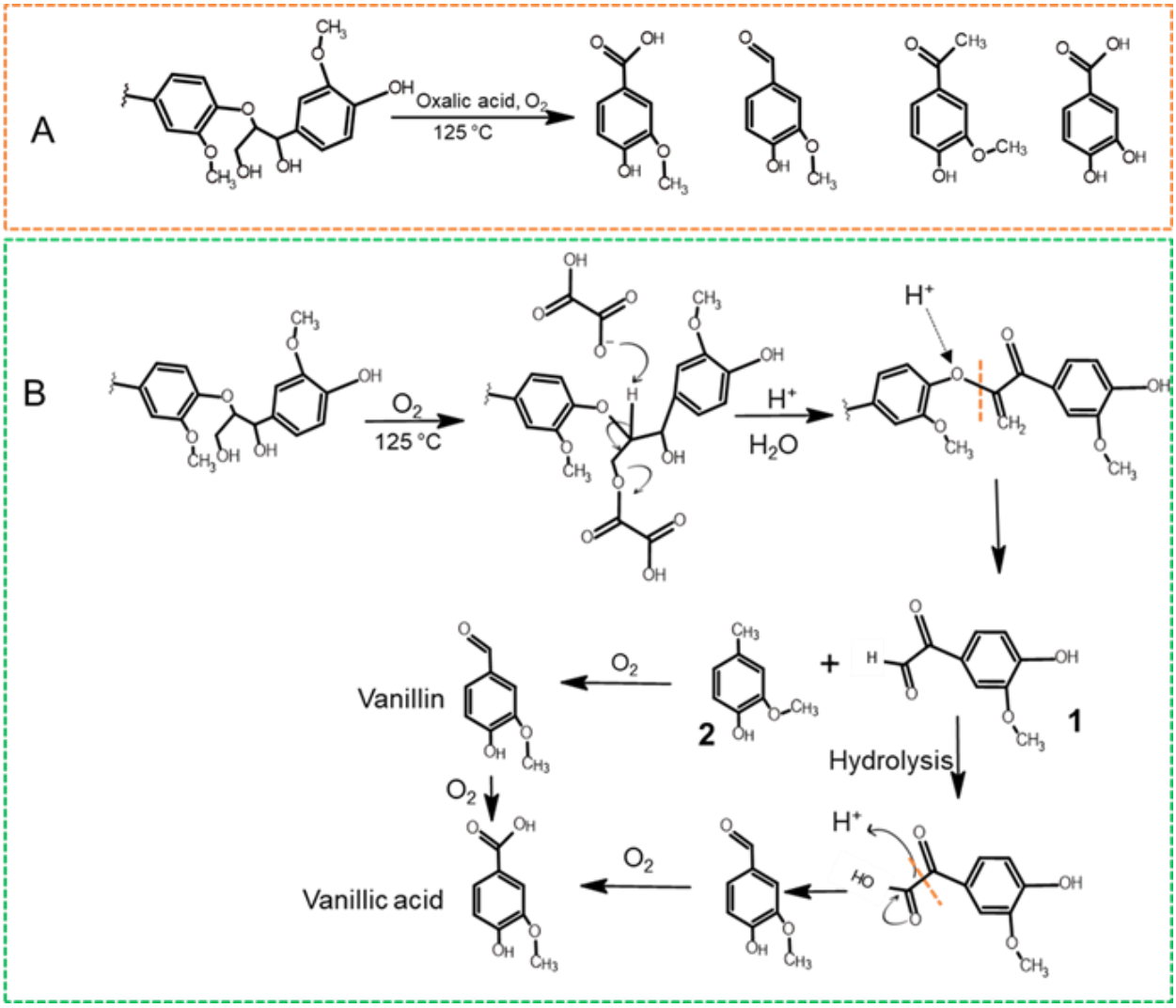

Figure 5.6: Proposed reaction mechanism of oxalic acid mediated lignin oxidation; A) major products, B) the proposed reaction pathways.

5.3.5. Comparison of different studies

Recent studies on the inorganic and organic acid-mediated lignin depolymerizations for phenolic compound productions are presented in Table 5.1. Inorganic acids, such as sulfuric acid, hydrochloric acid, and phosphoric acid, and organic acids, such as formic, peracetic, and oxalic acid, have been practiced for lignin depolymerization. The strategy mainly involves cleaving the aryl ether bonds (β-O-4). In an earlier study, a series of inorganic acids (H_2SO_4, H_3PO_4, and HCl)-mediated bagasse lignin depolymerization was conducted in methyl isobutyl ketone (MIBK) [16]. The authors reported 12-14 wt.% phenolic compound productions, where the maximum yield was reported as guaiacol (6 wt.%). In another study, pre-oxidized aspen lignin was depolymerized by formic acid, which led to 61.2 wt.% of total phenolic compound yields, including oligomers, such as syringyl (29.5 wt.%) and guaiacyl (18.3 wt.%). Only 3.5 and 2.9 wt.% were reported as vanillin and vanillic acid, respectively. Ma et al. depolymerized corn stover lignin with peracetic acid and obtained 28 wt.% (without catalyst) and 47 wt.% (in the presence of Nb_2O_5) phenolic product yields. However, they did not report any specific product selectivity. Since the PAA decomposes to acetic acid, no recovery of PAA and recyclability were not reported. Another study elaborated on the cleavage of the β-O-4 lignin model compound (Phenoxyacetophenone) by OxA-mediated aerobic oxidation to phenol and benzoic acid [19]. Learning from the study, Lindsay and colleagues demonstrated the depolymerization of pre-oxidized *Pinus radiata* milled wood lignin by OxA and the total phenolic compounds yield of 14 wt.% with a good selectivity toward vanillin [19]. However, they did not report the recyclability of the OxA on the lignin depolymerization and the product distributions. On the other hand, the current study oxidatively depolymerized softwood KL by OxA in the presence of oxygen and reported 41.8% phenolic compounds with ~22 wt.% and ~16 wt.% selectivity toward vanillin and vanillic acid generation, respectively. It can also be found that, after successfully recovering

from the process, parts of the OxA (45 wt.%) were recycled with no significant product loss (Figure 5.2f).

Table 5.1: Recent studies on acid-mediated lignin depolymerization toward phenolic compounds

Raw materials	Chemicals	Temp., °C	Time, h	Major products	Total Phenolic yield, wt.%	References
KL (5 wt.%)	Oxalic acid (2.5M), oxygen	125	1	vanillin, vanillic acid, phenolic compounds	Up to 41.8, 22% vanillin	Current study
Bagasse lignin (1.75 % (w/v)	sulfuric acid, Phosphoric acid, Hydrochloric acid 1% (w/w)	300	3	Guaiacol, 4-ethylphenol, guaiacol, Vanillin,	~14 (H_2SO_4) ~13 (H_3PO_4) ~12 (HCl), 4-6% Guaiacol	[16]
Oxidized aspen lignin (25 mg)	Formic acid (5ml, 85-95 wt.%)	110	24	phenol, guaiacol other phenolc compounds	61.2	[20]
Corn stover lignin (1g)	Peracetic acid (1g)	60	5	Phenolic compounds	28	[18]
Oxidized Milled wood lignin (36 mg)	Oxalic acid (360 mg), oxygen	100	24	Vanillin, phenolic compounds	14	[19]

5.3.6. A preliminary mass balance and market analysis

A priliminary mass balance was developed to investigate the process's economic feasibility. Table 5.2 describes a mass balance analysis for the products obtained from the reaction conditions of 5 wt.% KL in 1.25M OxA solution at 125°C for 60 mins with an initial oxygen pressure of 50 psi since other undetected phenolic compounds were low in this reaction condition. Around 30.9 wt.% of total phenolic compounds were produced from the reaction, while 68 wt.% lignin residue (URL and char) was collected after the reaction (Figure 5.1). However, the remaining 2.4% loss of lignin may be associated with the decomposition of lignin to CO_2 or other aliphatic carboxylic acid (i.e., formic acid) [19].

On the other hand, around 45-48 wt.% of OxA was directly collected from the aqueous phase after EA extraction (Figure 1). A part of the OxA remains in the soluble fraction (~30.6 wt.%) that was later determined from the HPLC analysis. In summary, around 78.6 wt.% of OxA was recovered from the process and can be reused without affecting the product yield (Figure 5.3) [19]. The remaining (21.4 wt.%) OA was probably decomposed into CO_2, CO, and formic acid during the reaction.

From the current study, 30.9 wt.% of total phenolic compounds could be produced with an estimated 15.3 wt.% and 11.7 wt.% yields for vanillin and vanillic acid, respectively (Figure 5.2d). These compounds have a significant global market demand in the food, flavor, and pharmaceutical industries. Only vanillin has a global market demand of around 20000 metric tons (MT) per year, mainly from petroleum sources [48]. KL and oxalic acid market prices are 260-500 USD/MT (Ľudmila et al., 2015) and 445 USD/MT, respectively [49]. The highest market prices for synthetic vanillin and vanillic acid are 40,000 and 80,000 USD/MT [50]. Considering the yields, approximately 153 kg of vanillin and 117 kg of vanillin and vanillic acid

can be produced from 1 MT of KL according to the current approach, which may have estimated current market values of 6,120 and 9,360 USD per MT of KL used, respectively. Moreover, the cost associated with OxA can be reduced since 78.6 wt.% of OxA can be recovered (~48 wt.% can be directly recovered after the OP and ~30.6 wt.% from the AP streams). The current study also demonstrated the reasonable recyclability of the OxA (45 wt.%) in two cycles with good vanillin and vanillic acid production yields. The current method developed a green process for the oxidative depolymerization of softwood KL to produce vanillin and vanillic acid with comparatively higher yields than the literature reports [19]. The study also emphasized the recovery of the OxA with the successful demonstrations of recyclability. Moreover, the depolymerization process does not involve any harmful chemicals since the primary solvent is water. This is in opposition to earlier studies in which harsh reaction conditions (e.g., HCl, H_2SO_4, etc.) and potent oxidizing agents (e.g., PAA) were reported.

Table 5.2: A preliminary mass balance analysis for the product produced under the conditions of 11.25 g oxalic acid in 100 mL of water (1.25 M), 125°C, 60 min, initial 50 psi oxygen.

Raw material	KL,	Residue (URL and char), g	Phenolic compounds, g	Conversion of lignin, wt.%	Loss, wt.%
Lignin	5	3.4 63% char 23% URL	1.5 (~30.9 wt.%)	84.3	2.4

Raw material	Initial used, g	Direct recovered after extraction, g	Left with phenolic compounds, g	Total possible recovery, wt. %	Loss, wt.%
OA	11.25	5.4 (~48 wt%)	3.44 (from HPLC, ~30.6%)	78.6 %	21.4

5.4. Conclusions

The current study reported the direct oxidative depolymerization of KL in OxA-mediated aqueous solution for vanillin and vanillic acid productions with a higher yield than previous work. The HPLC, ^{13}C, and HSQC-NMR analyses quantified the products and confirmed the absence of oligomers. The ^{1}H and HSQC-NMR analyses of the PDL showed that the β-O-4 linkages (C-O) were cleaved. The reaction mechanism described that KL was first depolymerized via cleaving β-O-4 linkages by OxA and then transformed into the final products. Finally, the two-time recyclability of the recovered OxA (45 wt%) showed no significant reduction in vanillin and vanillic acid yields.

References

[1] P. Figueiredo, K. Lintinen, J.T. Hirvonen, M.A. Kostiainen, H.A. Santos, Properties and chemical modifications of lignin: Towards lignin-based nanomaterials for biomedical applications, Progress in Materials Science 93 (2018) 233-269.

[2] R. Katahira, T.J. Elder, G.T. Beckham, A brief introduction to lignin structure, in *Lignin Valorization: Emerging Approaches*, Energy and Environmental series, The Royal Society of Chemistry, **19**2018, pp. 1-22.

[3] S. Sethupathy, G. Murillo Morales, L. Gao, H. Wang, B. Yang, J. Jiang, J. Sun, D. Zhu, Lignin valorization: Status, challenges and opportunities, Bioresource Technology 347 (2022) 126696. https://doi.org/https://doi.org/10.1016/j.biortech.2022.126696.

[4] A. Tejado, C. Pena, J. Labidi, J. Echeverria, I. Mondragon, Physico-chemical characterization of lignins from different sources for use in phenol–formaldehyde resin synthesis, Bioresource Technology 98(8) (2007) 1655-1663.

[5] A.G. Demesa, A. Laari, I. Turunen, M. Sillanpää, Alkaline partial wet oxidation of lignin for the production of carboxylic acids, Chemical Engineering &Technology 38(12) (2015) 2270-2278.

[6] J. Villar, A. Caperos, F. García-Ochoa, Oxidation of hardwood kraft-lignin to phenolic derivatives with oxygen as oxidant, Wood Science &Technology 35(3) (2001) 245-255.

[7] S. Laurichesse, L. Avérous, Chemical modification of lignins: Towards biobased polymers, J Progress in Polymer Science 39(7) (2014) 1266-1290.

[8] M.P. Pandey, C.S. Kim, Lignin depolymerization and conversion: a review of thermochemical methods, Chemical Engineering and Technology 34(1) (2011) 29-41.

[9] S.G. Santos, A.P. Marques, D.L. Lima, D.V. Evtuguin, V.I. Esteves, Kinetics of eucalypt lignosulfonate oxidation to aromatic aldehydes by oxygen in alkaline medium, Industrial & engineering chemistry research 50(1) (2011) 291-298.

[10] G. Wu, M. Heitz, E. Chornet, Improved alkaline oxidation process for the production of aldehydes (vanillin and syringaldehyde) from steam-explosion hardwood lignin, Industrial & Engineering Chemistry Research 33(3) (1994) 718-723.

[11] Q. Xiang, Y. Lee, Production of oxychemicals from precipitated hardwood lignin, Twenty-Second Symposium on Biotechnology for Fuels and Chemicals, Springer, 2001, pp. 71-80.

[12] H. Deng, L. Lin, Y. Sun, C. Pang, J. Zhuang, P. Ouyang, J. Li, S. Liu, Activity and Stability of Perovskite-Type Oxide LaCoO3 Catalyst in Lignin Catalytic Wet Oxidation to Aromatic Aldehydes Process, Energy & Fuels 23(1) (2009) 19-24. https://doi.org/10.1021/ef8005349.

[13] H. Deng, L. Lin, Y. Sun, C. Pang, J. Zhuang, P. Ouyang, Z. Li, S. Liu, Perovskite-type Oxide LaMnO3: An Efficient and Recyclable Heterogeneous Catalyst for the Wet Aerobic Oxidation of Lignin to Aromatic Aldehydes, Catalysis Letters 126(1) (2008) 106. https://doi.org/10.1007/s10562-008-9588-0.

[14] W. Schutyser, J.S. Kruger, A.M. Robinson, R. Katahira, D.G. Brandner, N.S. Cleveland, A. Mittal, D.J. Peterson, R. Meilan, Y. Román-Leshkov, Revisiting alkaline aerobic lignin oxidation, Green chemistry 20(16) (2018) 3828-3844.

[15] A. Toledano, L. Serrano, J. Labidi, Organosolv lignin depolymerization with different base catalysts, Journal of chemical technology & biotechnology 87(11) (2012) 1593-1599.

[16] P. Asawaworarit, P. Daorattanachai, W. Laosiripojana, C. Sakdaronnarong, A. Shotipruk, N. Laosiripojana, Catalytic depolymerization of organosolv lignin from bagasse by carbonaceous solid acids derived from hydrothermal of lignocellulosic compounds, Chemical Engineering Journal 356 (2019) 461-471.

[17] C. Dong, C. Feng, Q. Liu, D. Shen, R. Xiao, Mechanism on microwave-assisted acidic solvolysis of black-liquor lignin, Bioresource technology 162 (2014) 136-141.

[18] R. Ma, U. Sanyal, M.V. Olarte, H.M. Job, M.S. Swita, S.B. Jones, P.A. Meyer, S.D. Burton, J.R. Cort, M.E. Bowden, Role of peracetic acid on the disruption of lignin packing structure and its consequence on lignin depolymerisation, Green Chemistry 23(21) (2021) 8468-8479.

[19] A.C. Lindsay, S. Kudo, J. Sperry, Cleavage of lignin model compounds and lignin ox using aqueous oxalic acid, Organic & Biomolecular Chemistry 17(31) (2019) 7408-7415.

[20] A. Rahimi, A. Ulbrich, J.J. Coon, S.S. Stahl, Formic-acid-induced depolymerization of oxidized lignin to aromatics, Nature 515(7526) (2014) 249-252.

[21] S. Kudo, E. Honda, S. Nishioka, J.-i. Hayashi, Formation of p-Unsubstituted Phenols in Base-catalyzed Lignin Depolymerization, MATEC Web of Conferences, EDP Sciences, 2021, p. 05006.

[22] S.C. Gad, Peracetic Acid, in: P. Wexler (Ed.), Encyclopedia of Toxicology (Third Edition), Academic Press, Oxford, 2014, pp. 788-790. https://doi.org/https://doi.org/10.1016/B978-0-12-386454-3.01197-0.

[23] L. Das, P. Kolar, R. Sharma-Shivappa, J.J. Classen, J.A. Osborne, Catalytic valorization of lignin using niobium oxide, Waste and Biomass Valorization 8(8) (2017) 2673-2680.

[24] K. Skrodczky, M.M. Antunes, X. Han, S. Santangelo, G. Scholz, A.A. Valente, N. Pinna, P.A. Russo, Niobium pentoxide nanomaterials with distorted structures as efficient acid catalysts, Communications Chemistry 2(1) (2019) 129. https://doi.org/10.1038/s42004-019-0231-3.

[25] J.M. Jehng, I.E. Wachs, Niobium oxide solution chemistry, Journal of Raman spectroscopy 22(2) (1991) 83-89.

[26] L. Das, S. Xu, J. Shi, Catalytic oxidation and depolymerization of lignin in aqueous ionic liquid, Frontiers in Energy Research 5 (2017) 21.

[27] A. Diop, K. Jradi, C. Daneault, D. Montplaisir, Kraft lignin depolymerization in an ionic liquid without a catalyst, BioResources 10(3) (2015) 4933-4946.

[28] M. Tarnawski, K. Depta, D. Grejciun, B. Szelepin, HPLC determination of phenolic acids and antioxidant activity in concentrated peat extract—a natural immunomodulator, Journal of Pharmaceutical and Biomedical Analysis 41(1) (2006) 182-188. https://doi.org/https://doi.org/10.1016/j.jpba.2005.11.012.

[29] R. Roy, M.S. Rahman, T.A. Amit, B. Jadhav, Recent Advances in Lignin Depolymerization Techniques: A Comparative Overview of Traditional and Greener Approaches, Biomass 2(3) (2022) 130-154.

[30] S.C. Moldoveanu, Chapter 12 - Pyrolysis of Carboxylic Acids, in: S.C. Moldoveanu (Ed.), Pyrolysis of Organic Molecules (Second Edition), Elsevier2019, pp. 483-553. https://doi.org/https://doi.org/10.1016/B978-0-444-64000-0.00012-3.

[31] I.S. Shehatta, A.H. El-Askalany, E.A. Gomaa, Thermodynamic parameters of transfer and solution of oxalic acid in dimethylsulphoxide-water media, Thermochimica Acta 219 (1993) 65-72. https://doi.org/https://doi.org/10.1016/0040-6031(93)80483-Q.

[32] M. Thierry, A. Majira, B. Pegot, L. Cezard, F. Bourdreux, G. Clément, F. Perreau, S. Boutet- Mercey, P. Diter, G. Vo- Thanh, Imidazolium- Based Ionic Liquids as Efficient Reagents for the C− O Bond Cleavage of Lignin, ChemSusChem 11(2) (2018) 439-448.

[33] J. Higgins, X. Zhou, R. Liu, T.T.S. Huang, Theoretical Study of Thermal Decomposition Mechanism of Oxalic Acid, The Journal of Physical Chemistry A 101(14) (1997) 2702-2708. https://doi.org/10.1021/jp9638191.

[34] T. Aro, P. Fatehi, Production and application of lignosulfonates and sulfonated lignin, ChemSusChem 10(9) (2017) 1861-1877.

[35] A.W. Pacek, P. Ding, M. Garrett, G. Sheldrake, A.W. Nienow, Catalytic Conversion of Sodium Lignosulfonate to Vanillin: Engineering Aspects. Part 1. Effects of Processing Conditions on Vanillin Yield and Selectivity, Industrial & Engineering Chemistry Research 52(25) (2013) 8361-8372. https://doi.org/10.1021/ie4007744.

[36] S. Gonçalves, J. Ferra, N. Paiva, J. Martins, L.H. Carvalho, F.D. Magalhães, Lignosulphonates as an Alternative to Non-Renewable Binders in Wood-Based Materials, Polymers (Basel) 13(23) (2021). https://doi.org/10.3390/polym13234196.

[37] S. Sutradhar, N. Alam, L.P. Christopher, P. Fatehi, KOH catalyzed oxidation of kraft lignin to produce green fertilizer, Catalysis Today 404 (2022) 49-62.

[38] C. Pironti, M. Ricciardi, O. Motta, F. Camin, L. Bontempo, A. Proto, Application of 13C Quantitative NMR Spectroscopy to Isotopic Analyses for Vanillin Authentication Source, Foods 10(11) (2021) 2635.

[39] J. Feng, J. Jiang, Z. Yang, Q. Su, K. Wang, J. Xu, Characterization of depolymerized lignin and renewable phenolic compounds from liquefied waste biomass, RSC advances 6(98) (2016) 95698-95707.

[40] A. Setyawati, T.D. Wahyuningsih, B. Purwono, Synthesis and characterization of novel benzohydrazide as potential antibacterial agents from natural product vanillin and wintergreen oil, AIP Conference Proceedings, AIP Publishing LLC, 2017, p. 020121.

[41] K. Shi, J. Wang, Research on a Mixed Culture Technique of the White Rot Fungi Effect of Extracellular Lignin Peroxidase on Lignite Liquefaction, Frontiers in Energy Research 7 (2019) 133.

[42] H. Carreras, NMR Spectroscopy Principles, Interpreting an NMR Spectrum and Common Problems, Technology Networks (2021).

[43] A. Cassales, L.A. Ramos, E. Frollini, Synthesis of bio-based polyurethanes from Kraft lignin and castor oil with simultaneous film formation, International Journal of Biological Macromolecules 145 (2020) 28-41. https://doi.org/https://doi.org/10.1016/j.ijbiomac.2019.12.173.

[44] T.A. Amit, R. Roy, D.E. Raynie, Thermal and structural characterization of two commercially available technical lignins for potential depolymerization via hydrothermal liquefaction, Current Research in Green and Sustainable Chemistry 4 (2021) 100106.

[45] C. Crestini, H. Lange, M. Sette, D.S. Argyropoulos, On the structure of softwood kraft lignin, Green Chemistry 19(17) (2017) 4104-4121.

[46] H. Wang, T.L. Eberhardt, C. Wang, S. Gao, H. Pan, Demethylation of alkali lignin with halogen acids and its application to phenolic resins, Polymers 11(11) (2019) 1771.

[47] T. Ročnik, B. Likozar, E. Jasiukaitytė-Grojzdek, M. Grilc, Catalytic lignin valorisation by depolymerisation, hydrogenation, demethylation and hydrodeoxygenation: Mechanism, chemical reaction kinetics and transport phenomena, Chemical Engineering Journal 448 (2022) 137309. https://doi.org/https://doi.org/10.1016/j.cej.2022.137309.

[48] R. Ciriminna, A. Fidalgo, F. Meneguzzo, F. Parrino, L.M. Ilharco, M. Pagliaro, Vanillin: The Case for Greener Production Driven by Sustainability Megatrend, ChemistryOpen 8(6) (2019) 660-667. https://doi.org/10.1002/open.201900083.

[49] ProcurementResource, Oxalic Acid Price Trend and Forecast (2022).

[50] H. Ľudmila, J. Michal, Š. Andrea, H. Aleš, Lignin, potential products and their market value, Wood Res 60(6) (2015) 973-986.

Chapter 6

6.1. Conclusion and future work

The primary novelty and originality of the thesis was to conduct KOH-assisted direct aerobic oxidation of softwood KL to produce water-soluble lignin which can be utilized as ready-to-use green fertilizer and mid-range cement plasticizer. Another novelty of the thesis is the oxalic acid-mediated aerobic oxidation where softwood KL was selectively depolymerized to produce vanillin and vanillic acid. Moreover, no earlier studies reported catalytic activity (Nb_2O_5) to produce phenolic compounds. The research also focused on environmental concerns. In this research, oxidation processes (KOH and OxA-mediated) are considered green since no harmful solvents or chemicals were involved in the oxidation processes and no waste chemicals were generated, which would imply its limited environmental concerns.

In the first part of the thesis, different KOH-catalyzed oxidation approaches were conducted to increase the carboxylic acid groups of lignin. The increased carboxylic acid groups were determined by potentiometric titration methods, and ^{31}P-NMR was also performed to quantify its hydroxyl groups. The ^{31}P-NMR confirmed that KOH-catalyzed oxidation increased carboxylic acid groups of lignin from 0.43 to 2.07 mmol/g. However, the aliphatic and phenolic hydroxyl groups of lignin were significantly decreased. Moreover, the ^{1}H-NMR and HSQC-NMR analyses of the modified lignin showed significant disruption in aromatic regions (G-units) upon

oxidation. Based on the chemical analysis of the products, a schematic reaction mechanism was proposed. In addition, the samples were studied as green fertilizer to investigate the effect of lignin derivatives on physiological effects, such as plant growth, and chlorophyll content of maize seedlings. The findings were compared with commercial humic acid in another parallel experiment. The study showed that modified lignin increased the length of plants by 12% and 27% higher than the plants treated with humic acid and blank, respectively. The study also summarized that having sufficient carboxylic acid groups helped the nutrient transference to the plants and increased the carbon contents of the plants.

Furthermore, a series of KOH-assisted oxidation was carried out to investigate the effects of reaction parameters, such as lignin concentrations, temperature, oxygen consumption and pH on carboxylic acid group formation. The study revealed that the oxidation reaction under the conditions of 10 wt.% lignin in water, 210 °C, 100 psi initial oxygen for 30 min generated oxidized lignin (OKLB2) with the highest amount (2.6 mmol/g) of the carboxylic acid group and charge density (1.9 mmol/g). Structural changes during the oxidative modification were investigated and confirmed by FTIR, XPS and HSQC-NMR analyses. After that, the plasticizing performance of the samples with the highest carboxylic acid (OKLB2) was investigated. The adsorption analysis confirmed that having a significant amount of carboxylic acid groups (the hydrophilic ends) on lignin can facilitate its adsorption on the cement particles, while the unadsorbed COO^- groups of lignin derivatives can introduce electrical repulsion in the cement paste. It was observed that the OKLB2 exhibited higher flowability (18% at 0.25 wt.% dosages) compared to commercial lignosulfonate and plasticizer. Interestingly, OKLB2 increased the compressive strength of the cement by 45% more than the blank at 0.25 wt.% dosage. The study concluded that the oxidized lignin could be used directly as a mid-range water reducer (~18%).

In the last part of the thesis, the KL was depolymerized by oxalic acid-mediated oxidation to produce vanillin and vanillic acid. In this study, the effects of reaction parameters, such as reactants, temperature, time, and oxalic acid concentrations, on the yield and selectivity of phenolic were studied. The products were identified and quantified by HPLC analysis. It was observed that, regardless of the concentration of the lignin and oxalic acid, the maximum yield of phenolic compounds could be obtained at 125 °C for 60 min. The study summarized that oxalic acid was very selective for vanillin and vanillic acid productions. Moreover, the study demonstrated that the catalytic activity of Nb_2O_5 oxalic acid-mediated oxidation showed an excellent effect on product yields. The structural changes of the KL and unreacted lignin (recovered after the reaction) were analyzed by H-NMR and HSQC-NMR. A schematic reaction mechanism was proposed based on the major products obtained and the NMR analysis. Finally, the mass balance analysis showed that around 79wt.% of oxalic acid could be recovered and recycled (45 wt.%) in two cycles without reducing the product yields.

Overall, it was observed that softwood KL could successfully be oxidized in the presence of KOH to produce anionic hydrophilic lignin materials by introducing a significant amount of carboxylic acid groups. The final products could be utilized directly without any further purification process for such uses as green fertilizers and cement plasticizers. The oxalic acid-mediated KL oxidation showed a significant product selectivity toward vanillin and vanillic acid productions. In addition, the recovery and the recyclability of the oxalic acid suggested its possible use at an industry scale.

To investigate the effect of the oxidized lignin as fertilizers for plant growth, a field trial on different plants is suggested for future studies. The investigation of other physiological responses, such as hormonal activity, carbohydrate, and protein biosynthesis, can be considered

to understand how lignin derived fertilizers would affect the plant physiology. As a cement plasticizer, the effect of oxidized lignin on strength of cement with different formulas and in different environments could be studied to understand how lignin included cement would behave under different conditions. Moreover, the effect of the oxidized KL in construction grades of concrete admixtures could be studied. Furthermore, other commercial lignin products could be considered for the production of aromatic compounds to understand how different lignin products would generate aromatic compounds in oxalic acid-catalyzed oxidation processes. In addition, the influence of other transitional metal oxides/salts catalysts, such as CuO, $CuSO_4$, $FeSO_4$, $FeCl_3$, MnO eon the oxalic acid-mediated oxidation of lignin could be studied to understand how different catalysts would affect the oxidation of different lignin materials.

Chapter 7

Appendix

Chapter 3: KOH catalyzed oxidation of kraft lignin to produce green fertilizer.

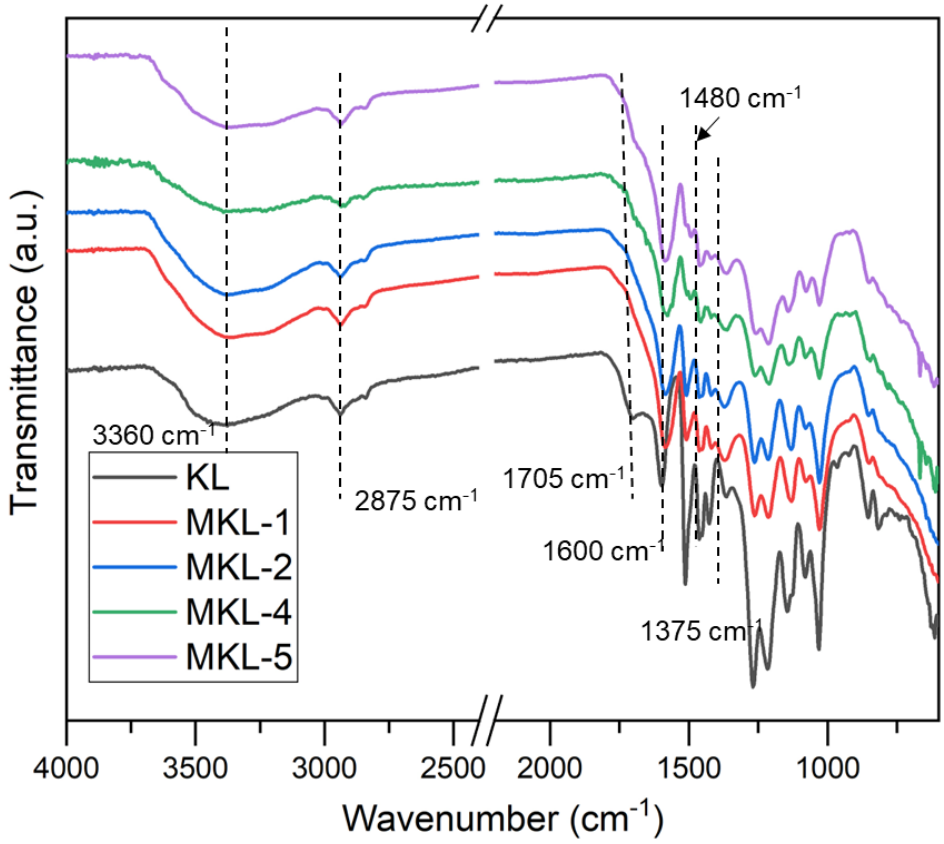

Figure A3.1: FTIR spectra of KL and MKLs

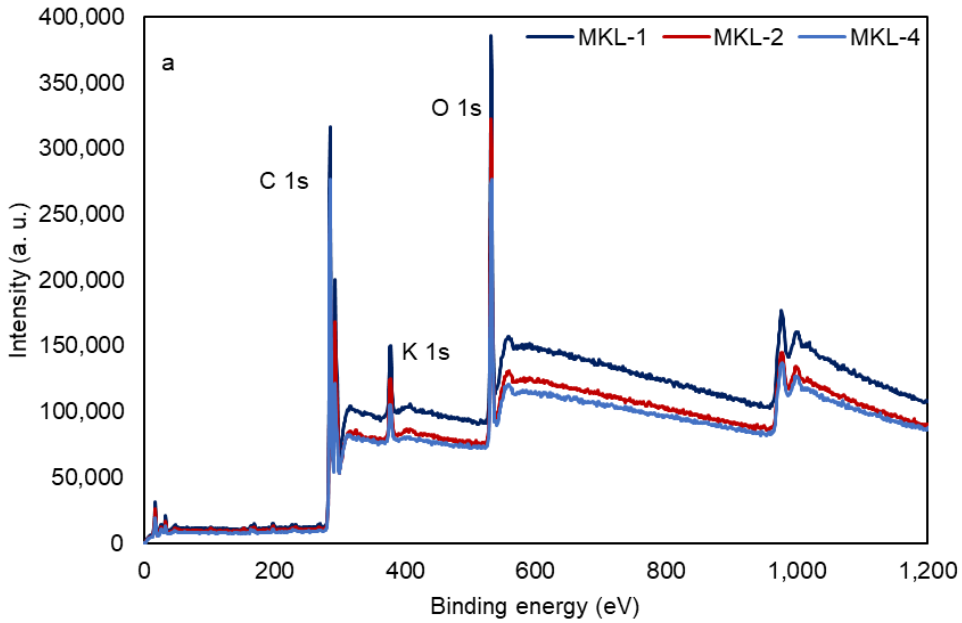
a
MKL-1
MKL-2
MKL-4
C 1s
O 1s
K 1s
Intensity (a. u.)
Binding energy (eV)
400,000
350,000
300,000
250,000
200,000
150,000
100,000
50,000
0
0
200
400
600
800
1,000
1,200

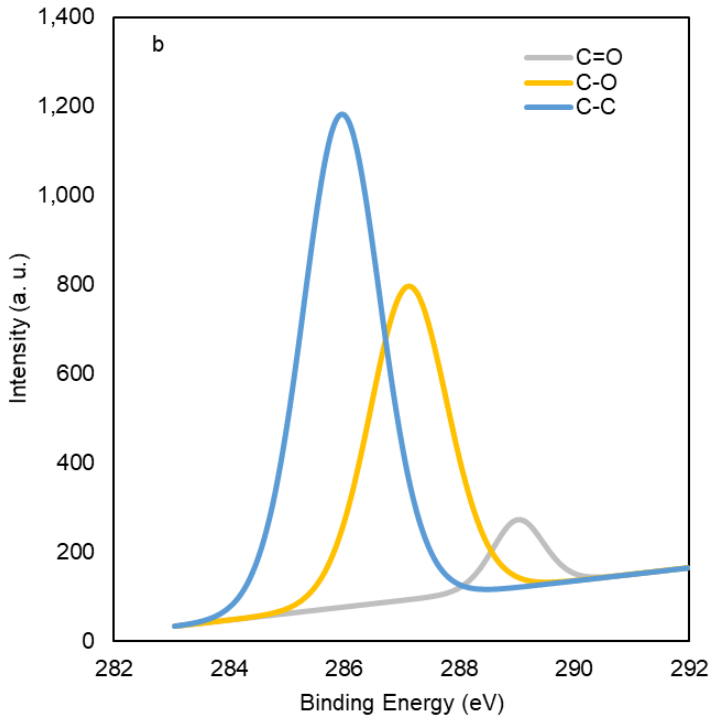
b
C=O
C-O
C-C
Intensity (a. u.)
Binding Energy (eV)
1,400
1,200
1,000
800
600
400
200
0
282
284
286
288
290
292

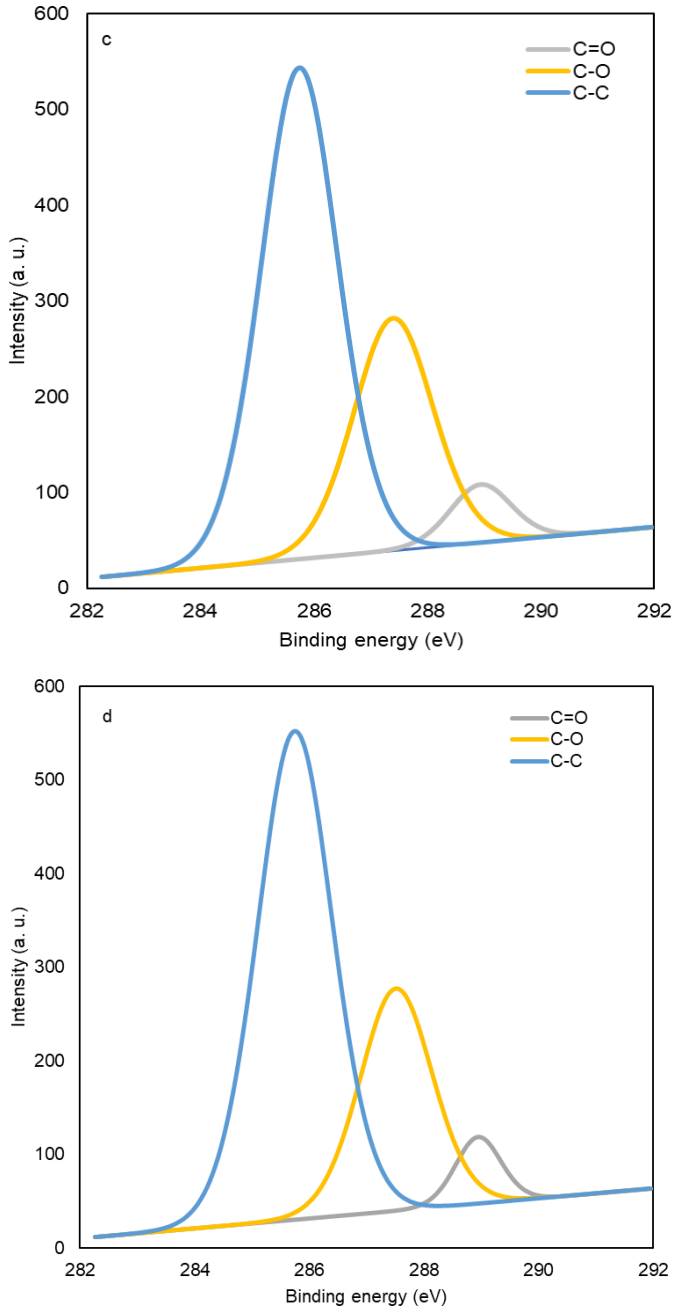

Figure A3.2: (a) XPS spectra of MKL-1, MKL-2 and MKL-4; (b) XPS scans (C 1s) for the MKL-1; (c) XPS scans (C 1s) for the MKL-2; (d) XPS scans (C 1s) for the MKL-4.

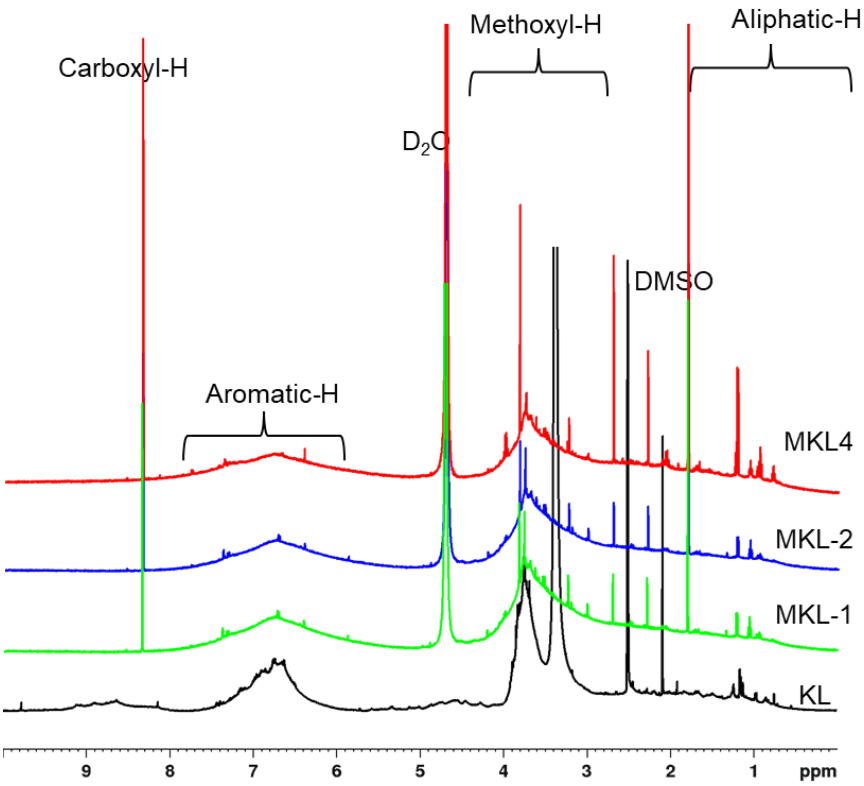

Figure A3.3: ^{1}H-NMR spectra of KL and MKLs.

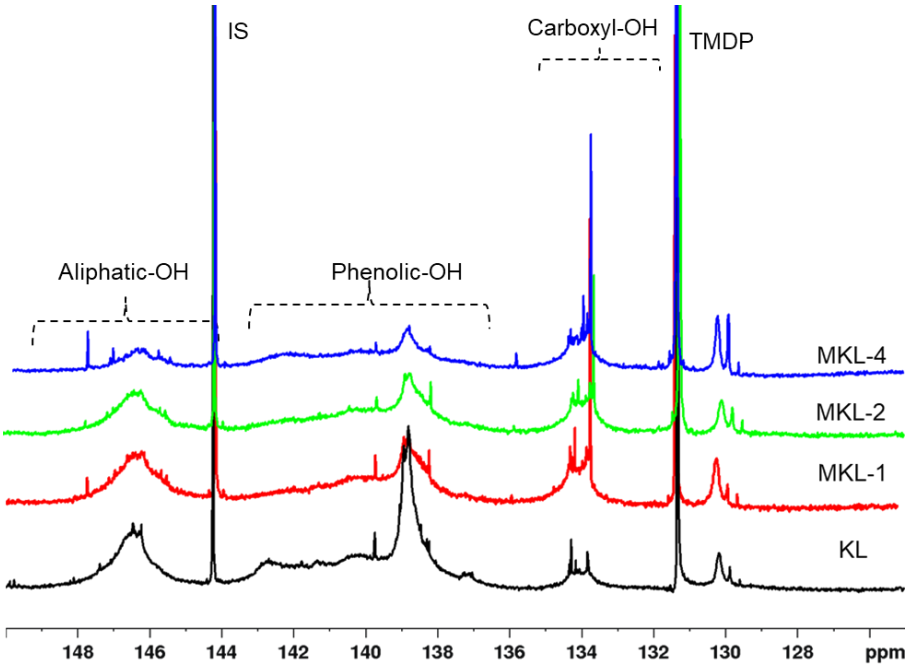

Figure A3.4: ^{13}P-NMR spectra of KL and MKLs

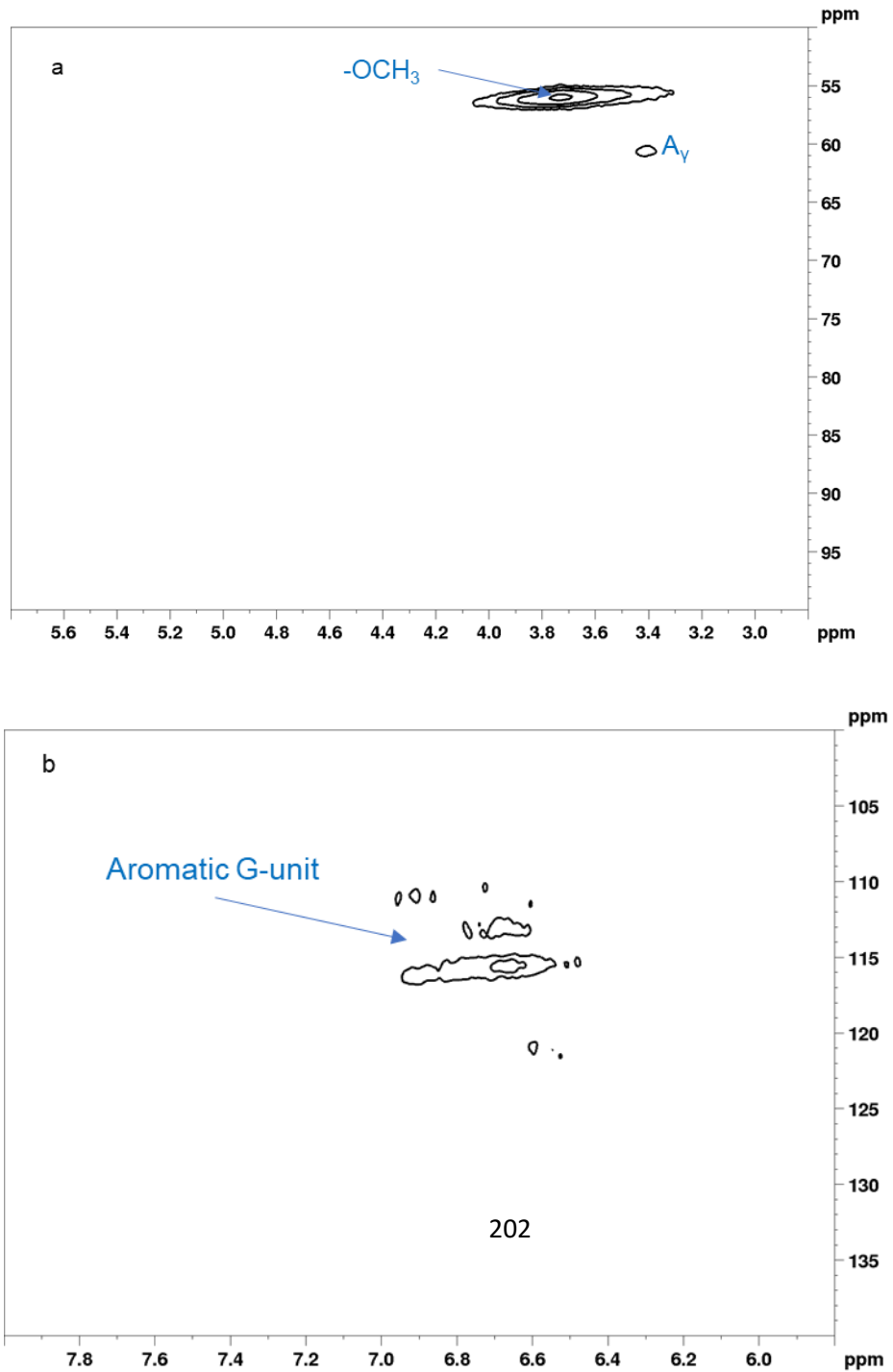

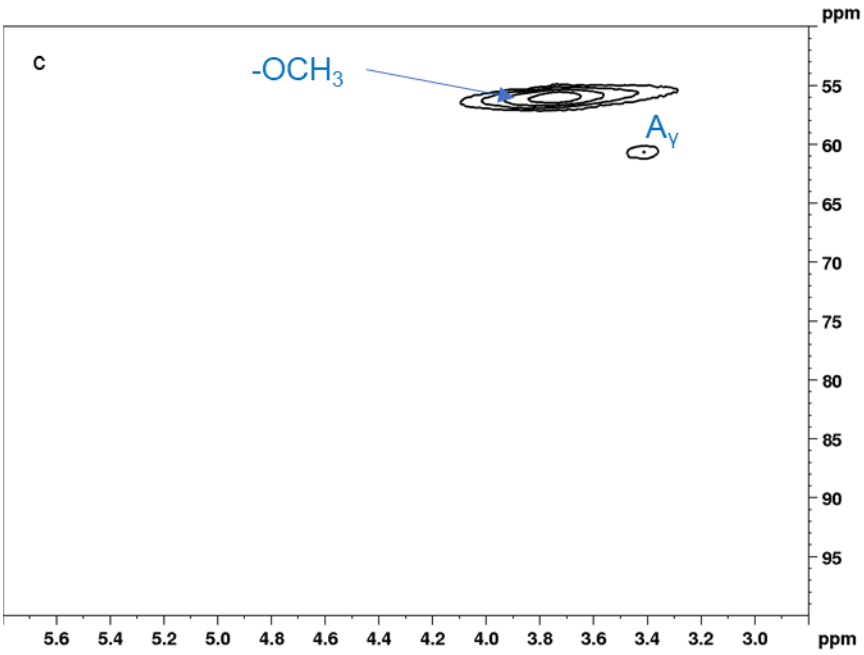
c
-OCH3
Aγ
ppm
55
60
65
70
75
80
85
90
95
5.6
5.4
5.2
5.0
4.8
4.6
4.4
4.2
4.0
3.8
3.6
3.4
3.2
3.0
ppm

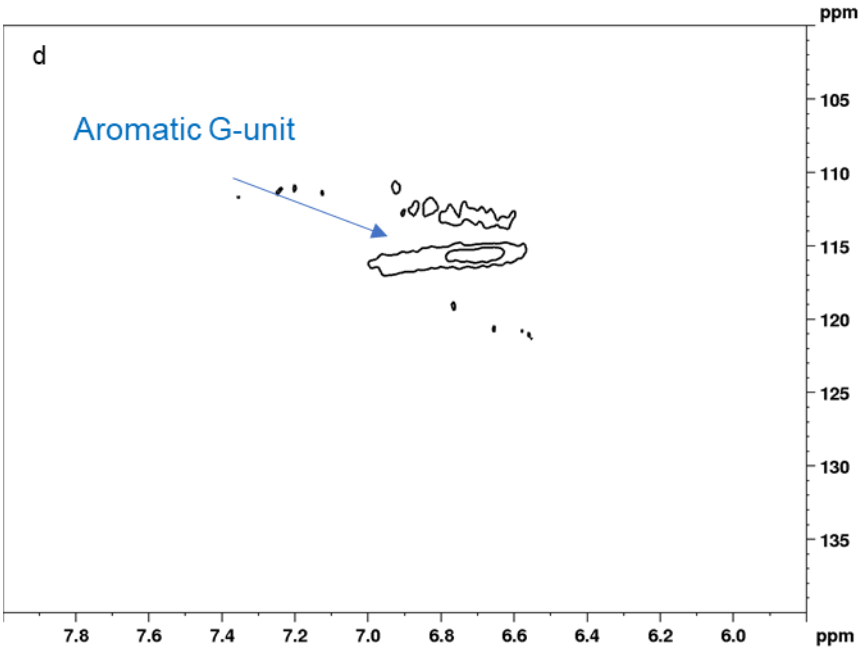
d
Aromatic G-unit
ppm
105
110
115
120
125
130
135
7.8
7.6
7.4
7.2
7.0
6.8
6.6
6.4
6.2
6.0
ppm

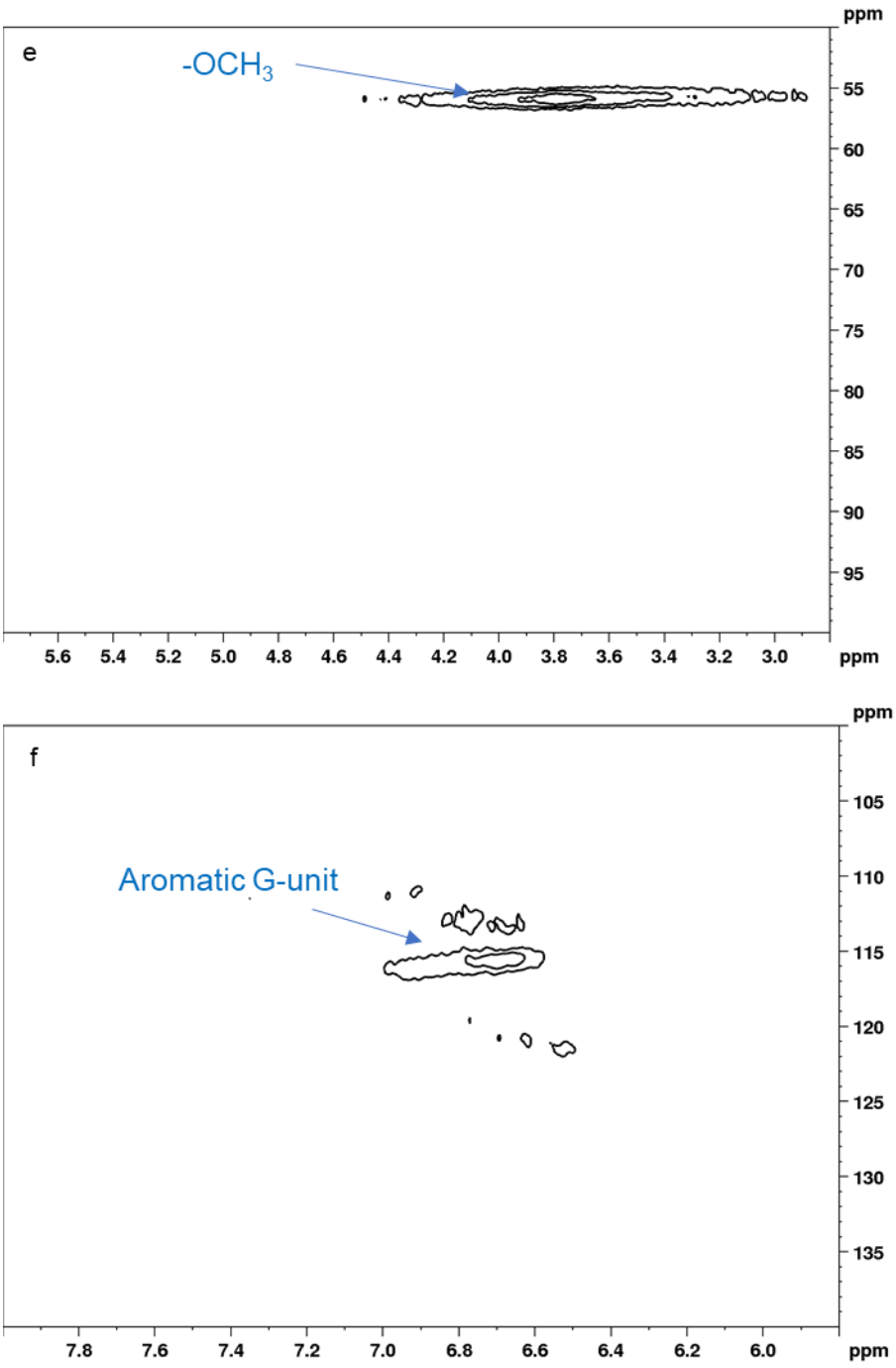

Figure A3.5: HSQC NMR spectra of MKL-1 for C-O aliphatic region (a) and aromatic region (b); MKL-2 for C-O aliphatic region (c) and aromatic region (d); MKL-4 for C-O aliphatic region (e) and aromatic region (f).

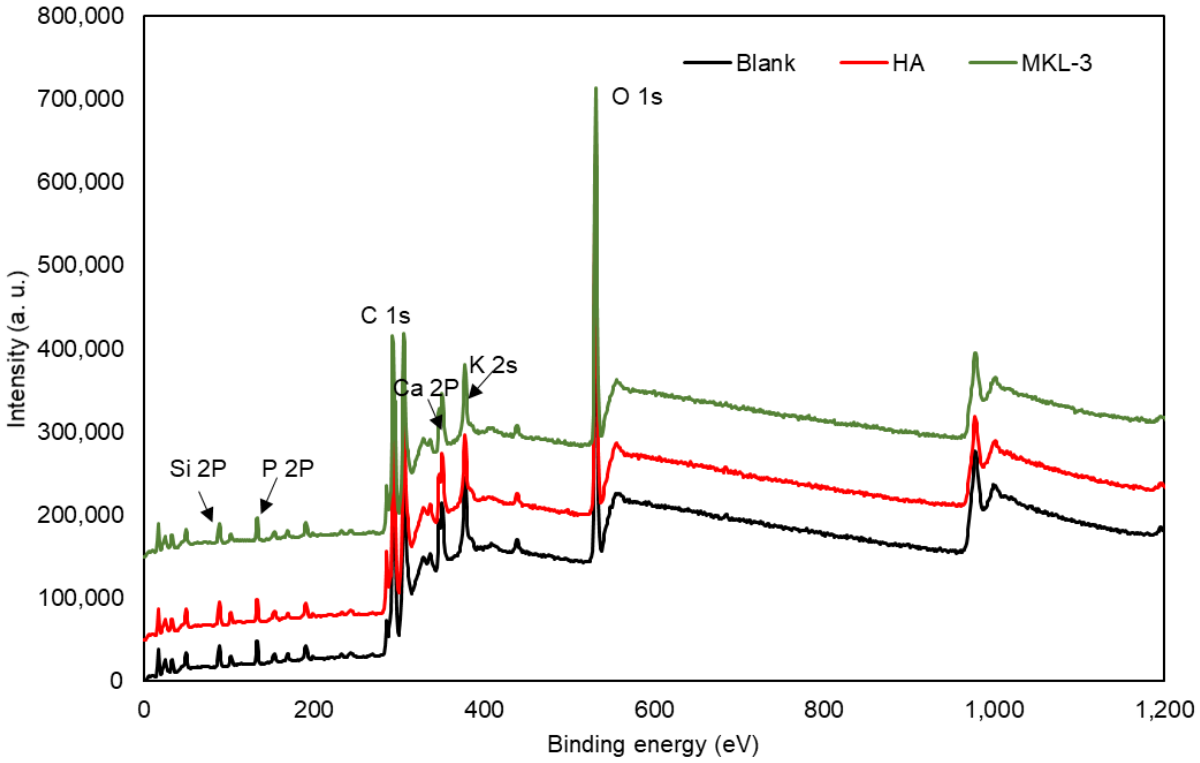

Figure A3.6: XPS wide spectra for the blank, HA, control and MKL-3 treated plant ash after 40 days.

Chapter 4: A green cement plasticizer from softwood kraft lignin

EXPERIMENTAL

Zeta potential Experiment

Zeta potential of solution containing the samples was determined by NanoBrook ZetaPALS (Brookhaven Instruments, Holtsville, New York, USA) at pH 7 and 10. First, 50 mg of dry samples were dissolved in 5 mL of deionized water, and its pH was adjusted by 0.1 M HCl and 0.1M KOH solution. Then, 1 ml of each solution was mixed with 1mM KCl solution and the zeta potential of these samples was measured.

Table A4.1: Detail experimental conditions, yields, molecular weights, and polydispersity.

Samples	Lignin, wt%	Temperature, °C	Yield before dialysis, wt.%	Yield after dialysis, wt.%	Mw, g/mol	Mn, g/mol	Mw/Mn
KL	NA	NA	NA	NA	7000	1200	5.83
OKLA1	5	180	84.3	55.1	3632	1904	1.9
OKLA2	5	210	82.3	54	3537	1946	1.8
OKLA3	5	240	77.5	51.3	3454	2028	1.7
OKLA4	5	270	72.6	46.4	3455	2127	1.6
OKLB1	10	180	77.5	58.4	3678	1844	2
OKLB2	10	210	75.4	57.2	3541	1950	1.8
OKLB3	10	240	75.2	55.4	3285	1935	1.7
OKLB4	10	270	71.9	57	3674	2192	1.7
OKLC1	15	180	77	56.8	3613	1821	2
OKLC2	15	210	71.6	55	3445	1874	1.8
OKLC3	15	240	71.7	53.8	3202	1882	1.7
OKLC4	15	270	68.5	55.2	4034	2404	1.7

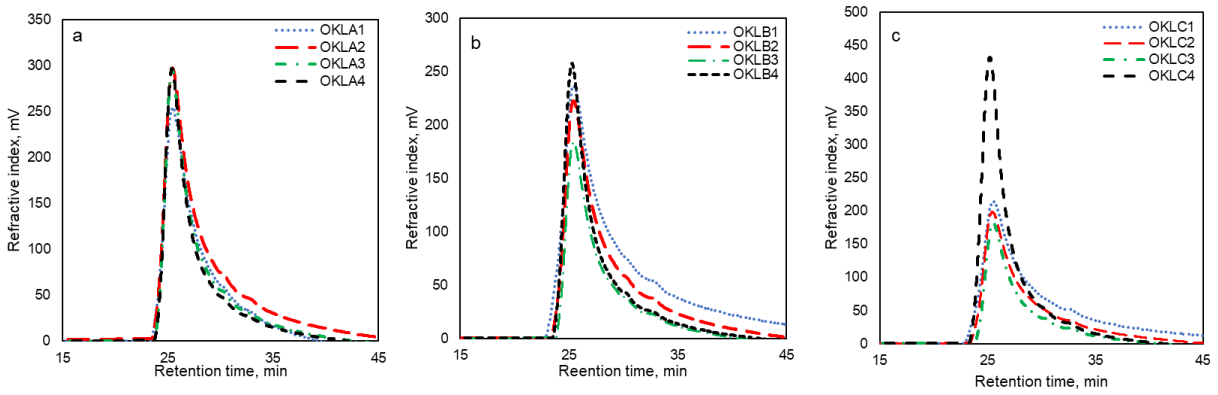

Figure A4.1: RI responses as a function of retention time of OKLAs (a), OKLBs (b), OKLCs (c)

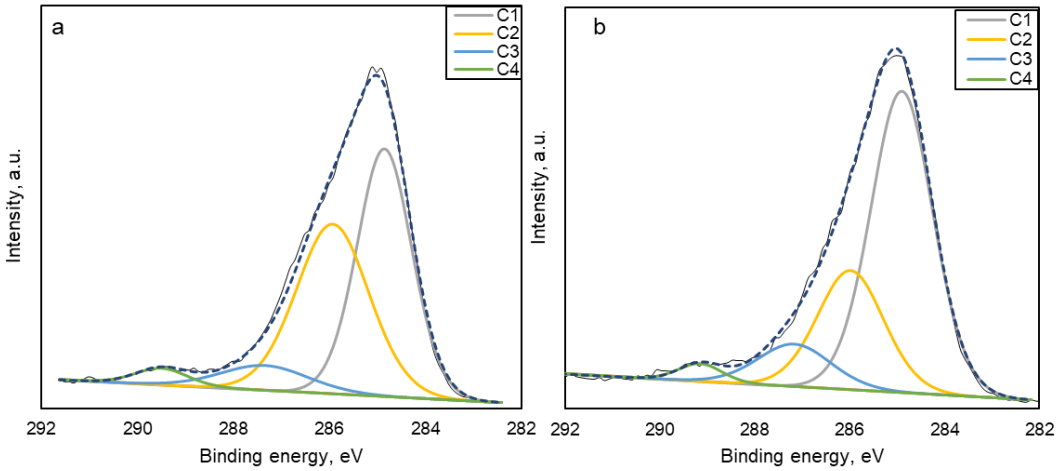

Figure A4.2: XPS C-scan of the samples OKLC3 and OKLC4.

Table A4.2: Relative abundances from XPS analysis

		Mass concentration, %	
Bond types	Assignments	OKLC3	OKLC4
C1	C-H, C-C	50.6	61.34
C2	C-OH/C-O-C	37.5	26.0
C3	C=O, carbonyl	8.39	10.18
C4	C=O, carboxylic	3.48	2.49

Zeta potential discussion

Figure S3 describes the effects of ZP on CD at pH 7 and 10. It can be observed that at pH 10, the negative ZP increases with increasing negative CD. The samples having highest CD of 1.9 meq/g (OKLB2) exhibits more negative charge. Similar phenomenon also observed in a recent study, where KL was oxidized by NaOH and H_2O_2 and showed more negative ZP (-39 mV at pH 6) due to more negative CD[1]. On the other hand, at pH 7, there were no significant effect on ZP which attributing the protonation of the carboxylic groups[2]. The remaining negative charge can be due to the available phenolic-OH and rest of the carboxylic groups in the solution[2].

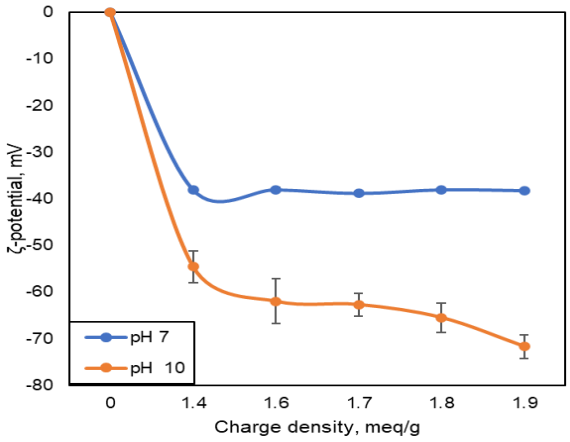

Figure A4.3: Effects of zeta potential on charge density at pH 7 and 10.

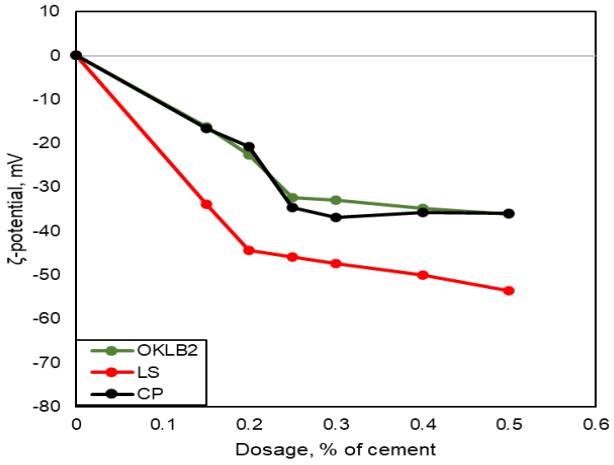

Figure A4.4: Zeta potential of the same samples before at same pH (pH ~11).

REFERENCES

(1) Aldajani, M.; Alipoormazandarani, N.; Fatehi, P., Two-Step Modification Pathway for Inducing Lignin-Derived Dispersants and Flocculants. *Waste and Biomass Valorization* **2022,** *13* (2), 1077-1088.
(2) Klapiszewski, Ł.; Wysokowski, M.; Majchrzak, I.; Szatkowski, T.; Nowacka, M.; Siwińska-Stefańska, K.; Szwarc-Rzepka, K.; Bartczak, P.; Ehrlich, H.; Jesionowski, T., Preparation and characterization of multifunctional chitin/lignin materials. *Journal of Nanomaterials* **2013,** *2013*.

Chapter 5: Oxalic acid-mediated oxidative depolymerization of Kraft lignin for vanillin and vanillic acid production

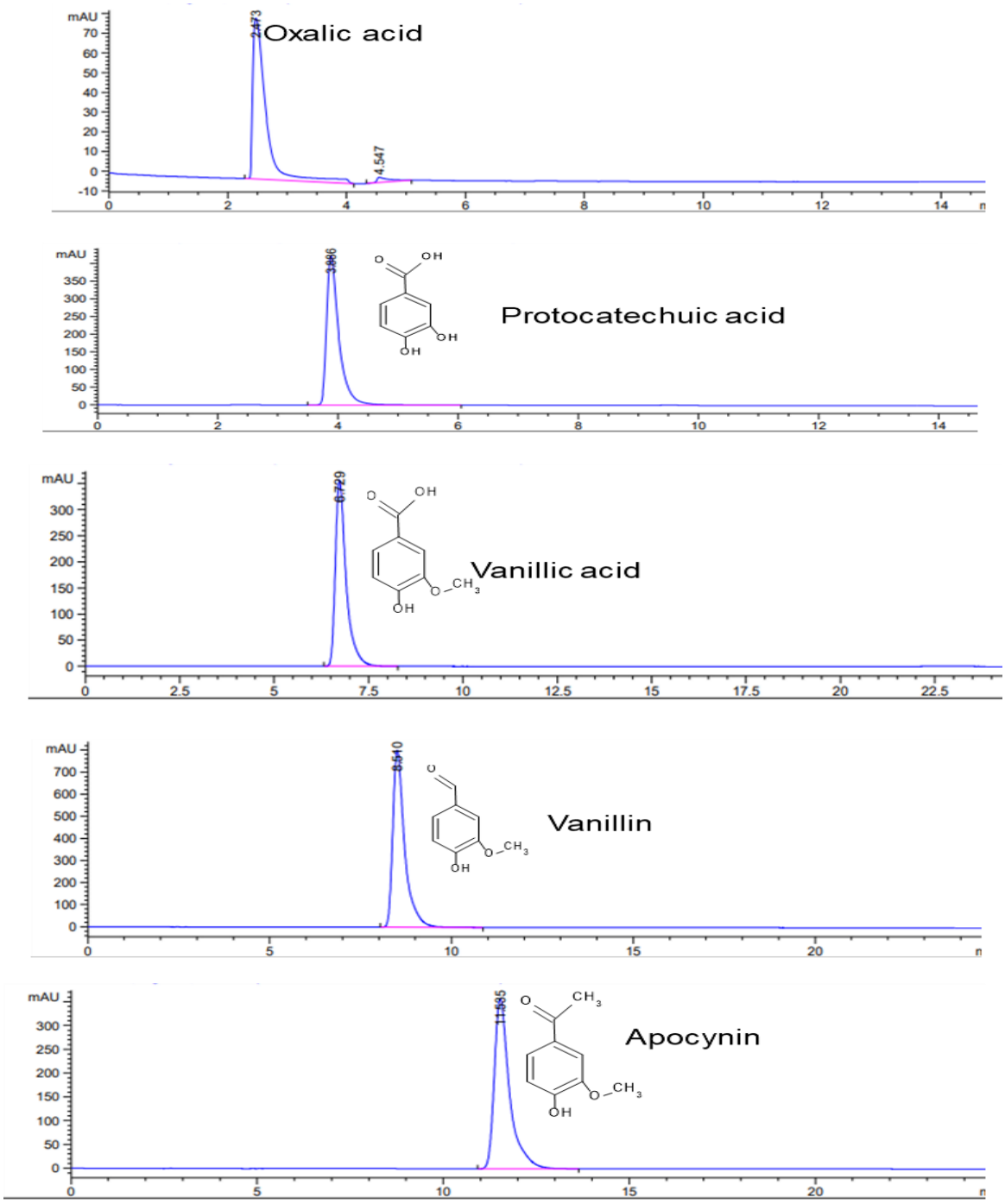

HPLC analysis of the standards and extracted products :

Figure A5.1: HPLC standards of OxA, Protocatechuic acid, vanillic acid, vanillin and apocynin.

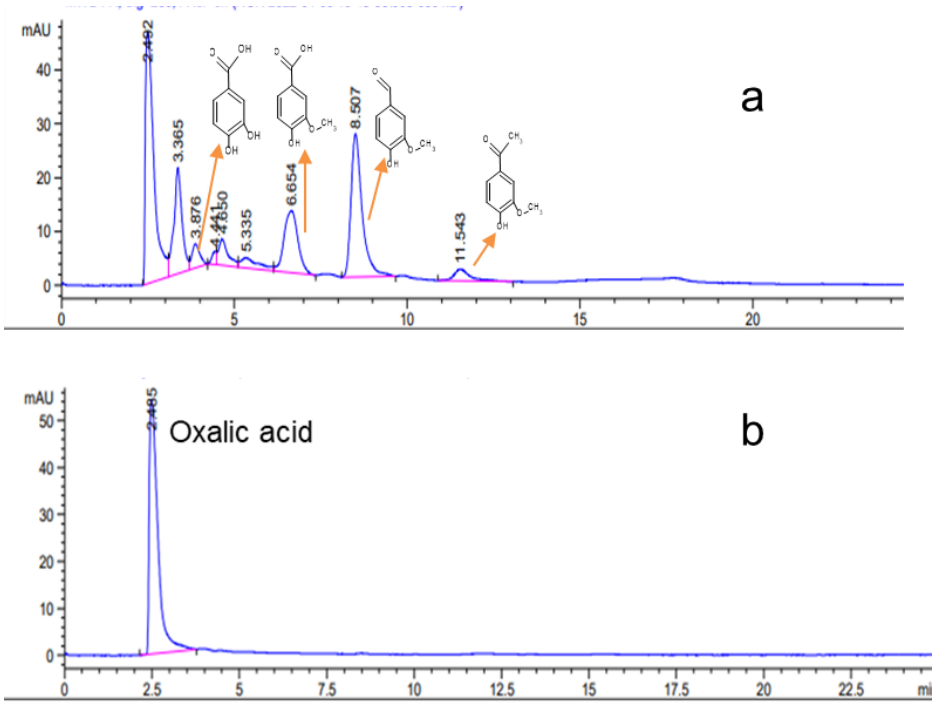

Figure A5.2: HPLC analysis of phenolic compounds from EA soluble fractions(a); recovered OxA from the aqueous phase after EA extraction.

Effects of Nb_2O_5 catalytic effects on higher reaction time and higher OxA concentration

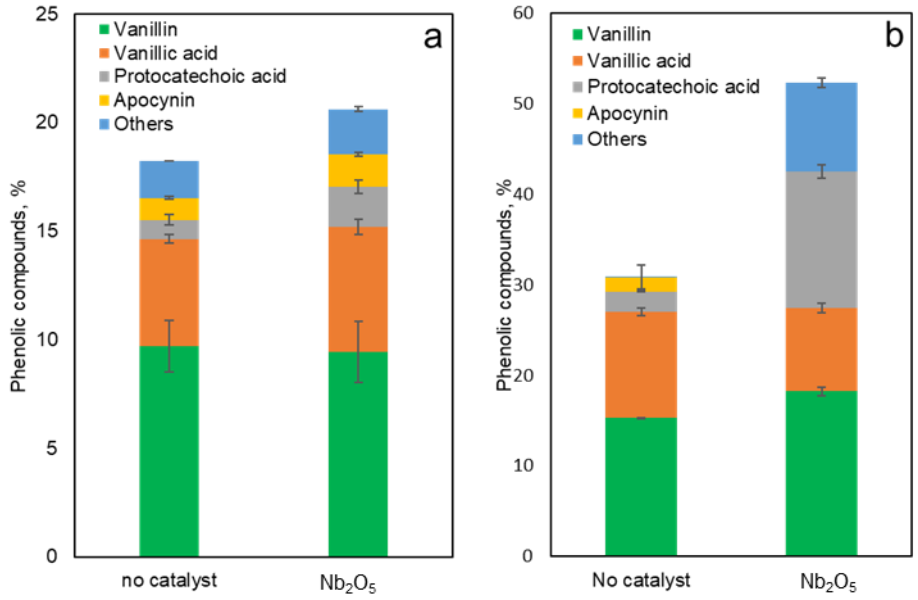

Figure A5.3: (a)Effect of Niobium pentoxide on phenolic yields at higher reaction time, reaction condition: 5 g KL, 4.5 g OxA in 100 ml of water (0.5 M), 125 ° C, **120 min**, initial 50 psi oxygen, Nb_2O_5-0.5 g. (b) Effect of Niobium pentoxide on phenolic yields at **1.25 M OxA**, reaction condition: 5 g KL, 11.25g OxA in 100 ml of water (1.25 M), 125 ° C, 60 min, initial 50 psi oxygen, Nb_2O_5-0.5 g.

FTIR analysis

Table A5.1: The major FTIR peak assignments for KL, PDL and char.

Wave number (cm^{-1})	Peak assignments
3360	Phenolic and aliphatic hydroxyl groups
2870	Methoxyl groups attached to aromatic rings
1705	C=O stretching
1504	Aromatic ring stretching
1330-1400	Deformation of aromatic G-units
1145	C-H plane vibration for G-units

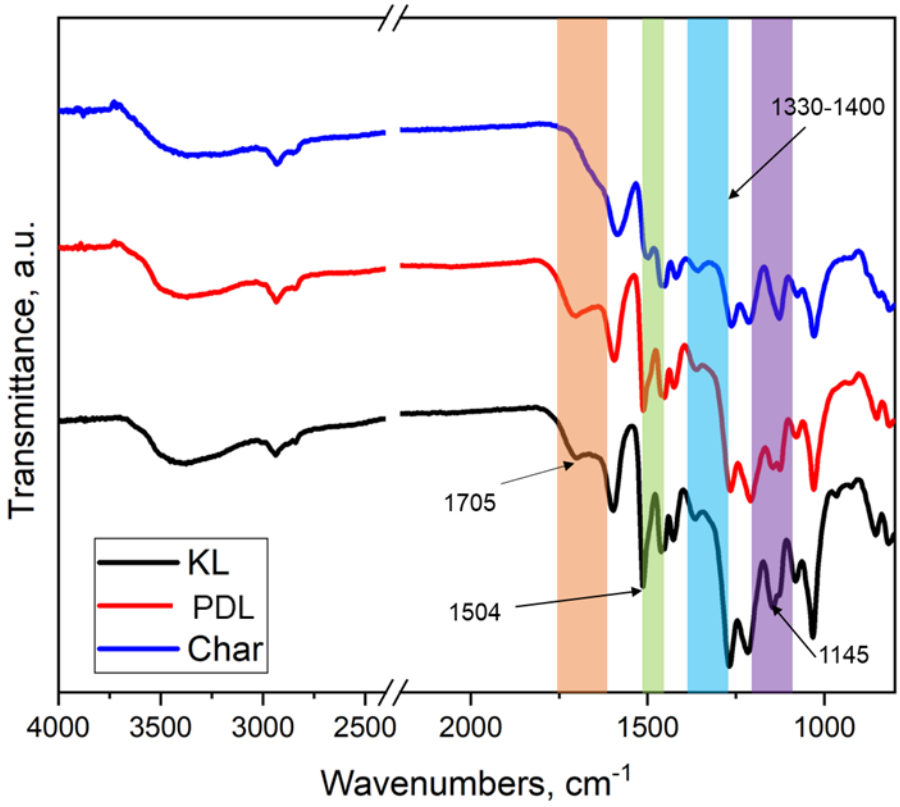

Figure A5.4: FTIR spectra of KL, PDL and char.

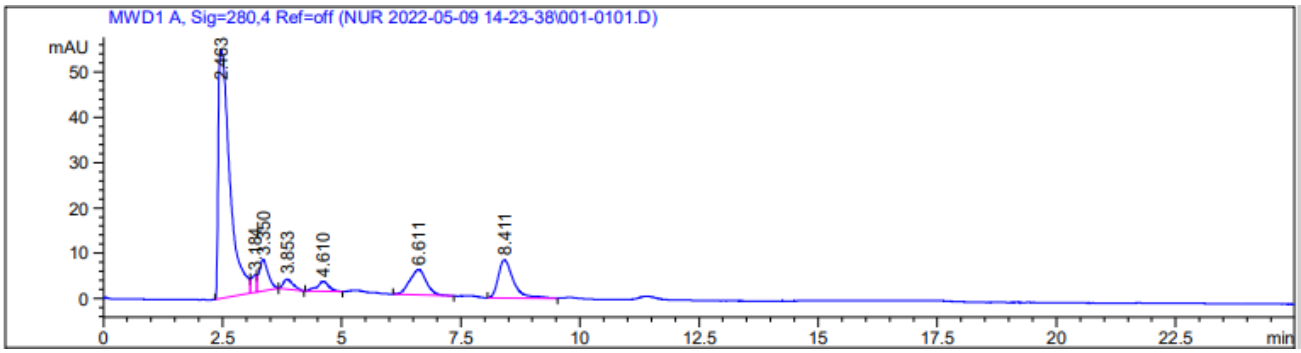

Peak #	RetTime [min]	Type	Width [min]	Area [mAU*s]	Height [mAU]	Area %
1	2.463	BV	0.2499	921.60522	54.88189	64.3567
2	3.184	VV	0.1157	30.07514	3.82545	2.1002
3	3.350	VB	0.1933	90.77055	6.90679	6.3386
4	3.853	BB	0.2108	31.24260	2.18460	2.1817
5	4.610	BB	0.2535	38.35382	2.19842	2.6783
6	6.611	BB	0.3353	135.24895	5.61022	9.4446
7	8.411	BB	0.3236	184.73148	8.43158	12.9000

Figure A5.5: HPLC analysis for the products generated from the condition of 5g KL, 125 °C, 60 min at 1.25M OxA.